A CYCLIC ELECTRODIALYSIS PROCESS

Investigation of Open Systems

by

MOHAMMED ELAMIEN ABU-GOUKH

B.Sc. (Hons.), University of Khartoum, 1970

A THESIS SUBMITTED IN PARTIAL FULFILLMENT OF
THE REQUIREMENTS FOR THE DEGREE OF

DOCTOR OF PHILOSOPHY

in

THE FACULTY OF GRADUATE STUDIES
Department of Chemical Engineering

We accept this thesis as conforming
to the required standard

THE UNIVERSITY OF BRITISH COLUMBIA

November, 1976

In presenting this thesis in partial fulfilment of the requirements for

an advanced degree at the University of British Columbia, I agree that

the Library shall make it freely available for reference and study.

I further agree that permission for extensive copying of this thesis

for scholarly purposes may be granted by the Head of my Department or

by his representatives. It is understood that copying or publication

of this thesis for financial gain shall not be allowed without my

written permission.

Department of ___Chemical Engineering___

The University of British Columbia
2075 Wesbrook Place
Vancouver, Canada
V6T 1W5

Date ___Dec. 16, 1976___

ABSTRACT

Cyclic electrodialysis is a novel separation process in which a
modified membrane stack is operated in a periodic unsteady-state manner.
Repeated reversals of polarity could avoid the main problems encountered in
conventional electrodialysis; fouling and scale formation on the membranes.

In cyclic electrodialysis the standard electrodialysis stack is
converted into an adsorption-desorption stack with only one set of flow
channels, the other set being replaced by storage compartments. These
compartments are in the form of three-layer membranes consisting of an
anion and a cation selective membrane enclosing a core of non-selective
material. The depleted and enriched products are produced successively
in the single set of channels instead of simultaneously in adjacent channels.
The process is potentially applicable for commercial desalination of brackish
water to make it potable, to remove harmful ions from discharge waters,
or to concentrate ionic solutions for recovery of valuable materials.

Previously reported experiments with aqueous NaCl solutions in a
closed (batch) system showed that a large separation factor could be obtained
in cyclic electrodialysis. Batch operation is somewhat analogous to total
reflux in distillation. The present work extends the earlier work to
potentially more useful operating conditions in which feed is supplied and
product removed.

A constant-rate model has been developed for the process and used
extensively throughout the work as a simple and efficient tool to compare

various operating cycles and modes of operation. Scattered articles

in the literature on the resistance of an electrodialysis stack have been

compiled to develop a stack resistance model. Good agreement was obtained

between the model predictions and measured values of resistance.

Experimental apparatus is described and the effects of the following

eight system parameters are reported:

    (i)   Demineralizing path length

  (ii)   Production rate

 (iii)   Pause time

  (iv)   Applied voltage

   (v)   Initial concentration

  (vi)   No-pause operation

 (vii)   Pure-pause operation

(vii)   Semi-symmetric operation

Large separations were achieved for asymmetrical paused operation with

long demineralizing path, long pause time, high applied voltage, low feed

concentration and small production rate. Despite the strong trade-off

between production rate and separation, a separation factor as high as 50

was obtained at the highest production rate used. This value is higher

than that obtained in commercial plants currently in use.

The process looks promising and is worth further consideration.

TABLE OF CONTENTS

LIST OF TABLES

LIST OF FIGURES

ACKNOWLEDGEMENT

CHAPTER 1

Introduction and General

Water is the most important chemical compound on Earth. When men

settled down to agriculture and farming, they built their houses near

potable water resources, such as rivers and lakes. Increasing the size

of settlements augmented the needs of fresh water supply. The theoretical

minimum water requirements, including agriculture, to sustain human life

are about 1.1 m^3 per person per day, assuming that man can live on bread

alone. The introduction of 0.5 kg of animal fat and protein to the diet

increases the water requirement for subsistence to about 9.5 m^3 per person

per day (Bradley, 1962). Increasing demand for water caused by the rising

standard of living and by the increase in population, irresponsible wasting

of water in many large cities, and above all pollution of natural water

reserves with industrial waste and sewage, have brought many regions in

various countries close to the critical point where existing resources can

no longer satisfy the growing demand. The situation will become worse if

adequate means are not adopted in time.

Although the annual precipitation on Earth's surface might be

sufficient, the uneven distribution of rainfall does not meet the human needs

in all regions of the world. In several arid areas, existing water

resources are saline, exceeding the limit of potable water which is set as

1

500 mg/l for total dissolved solids. Actually there are many communities in various countries which are still supplied with water containing over 1000 mg/l total dissolved solids and sometimes up to 3000 mg/l. For such brackish and similar polluted waters treatment by distillation is not economically feasible and efforts have been made to resort to other processes such as electrodialysis. However, conventional electrodialysis has achieved only partial success in brackish water demineralization despite many theoretical advantages it offers over other processes. Under steady state operation, conventional electrodialysis is subject to mud and scale build-up on the membrane surfaces which may hinder the transfer of ions through the membranes, thus decreasing the capacity of the unit. The deposit may partially block flow channels, increasing pumping cost, and may react with and damage the membranes, reducing the selectivity and efficiency of the separation (Matz, 1965 and Korngold, 1970).

Periodic current interruptions and/or reversals have been employed in standard electrodialysis plants to reduce polarization effects and deposition of particulates on the membranes (Matz, et al., 1962; Calvit and Sloan, 1965). Based on current reversal technique, Lacey (1965, 1968) invented an electrosorption stack of much simpler construction than conventional electrodialysis stacks. Electrosorption can be considered as a one-cycle process without reflux. This idea was further modified and developed into cyclic electrodialysis by Thompson and Bass (1972, 1974). Cyclic electrodialysis is a cyclic separation process which applies the periodic flow-reversal technique to an electrically driven electrosorption stack. The process has a wide field of potential applications such as:

    i)   Brackish water demineralization

    ii)   Brine production from sea water

iii) Radioactive waste decontamination

iv) Selective separation of monovalent salt from divalent and other polyvalent salts

v) In the food industries it may be used for desalination of cheese whey and de-acidification of orange juice and treatment (mainly de-ashing) of sugars and syrups and related compounds

vi) Other potential applications outside the food industry concern the treatment of leach solutions in metallurgy, waste pickle-liquor recovery and waste sulfite-liquor recovery.

Although cyclic electrodialysis may be most economical for the conversion of brackish waters (up to 10,000 ppm) to potable water of 500 ppm, nevertheless specific conditions can create other situations when the process could become unexpectedly economical. For example, there seems to be a large potential demand for sea water conversion on the 2-5 m^3/h scale for tourist resorts. In these cases, the amortisation and interest charges tend to be very high and the utilisation factor is often as low as 33% per annum. Capital cost is therefore overwhelmingly the most important factor, and it appears that the process may provide the cheapest capital plant for meeting these requirements, although, at this salinity level, the power cost of cyclic electrodialysis would be higher than the other competitive processes.

Cyclic electrodialysis has been investigated in a closed system and separation factors of several hundreds were reported for most of the runs with aqueous sodium chloride solutions (Bass, 1972). The present work is an extension of the previous work to an open system which represents a more useful mode of operation. The main objectives are to analyze the potential of the cyclic process on a continuous basis and to investigate systematically

the effect of the various design and operating parameters on the performance of the process. The present program makes a rather extensive study and exploration of the system within the design parameters and it provides information that should be useful in further study and in optimizing the system.

CHAPTER 2

Theory and Review

2.1. Desalting Processes

Desalting techniques potentially useful as commercial separation processes may be classified into two general categories, as shown in Table I:

a) Processes that remove pure water from solution

b) Processes that remove salts from solution

The most developed process in category (a) is distillation. Freezing is a process currently being developed, while hydrate formation is still in the experimental stage. Reverse osmosis, after a long period of membrane development, is entering the field of commercial operation.

The latent heat for changing phase is an important factor in the overall economics of distillation processes while the degree of salinity of the raw water is of little importance. This process is therefore equally suitable for desalting seawater or brackish water. The same applies for freezing. However, the feed concentration is important in reverse osmosis, as the required counterpressure depends greatly upon the salt content of the raw water.

The most developed process in category (b) is electrodialysis, and work has been done with ion exchange. The economics of these processes depends closely on the salt content of the raw water, which determines the amount of electric power required, or the consumption of chemicals needed

Table I Classification of Main Desalination Processes

Processes that Separate

Water from Solution	Salts from Solution

---

1. Distillation

    Vertical tube evaporator
    Horizontal tube evaporator
    Multi-stage flash evaporator
    Vapor compression
    Solar evaporation

1. Ionic processes

    Ion exchange
    Electrodialysis
    Transport depletion
    Osmionic
    Piezodialysis
    Electrochemical
    Biological Systems

2. Reverse osmosis

2. Other processes

    Liquid-liquid extraction

3. Crystallization

    Freezing
    Hydrate formation

---

for the regeneration of the resins. Hence, these processes are more suitable for the purification of brackish waters.

Table II shows the number and capacity of plants by process and by geographic location. (O'Shaughnessy, 1973). Multi-stage flash evaporation accounts for 65% of the total capacity of the distillation plants. Two regions which represent large centres of desalting are the islands in the Caribbean Sea, and the Middle East, including countries around the Persian Gulf.

A listing of most electrodialysis plants having a capacity of 100,000 gpd or more is given in Table III. It has also been reported that approximately 300 electrodialysis plants have been constructed and installed in the U.S.S.R. (Lynch and Mintz, 1972).

2.2. Some Economic Aspects of Selective and State-Change Processes

Selective processes such as electrodialysis achieve separation without a change of phase of any component in the system. Such processes have economical advantages over state-change processes such as distillation and freezing.

The methods of separation that rely on a change of state involve a high rate of energy circulation in the system, because the heat of fusion or vaporization of the solvent must be supplied. In general, this energy is many times larger than the energy theoretically needed to separate the salt from the solvent; and the energy required for vaporization or fusion must be recovered and reused to make such processes practical. The losses and inefficiencies in any system tend to be proportional to the energy

Table II Total number and capacity of desalting plants exceeding 25000 gpd (95 m^3/day)*
P = plants number; a = data in 1000 m^3/day; b = data in Mgd.

Geographic Location	Total distillation plants			Electrodialysis			Reverse Osmosis			Freezing Processes			Total desalination plant capacity			
	P	a	b	P	a	b	P	a	b	P	a	b	P	a	b	%
United States ...	281	161.7	42.7	15	21.6	5.7	24	9.1	2.4	1	0.3	0.1	321	192.7	50.9	14.63
U.S. Territories	16	47.8	12.6							1	0.3	0.1	17	48.1	12.7	3.65
N. America except U.S.	13	32.5	8.6				1	1.1	0.3				14	33.6	8.9	2.56
South America ...	24	18.5	4.9	2	1.9	0.5				1	0.4	0.1	27	20.8	5.5	1.58
Caribbean Islands	37	99.2	26.2	1	0.1	0.1	1	1.1	0.3				39	100.4	26.6	7.65
Europe Continental ...	102	174.9	46.3	12	16.3	4.3	2	0.2	0.1	1	0.4	0.1	117	191.8	50.8	14.60
England and Ireland	63	59.8	15.8	1	0.1	0							64	59.9	15.8	4.54
U.S.S.R.	12	111.7	29.5	1	0.1	0							13	111.8	29.5	8.48
Asia	29	21.2	5.5				4	3.4	0.9				33	24.6	6.4	1.84
Middle East and Persian Gulf ..	77	405.0	107.0	18	8.7	2.3	1	0.1	0				96	413.8	109.3	31.41
Africa	55	92.8	24.5	10	22.0	5.8							65	114.8	30.3	8.71
Australia	5	4.5	1.2	1	0.1	0							6	4.6	1.2	0.34
Total Plants	714			61			33			4			812			
Total Mgd			324.8			18.7			4.0			0.4			347.9	
Total 1000 m^3/day		1229.7			70.8			15.0			1.4			1316.9		
Plants %	87.93			7.51			4.06			0.49			100.0			
Capacity %			93.36			5.38			1.15			0.11			100.0	100.0

* From O'Shaughnessy, F. "Desalting Plant Inventory Rept. No. 4 (1973), ed. by the U.S. Office of Saline Water."

Table III Large Electrodialysis Plants – Over 100,000 gpd*

Plant Location	Actual or Planned Year of Start-up	Feedwater Salinity ppm	Manufacturer	Capacity gpd
Brindisi, Italy	1971	2,000	Ionics	1,300,000
Buckeye, Ariz.	1962	2,200	Ionics	650,000
Pantelleria, Italy	1971	4,500	Ionics	265,000
Siesta Key, Fla.	1969	1,300	Ionics	1,500,000
Aramco, Dhahran, Saudi Arabia	1961	2,700	Ionics	115,000
Bahrain Petroleum Co., Bahrain, Persian Gulf	1964	3,150	Ionics	100,000
Anaconda Copper Co., Chile	1970	2,200	Ionics	265,000
Industrial Co., Tex.	1969	2,500	Ionics	880,000
Automobile Factory, Bari, Italy	1970	2,000	Ionics	530,000
U.S. Army N.M.	1970	3,100	Ionics	100,000
Al Saudi Co., Al Khobar, Saudi Arabia	1967	2,800	Ionics	100,000
Gillette, Wyo.	1971	2,500	Ionics	1,500,000
Port Mansfield, Tex.	1965	2,400	Ionics	265,000
Ras Gharib, Egypt	1971		Ionics	113,000
El Adem, Libya	1971		Ionics	170,000
Bahrain Hospita, Bahrain	1971		Ionics	105,000
Benghazi, Libya	Under construction	2,000	Wm. Boby Co.	5,000,000
Moshabei, Sadeh, Israel	1971	2,300	Tahal Consulting Engineers	1,250,000
Heinekens Brewery, Rotterdam, Netherlands	1968	1,100	Wm. Boby Co.	177,000
Zliten, Libya	1968	4,400	Wm. Boby Co.	105,000
Kazakstan, U.S.S.R.	Under construction		Unknown	500,000

* From Lynch and Mintz, J. Am. Water, <u>64</u>, 711 (1972)

circulation; and, to a first approximation at least, the energy needed to operate a distillation system will be a definite fraction of the heat of vaporization of the solvent and independent of the amount of solute present (Shaffer & Mintz, 1966). On the other hand, processes that are based on selective transport require energy at a rate that varies with the theoretical minimum energy (Helmholtz free energy) needed to produce a desalted and concentrated stream from a saline feed water i.e. while the salinity does not affect the practical energy requirements for a process such as distillation, it does make a great deal of difference to a process such as electrodialysis. For further discussion on theoretical and actual energy requirements for a desalting process refer to Appendix F.

The energy losses in the selective transport systems arise primarily as a result of the desire to maintain practical production rates; thus necessitates the use of substantial driving forces instead of infinitesimal forces, which would cause the processes to take place slowly and reversibly.

The net result of these considerations can best be seen by examining Figure 1, (Shaffer & Minrz, 1966) which compares the energies actually required for distillation and electrodialysis with the theoretical require- ments at various salinities and fixed blowdown and product specifications.

According to this graph distillation is more economical for de- mineralizing high-salinity waters while electrodialysis is more attractive for brackish waters up to about 10,000 ppm.

2.3. Electrodialysis

Electrodialysis is a selective transport process, in which the partial separation of the components of an ionic solution is induced by an electric current. The separation is accomplished by placing ion selective
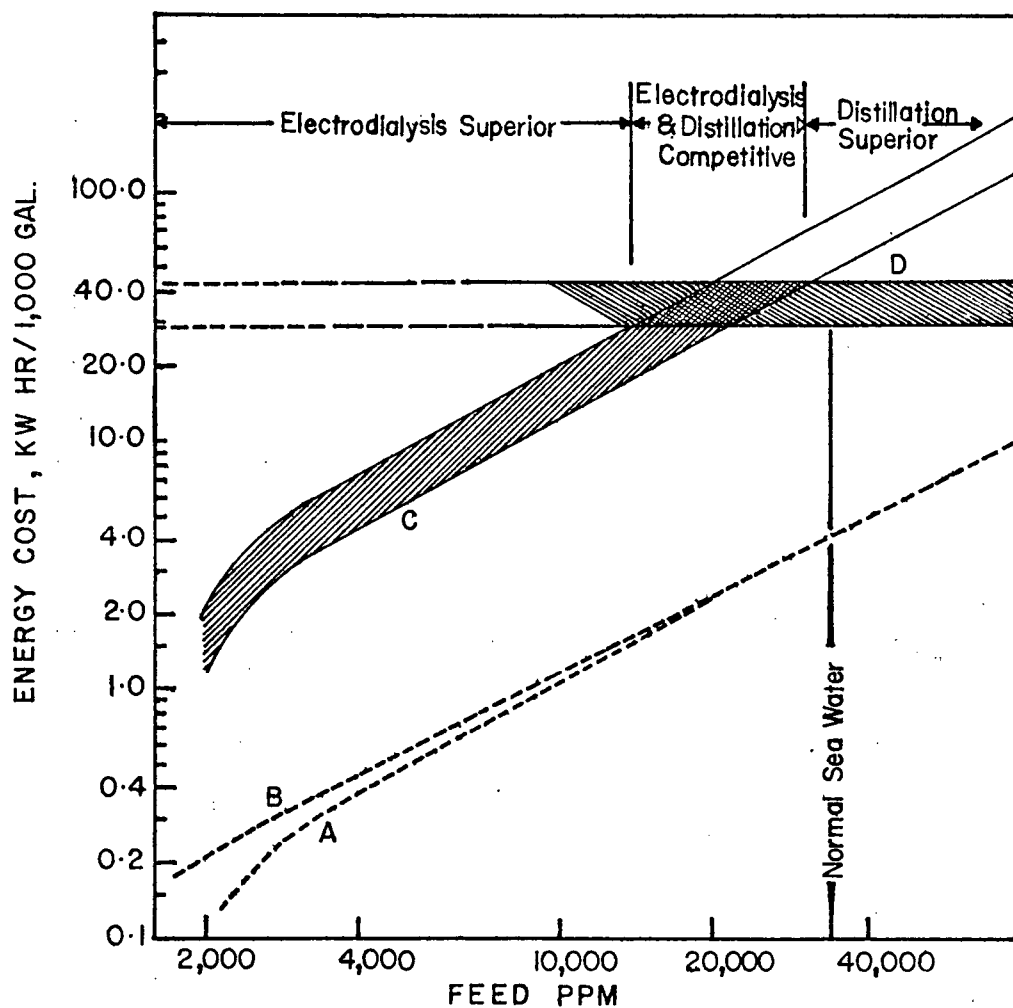
FIGURE I

Comparison of energy costs for distillation and electrodialysis of salt
water. Basis : Average equivalent weight of salt = 60 ; blowdown concentration
β = two times feed concentration ; distillation to produce pure water;
and electrodialysis to produce 0.005 -N (300 - ppm) product .
(A) Theoretical energy for electrodialysis ; (B) theoretical energy for distillation;
(C) estimated actual energy for electrodialysis , and (D) estimated
actual energy for distillation. (Spiegler , 1966) .

membranes across the path of the current flow. The process takes advantage of the ability of the membranes to discriminate between differently charged ions and the origin of separation lies in this membrane's selectivity.

If non-selective membranes that are permeable to ions (e.g. cellophane) are used in electrodialysis processes, electrolytes can be separated from non-electrolytes. On the other hand, with membranes that are more permeable to univalent ions than to multivalent ions, electrodialysis can be used to simultaneously separate and concentrate univalent ions from solutions containing mixtures of uni- and multivalent electrolytes.

Electrodialysis differs fundamentally from the great majority of electrochemical processes in that it does not utilize the electrode reactions. Electrodes do, of course, have to be incorporated in an electro-dialysis plant, but they serve the purely ancillary purpose of applying the EMF. They are in fact a necessary evil, since they involve a great deal of extra complication in the design and operation of the plant.

A pioneer book on electrodialysis, edited by Wilson (1960), describes the process and the use of ion exchange membranes in water desalting. Chapters in books by Tuwiner (1962), Spiegler (1962, 1966 a), Sporn (1966), Popkin (1968) and Kuhn (1971) also describe electrodialysis mainly as a desalination process. Lacey and Loeb (1972) consider various applications of the process such as concentration of electrolytes in dilute solutions, processing of cheese whey and recovery of constituents from pulping liquors. Recently Hwang and Kammermeyer (1975) have reviewed the process.

The electrodialysis process uses cells consisting of many (at least three) compartments formed alternatively by an anion exchange membrane and a cation exchange membrane placed between an anode and a cathode as shown in Figure 2.
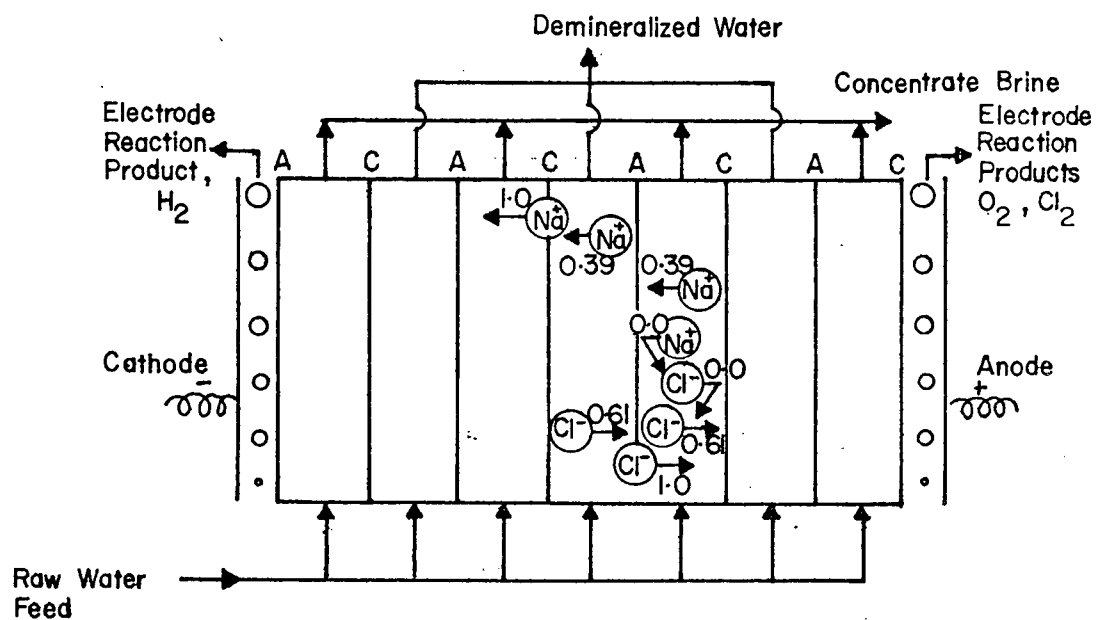
FIGURE 2
Multiple-chamber alternate-membrane electrodialysis.cell.
A,the anion-selective membrane; C,the cation-selective
membrane. Transport numbers are shown above or below
arrows.

The saline water feed is pumped through the compartments of the membrane stack and, when a direct current potential is applied, cations migrate toward the cathode and anions migrate toward the anode. Cations pass easily through the cation-permeable membrane and are blocked from further transfer by the anion-permeable membrane. Similarly, anions have free passage through the anion-permeable membrane and are stopped at the cation permeable membrane. As a result the adjacent cells become alternately diluting and concentrating compartments.

2.3.1. Electrodialysis Stack

The essential elements of a membrane stack are:

(a) a large number of ion-permeable membranes arranged in the correct order.

(b) gaskets and spacers to provide sealing between compartments and to maintain proper distances between membranes.

(c) manifold systems to direct feed, product and waste streams into and out of the compartments without leakage.

(d) electrodes and conductors.

(e) a pair of strong presses to hold the above-mentioned parts in place.

The multicell electrodialysis stacks are normally assembled in the same fashion as a plate-and-frame filter press (Figure 3).

In addition to the stack, which is the actual part that effects the desalination, electrodialysis plants consist of:

I Hydraulic equipment and auxilaries such as pipes, pumps, valves, filters, raw water supply, concentrate disposal.

Demineralized solution

Concentrating solution

Electrode _ Rinse solution

Feed Solution

1 Electrode

2 Cation_ Exchange Membrane

3

4 Anion_ Exchange Membrane

5 Many More Membranes, Spacer Frames, And Another End Frame
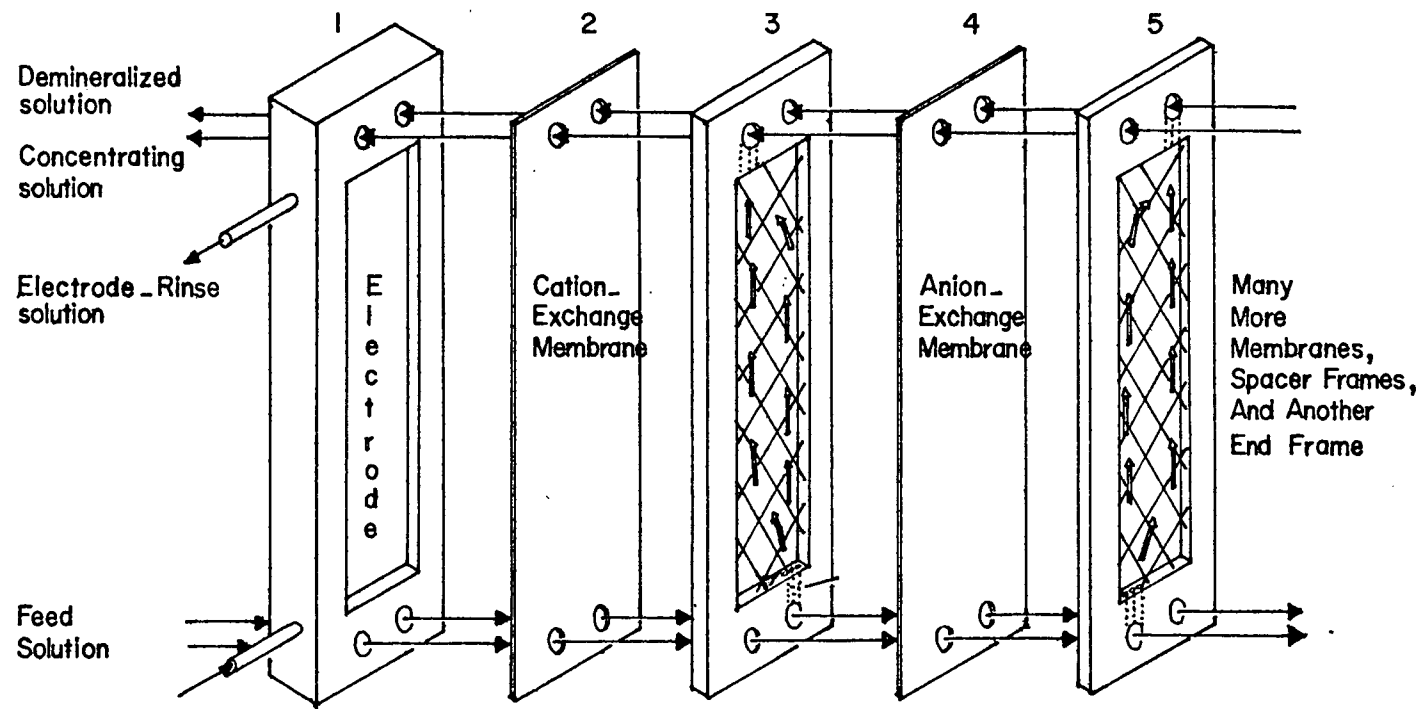
FIGURE 3

Exploded view of components in an electromembrane stack.

II A power supply with transformers and rectifiers and associated

electrical and control instrumentation.

2.3.2. Stack Size and Capacity

(i) Cell size

Electrodialysis cell dimensions are limited only by the availability

of suitably sized membrane sheets and the practicability of handling the

gaskets and membrane materials. Weiner and co-workers at the University of

California have developed a 10-foot-long stack to study polarization effects

(Weiner, et al., 1964).

In order to increase desalination and to reduce operating costs, the

area of each cell-pair should be as large as practicable. One of the size

limitations is the fact that membrane stacks need, at periodic intervals,

to be dismantled in order to remove solid deposits formed during operation.

It is necessary that the stack should be relatively small in order to be

conveniently handled. In addition, large size membranes which are generally

mechanically weak, tend to tear and break more readily during handling.

The practice today is to limit the unit surface area to a maximum of

about $2m^2$ (2 by 1 meter), and to design the stacks to comprise a number of

relatively small sub-units to facilitate handling. The largest cell in

commercial use up to 1974 was 150 x 50 cm.

(ii) Number of Cell Pairs

A cell pair is the repeating unit in an electrodialysis stack. It

consists of a diluting and a concentrating compartment together with a

cation- and an anion-permeable membrane.

The number of cells in a stack is mainly limited by engineering

considerations such as:

(a) the total voltage that can be safely applied,

(b) the size of the manifold that can distribute flow evenly

into each flow channel,

(c) the structural stability of the stack,

(d) the ease of assembly and repair.

Since the failure of a single membrane can impair stack performance,
the number of membranes in a stack is limited by the life or reliability of
the membranes and the anticipated frequency of other service requirements.
The requirements for staging also make it desirable in some cases to have
several small stacks rather than one large one. Usually several small
subassemblies or "packs" containing about 50 cell pairs (100 membranes) are
used. These packs are then used as the building blocks for a plant of the
required size. As many as 10 of these packs can be placed into a single
press. A single set of electrodes may be used for the entire assembly,
or several electrodes may be used to provide electrical staging.

(iii) Stack Capacity

The desired product salinity is achieved by passing the feed liquid
through several stacks in series, while desired plant throughput is
obtained by operating several electrodialysis paths in parallel.

The largest stacks in operation in 1970 handled dilute flows of
about 250,000 gal/day. For larger production parallel arrangement of these
stacks was planned, rather than scale-up of single stacks. The largest
electrodialysis desalting plant in the world is in Benghazi, Libya, con-
structed by William Boby and Company, England after 1972. It has a
production capacity of 5×10^6 gal/day as shown in Table IV. The plant has
16 parallel trains each of 2 stacks in series, each stack with a capacity of
about 310,000 gal/day.

Table IV   Technical details of Benghazi (Libya) and
           Siesta Key (Florida) Electrodialysis Plants*

	Benghazi	Siesta Key Stage 1	Stage 2
Rated output, m^3/h net	800	188	310
Waste water, % of output	8	17	
Raw water, ppm total dissolved solids	2,000	1,300	
Number of parallel trains	16	7	12
Stacks/train	2	2	
Total number of cell pairs	9,600	4,200	7,200
Total membrane area, m^2	15,000	3,900	6,700

* From Solt, Chap. 12 in Kuhn (ed.), "Industrial Electrochemical Processes"

2.4. Membrane Technology

An ion-exchange membrane is an ion exchanger in sheet form and its physical chemistry is to a large extent also the physical chemistry of ion exchange resins.

Ion exchange resins consist of two principal parts: a structural portion or a backbone (a polymer matrix) and a functional portion or an ion-active group. The synthesis of an organic ion-exchanger involves the chemical substitution of an ion-active group and a polymerization reaction. The substitution may precede the polymerization or vice-versa.

Most ion exchangers currently in large scale use are based on synthetic resins, usually polystyrene $[RO - (CH_2 - \underset{\phi}{CH})_n - OR]$ copolymerized with divinylbenzene $[C_6H_4 (CH:CH_2)_2]$ to provide the requisite amount of cross linking. The functional group may be acidic or basic with different degree of strength of acidity or basicity.

Strongly-acid (cationic) resins generally contain bound sulfonic acid groups $(-SO_2OH)$, while strongly basic resins (anionic) contain quaternary ammonium groups fixed to a polystyrene-divinylbenzene matrix (Pepper, et al., 1953).

Some ion-exchange membranes are made by mixing ion-exchange resins with a polymeric binder and casting or extruding a sheet from the mixture, while others are manufactured by methods that exactly parallel the production of ion-exchange resins - i.e. styrene and divinylbenzene are copolymerized in sheet form, and the resulting structure is then chemically treated to give the sheet ion-exchange properties. The details of methods for making ion-exchange membranes have been reviewed by Wilson (1960), Friedlander and

Rickles (1966), Lacey (1972), Chiolle, et al. (1973) and Laskorin, et al. (1973). An excellent summary of preparative methods found in the U.S. Patent literature is given by McDermott (1972).

An industrially useful membrane should have the following properties:

1. High ion selectivity - cation-permeable membranes should exclude the passage of anions, and vice-versa.

2. Low electrical resistance - permitting a free flow of counter-ions through the membranes at low energy requirements.

3. High mechanical strength - toughness, flexibility, and crack resistance are important, not only to the service life of the membrane, but also to construction, servicing and, therefore, the cost of electrodialysis plants.

4. High chemical stability - resists hydrolytic, oxidative, and other forms of degradation.

5. Resistance toward fouling by scale deposits and plugging by large polyvalent organic ions present in the solutions to be treated.

The properties of a number of commercially available ion-exchange membranes have been tabulated by Shaffer and Mintz (1966) and Lacey and Loeb (1972).

A bibliography on membrane technology, pertaining to saline water desalination and ranging from 1908 to 1962 has been compiled by the Office of Saline Water (Mangan, et al., 1963). A comprehensive review of the physical chemistry of ion-selective membranes has been given by Malherbe and Mandersloot (1960).

2.4.1. Membrane Selectivity

One of the basic characteristics of an ion-exchange membrane is the selectivity, which is defined as the ability of the membrane to distinguish between oppositely charged species leading to the preferential uptake of counter-ions and exclusion of co-ions. Counter-ions and co-ions are the mobile ions possessing charges opposite and similar in sign respectively to the membrane fixed ions.

When a cation-selective membrane is immersed in an electrolyte solution the cations in solution will enter into the resin matrix and replace the cations present, but anions are prevented from entering the matrix by the repulsion of the anions affixed to the resin. The opposite phenomena takes place when an anion selective membrane is immersed in an electrolyte solution; the fixed cationic groups permit intrusion and exchange of anions from an external source, but exclude cations. This type of exclusion is called Donnan exclusion.

(i) Permselectivity

Selectivity is usually reported in terms of permselectivity, P, which is the increase in transport number over the value in free solution due to the presence of the membrane and it is given by:

$$P = \frac{\bar{t} - t}{1 - t} \qquad (1)$$

where:

$\bar{t}, t$ = transport numbers of counter-ions in membrane and in free solution respectively

$(\bar{t} - t)$ = increase in transport number over the value in free solution

(1-t) = the maximum possible increase or the increase that would be

observed in the case of an ideally selective membrane.

Both p and $\bar{t}$ are functions of concentration. They decrease as the external electrolyte concentration increases as shown in Figure 4.

(ii) Donnan Exclusion

According to the Donnan principle the chemical potential of the salt in the solution external to the membrane must be equal to the chemical potential of the salt inside the membrane, i.e.

$$RT \ln a_{\pm}^2 = \bar{\nu}\Delta\rho + RT \ln \bar{a}_{\pm}^2 \qquad (2)$$

where:

$a_{\pm}$, $\bar{a}_{\pm}$ are the ionic activities in free solution and in membrane

phases respectively

$\bar{\nu}$ is the partial molar volume, cm^3/mole

$\Delta\rho$ is the difference in internal pressure between the mem-

brane and the solution phase called the "swelling pressure"

of the membrane

The pressure-volume term arises from the free energy change due to the difference between the osmotic pressure of the solutions inside and outside the membrane (Wilson, 1960). In the absence of large pressure differences between the interior and the external phase, the Donnan principle requires that:

$$(a_+)^{\nu+} \cdot (a_-)^{\nu-} = (\bar{a}_+)^{\nu+} \cdot (\bar{a}_-)^{\nu-} \qquad (3)$$

where:
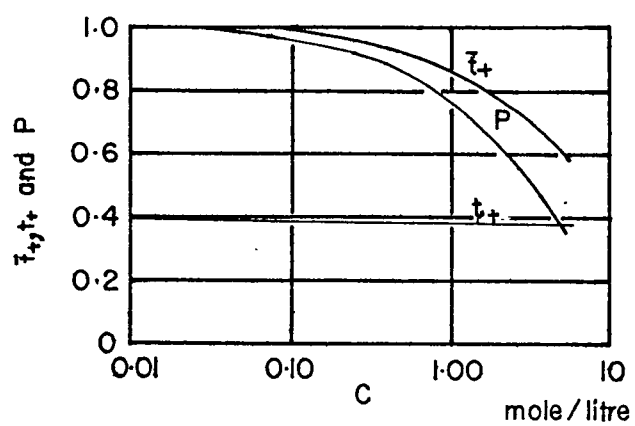
FIGURE 4
Dependence of counterion transport
numbers and permselectivity upon external
concentration. (Wilson, 1960).

$a_{\pm}$ are the ionic activities

ν's are the stoichiometric coefficients for electrolyte $M_{\nu+}X_{\nu-}$

and the barred symbols refer to the membrane phase.

For uni-univalent electrolyte, $\nu+ = \nu- = 1.0$, and Eq.(3) reduces to:

$$\gamma_{\pm}^{2} \, C_{k} \, C_{j} \;=\; \bar{\gamma}_{\pm}^{-2} \, \bar{C}_{k} \, \bar{C}_{j} \tag{4}$$

where $\gamma_{\pm}$ is the mean ionic activity coefficient, defined generally as

$$\gamma_{\pm}^{\nu} \;=\; \gamma_{+}^{\nu+} \cdot \gamma_{-}^{\nu-} \tag{5}$$

where $\nu = \nu^{+} + \nu-$; subscripts j and k refer to co-ion and counter-ion respectively.

Since both the solution and the membrane must be electrically neutral, this requires that:

In membrane; $\quad \bar{C}_{k} = \bar{C}_{j} + \bar{C}_{x}$ $\tag{6}$

In solution; $\quad C_{k} = C_{j} = C$ $\tag{7}$

where $\bar{C}_{x}$ is the fixed ion concentration in the membrane.

Substitute Eqs.(6) and (7) into (4) and replace activities by concentrations:

$$C_{j} \, C_{k} \;=\; \bar{C}_{j} \, (\bar{C}_{j} + \bar{C}_{x}) \tag{8}$$

Assume $\quad \bar{C}_{j} + \bar{C}_{x} = \bar{C}_{x}$ then

$$\bar{C}_{j} \;=\; \frac{C^{2}}{\bar{C}_{x}} \tag{9}$$

Eq.(9) shows how the selectivity of a membrane is affected in opposite directions by the external salt concentration, C, and the fixed-ions concentration in the membrane, $\bar{C}_{x}$. The higher the concentration of fixed ions, the greater the selectivity ($\bar{C}_{j} \to 0$ as $\bar{C}_{x} \to \infty$) while ($\bar{C}_{j} \to C$ as $C \to \bar{C}_{x}$).

In a typical electrodialysis system, the concentration outside the membrane may range from 0.001 to 0.1 m, while it is usually possible to make the molality inside the membrane fall in the range 1 to 5 m. According ingly Eq.(9) guarantees that $2 \times 10^{-7} \leqslant \bar{C}_j \leqslant 10^{-2}$ (Shaffer and Mintz, 1966). From Eq.(9) it is clear that the current carried by some ions in the system can be made very small. In the extreme case of ideally selective membrane the co-ions are completely excluded and the whole current is carried by the counter-ions alone through the membrane.

Figure 5a shows a negative membrane (cation-exchanger) in sodium chloride solution and it illustrates the basic operating principle involved in all electrodialysis processes i.e. on the left side the electric current carries sodium ions to the membrane at the rate $t + i/F$ and these ions disappear across the membrane at the rate $\bar{t} + i/F$ where F is Faradays constant and i is the current density. The net result of the passage of 1 Faraday is the removal of $\bar{t}_+ - t_+ = 0.6$ mole of salt from the solution immediately adjacent to the lefthand face of the membrane and the appearance of a like quantity ($t_- - \bar{t}_- = 0.6$) in the solution adjacent to the righthand face. (For sodium chloride, $t_+ \simeq 0.4$ and $t_- \simeq 0.6$).

2.4.2. Membrane Polarization

Concentration polarization at the surfaces of the ion-exchange membranes limits the current density and the production rate in an electrodialysis unit. Polarization is a natural result of the separation mechanism and it increases as the selectivity of the membrane increases; there is no way to prevent concentration polarization other than by stopping the current flow. Due to the differences in the transport numbers of ions in the solutions and in the ion-exchange membranes two boundary layers with
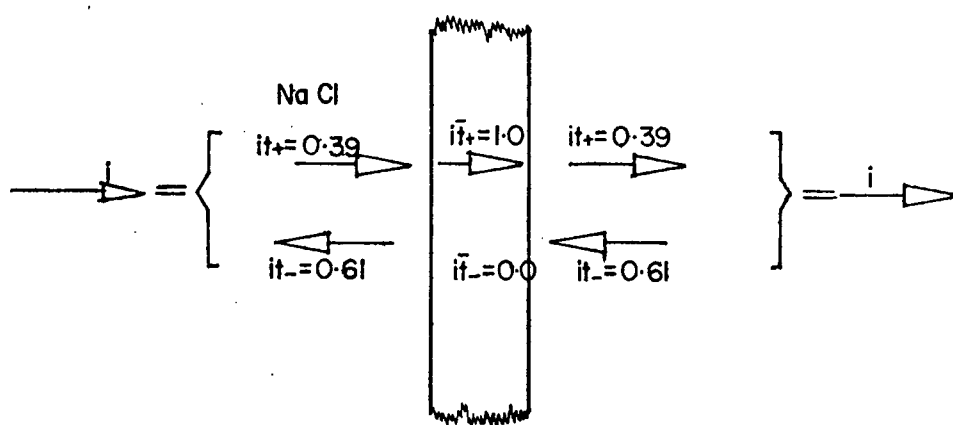
FIGURE 5a
Ion transport across a permselective membrane,
showing current i and transport number t.
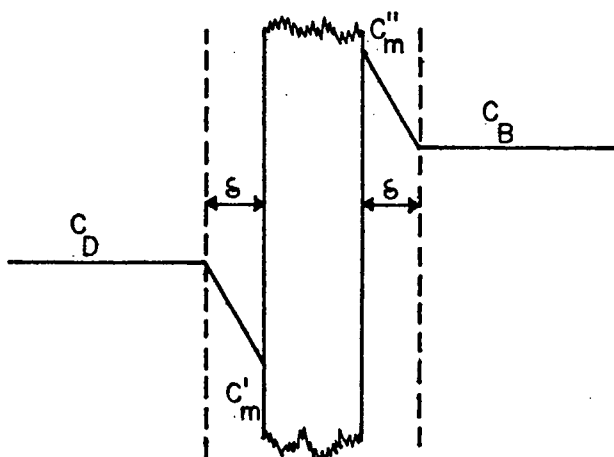
FIGURE 5b
Concentration profile across a permselective membrane
in an electrodialysis stack.

opposite concentration gradients are formed at the opposite sides of each membrane (Figure 5b).

In a well-stirred system the film model (Nernst layer model) can be adopted and the concentration gradient on the dilute side approximated by $\frac{C_D - C_m'}{\delta}$ where

C_D, C_m' are the concentration of the bulk solution and the concentration at the membrane surface respectively

δ is the Nernst film thickness

In a steady state operation, the rate of arrival of salt at the membrane-solution interface must equal the rate of removal of salt i.e. at a cation-permeable membrane we have:

$$\frac{\bar{t}_+ - t_+}{zF} \, i \; = \; D \, \frac{\Delta C}{\delta} \tag{10}$$

where D = lateral diffusion coefficient across boundary layer

$\Delta C = C_D - C_m'$

z = valence

In the limiting case when $C_m' \to 0$, $\Delta C \to C_D$; the corresponding limiting current density, i_{lim}, is given by

$$i_{lim} \; = \; \frac{zFDC_D}{\bar{t}_+ - t_+} \, \frac{1}{\delta} \tag{11}$$

Polarization is a result of mass transfer limitations adjacent to the membrane-solution interfaces. It occurs when ion depletion by electro-dialysis exceeds the rate of ion diffusion into the boundary layer from the bulk solution, and it becomes appreciable when the bulk solution concentration C_D, is low and the diffusion layer is thick so that the concentration gradient is low.

(i) Consequences of Polarization

In practice a considerably lower current density than i_{lim} is used.

As C'_m approaches zero the resistance increases and efficiency drops

tremendously. The concentration of H^+ and OH^- ions in an aqueous solution

is about 10^{-7} mole/liter, and the mobilities of these ions are 3 to 5 times

greater than the mobilities of the other common ions. As soon as C'_m

approaches 5×10^{-6} mole/liter, an appreciable amount of current will be

carried by hydrogen and hydroxyl ions. This results in the following

effects:

(1) An enormous increase in the power consumption due to:

(a) More current flowing per unit of salt removed e.g. if

$(u_{Na}+)(C) = (u_H+) \, 10^{-7}$ where u is the ionic mobility then

Na^+ and H^+ ions will transfer at equal rates. In this case

even an ideal membrane would function with an effective

current efficiency, η_I, of only 50 per cent, because H^+

transfer does not contribute to desalting.

(b) More energy dissipation in the boundary layer resulting

from the poor conductivity of nearly pure water ($k_{H_2O} =$

4×10^{-8} ohm^{-1} cm^{-1}).

(c) The energy required to ionize the water molecules

(dissociation energy of water splitting).

(d) An increase of the back emf's due to polarization layers.

(2) Deviation from neutrality in the polarized layer or the

alteration of the pH's of the process streams. Acidity can develop on the

cathode side of cation-permeable membrane and alkalinity on the anode side

of anion-permeable membrane. As most brackish waters are nearly saturated

with scale-forming materials, any transfer of H^+ or OH^- into or out of a

local region will generally cause serious scale and precipitation problems

e.g. $Mg(OH)_2$ precipitation may be expected at pH > 10 (i.e. $C_{OH^-} \simeq 10^{-4}$).

(3) Polarization changes the electrochemical properties of the mem-

branes and may result in membrane deterioration if they are not stable to

wide pH variation. (Wilson, 1960). Anion-permeable membranes are most

affected by this.

In practice, polarization is held to reasonable values by controlling

the ratio of current density to the normality of the dilute stream, i/C_D,

and by designing the system to make δ as small as possible. It should be

noted that the polarization limitation rather than the results of economic

optimization generally controls the operating current density in practical

electrodialysis installations.

In any practical apparatus, the picture is far more complex than this.

Where there are cells fed in parallel from a manifold, it is impossible to

have exactly the same liquid velocity in each cell. Cooke (1967) and Solt

(1967) have drawn attention to the fact that, even within an individual

cell in the most ideal situation, the local conditions of mass transfer are

not uniform over the whole area through which current is passing.

(ii) <u>Polarization Control</u>

Polarization can not be avoided completely, but it can be held to

reasonable values by controlling the ratio of current density to the

normality of the dilute stream, i/C_D and by making the thickness of the

diffusion layer, δ, as small as possible.

There is little that can be done about the bulk concentration when the

diluted stream is the required product. However, δ can be reduced by high

solution flow velocity and the introduction of turbulence promoters such as spacers or screens that cause local eddying or turbulence (Hoek, 1956). Both of these measures add to the power consumed in circulating the process fluids, but they reduce the stack power consumption and allow operation at higher current densities with an acceptable level of polarization.

An alternative method of reducing polarization was reported by Spiegler (1963) who reversed the current for a fraction of a second after each several seconds of operation. Partial confirmation of the efficacy of this technique was obtained in the Webster, South Dakota, demonstrative plant (OSW, 1964 a).

2.4.3. Scaling and Fouling of Membranes

Concentration polarization is often linked with other problems in practice such as membranes scaling and fouling. An increase in the pH of the solution due to polarization promotes the formation of alkaline precipitates, such as calcium carbonate and magnesium hydroxide on the membrane surface. On the dilute-stream side of the anion-permeable membrane the depletion of the more mobile anions encourages the deposition of large polyanions onto the membrane surface. Polyanions commonly found in brackish waters are humic acids, silic acids, phenols, proteins and polyphosphates (OSW, 1963).

Scaling of membranes causes additional electrical and flow resistance, a decrease in electrodialysis efficiency and an increase in pumping power requirements. Scale deposits can be found within the membrane gel structure, which is known as fouling and results in rapid embrittlement and physical deterioration of membranes.

Several methods have been attempted to control membrane scaling and fouling and can be summarized in the following:

(i) Current Density reduction

Scale formation is particularly pronounced at high current densities. Reducing the current density may reduce scaling.

(ii) Pre-treatment for cation removal

Pre-treatment by cation-exchange requires all the feed to be passed through a cation-exchange bed, in order to remove calcium and magnesium. Cations may be partially removed by a preliminary lime or lime-soda treatment followed by filteration. Such pre-treatments add considerably to operating costs and would be unjustifiable economically except for specific applications.

(iii) Acid Treatment of Concentrate

Acidification to a pH level low enough to prevent precipitation is commonly practised, but even this method may not completely prevent scale formation at the surfaces of or within the membranes. The addition of sulphuric acid to keep pH below 5.0 for prevention of $Ca\ CO_3$ scaling was reported by Watanabe, et al. (1972) and Asawa, et al. (1973).

Although acidification adds to the direct cost of desalting, the added cost was considered to be partly offset by savings in energy consumption due to a lower overall electrical resistance. (Furukawa, 1968).

(iv) Reversed Polarity

Periodic reversal of electrode polarity has been proposed to dissolve scale and control membrane fouling (Matz, 1965).

Wherever the membranes were suspected of producing a sieve or filtering effect, rather than acting as a pure ion-transfer medium, current reversal was practiced on a periodic basis to discharge electrochemically entrapped colloids and/or macromolecules so as to restore the original

membrane properties. Although the effectiveness of this procedure depends on the type of membrane and the nature of the contaminants that foul it, the reversal of hydrogen and hydroxyl ion transfer and the accompanying interchange of pH effects at the membrane surface is probably the significant defouling factor.

(v) Pulsating Current

Pulsating current is sometimes used when reversed polarity is not able to prevent rapid accumulation of scale. In this method very brief pulses of reverse current are applied to produce current reversal or current interruption (Matz, et al., 1962). This technique tends to alleviate scaling problems and also apparently improves the efficiency of an operating electrodialysis stack (Israel, 1961).

2.5. Process Efficiency

2.5.1. Principal Energy Sinks

The actual energy required to operate an electrodialysis process exceeds that theoretically required for the following reasons:

(i) Power losses attributable to resistance i.e. the power that will be dissipated by the Joule heating of the membranes and the electrolyte solution.

(ii) Power losses attributable to concentration polarization i.e. the power required to overcome the overpotentials that exist at the membrane-solution interfaces.

(iii) Power losses attributable to electrode reaction and the IR drop in the rinse solution streams in the electrodes compartments.

(iv) Low current efficiency.

The overall efficiency of an electrodialysis stack, η, can be expressed as a product of four principal efficiencies:

(a) Three voltage terms: η_R associated with the total resistance, η_c associated with the concentration polarization effects and η_e associated with the electrode reactions.

(b) The current efficiency, η_I

i.e. $$\eta = \eta_R \, \eta_c \, \eta_e \, \eta_I \tag{12}$$

where η_e is primarily a function of the stack design (e.g. number of cell pairs), η_c depends mainly on the operating conditions (e.g. current density), while η_R depends on both design factors such as cell spacing, membrane type and thickness and on operating conditions.

(a) <u>Voltage Terms</u>

The major inefficiency in stack operation is associated with the first and second terms in Eq.(12), $\eta_R \eta_c$. These terms are considered in Chapter 3.

In multiple-membrane stacks used in electrodialysis, the energy consumed in electrode processes, η_e, does not contribute to the desired separation and hence the relative effect of this energy consumption can be reduced considerably by increasing the number of membrane cell pairs used in series with a given pair of electrodes. The electrode reactions and the polarization effects are considered briefly in Appendix A.

The total external voltage, E_T, that is needed to operate a practical electrodialysis stack is the sum of 3 principal potential drops:

$$E_T = E_e + E_R + E_c \tag{13}$$

where

E_e = potential drops associated with the electrodes and electrode

streams (including electrode potential and overpotentials)

E_R = the IR drops in the solutions and membranes

E_c = concentration potential across the membranes and at the membrane-solution interfaces.

A voltage efficiency term associated with the electrode reactions, η_e, can be defined for the stack as a whole by

$$\eta_e = 1 - \frac{E_e}{E_T} = \frac{E_c + E_R}{E_T} = \sum_j \frac{(e_R + e_c)_j}{E_T} \tag{14}$$

where e_R, e_c are defined in a same way as E_R and E_c but they refer to one cell pair instead of the whole stack. A cell pair consists of two membranes and their two associated solution passages.

From Eq.(14), it is obvious that whatever the individual values of e_R and e_c for the design selected, η_e will approach 1.0 as the number of cell pairs, j, is increased.

Usually the energy consumed at an electrode is of the same order as that consumed by one cell pair. Belfort, et al. (1968) showed in their studies of two electrodialysis plants: Webster, South Dakota and Buckeye, Ariz. that the electrode polarization is a minor factor, making up less than half per cent of the total potential drop.

(b) Current Efficiency, η_I

In any practical electrodialysis system, it is generally found that the amount of current required to produce a given amount of desalting exceeds the theoretical amount calculated on the basis of current flow through ideal membranes.

The current efficiency, η_I, is defined as

$$\eta_I = \eta_F \eta_W \qquad (15)$$

where η_F is the Faraday efficiency, which is defined as the ratio of the salt transferred to the theoretical current requirement

$$\eta_F = \frac{(\text{equivalent of salt transported})}{(\text{Faraday of electricity passed})(\text{number of membrane pairs employed})} \qquad (16)$$

η_W is the result of water transport through the membranes. When the feed is of low salinity, as with brackish water, the effect of water transfer is usually small and the water transfer term, η_W, can be assumed to be unity.

A more detailed discussion of the current efficiency is considered in Appendix B.

2.6. Variants of Electrodialysis

Several variants of the electrodialysis process have been developed to overcome some of the problems that have been encountered with conventional electrodialysis. For instance, the anion-selective membranes used in conventional systems are particularly troublesome because of vulnerability to fouling and scaling, so attempts have been made to replace them by either neutral (nonselective) membranes (in transport depletion) or by cation-exchange membranes (in electrogravitational demineralization).

2.6.1. Transport Depletion

The transport depletion process is a variant of electrodialysis in which an array of alternate cation exchange and nonselective membranes is used as shown in Figure 6. This concept was first suggested by Deming and
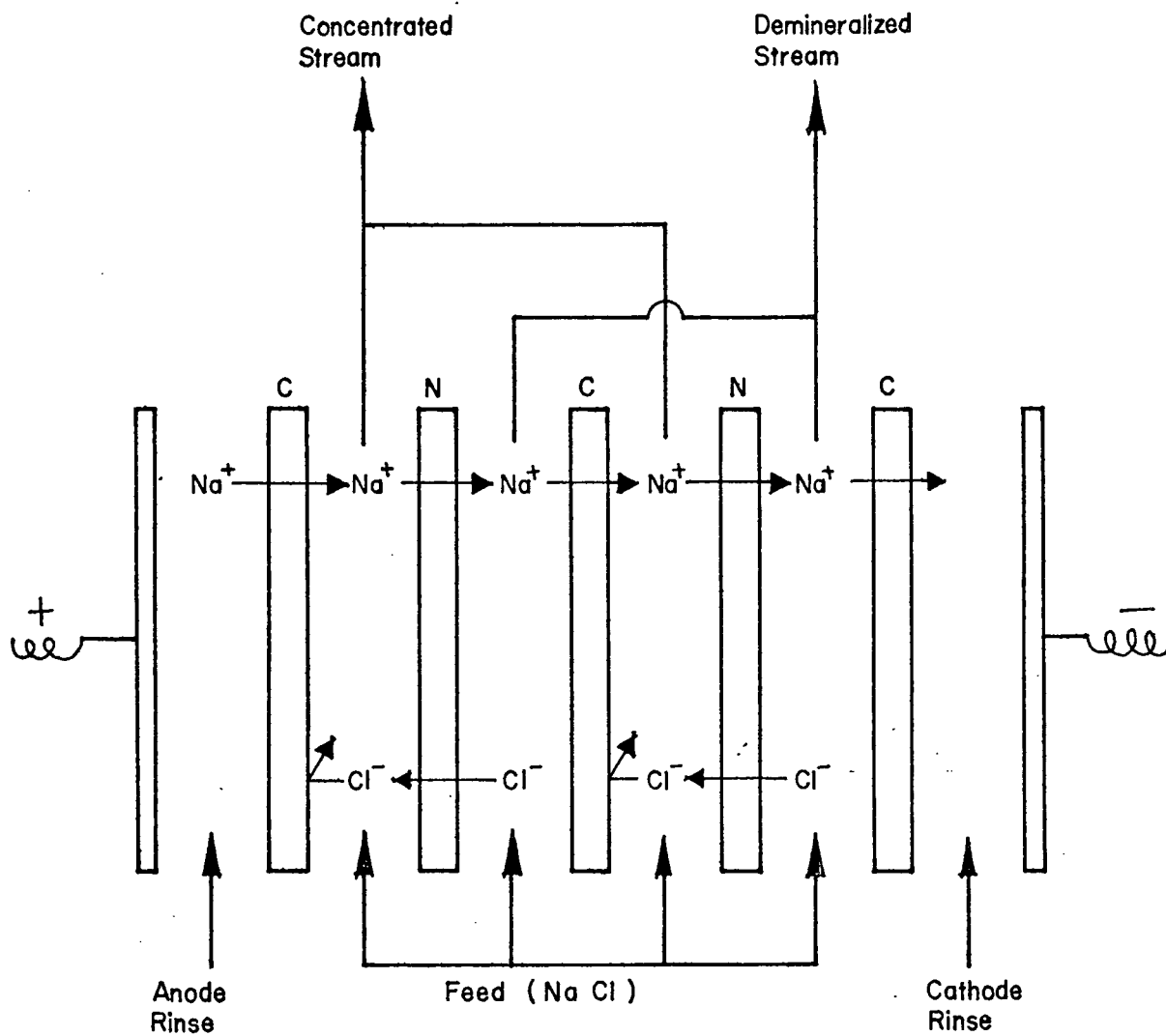
FIGURE 6
The cation-neutral transport depletion process;
C, cation-selective membrane
N, neutral membrane.

Kollsman (1959) and developed by Lacey (1963).

When direct electric current is passed, depleted and concentrated boundary layers form at the two sides of the cation exchange membranes, but not at the nonselective neutral membranes. The latter serve only to separate the depleted and concentrated boundary layers from each other and, in doing so, create alternate diluting and concentrating compartments. Neutral membranes have little tendency to polarize or foul, thus their use trades off the chemical and mechanical disadvantages of anion-exchange membranes for higher power costs, e.g. for solutions of K Cl ($t_+ = 0.5 = t_-$), passage of one Faraday shifts 1 mole of salt from diluate to concentrate when alternating ideally selective cation- and anion-exchange membranes are used in conventional electrodialysis, while only ½ mole is shifted in transport depletion. Therefore, to achieve the same production rate in the transport depletion stacks as in the basic electrodialysis stack, twice the current is needed. The voltage is then also nearly twice, hence the power costs almost quadruple. However, by eliminating the anion membranes the capital cost drops. It appears that the power consumption is not the decisive factor in electrodialysis since the major desalination costs do not reside in the energy requirements but in the investment costs for equipment or the replacement costs for the membranes (Shaffer and Mintz, 1966).

The economics of the transport depletion process have been studied by Huffman (1969) and Redman (1971). Lacey estimated a cost reduction of 8% compared with the normal electrodialysis. The process development continues in the belief that the simplicity of the plant and its freedom from trouble in the field will out-balance the increased power cost (Solt, 1971).

2.6.2. Electrogravitational Demineralization

The term "electrogravitation" was first suggested by Murphy (1950). Electrogravitational demineralization may be achieved in a cell in which only cation exchange membranes are used, as shown in Figure 7. When a direct electric current is passed depleted and concentrated boundary layers form at each side of the membrane, but the solution in the depleted boundary layer rises and collects at the top of the depleted compartment because its density is lower than that of the bulk of the solution. Similarly the solution in the concentrated boundary layer slides downward and collects at the bottom of the enriched compartment. Additional density differences are obtained because the depleted solution has higher electrical resistance than the bulk, and gets hotter.

The process is extremely simple to construct and operate. The membranes may be placed loosely or simply hung in a tank fitted with electrodes; edge seals on the compartments are not necessary; imperfections in the membranes, even holes, will not seriously affect performance. Current leakage through holes or around edges may waste power, but will not interfere with the operation of the system.

Very high concentration gradients can be achieved in the process. Mintz and Lang (1965) have shown that concentration gradients of greater than 100 to 1 can be obtained in cells only 6 in. high. Studies by Lang and Huffman (1969) showed that electrogravitation is not competetive with other processes for demineralizing saline water but may be of interest for some industrial separations.
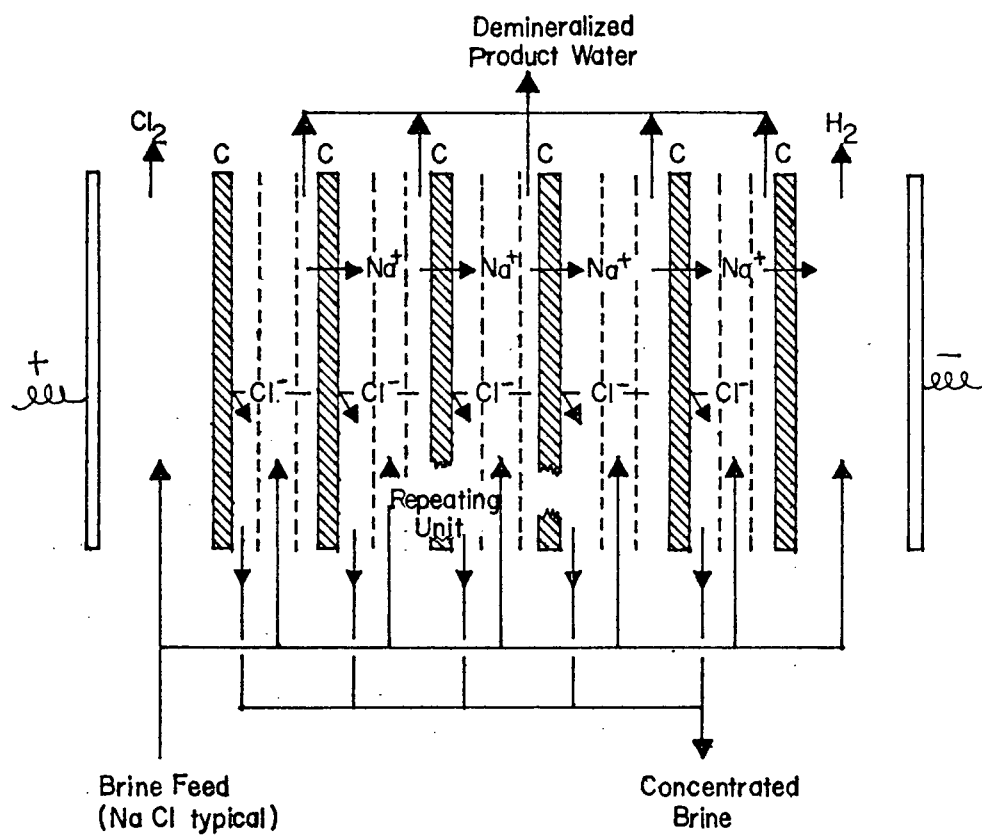
FIGURE 7

Electrogravitation with cation-selective membranes.

2.7. Cyclic Processes

2.7.1. Electrosorption

Electrosorption is a modification of electrodialysis which was first conceived by Lacey and Lang (1964, 1968). It is a one-cycle process without reflux.

An electrosorption demineralizer consists of many electrosorption membranes arranged between a pair of electrodes, so that solution compart-ments are formed between the parallel membrane surfaces as shown in Figure 8. An electrosorption membrane, which is the fundamental desalting unit, is a three-layer membrane comprising a neutral inner layer (which may be a spacer or merely solution) sandwiched between a cation- and an anion-exchange membrane. When a direct current is passed through the system cations and anions are transported (in opposite) directions from the external solution into the electrosorption membranes. The external solution is depleted while that within the membranes becomes highly concentrated. After 20-50 minutes of sorption the direction of the current is reversed and the trapped ions accumulated inside the membranes are driven back to the external solution to regenerate the membranes. The external solution is sent to waste during this step.

2.7.2. Cyclic Electrodialysis

Cyclic electrodialysis is a novel cyclic separation process, which uses periodic flow reversal applied to an electrically driven electro-sorption stack. The process has been studied and described by Bass (1972), Bass and Thompson (1973). In this process cyclic times ranging between 30 seconds and 2 minutes were used with the voltage and flow direction
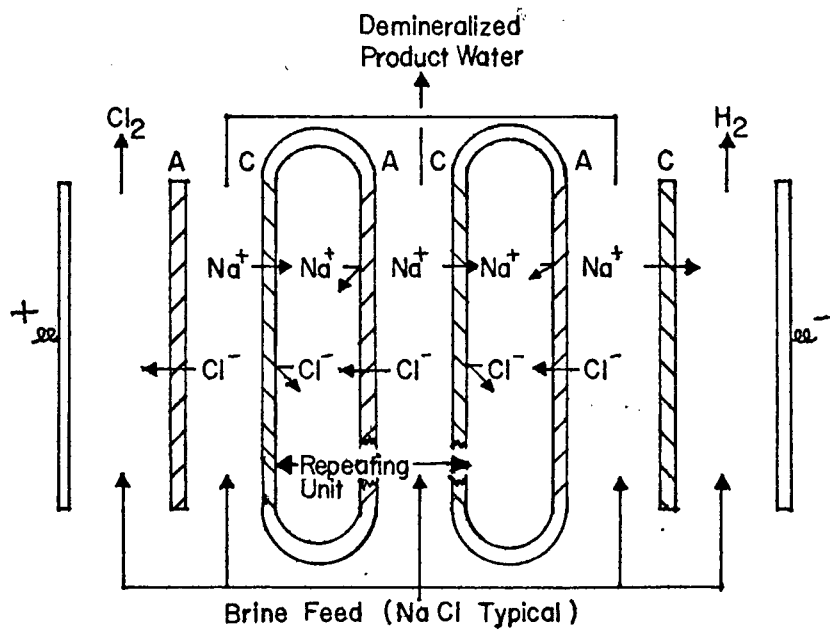
FIGURE 8

Electrosorption Process .

reversed every half cycle. A concentration difference between the ends of the apparatus is built up with repeated cycling. Separation factors of several hundreds were reported for most of the experiments with aqueous sodium chloride solutions in a closed system. The present work is an extension of cyclic electrodialysis to an open system.

Cyclic electrodialysis usually requires more electrical energy per unit of product water than conventional electrodialysis, due to the regeneration step. The cost of this additional energy must be balanced against savings in capital and operating costs resulting from:

(i) Extreme simplicity of the manifolding and distributing systems. Lower cost of the stack is possible because only one stream of solution is withdrawn at any one time.

(ii) The "sealed-envelope" or "membrane sack" character of electrosorption membranes simplifies the stack construction and results in a better membrane utilization factor. Since the membranes are not used to separate brine and dialystate flow channels, they may be as small as the active interior of the stack. A membrane utilization factor of about 95% is obtained, whereas the factor is only about 70% to 75% in conventional electrodialysis stacks (Lacey, 1968). This results in a lower membrane replacement cost and a lower stack capital cost.

(iii) With electrosorption, no pretreatment was needed to remove iron or manganese from feed waters. With feeds containing either $CaSO_4$ or $Ca(HCO_3)_2$, precipitates within membranes did form at high pH values, but these were easily and quickly removed by reversed current flow during desorption without causing any cell blockage or damage to the membranes (Lacey, 1967). It is expected that this would also be true for cyclic electrodialysis.

(iv) Increased throughputs are possible because current densities more closely approaching the limiting current density can be used without experiencing permanent damage to the membranes or stack due to precipitates.

(v) A high degree of desalination can be obtained in a single stack (Bass, 1972).

(vi) The periodic reversed polarity technique provides a repeated rejuvenation of the membranes. So far no problems with membrane deterioration have been encountered.

(vii) In cyclic electrodialysis only cheap graphite electrodes need to be used. Such electrodes proved to be satisfactory in a long-term operation.

Cyclic electrodialysis has some similarities to thermal parametric pumping. In both processes the flow of a mobile phase is periodically reversed and in both processes the origin of separation lies in the ability of the system to store solute temporarily in the fixed phase, withdrawing it from the lean end and subsequently adding it to the rich end of the processing stream.

2.7.3. Parametric Pumping

The term parametric pumping was first introduced by Wilhelm, et al. in 1966 (Wilhelm, et al., 1966 a, 1966 b). It refers to a dynamic principle of separation based on periodic synchronous coupling of two cyclic fields or two transport steps (Wilhelm and Sweed, 1968 a; Wilhelm, et al., 1968 b). Parametric pumping has been reviewed in details by Sweed (1971, 1972) and Wankat (1974).

The system of a direct thermal parametric pumping consists mainly of a jacketed column packed with an adsorbent bed as shown in Figure 9a, a constant-rate, positive displacement dual-syringe infusion-withdrawal pump, sources of hot and cold water for the jacket (not shown in the figure), and a programmed cycle timer. The timer is adjusted to reverse periodically the direction of the fluid stream; also to cycle the jacket temperature by connection to hot or cold sources. Both alterations have the same frequency (i.e. every half cycle) and are in phase.

The fluid is heated during the upward stroke and cooled during the downward stroke. The adsorbent holds more solute when the fluid is cool. Thus the solute is held by the adsorbent on the cold half cycle and released to the fluid on the hot half cycle. A multiple succession of these adsorption-desorption actions tends to cause accumulation of solute at one end of the column and depletion at the other end. Eventually, under ideal conditions, all of the solute will be "pumped" to the upper reservoir and the lower reservoir will contain no solute. In the present case the "pump" is identified as the oscillatory thermal field; the flow displacements between fluid and solid phases simply keep the system in a state of disequilibrium.

The four basic requirements for implementing the principle of para-metric pumping (according to Sabadell and Sweed, 1970) are:

1. The existence of a two-phase system.

2. An equilibrium distribution of the component being separated between the phases.

3. An alternating relative velocity between the phases.

4. An alternating interphase mass flux obtained by periodically
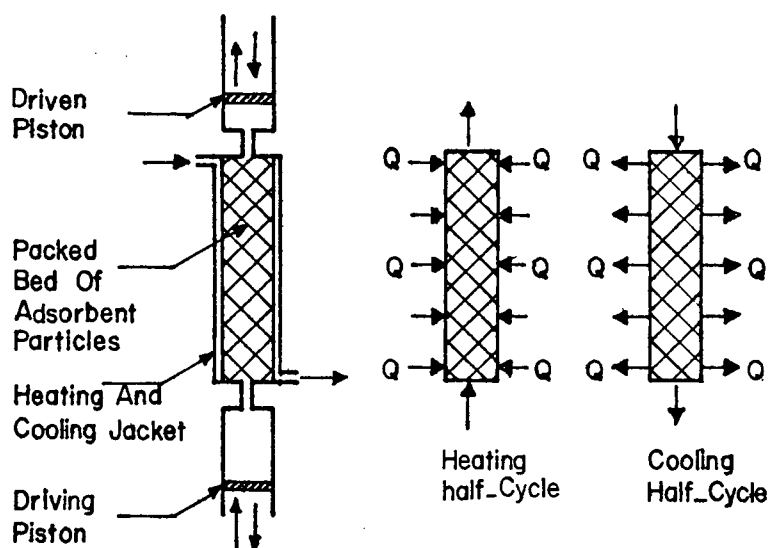
FIGURE 9a
Diagram of column for direct mode P.P. .
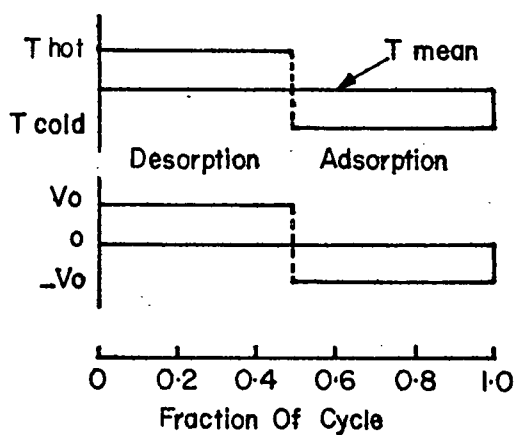
FIGURE 9b
Velocity and temperature at a point in the bed
as a function of time .

changing one or more of the intensive thermodynamic variables that affect equilibrium e.g. temperature.

Although thermal parametric pumping results in a large separation in the system toluene-n-heptane-silica gel, with a separation factor of 10^5 in batch operation (Wilhelm, et al., 1968 b) and of over 600 in an open system (Chen, et al., 1972 a), it gives only a modest separation in the system Na Cl - H_2O - ion resin with a separation factor of 10 in a closed system (Sweed and Gregory, 1971) and a separation factor of 2.0 in an open system (Wilhelm et al., 1966 a; Sweed and Gregory, 1972).

2.7.4. Cyclic electrodialysis and Parametric Pumping

Despite the prementioned similarities between cyclic electrodialysis and parametric pumping, the two processes are different with regard to the nature of the driving force and process design, limitations and applications.

In parametric pumping separation is achieved at the expense of thermal energy. By changing the temperature and reversing the fluid flow every half cycle the system is kept in a state of disequilibrium, thus molecules diffuse from one phase into another. In cyclic electrodialysis an external electric field is applied and bodily forces are exerted on the ions that are transferred from one region into another across the stack.

A parametric pumping process consists essentially of a column packed with a suitable adsorbent bed while cyclic electrodialysis stack comprises well-defined parallel flow channels between membrane sheets.

While parametric pumping operation is controlled by equilibrium considerations, electrically driven separation process such as cyclic electrodialysis is governed by finite rates of mass transfer and usually operate at concentrations far from equilibrium. The rate of mass transfer is

approximately proportional to the current flowing and is thus to some

extent under the direct control of the experimenter.

Finally cyclic electrodialysis deals only with ionic solutions

whereas parametric pumping is not limited to these solutions. However,

within the specific field of separation of ionic solutions, cyclic electro-

dialysis looks more promising since it is not constrained by the chemical

nature of the system. In parametric pumping a large separation is only

expected when the shift of equilibrium with temperature of the particular

system is large.

CHAPTER 3

System Models

3.1. Stack Resistance Models

The apparent resistance of an electrodialysis stack is determined
by multiplying the apparent resistance of one cell pair by the number of the
cell pairs and making some allowance for the electrode system.(Generally
ignoring the electrode system contribution towards the total stack resis-
tance will result in only minor error). A cell pair consists of two ion-
exchange membranes and their associated flow channels. The apparent
resistance comprises the electrical resistance of the solutions and the
membranes together with the back emf's caused by polarization. These back
emf's oppose the applied voltage and thus represent an apparent resistance.

In the development of these analyses two approaches can be dis-
tinguished which are designated as "non-ohmic" and "ohmic". The non-ohmic
analysis is an analytical approach which takes into account the variation of
the apparent resistance with current density. This approach breaks down
the total resistance into several resistive elements, evaluates the con-
tribution of each element independently and sums them to get the total
value. The ohmic analysis is an empirical approach which assumes proportion-
ality between current and voltage in the electrodialysis stack.

3.1.1. Non-ohmic Analysis

When a voltage is applied across an electrodialysis stack, the initial
current is roughly proportional to the voltage, but as the current flows

through the apparatus concentration gradients and discontinuities are established and the apparent resistance of the stack increases. Apparent resistance comprises the electrical resistances of the solutions and the membranes, and the back electromotive forces (membrane potentials and diffusion potentials) caused by concentration polarization.

Figure 10 shows schematically the concentration profiles in an electrodialysis cell pair. The cell pair contains the concentrated and depleted bulk solutions, the two membranes, and the four boundary layers in which the concentrations of salts in the solution near the membrane vary considerably. The electrical circuit in Figure 10 is an analog of the electrodialysis cell pair. The battery symbols represent the concentration potentials, and the resistor symbols represent the resistances of membranes and segments of solution. This analog can be used to develop an equation for the total potential across a cell pair.

(i) Diffusion layer resistance

The voltage from 1 to 2 in the depleted diffusion layer is the algebraic sum of the diffusion potential and the IR drop from point 1 to point 2

$$E_{1-2} \Big|_z = \frac{RT}{F} \int_1^2 (t_d^- - t_d^+) d \ln(\gamma C)_z + i \int_1^2 \rho_{x,z} dx \qquad (17)$$

where R is the gas law constant, T is the absolute temperature, F is Faraday's constant; t^-, t^+ are the transport numbers of anion and cation respectively in solution, C is the solute concentration in eq./cm^3, γ is the activity coefficient, $\rho_{x,z}$ is the resistivity of the solution at the coordinate point x,z, Ω-cm, where x is the distance from the membrane surface and z is the distance from the inlet along the flow path. The subscript d refers to the depleting solution.
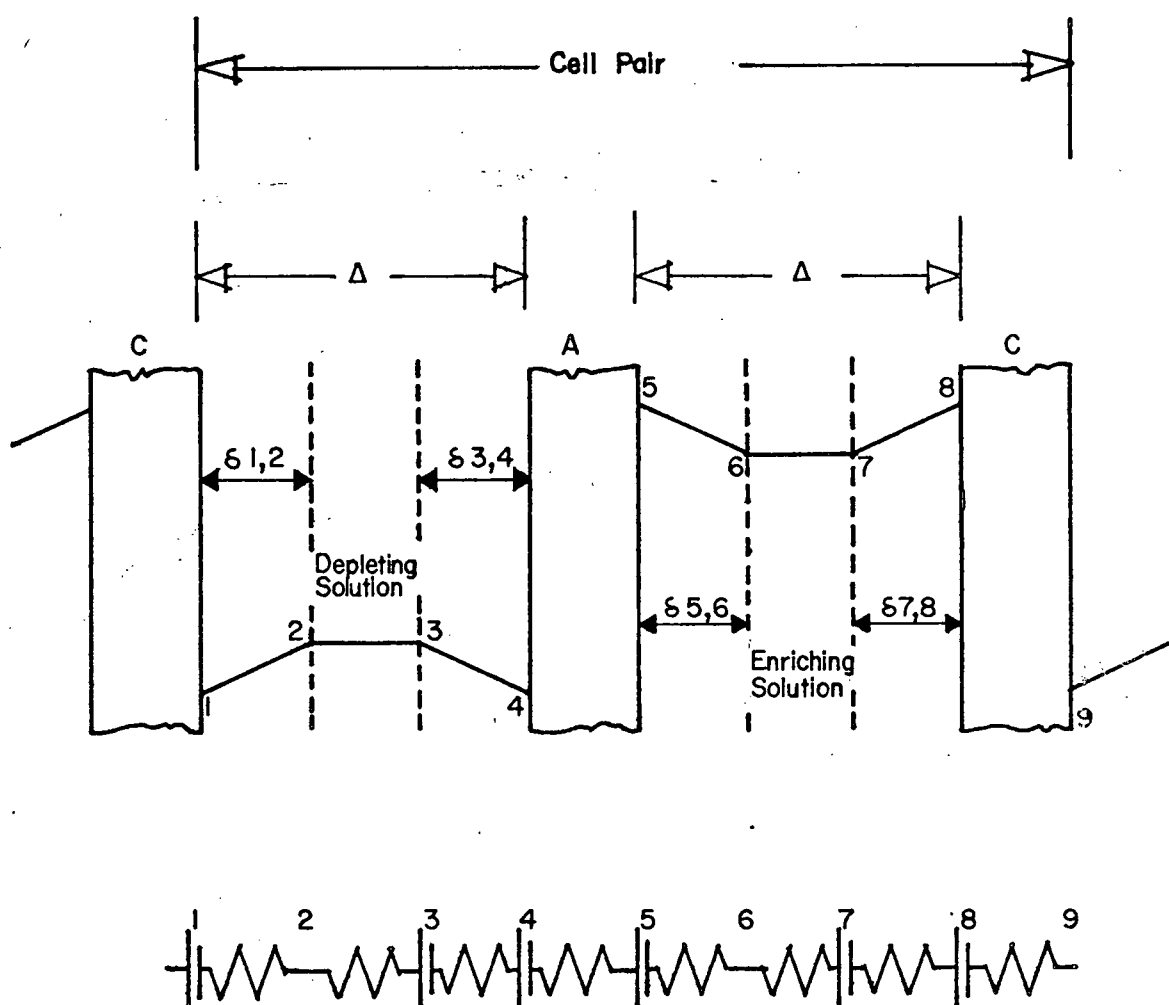
FIGURE 10

Simplified concentration profiles in an electrodialysis cell pair and the analogous electrical circuit.

The equivalent resistance of the diffusion potential (first term on R.H.S. of equation (17)) is given by

$$(R_{\phi,d})_z = \frac{RT}{Fi} (t_d^- - t_d^+) \ln \frac{(\gamma_2 C_2)_z}{(\gamma_1 C_1)_z} \tag{18}$$

Integration of Equation (18) along the flow path (z coordinate) results in (refer to Figure 11)

$$\frac{1}{R_{\phi,d}} = \frac{Fi}{m\ RT\ (t_d^- - t_d^+)} \int_{z=0}^{m} \ln \frac{(\gamma_1 C_1)_z}{(\gamma_2 C_2)_z}\ dz \tag{19}$$

where $R_{\phi,d}$ is the equivalent resistance of the diffusion potential per unit area of the depleted layer.

The diffusion layer resistance that the dialyzing current must pass through (the second term on the R.H.S. of equation (17)) is calculated by performing a double integration across the diffusion layer (x coordinate) as well as along the flow path (z coordinate) as indicated in Figure 11.

$$\frac{1}{R_{\delta,d}} = \frac{1}{m} \int_{z=0}^{m} \left[\int_{x=0}^{\delta} \rho_{x,z}\ dx \right]^{-1} dz \tag{20}$$

where $\rho_{x,z}$ is obtained from the basic definition of resistivity:

$$\rho_{x,z} = \frac{1000}{(\Lambda_v)_{t°C}\ C_{x,z}} \tag{21}$$

$(\Lambda_v)_{t°C}$ is the equivalent solution conductance at average concentration of salts and t°C. It can be evaluated from the Onsager equation at various temperatures and concentrations

$$(\Lambda_v)_{t°C} = (\Lambda_\infty)_{t°C} - [A + B\ (\Lambda_\infty)_{t°C}]C^{\frac{1}{2}} \tag{22}$$

$$(\Lambda_\infty)_{t°C} = (\Lambda_\infty)_{25°C}\ [1 + 0.023\ (t - 25)] \tag{23}$$

where
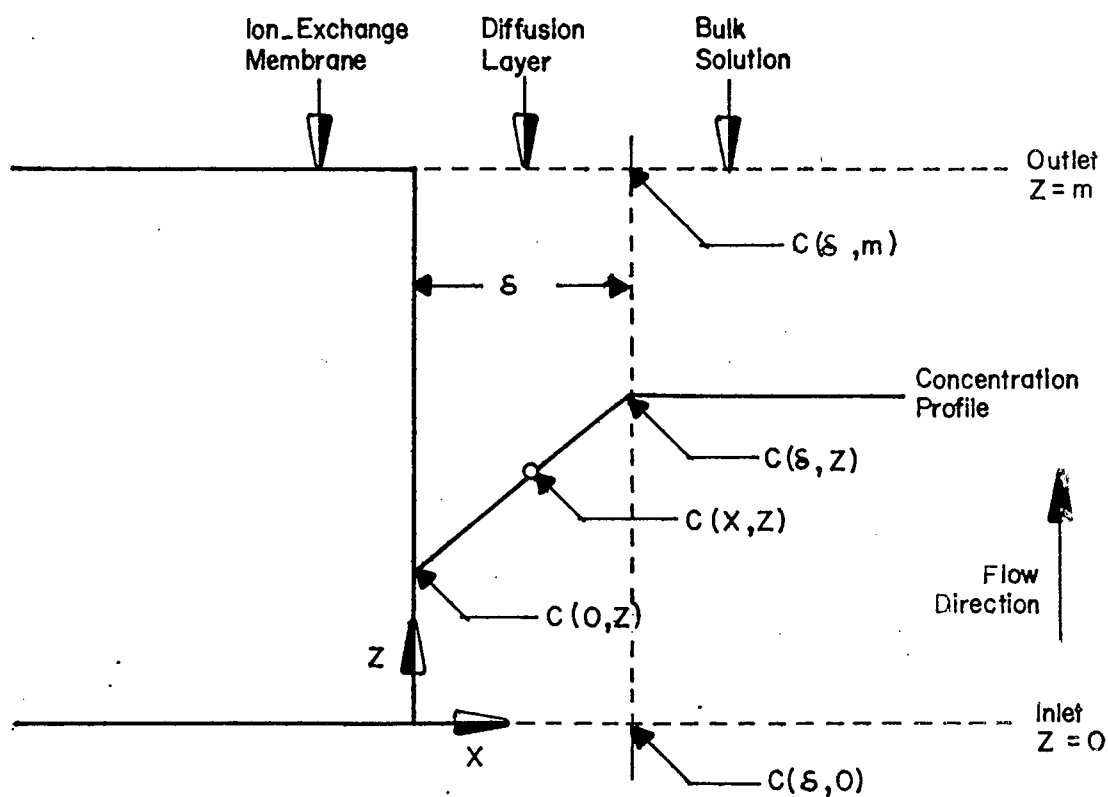
FIGURE II

Diagram of the concentration profile and the diffusion layer on the dialysate side of an electrodialysis ion exchange membrane.

$(\Lambda_\infty)_{t°C}$ is the equivalent conductance at infinite dilution and $t°C$.

After $\rho_{x,z}$ from Eqs. (21), (22) and (23) is substituted in Eq. (20), $C_{x,z}$ as a function of x and z has to be evaluated from the boundary conditions. To relate the concentration at the membrane surface $C(0,Z)$ with the diffusion layer-bulk interface concentration, $C(\delta,Z)$, the Nernst idealized equation will be used (this model is considered in Appendix C):

$$\frac{dc}{dx} = \frac{C(\delta,Z) - C(0,Z)}{\delta} \tag{24}$$

From the Nernst equation and realizing that at the limiting current density, i_{lim}, surface concentration $C(0,Z)$ approaches zero,

$$C(0,Z) = (1 - k)\, C(\delta,Z) \tag{25}$$

where k is the ratio of the operating to limiting current density i.e.

$$k = \frac{i_{oper}}{i_{lim}} \tag{26}$$

At any point (x,z) within the boundary layer $C(x,z)$ is given in terms of bulk solution concentration $C(\delta,Z)$, diffusion layer thickness, δ, and the current density ratio, k by the following relation (using equations (24) and (25)):

$$C(x,z) = C(0,z) + \frac{x[C(\delta,z) - C(0,z)]}{\delta}$$

$$= [(1-k) + \frac{kx}{\delta}]\, C(\delta,Z) \tag{27}$$

The diffusion layer thickness, δ, the limiting current density, i_{lim}, the operating current density, i_{oper}, and the bulk solution concentration, $C(\delta,Z)$ must be evaluated before equation (27) can be used.

The diffusion layer thickness

The diffusion layer thickness, δ, is obtained from Equation (11) in terms of limiting current density as:

$$\delta = \frac{C(\delta,m)\ FD}{i_{lim}\ (\bar{t} - t)} \tag{28}$$

Limiting current density, i_{lim}, will occur when the exit concentration of the dilute stream $C(0,m)$ shown in Figure 11 reaches zero. The limiting current density can be determined experimentally as shown by Rosenberg and Tirrel (1957), Cowan and Brown (1959) and Cooke (1961). Once i_{lim} is obtained, δ can be calculated.

The current density ratio, k

Using Faraday's Law and a material balance, the capacity is defined as,

$$Cap = \frac{i\ \eta\ Ap\ n}{F} = F_d\ n\ C_{di}\ f \tag{29}$$

where capacity is in g-equiv. transferred/sec., η is current efficiency, Ap is the active membrane area [i.e. area available for demineralization] (cm^2), n is the number of membrane pairs, F is Faraday No. (coulombs/g-equiv), F_d is dilute stream exit flow rate (lit/(sec)(channel)), C_{di} is dialysate inlet bulk concentration (g-equiv/lit), and f is fraction desalted.

From Eq. (29) we have

$$i_{oper} = \frac{F\ F_d\ C_{di}\ f}{\eta\ Ap}\ amps/cm^2 \tag{30}$$

From the limiting current value and Equation (30), the current density ratio, k, can be obtained.
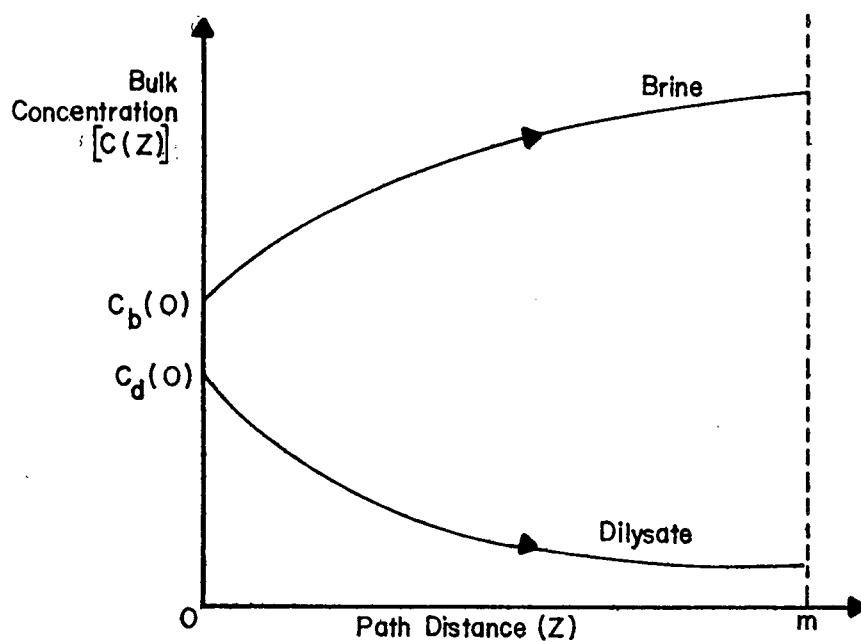
FIGURE 12 a
The concentration profiles (exponential) of both the the dialysate and brine streams.
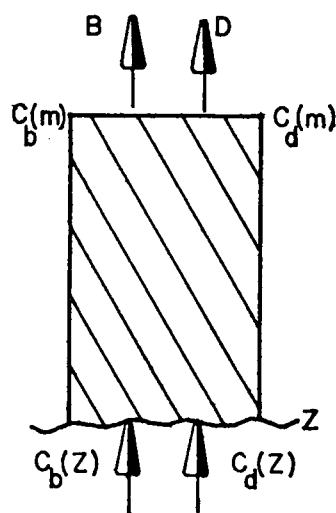
FIGURE 12 b
The material balances of both the dialysate and brine streams.

Bulk solution concentration, $C(\delta, Z)$

Based on the traditional treatment of electrodialysis the dialysate bulk stream concentration can be assumed to decay exponentially with the distance Z from the feed point as shown in Figure 12a. On evaluating each bulk solution as a function of path distance Z we get for the dialysate

$$C_d (Z) = C_d (0) e^{-\alpha Z} \tag{31}$$

and from a material balance on the salt at a distance Z along the path length and the top of the unit (at $Z = m$) we get for the brine (refer to Figure 12b):

$$C_b (Z) = [C_b(m) + (\frac{Fd}{Fb}) C_d(m)] - [(\frac{Fd}{Fb}) C_d(0)]e^{-\alpha Z} \tag{32}$$

On substituting equation (31) into (27) a general expression for the local concentration, $C(X,Z)$, can be obtained:

$$C(x,Z) = [(1-k) + \frac{kx}{\delta}] C(\delta,0) . e^{-\alpha Z} \tag{33}$$

By substituting values from equations (21), (22), (23), (25), (26), (28), (30) and (33); equations (19) and (20) can be integrated.

From equations (19) and (20) the apparent resistance per unit area of the depleted diffusion layer is given by:

$$
\begin{aligned}
R_d &= R_{\phi,d} + R_{\delta,d} \\
&= \frac{m \, RT \, (t_d^- - t_d^+)}{Fi} \left[-\int_{z=0}^{m} \ln \frac{(\gamma_1 C_1)_z}{(\gamma_2 C_2)_z} \, dz \right]^{-1} \\
&\quad + m \left[\int_{z=0}^{m} \left[\int_{x=0}^{\delta} \rho_{x,z} \, dx \right]^{-1} dz \right]^{-1}
\end{aligned} \tag{34}
$$

A combined expression for the apparent resistances of the two depleted diffusion layers is given by (refer to Figure 10)

$$
R_d = R_{\delta(1-2)} + R_{\delta(3-4)}
$$

$$
= \frac{m\,RT\,(t_d^- - t_d^+)}{Fi} \left[\int_{z=0}^{m} \ln \frac{(\gamma_1 C_1)_z}{(\gamma_4 C_4)_z}\, dz \right]^{-1}
$$

$$
+ 2m \left[\int_{z=0}^{m} \left[\int_{x=0}^{\delta} \rho_{x,z}\, dx \right]^{-1} dz \right]^{-1} \qquad (35)
$$

The combined apparent resistance of the two enriched diffusion layers can be obtained in a similar way:

$$
R_e = R_{\delta(5-6)} + R_{\delta(7-8)}
$$

$$
= \frac{m\,RT\,(t_e^- - t_e^+)}{Fi} \left[\int_{z=0}^{m} \ln \frac{(\gamma_5 C_5)_z}{(\gamma_8 C_8)_z}\, dz \right]^{-1}
$$

$$
+ 2m \left[\int_{z=0}^{m} \left[\int_{x=0}^{\delta} \bar{\rho}_{x,z}\, dx \right]^{-1} dz \right]^{-1} \qquad (36)
$$

where $\bar{\rho}_{x,z}$ is the resistivity at any point (x,z) within the enriched diffusion layer.

(ii) The bulk solution resistance

The electrical resistance of a solution-filled compartment Δ cm thick is

$$
\rho_{sol} = \frac{\Delta}{C\Lambda} \quad ohm - cm^2 \qquad (37)
$$

The resistances of the bulk depleting and enriching solutions are given by

$$R_b = R_{b,d} + R_{b,e}$$

$$= m(\Delta - 2\delta) \left\{ \left[\int_{z=0}^{m} (C_2 \Lambda_2)_z \, dz \right]^{-1} + \left[\int_{z=0}^{m} (C_6 \Lambda_6)_z \, dz \right]^{-1} \right\} \quad (38)$$

(iii) <u>The membrane resistance and potential terms</u>

The resistance of a membrane cannot be calculated by a simple method but it can be measured or obtained from the manufacturer. Although direct current is used in electromembrane processes, alternating currents are usually used to measure the electrical resistance of membranes because concentration gradients that are present with direct current systems are not formed with alternating current and the resistance of the membrane itself can be more easily determined. However, the resistance of a membrane to alternating current is usually lower than the resistance to direct current (Spiegler, 1966). If precise values are needed the resistance to direct current should be determined under conditions of membrane use.

There are concentration discontinuities at the membrane-liquid interface in an ion-exchange membrane as a result of the Donnan equilibrium. Figure 13a shows the concentration distribution in a cation exchange membrane. The concentrations of the anions and cations are equal in the outside solution but deviate from each other within the membrane. The upper line is cation concentration, C^+, and the lower line is anion concentration.

The total membrane potential, E_m, is the sum of three potential differences as shown in Figure 13b.

$$E_m = E_{d_1} + E_H + E_{d_2} \quad (39)$$

where E_{d_1}, E_{d_2} are the two potential jumps occurring at the membrane faces, which form the Donnan potential.

1	2	3
Electrolyte a_1 (c_1)	Membrane	Electrolyte a_3 (c_3)
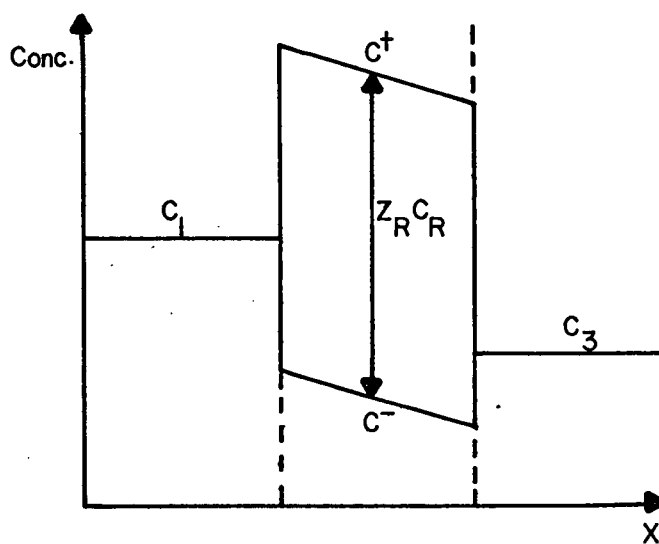
FIGURE 13a

Concentration distribution in a cation-exchange membrane $Z_R C_R$ is the concentration of fixed charge in membrane.
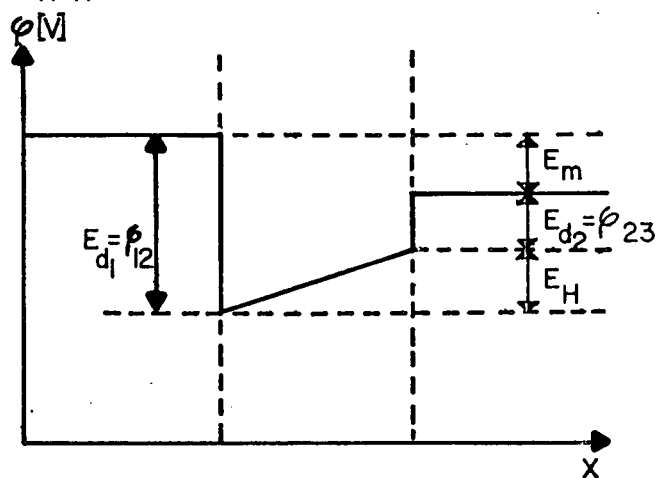
FIGURE 13b

Schematic potential distribution through a cation-exchange membrane.

E_H is the Henderson term which is the diffusion potential existing in the interior of the membrane.

The detailed expressions of the Donnan terms and Henderson term are given by Vetter (1967). A simplified expression for the electrical potential difference across a membrane in contact with uni-univalent electrolyte solutions of activities a_m' and a_m'' on the opposite sides is given by

$$E_m = \frac{RT}{F}(t_c^+ - t_c^-) \ln \frac{(a_m'')_z}{(a_m')_z} \tag{40}$$

where t_c^+, t_c^- are the cation and anion transport numbers in a cation-exchange membrane.

The membrane potentials oppose the applied electrodialysis potentials when ions are transferred from lower to higher concentrations. The resistance per unit area due to potentials of a cation and an anion membrane is given by

$$R_m = R_{ma} + R_{mc} + \rho_a + \rho_c$$

$$= \rho_a + \rho_c + \frac{mRT}{Fi} \left\{ \left[\int_{z=0}^{m} \left[(t_a^- - t_a^+)_z \ln \frac{(\gamma_5 C_5)_z}{(\gamma_4 C_4)_z} \right]^{-1} dz \right]^{-1} \right.$$

$$\left. + \left[\int_{z=0}^{m} \left[(t_c^- - t_c^+)_z \ln \frac{(\gamma_9 C_9)_z}{(\gamma_8 C_8)_z} \right]^{-1} dz \right]^{-1} \right\} \tag{41}$$

where subscripts a and c refer to anion- and cation-exchange membrane respectively

ρ_a, ρ_c are the anion and cation membrane resistance per unit area

R_{ma}, R_{mc} are the equivalent resistance per unit area due to anion and cation membrane potential.

The apparent resistance of a cell pair

The apparent resistance per unit area of a cell pair, R_π, is given by

$$R_\pi = R_d + R_e + R_b + R_m \tag{42}$$

where R_d, R_e, R_b and R_m are defined by equations (35), (36), (38) and (41) respectively.

The apparent resistance per unit area of a cell pair can be evaluated by considering a local resistance at any level Z together with the average bulk concentrations of the solutions. In this case equation (42) reduces to (refer to Figure 10)

$$
\begin{aligned}
R_{\pi,Z} = \delta &\left[\frac{\ln C_1\Lambda_1/C_2\Lambda_2}{(C_1\Lambda_1 - C_2\Lambda_2)} + \frac{\ln C_3\Lambda_3/C_4\Lambda_4}{(C_3\Lambda_3 - C_4\Lambda_4)} + \frac{\ln C_5\Lambda_5/C_6\Lambda_6}{(C_5\Lambda_5 - C_6\Lambda_6)} \right. \\
&\left. + \frac{\ln C_7\Lambda_7/C_8\Lambda_8}{(C_7\Lambda_7 - C_8\Lambda_8)} \right] \\
&+ (\Delta - 2\delta)\left(\frac{1}{C_2\Lambda_2} + \frac{1}{C_6\Lambda_6} \right) + \rho_a + \rho_c \\
&+ \frac{RT}{Fi} \left[(t_d^- - t_d^+) \ln \frac{\gamma_4 C_4}{\gamma_1 C_1} + (t_e^- - t_e^+) \ln \frac{\gamma_8 C_8}{\gamma_5 C_5} \right. \\
&\left. + (t_a^- - t_a^+) \ln \frac{\gamma_5 C_5}{\gamma_4 C_4} + (t_c^- - t_c^+) \ln \frac{\gamma_9 C_9}{\gamma_8 C_8} \right]
\end{aligned} \tag{43}
$$

The subscripts d and e refer to the depleting and enriching solutions and a and c refer to the anion- and cation-exchange membranes. The numerical subscripts refer to the corresponding numbers in Figure 10.

Eq. (43) is based on the following assumptions:

(i) Validity of Nernst idealized model (refer to appendix C)

(ii) A uni-univalent electrolyte system

(iii) Solution-filled compartments without spacers; each of the same

thickness Δ and with two diffusion layers each of the thickness δ

(iv) Constant transport numbers of the membranes and solutions over the range of concentrations of interest

(v) Single-ion activities can be replaced by molalities and mean activity coefficients.

Simplifying Assumptions

Even the simplified equation of the apparent resistance of a differential area of a cell pair i.e. Eq. (43) is cumbersome and time-consuming. It can be simplified by making several assumptions, most of which can be approached in practice. The first simplifying assumption that can be made is that the two diffusion layers in each of the flow channels are identical and the boundary layer thickness on the two membrane faces is the same. With this assumption the concentration profiles become symmetrical i.e. $C_1 = C_4$ and $C_5 = C_8$ and the two junction potentials (the concentration potentials in the boundary layers) cancel out as shown in Figure 14. The assumption implies that:

(a) $(\bar{t} - t)_a = (\bar{t} - t)_c$

where $\bar{t}$, t are the transport numbers of counterion in membrane and solution phase respectively and subscripts a, c refer to anion- and cation-selective membrane.

(b) Same hydrodynamic conditions prevail in the boundary layers in the flow channels i.e.

$$\delta_{1,2} = \delta_{3,4} = \delta_{5,6} = \delta_{7,8} = \delta$$
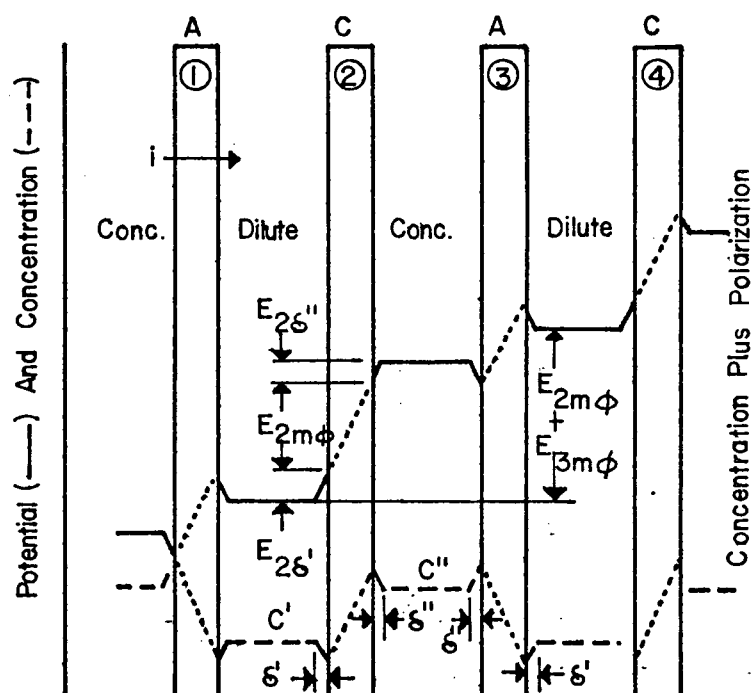
FIGURE 14

Back emf due to concentration and polarization
(neglecting IR effects) when current is flowing as marked (Spiegler,1966).
Dashed lines , concentration ; solid lines   potential
A ,anion_permeable   membrane ;   C , cation_ permeable   membrane .

According to this assumption Eq. (43) reduces to

$$R_{1-9} = 2(\bar{t} - t_c) \frac{RT}{Fi} \ln \frac{\gamma_5 C_5}{\gamma_4 C_4} + 2\delta (\frac{\ln C_2 \Lambda_2 / C_1 \Lambda_1}{C_2 \Lambda_2 - C_1 \Lambda_1} + \frac{\ln C_6 \Lambda_6 / C_5 \Lambda_5}{C_6 \Lambda_6 - C_5 \Lambda_5})$$

$$+ (\Delta - 2\delta)(\frac{1}{C_2 \Lambda_2} + \frac{1}{C_6 \Lambda_6}) + \rho_a + \rho_c \qquad (44)$$

where $\bar{t}$, t_c are the transport numbers of counterions and co-ions in the membrane phase.

Eq. (28) can be used to estimate the boundary layer thickness, δ. Other terms which are not accessible to direct measurement in Eq. (44) are the interfacial concentrations, C_1 and C_5. These can be eliminated as follows:

Eq. (10) can be written as

$$\frac{dc}{dx} = \frac{C_2 - C_1}{\delta} = \frac{i}{B} \qquad (45)$$

where the constant B, which depends only on the nature of the dissolved electrolyte and of the membrane, is defined as

$$B \equiv \frac{FD}{(\bar{t} - t)} \qquad (46)$$

substitute Eq. (11) into Eq. (46)

$$\delta = \frac{B C_2}{i_{lim}} \qquad (47)$$

Therefore we get

$$C_1 = C_2 (1 - \frac{i}{i_{lim}}) = C_2 (1 - k) \qquad (48)$$

Similarly by assuming the same concentration in both diffusion layers we get

$$C_5 = C_6 + \frac{\delta i}{B} = C_6 \left(1 + \frac{k}{ns}\right) \qquad (49)$$

where ns is the separation factor defined by

$$ns = \frac{C_e}{C_d} = \frac{C_6}{C_2} \qquad (50)$$

The following further simplifying assumptions can be made.

• The equivalent conductance is independent of concentration over the limited range of interest i.e.

$$\Lambda_1 = \Lambda_2 = \ldots\ldots\ldots = \Lambda$$

• The activities are equal to the concentrations,

$$\gamma_1 = \gamma_2 = \ldots\ldots\ldots = 1.0$$

With these assumptions together with Eqs. (48) and (49) Eq. (44) reduces to

$$R_{1-9} = 2 \frac{RT}{Fi} \left[(\bar{t} - t_c) \ln \frac{ns + k}{1 - k} \right] + \frac{2FD}{(\bar{t} - t)\Lambda i} \ln \frac{1 + k/ns}{1 - k}$$

$$+ \frac{\Delta - 2\delta}{\Lambda} \left(\frac{1}{C_2} + \frac{1}{C_6}\right) + \rho_a + \rho_c \qquad (51)$$

where k and ns are defined by Eqs. (26) and (50) respectively and $\bar{t}$, t_c are the transport numbers of the counterion and co-ion respectively in the membrane. For ideally selective membranes

$$(\bar{t} - t_c) = 1.0$$

Instead of integrating over the whole flow path, a considerable simplification is achieved by using logarithmic mean values of the bulk concentrations, $\bar{C}_2$ and $\bar{C}_6$ together with Eq. (44) or (51) to evaluate the apparent resistance of a complete cell pair.

Finally it should be noted that all these expressions for the apparent resistance of a cell pair, namely Eqs. (42), (43), (44) and (51) have to be modified to take into account the effects due to:

(a) Presence of spacers in spacer filled configurations

(b) Ohmic resistance due to scale. Scales, such as $CaSO_4$, $CaCO_3$, $Mg(OH)_2$ etc., can precipitate out of solution and deposit on the membrane surfaces at points of low velocity.

3.1.2. Ohmic Analysis

This analysis assumes proportionality between current and voltage in the electrodialysis stack. It is an empirical approach to evaluate stack resistance. For a cell of given design and membrane type, it is a relatively simple matter to use a laboratory model to obtain an empirical set of resistance values as a function of typical operating conditions. These values may then be used to design a full-scale plant. This data may be expressed as the resistance of 1 cm^2 of one cell pair in ohm-cm^2, as a function of external solution concentrations.

Although the actual correlation of cell-pair resistance, R_p, with solution concentration may take the form of a polynomial power series such as $R_p = a + bC + cC^2$ etc, or an exponential form $R_p = \alpha \, C^B$ as shown by Tye (1963), Mason and Kirkham (1959) have suggested the following expression for the local resistance per unit area of a cell pair:

$$R_p = \frac{K_1}{\bar{C}} + K_2 - K_3 \, \bar{C} \tag{52}$$

where K_1, K_2 and K_3 are constants for a given spacer geometry, ionic composition, membrane type and temperature. $\bar{C}$ is the local "average" concentration calculated from

$$\frac{1}{\bar{C}} = \frac{1}{1 + r} \left(\frac{1}{C_d} + \frac{r}{C_c} \right) \tag{53}$$

Here C_d and C_c are the local diluate and concentrate concentrations, and r is the ratio of spacer thicknesses in the concentrate and in the dilute compartment (frequently r is unity).

At low values of $\bar{C}$ (i.e. in dilute solutions), the K_3 term becomes negligible and Eq. (52) reduces to the form

$$R_p = \frac{K_1}{\bar{C}} + K_2 \tag{54}$$

In dilute solutions the electrical resistance of strong electrolytes is approximately inversely proportional to concentration, and the electrical resistances of commercial ion exchange membranes are relatively independent of changes in electrolyte concentration. This is true up to about 0.1 N (Mason, 1959). Thus Eq. (54) can be considered to consist of a solution resistance term, $\frac{K_1}{\bar{C}}$, plus a membrane resistance term, K_2. The K_3 term in Eq. (52) allows for non-linearity between solution concentration and conductance, and for decrease in membrane resistances with increasing solution concentration. At electrolyte concentrations higher than 0.1 N the membrane resistance begins to decrease with increasing electrolyte concentration because of the increased conductivity of the electrolyte in the resin.

Allowances for membrane potentials which oppose the applied voltage and thus represent an apparent resistance, and for resistance increases due to concentration gradients in the diffusion layers is made in choosing the numerical values of K_1, K_2 and K_3. The K's can be estimated from tabulated values of solution and membrane resistance.

The stack resistance is calculated from the solution concentration by either using the logarithmic mean concentration or by integrating over the

whole flow path.

Integration Procedure

The local value, at any level z along the flow path, of the resistance per unit area of a cell pair $(R_p)_z$ can be integrated over the membrane area (pa) available for desalination to obtain the total resistance of a cell pair, R_p.

$$\frac{1}{R_p} = \int_o^{pa} \frac{da}{(R_p)_z} \qquad \text{cell pair}/\Omega \tag{55}$$

where a, is the actual membrane cross-sectional area, cm^2 (a = m x n); and p is the fraction of membrane area available for desalination.

$$pa = pnz \ cm^2$$

$$pda = pndz \ cm^2$$

where n is the membrane width (cm) and z is the coordinate system along a membrane surface (refer to Fig. 11) transposing variables,

$$\frac{1}{R_p} = pn \int_{z=0}^{m} \frac{dz}{(R_p)_z} \tag{56}$$

From Eqs. (52), (53)

$$(R_p)_z = \frac{K_1}{C_a(z)} + K_2 - K_3 \ C_a(z) \tag{57}$$

and

$$\frac{1}{C_a(z)} = \frac{1}{1+r} \left[\frac{1}{C_d(z)} + \frac{r}{C_b(z)} \right] \tag{58}$$

Variations of $C_d(z)$ and $C_b(z)$ with z, will make $C_a(z)$ a function of z.

$$C_a(z) = f(z) \tag{59}$$

$$(R_p)_z = [\frac{K_1}{f(z)} + K_2 - K_3 f(z)] \tag{60}$$

Substituting Eq. (60) into Eq. (56),

$$\frac{1}{R_p} = pn \int_0^m [\frac{K_1}{f(z)} + K_2 - K_3 f(z)]^{-1} dz$$

$$= pn \int_0^m \{ K_1 + K_2 f(z) - K_3[f(z)]^2 \}^{-1} f(z) \, dz \tag{61}$$

f(z) is obtained by substituting values of the bulk solutions from Eqs. (31) and (32) into Eq. (58)

$$f(z) = C_a(z) = \frac{(1+r)(C_d(0)e^{-\alpha z})\{[C_b(m) - (F_d/F_b)C_d(m)] + [(F_d/F_b)C_d(0)e^{-\alpha z}]\}}{\{[C_b(m) - (F_d/F_b) C_d(m)] + C_d(0)e^{-\alpha z} [(F_d/F_b) + r]\}}$$

$$\cdots\cdots\cdots (62)$$

Thus, substituting into Eq. (61) for f(z) or $C_a(z)$, the cell pair resistance, R_p, can be evaluated. Small intervals (Δz) can be chosen to evaluate the integral as a summation

$$\frac{1}{R_p} = pn \sum_{z=0}^{m} \frac{C_a(z) \, \Delta z}{K_1 + K_2 C_a(z) - K_3 C_a(z)^2} \tag{63}$$

3.2. Mass Transfer Models

The differential equation of material conservation for a component in the flow system shown in Figure 15 is:

Adsorbent
Phase,(s)

Fluid
Phase,(f)

dz

z
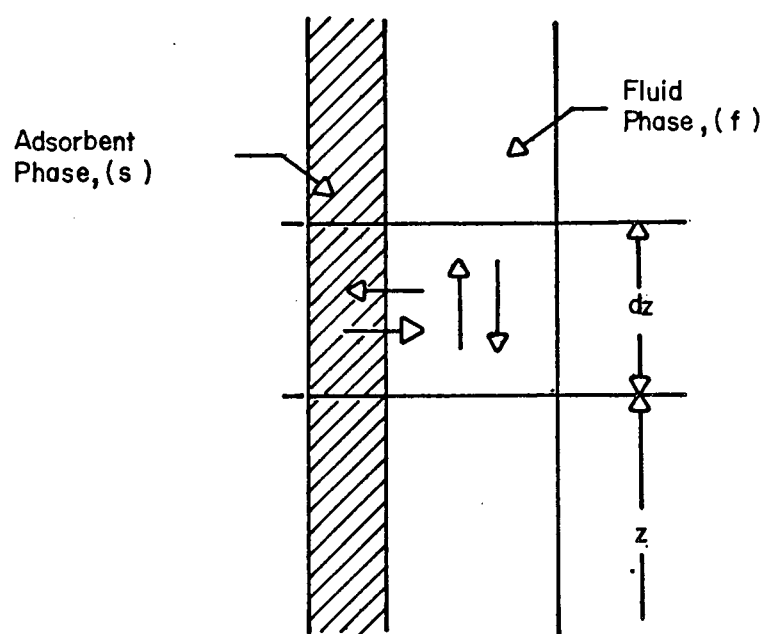
FIGURE 15

Differential section of column.

$$\frac{\partial C_f}{\partial t} + v\frac{\partial C_f}{\partial z} - D\frac{\partial^2 C_f}{\partial z^2} + \left(\frac{1-\epsilon}{\epsilon}\right)\frac{\partial C_s}{\partial t} = 0 \tag{64}$$

$\quad$ (a) $\qquad$ (b) $\qquad$ (c) $\qquad$ (d)

where C_f and C_s are the concentrations of the component transferred in the mobile and stationary phases respectively, v is the displacement velocity, D is solute diffusivity, ϵ is void fraction.

Equation (64) is sometimes called the chromatography equation. The terms in this equation express mass conservation contributions attributable to the following mechanisms:

(a) = interstitial, fluid phase transient

(b) = axial convection

(c) = axial fluid-phase diffusion

(d) = adsorptive phase transient

Together with an equation relating local values of C_s to C_f, and appropriate boundary conditions, Equation (64) applies during every sub-interval of a cyclic flow process.

3.2.1. Equilibrium Model

Pigford et al. (1969) used Equation (64) to develop a simple "equilibrium model" for thermal parametric pumping. The basic assumption in this model is that the solid and fluid are locally in equilibrium. This assumption greatly simplifies the equations since rate information is not needed. In addition, axial dispersion was neglected and the equilibrium relationship was assumed to be linear. With these assumptions the resulting equation is a hyperbolic partial differential equation which can be solved analytically by the method of characteristics developed by Acrivos (1956). The characteristic lines can be used to show graphically the development of the separation, and to show

when separation will not occur; thus the model offers algebraic solutions that can be used for a rapid calculation of parapump separation. The equilibrium theory was generalized by Aris (1969) and extended to an open system by Gregory and Sweed (1970), Chen and Hill (1971) and it was further extended by Thompson and Bowen (1972) to predict separation in a two-column arrangement where the two columns are operated back-to-back to minimize mixing.

Although the equilibrium model is compact and easy to apply it ignores dispersive effects which limit separation in a real system, hence it can not predict the ultimate steady-state separation (Rice, 1973). Gupta and Sweed (1972) have extended the equilibrium model to take into account axial mixing. Foo and Rice (1975, 1976) used a more general temperature dependence in the linear isotherm along with the dissipative forces associated with axial dispersion, film resistance and pore diffusion to predict the ultimate separation in closed parapumps. Mass transfer between the moving phase and the stationary phase is assumed to take place instantaneously in the equilibrium model and hence the cycle durations do not enter into the solutions predicted by the model. Since the cycle duration may be assigned any arbitrary value, the equilibrium model solutions are not functions of real time and the model can only serve as in idealization that predicts the best possible separation.

Electrically driven separation processes such as electrodialysis are governed by finite rates of mass transfer and usually operate at concentrations far from equilibrium. The rate of mass transfer is proportional to the current flowing (within a certain range of concentration) and is thus to some extent under the direct control of the experimenter. Cyclic

operation of such systems may therefore be better represented by a rate model than by equilibrium theory.

3.2.2. Rate Models

Two rate models will be considered here:

(a) constant rate model

(b) concentration-dependent rate model

The basic assumption in each of these models is that the equilibrium condition may be disregarded altogether, i.e. if the two phases were left in stationary contact for a sufficiently long period of time, the adsorbate would be transferred completely into one of the phases. These models also assume that the capacity of the storage layers is large enough that it does not impose a limit on mass transfer during the cycle. Axial dispersion is neglected and the fluid is assumed to be incompressible and have constant density. The complete operating cycle is divided into a number of sub-intervals; whenever the fluid velocity changes at the end of these periods it is assumed that it changes in a stepwise manner, while it remains constant during each of these sub-intervals. Furthermore, a system in which one void volume is displaced every half cycle is considered.

Concentration changes predicted by the rate models are functions of time, in contrast to the equilibrium model solutions which are functions of the number of cycle but not of real time.

(a) Constant rate model

A constant rate of interphase mass transfer, uniform everywhere within the cell, requires a constant, uniform, distribution of electric current. Uniformity can be approximated by connecting a number of short stacks together in series both electrically and hydraulically, as shown in Figure 16.

Dialysate Production   Brine Production
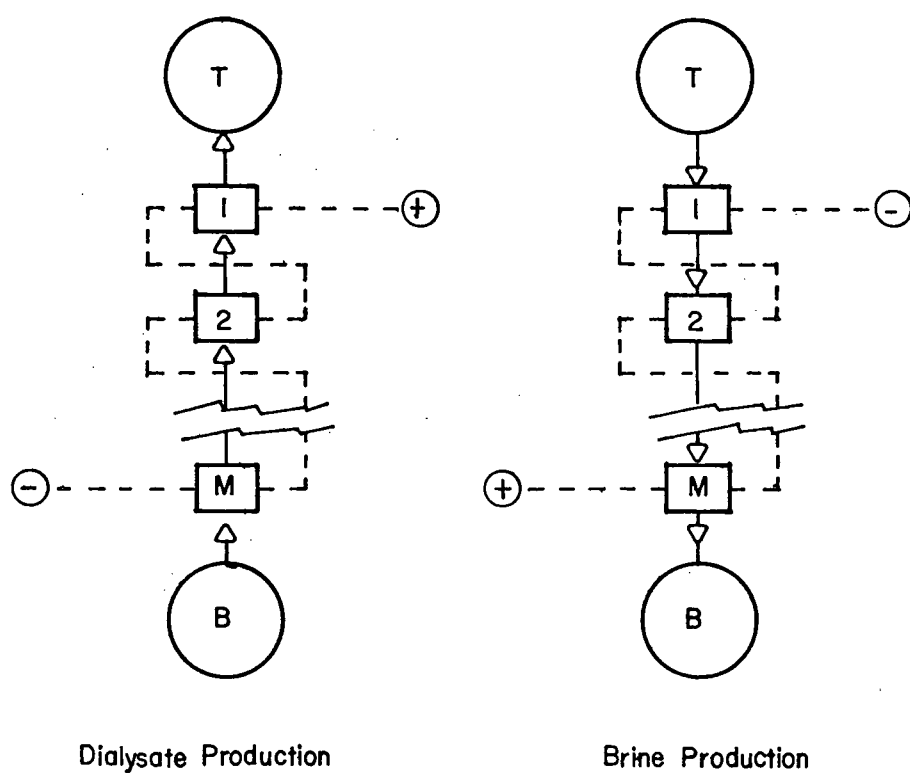
FIGURE 16

Series connection of ED modules to approximate constant_rate operation.

Constant current can be maintained by a suitable power supply. This will ensure constant mass transfer until the solute concentration drops low enough at some point in the apparatus that water splitting occurs and solvent ions start to carry a significant portion of the current. While constant-rate operation is not very practical, an examination of some of the consequences of this model is of interest since it illustrates limiting conditions.

If the rate of mass transfer is held constant, and axial diffusion is neglected, Equation (64) simplifies to

$$\frac{\partial C_f}{\partial t} + v \frac{\partial C_f}{\partial z} = - \left(\frac{1 - \varepsilon}{\varepsilon} \right) \frac{\partial C_s}{\partial t} = K \text{ (constant)} \tag{65}$$

during any sub-interval of the cycle.

(i) Synchronous (in-phase) operation

If the total cycle period T is composed of two equal sub-intervals, with simultaneous reversal of both the flow direction and the direction of mass transfer, then the constant in Equation (65) can be written $K = - K_1$ during the demineralizing half-cycle and $K = K_2$ during enrichment i.e.

$$\frac{dC_f}{dt} = - \rho \frac{dC_s}{dt} = - K_1 \quad ; \text{ for demineralization} \tag{66}$$

$$\frac{dC_f}{dt} = - \rho \frac{dC_s}{dt} = K_2 \quad ; \text{ for enrichment} \tag{67}$$

where $\rho = \dfrac{1 - \varepsilon}{\varepsilon}$

If we consider $K_2 > K_1$ and demineralization takes place for time $\frac{T}{2}$; then to maintain the material balance of the system the enrichment period should be Δt where

$$\Delta t = \frac{T \, K_1}{2 \, K_2} \tag{68}$$

during the rest of enrichment half cycle i.e. $\frac{T}{2} (1 - \frac{K_1}{K_2})$ the voltage can

be switched off to save power.

The graphical solution of the model Equations (66, 67, 68) gives the

following result (refer to Appendix D):

$$\frac{C_{T,n}}{C_o} = 1 - \frac{T \, K_1}{4 \, C_o} - \frac{T \, K_1}{4 \, C_o} (1 - \frac{K_1}{K_2})(n - 1) \tag{69}$$

$$\frac{C_{B,n}}{C_o} = 1 + \frac{T \, K_1}{4 \, C_o} (1 - \frac{K_1}{K_2})n \tag{70}$$

where C_T, C_B are the top (demineralized) product and the bottom (enriched)

product respectively

C_o is the initial concentration; $C_{f(t=0)} = C_{s(t=0)} = C_o$

n is the number of cycles

From Equations (69, 70) it is clear that maximum separation occurs when

$K_2 \gg K_1$ or when $\frac{K_1}{K_2} \to 0$. In this case the separation factor, ns is given

by

$$ns = \frac{C_{B,n}}{C_{T,n}} = \frac{1 + \dfrac{TK_1 n}{4 \, C_o}}{1 - \dfrac{TK_1 n}{4 \, C_o}} \tag{71}$$

It is also obvious that when $K_1 = K_2$, no separation occurs after the first

cycle. The concentration of solute stored within the membranes returns to

its initial value at the end of each cycle and the average top and bottom con-

centrations (Equations 69, 70) do not change after the first cycle.

Figure 17 illustrates successive concentration profiles in the stack
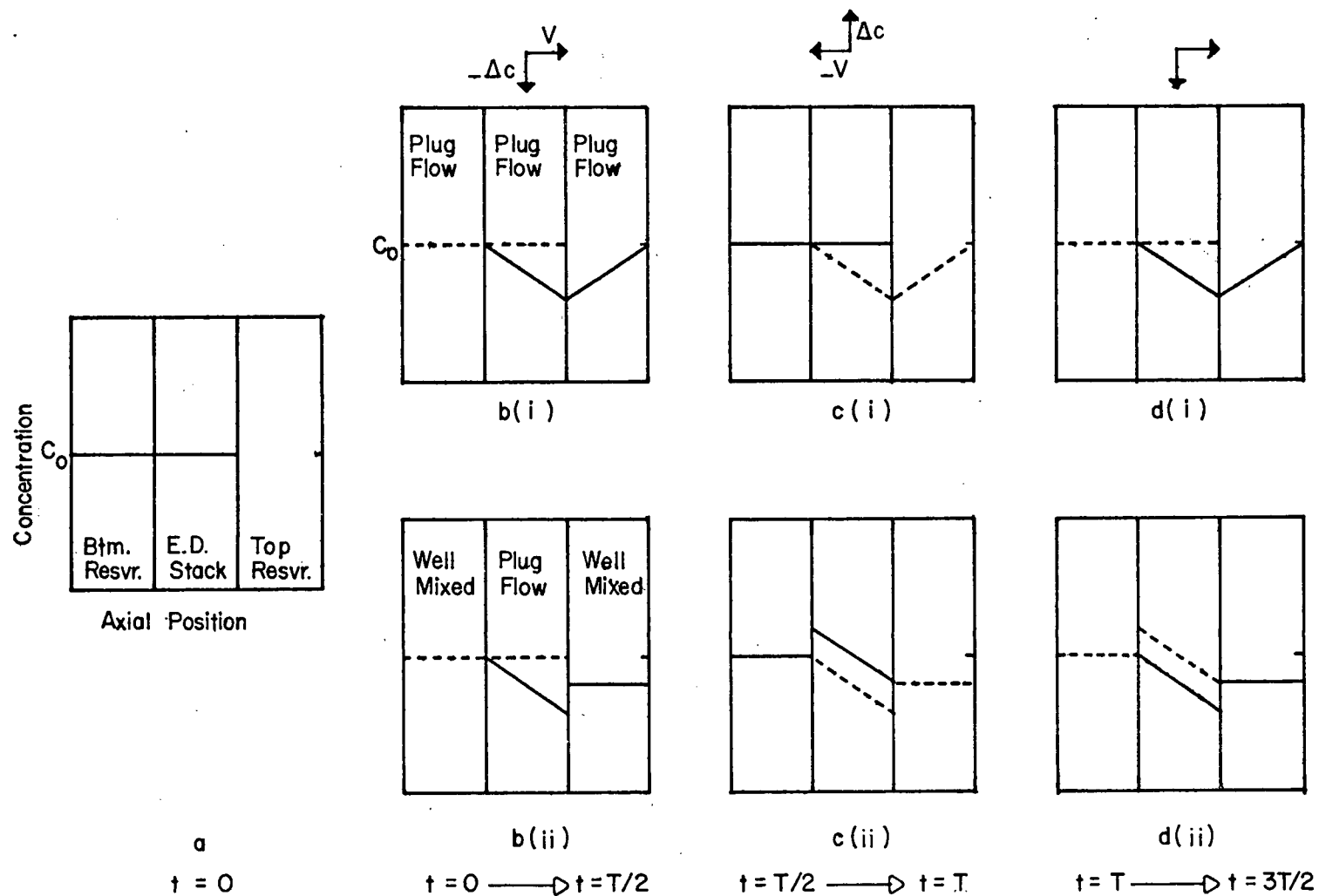
FIGURE 17

Concentration profiles predicted by constant_rate model with equal rates_continuous cyclic displacement of fluid and mass transfer. Case (i), the top row, assumes no mixing in the end reservois, while case (ii) assumes well mixed end reservoirs.

and in the end reservoirs when $K_1 = K_2$. For simplicity it is assumed that the end reservoirs have the same volume and the same L/D ratio as the cell interior. The initial concentration profile is shown in (a), Figure 17. After the first half-cycle the conditions are either as shown in (bi) (if no mixing takes place in the end reservoir) or in (bii) (if the end reservoir is well mixed). The fluid in the top reservoir is displaced back through the column to produce the profiles shown in (ci) or (cii) at the end of the first complete cycle, when the mean concentration in the bottom reservoir has returned to the value it had in (c). Figure 17(d) shows conditions at the end of the 3rd half cycle, which are identical with (b).

In order to obtain separation we must either:

(i)   make $K_2 > K_1$, or

(ii)   modify the cycles by periodically interrupting the electric current, or

(iii) modify the cycles by periodically interrupting the fluid flow, or

(iv)   introduce lag between current and flow cycles i.e. use out-of-phase operation

Case (i) has already been considered. Thompson et al. (1974) has discussed the other three cases as shown in the following sections.

(ii) Interrupted Current operation

This is a more general and more useful type of operation than case (i). Here the current is turned off during a part of every half cycle. Figure 18 shows the flow and current cycles for this kind of operation. During the first half-cycle both flow and mass transfer take place for period τ_1, at which point the current is turned off and flow continues for period τ_2. A

similar sequence, τ_3 and τ_4, follow during the second half-cycle. From the material balance on the salt

$$K_1 \tau_1 = K_2 \tau_3 \qquad (72)$$

and from the material balance on the solvent

$$\tau_1 + \tau_2 = \tau_3 + \tau_4 \qquad (73)$$

If β is the fraction of the first half-cycle during which the current is on ($\beta = \tau_1/(T_2/2)$), then the successive intervals are;

$$\tau_1 = \beta \left(\frac{T}{2} \right)$$

$$\tau_2 = (1 - \beta) \left(\frac{T}{2} \right)$$

$$\tau_3 = \frac{K_1}{K_2} \beta \left(\frac{T}{2} \right)$$

and $\qquad \tau_4 = (1 - \frac{K_1}{K_2} \beta) \left(\frac{T}{2} \right) \qquad (74)$

Figure 18 shows concentration profiles at consecutive intervals in a batch separation, for simplicity a system in which the end reservoirs remain unmixed is illustrated. The dotted lines represent the concentration at the beginning of each period τ_i and the solid lines show the profile at the end of each period. Subsequent cycles result in a progressive build up of the concentration wave.

The average top product concentration after n cycles is given by

$$\frac{C_{T,n}}{C_o} = 1 - \frac{TK_1}{4C_o} \beta (2 - \beta) - \frac{TK_1}{4C_o} \beta [2 - \beta (1 + \frac{K_1}{K_2})] (n - 1) \qquad (75)$$

and the average concentration of the bottom (enriched) product is
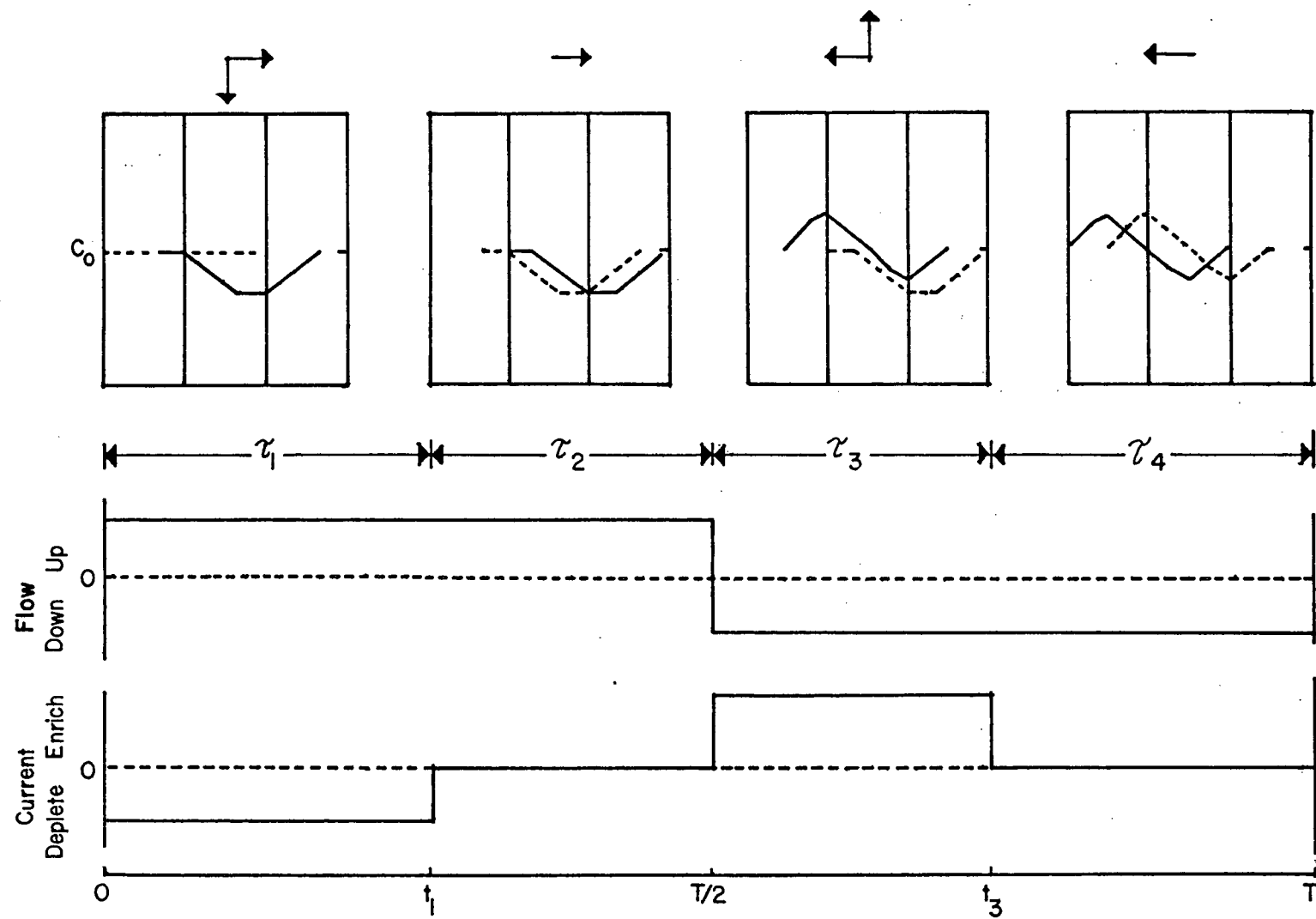
FIGURE 18

Concentration profiles – interrupted current cycle.

$$\frac{C_{B,n}}{C_o} = 1 + \frac{TK_1}{4C_o} \beta [2 - \beta (1 + \frac{K_1}{K_2})] n \qquad (76)$$

If $K_1 = K_2$ and $\beta = 1$ separation ceases after 1 cycle. It is possible to choose a value of β that gives continuing separation for any specified value of K_1/K_2. Differentiation of equation (75) or (76) shows that the most rapid increase in separation will be obtained when

$$\beta = \frac{K_2}{K_1 + K_2} \qquad (77)$$

Under these conditions the separation factor is given by

$$ns = \frac{1 + \frac{TK_1}{4C_o} \beta n}{1 - \frac{TK_1}{4C_o} \beta (n - \beta + 1)} \qquad (78)$$

Thus, if $K_1 = K_2$, best separation is obtained by setting $\beta = \frac{1}{2}$, so that $\tau_1 = \tau_2 = \tau_3 = \tau_4$ and the separation factor is

$$ns = \frac{1 + \frac{TK_1}{8C_o} n}{1 - \frac{TK_1}{8C_o} (n + \frac{1}{2})} \qquad (79)$$

$n_{max} = (\frac{8C_o}{TK_1} - \frac{1}{2})$. If $n > n_{max}$, then n_{max} must be used.

If $K_2 \gg K_1$, $\beta = 1$ and the separation factor is

$$ns = \frac{1 + \frac{TK_1}{4C_o} n}{1 - \frac{TK_1}{4C_o} n} \qquad (80)$$

provided that $n < \frac{4C_o}{TK_1}$

Since the current is only on for fraction β of each cycle, the amount of separation obtained for a given amount of current consumed is approximately the same in equations (79) and (80).

If a real system is operated with $K_2 > K_1$, but with no externally controlled interruption of the current, as in case (i), the concentration in the storage layers must continually decrease in successive cycles. After a number of cycles the concentration will drop to near zero part way through a depletion half cycle, causing the electrical resistance to become very large. If the voltage is controlled at a constant value the current must then become very small, so that, from this cycle onward, the system will behave as if the current were interrupted part way through each depletion cycle.

(iii) Interrupted flow operation

A third type of operating cycle is shown in Figure 19. Here the fluid displacement, rather than the current, is periodically interrupted. The current is turned on at the beginning of the cycle, to demineralize the solution, but flow does not start until the end of pause time τ_1. The fluid is displaced upward during period τ_2 while the current remains on and further demineralization takes place. The polarity is reversed at the start of period τ_3 and a similar sequence of flow pause followed by downward displacement completes the cycle. The complete cycle time T consists of the two pause periods τ_1 and τ_3 and the displacement periods τ_2 and τ_4. In the subsequent work based on this operating cycle the displacement periods are kept constant and the cycle time T varies with the pause time used.

From the material balance on the salt

$$K_1 (\tau_1 + \tau_2) = K_2 (\tau_3 + \tau_4) \tag{81}$$

and from the material balance on the solvent

$$\tau_2 = \tau_4 \tag{82}$$

If pause τ_1 lasts for a fraction $\frac{\alpha}{2}$ of the total cycle time T, then the successive intervals are:

$$\tau_1 = \alpha(\frac{T}{2})$$

$$\tau_2 = \frac{TK_2}{K_1 + K_2} - \alpha(\frac{T}{2})$$

$$\tau_3 = T(\frac{K_1 - K_2}{K_1 + K_2}) + \alpha(\frac{T}{2})$$

and

$$\tau_4 = \tau_2 \tag{83}$$

Figure 19 illustrates the way in which the concentration profile develops in a closed system with no mixing in the end compartments.

The average top-compartment concentration after the nth cycle is given by

$$\frac{C_{T,n}}{C_o} = 1 - \frac{TK_1}{4C_o}(\alpha + \frac{2K_2}{K_1 + K_2}) - \frac{TK_2}{4C_o}\{(1 + \frac{K_1}{K_2})\alpha + 2(\frac{K_1 - K_2}{K_1 + K_2})\}(n-1)$$

$$\ldots\ldots\ldots\ldots \tag{84}$$

and the bottom concentration is

$$\frac{C_{B,n}}{C_o} = 1 + \frac{TK_2}{4C_o}\{(1 + \frac{K_1}{K_2})\alpha + 2(\frac{K_1 - K_2}{K_1 + K_2})\}n \tag{85}$$

If $K_1 = K_2$ the separation factor is given by
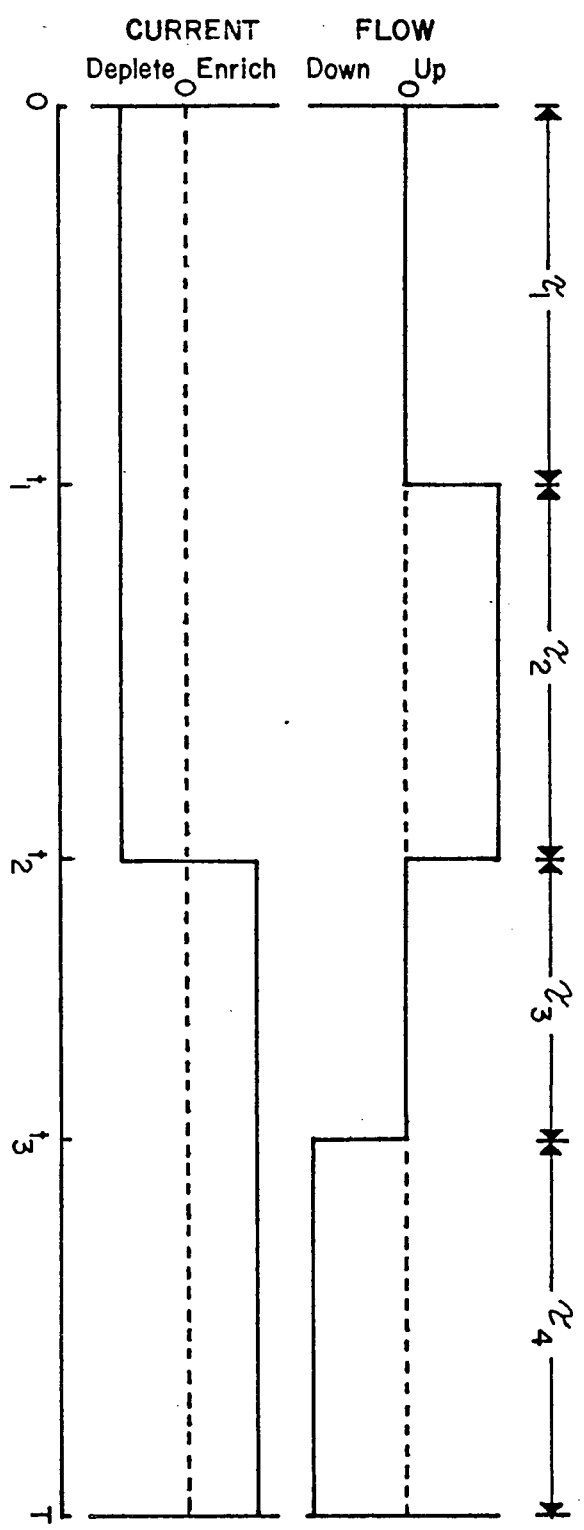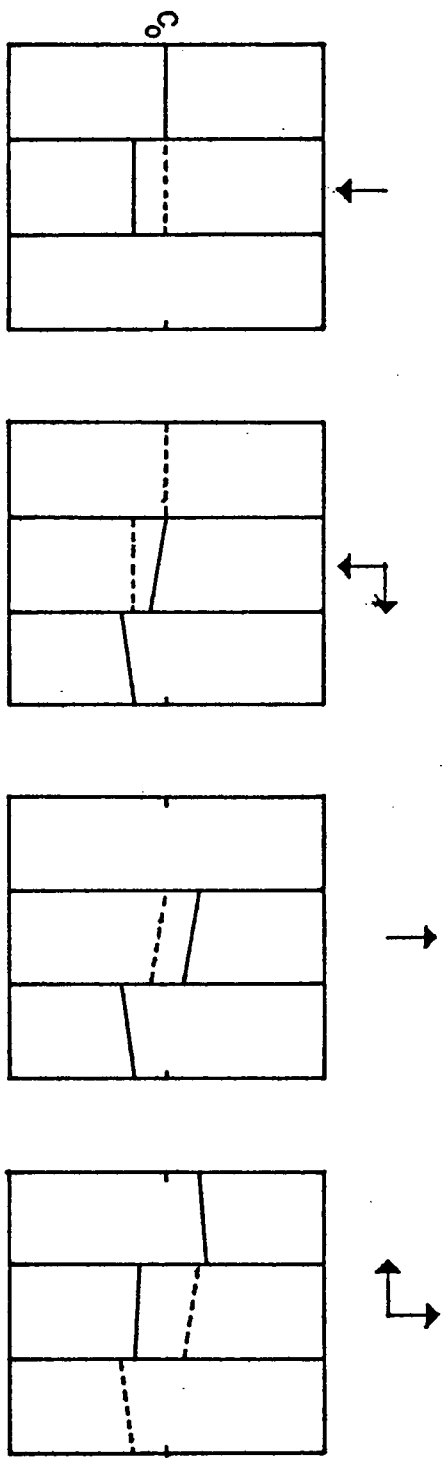
FIGURE 19

Concentration profiles - interrupted flow cycle.

$$ns = \cfrac{1 + \cfrac{TK_1}{2C_o} \alpha\, n}{1 - \cfrac{TK_1}{2C_o} \alpha\, (n + \cfrac{1-\alpha}{2\alpha})} \qquad (86)$$

Provided that $o < \alpha < 1$ and $n_{max} = (\dfrac{2C_o}{TK_1\alpha} - \dfrac{1-\alpha}{2\alpha})$.

If $n > n_{max}$, then n_{max} must be used.

Obviously, best separation is obtained as $\alpha \to 1$, giving an operating cycle with relatively long flow-pauses and rapid displacement. This special case may be referred to as instantaneous displacement operation or pure-pause operation in comparison with continuous displacement operation of Case (i). As $\alpha \to 1$, the separation is given by

$$ns = \cfrac{1 + \cfrac{TK_1}{2C_o} n}{1 - \cfrac{TK_1}{2C_o} n} \qquad (87)$$

which is double the value predicted by case (i) in its best operating conditions (Equation 71).

(iv) Out-of-phase operation

Figure 20 illustrates the concentration profiles at successive quarter cycles after the start for a constant rate process operating with the current cycle 90° out-of-phase with the displacement. It is assumed that the rate constants K_1 and K_2 are equal and that the effluent remains unmixed in the end reservoirs. In contrast to in-phase operation, out-of-phase operation leads to a continuing build-up of the concentration wave.

If the current switching leads the flow switching by time τ, and $\gamma \equiv \dfrac{2\tau}{T}$, the average top and bottom concentration transients after the nth cycle are
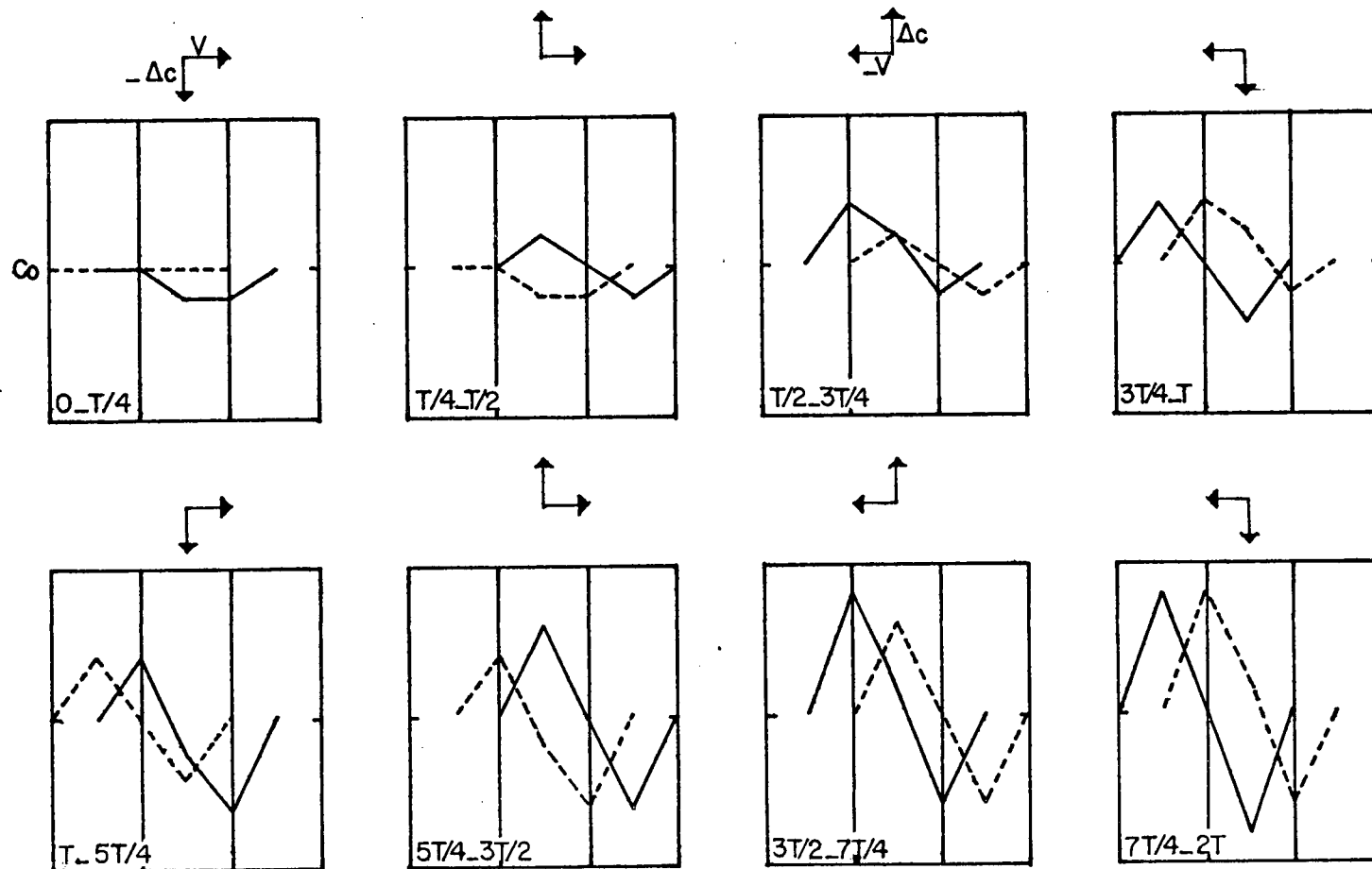
FIGURE 20

Concentration profiles predicted by constant_rate model_continuous cyclic displacement of fluid and mass transfer. The mass transfer cycle is 90° out _ of _ phase with the displacement cycle.

given by:

$$\frac{C_{T,n}}{C_o} = 1 - \frac{TK_1}{4C_o} [1 - 2\gamma^2] - \frac{TK_1}{C_o}(1 - \gamma)(\gamma)(n-1) \tag{88}$$

$$\frac{C_{B,n}}{C_o} = 1 + \frac{TK_1}{C_o}(1-\gamma)(\gamma) n \tag{89}$$

in the interval $o \leqslant \gamma \leqslant \frac{1}{2}$. The concentrations change linearly with the number of cycles and the greatest rate of change occurs when $\gamma = \frac{1}{2}$. This is in marked contrast to the results of the equilibrium model of parametric pumping, which predicts best separation when transfer and displacement cycles are in phase and no separation when they are 90° out of phase (Pigford et al., 1969 a). The separation factor when $\gamma = 0$ is given by

$$ns = \frac{1}{1 - \frac{TK_1}{4C_o}} \tag{90}$$

i.e. separation ceases after 1 cycle. When $\gamma = \frac{1}{2}$ the separation factor is

$$ns = \frac{1 + \frac{TK_1}{4C_o} n}{1 - \frac{TK_1}{4C_o}(n - \frac{1}{2})} \tag{91}$$

$n_{max} = (\frac{4C_o}{TK_1} + \frac{1}{2})$. When $n > n_{max}$, then n_{max} must be used.

Figure 21 shows concentration profiles in a possible arrangement of two units operated together, with the top of one cell connected directly to the top of the other and the bottoms of the cells connected together through a reversible pump. With this configuration no end reservoirs are needed and the concentration wave builds up twice as rapidly as with a single unit.
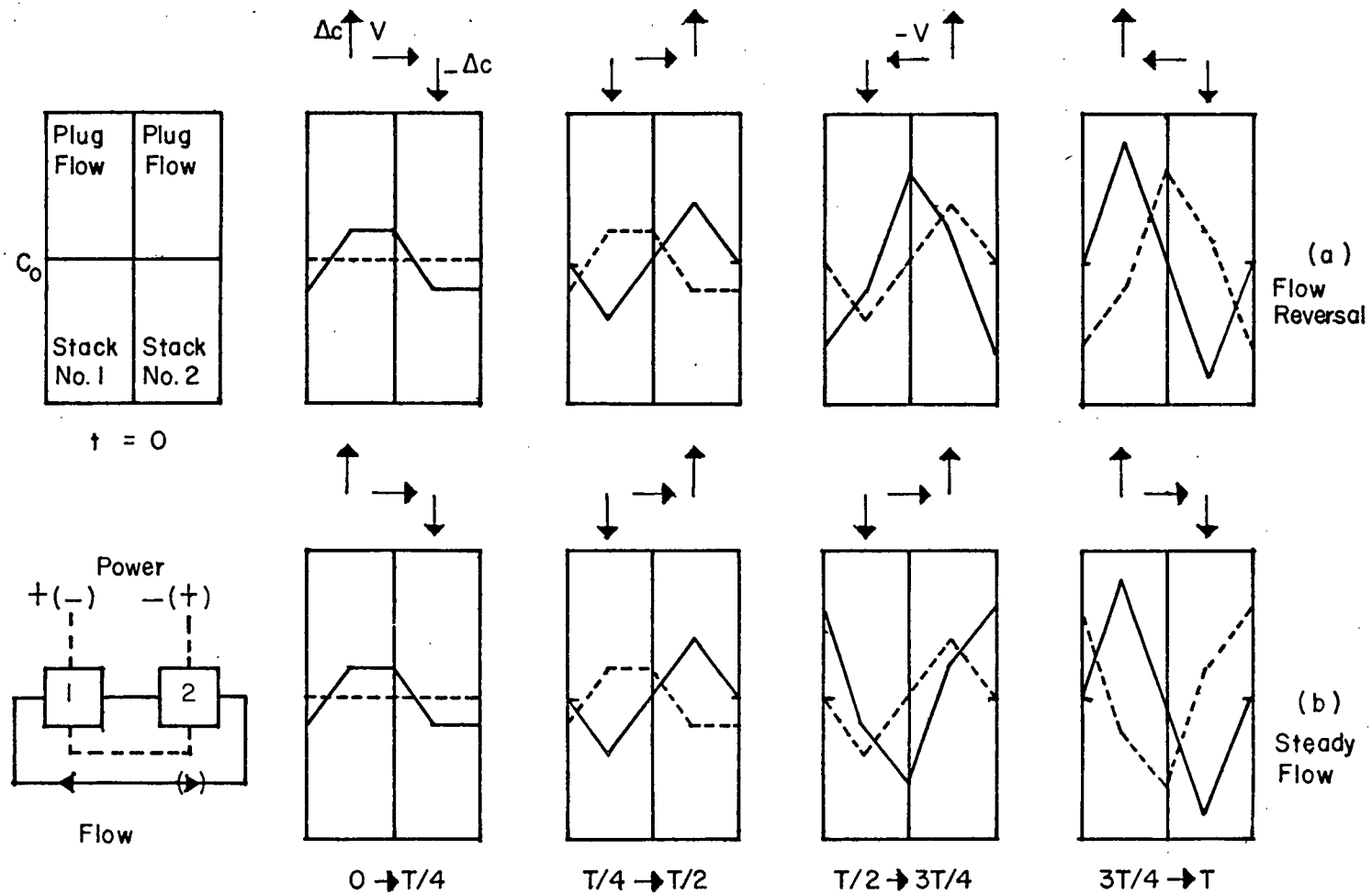
FIGURE 21

Back_to_back operation of two units.
Case (a) , the top row , operates with cyclic displacement of fluid , 90° out_of_phase mass transfer.
Case (b), operates with no flow reversal , cyclic mass transfer.

Note that the concentration profile in Figure 21(a) is symmetrical at the
end of each half cycle. Because of this symmetry either periodic flow
reversal or continuous flow, Figure 21(b), lead to similar separation. In
the first method of operation an oscillating concentration wave is generated,
which grows with time, while in the second method a rotating wave is produced
which grows at the same rate. A third possibility would be to operate a
number of units in series to generate a travelling wave, growing as it moves
along. Operation of equilibrium systems in this manner has been discussed by
Pigford et al. (1969 b).

Comments on various operations of the constant-rate model

By comparing the separation obtained in the four cases discussed
previously, it can be noticed that the concentrations change faster in
case (iii) than with either of the other cases considered. Since mass trans-
fer during displacement contributes little to the final separation in pause
operation (case (iii)), some economy in electric power consumption might be
obtained by turning the current off during all or part of the displacement
periods.

(b) Concentration-dependent rate model

While it is possible to operate the process in a constant current/con-
stant rate mode, it is more convenient to apply a constant potential to the
electrodes. The local current density is then a function of the concen-
trations along the current path and of the effective voltage.

If the applied voltage is $\Delta\phi$, and the voltage available to the stack
is $\Delta\phi'$ (after ohmic losses and overpotentials in the electrode compartment are
allowed for), then the current through the stack is given by

$$I = \frac{\Delta\phi' - \Delta\phi_{DON}}{\Sigma R} \tag{92}$$

where $\Delta\phi_{DON}$ is the Donnan potential across the membranes of the stack. The resistance is the sum of three terms, R_m - the resistance of the membranes, R_f - the integral resistance of the fluid in the flow channels, and R_s - the integral resistance of the fluid stored in the core layers within each membrane pair. The fluid resistance terms comprise the bulk fluid resistance together with the associated boundary layers resistances.

Under the operating conditions for most experiments the Donnan potential was small compared to the applied potential, so that the current density was mainly controlled by the largest resistance in the current path. Low concentrations, and hence high resistances, occurred in the flow channels during most of the depletion part of an operating cycle, and in the membrane cores during enrichment. Accordingly the following rate laws were assumed

$$\rho \frac{\partial C_s}{\partial t} = a_1 C_f \qquad \text{(during depletion)} \tag{93}$$

$$\frac{\partial C_s}{\partial t} = - a_2 C_s \qquad \text{(during enrichment)} \tag{94}$$

Substituting these equations into equation (64), and neglecting axial diffusion, leads to a set of equations that can be solved analytically for some boundary conditions. Solutions have been obtained (Bass, 1972) for the interrupted-flow operating cycle previously described provided mass transfer is restricted to the flow-pause periods and the displaced fluid volume is equal to the void volume. Under these conditions, the average dialystate and brine concentrations after n cycles are

$$\frac{C_{T,n}}{C_o} = p^n \tag{95}$$

$$\frac{C_{B,n}}{C_o} = 2 + \rho - p^n - \rho q^n - q p^{n-1} (1 - p) \sum_{\ell=o}^{\ell=n-1} \left[\frac{q}{p} \right]^\ell \tag{96}$$

where

$$p = \exp\left(- \frac{a_1 T}{2}\right)$$

$$q = \exp\left(- \frac{a_2 T}{2}\right)$$

$$\rho = \frac{1 - \varepsilon}{\varepsilon}$$

An alternative semi-empirical approach can be developed by assuming a concentration-dependent mass transfer rate similar to Equations (93, 94)

$$\rho \frac{\partial C_s}{\partial t} = k_1 C_f \quad \text{(during depletion)} \tag{97}$$

By considering the overall material balance for the solute and the limiting separation a general solution of the system is obtained in which the average dialystate and brine concentrations after n cycles are given by

$$\frac{C_{T,n}}{C_o} = \exp\left(\frac{-k_1 Tn}{2} \right) + k_2 \left[1 - \exp\left(\frac{-k_3 Tn}{2} \right) \right] \tag{98}$$

$$\frac{C_{B,n}}{C_o} = 2 - \exp\left(\frac{-k_1 Tn}{2} \right) - k_2 \left[1 - \exp\left(\frac{-k_4 Tn}{2} \right) \right] \tag{99}$$

This solution can be simplified by assuming that $k_3 = k_4 = k_1$ in this case Equations (98, 99) reduce to

$$\frac{C_{T,n}}{C_o} = \exp\left(\frac{-k_1 Tn}{2} \right) + k_2 \left[1 - \exp\left(\frac{-k_1 Tn}{2} \right) \right]$$

$$= k_2 + (1 - k_2) \exp\left(\frac{-k_1 Tn}{2} \right) \tag{100}$$

$$\frac{C_{B,n}}{C_o} = 2 + (k_2 - 1) \exp\left(\frac{-k_1 Tn}{2} \right) - k_2 \tag{101}$$

where k_1, k_2 are constants which are functions of system and operating parameters.

If we assume flow channel and storage compartment are of the same capacity and dimensions (as is the usual case) then $\rho = 1.0$ and Equations (95, 96) will be a special case of Equations (98, 99) where the constants are given by

$$k_1 = a_1, \; k_2 = -1, \; k_3 = 0 \text{ and } k_4 = a_2$$

3.2.3. Comment on Constant-Rate Model

Although the constant-rate model is compact and easy to apply it ignores dispersive and current-limiting effects which limit separation in a real system; hence it can not predict the ultimate steady-state separation. However, the model offers simple algebraic solutions to a complicated system which can be utilized to show graphically the development of the concentration profiles and to indicate when separation will not occur. The model has been used extensively in the present work to compare various operating cycles and modes of operation.

CHAPTER 4

The Cyclic Electrodialysis Process –
Objectives, Techniques and Apparatus

4.1. Objectives of the Program

The primary objectives of this experimental program were; to
explore the possible regions of application of cyclic operation in an open
electrodialysis system, to screen system parameters and to determine their
relative importance.

Previous work in a batch system (Bass, 1972) showed that the most
important operating parameters were the displacement cycle, the applied volt-
age and the initial concentration. These were further investigated here
together with the effect of production rate. An open system offers a high
degree of freedom with regard to introduction of feed and withdrawal of
products, and a variety of different operating modes were considered. The
modular construction of the ED cell allowed crude measurements to be made
of the axial distribution of current and probe voltage during the cycle and
also permitted the effect of channel length to be investigated.

The constant-rate model discussed in Chapter 3 predicted that the
interrupted flow operation would result in the best separation compared to the
other cycles studied (synchronous, out-of-phase and interrupted current

cycles). The experimental part of the work was based mainly on this
interrupted flow cycle. The cycle is most conveniently described with
reference to a single electrodialysis stack, however two stacks close-
coupled in a back-to-back configuration were used in most of the
experimental work.

4.2. Single Stack Operation

Figure 22 illustrates the sequence of events that make up a complete
operating cycle. The electrodialysis cell (ED cell) is shown schematically
as a rectangular box with an internal shaded area symbolizing the
sorption membrane stack. Two well mixed reservoirs (circles in Figure 22)
are connected to the ends of the ED cell. Partial shading of the circles
indicates the liquid content of these reservoirs at different times during
the cycle. Figure 22 shows batch operation but it can be modified to
allow for feed addition and product removal in various ways during the
cycle.

The interior of the cell is divided by many parallel ion-selective
membranes into two regions; a set of flow channels connecting the inlet and
outlet ports, and an interleaved set of closed "capacity cells" or membrane
stack. Depending on the direction of the electric current, ions are either
transferred from the solution in the flow channels to that in the capacity
cells or vice-versa. During the first half cycle the applied electric
potential is controlled to produce a positive square wave. The membranes
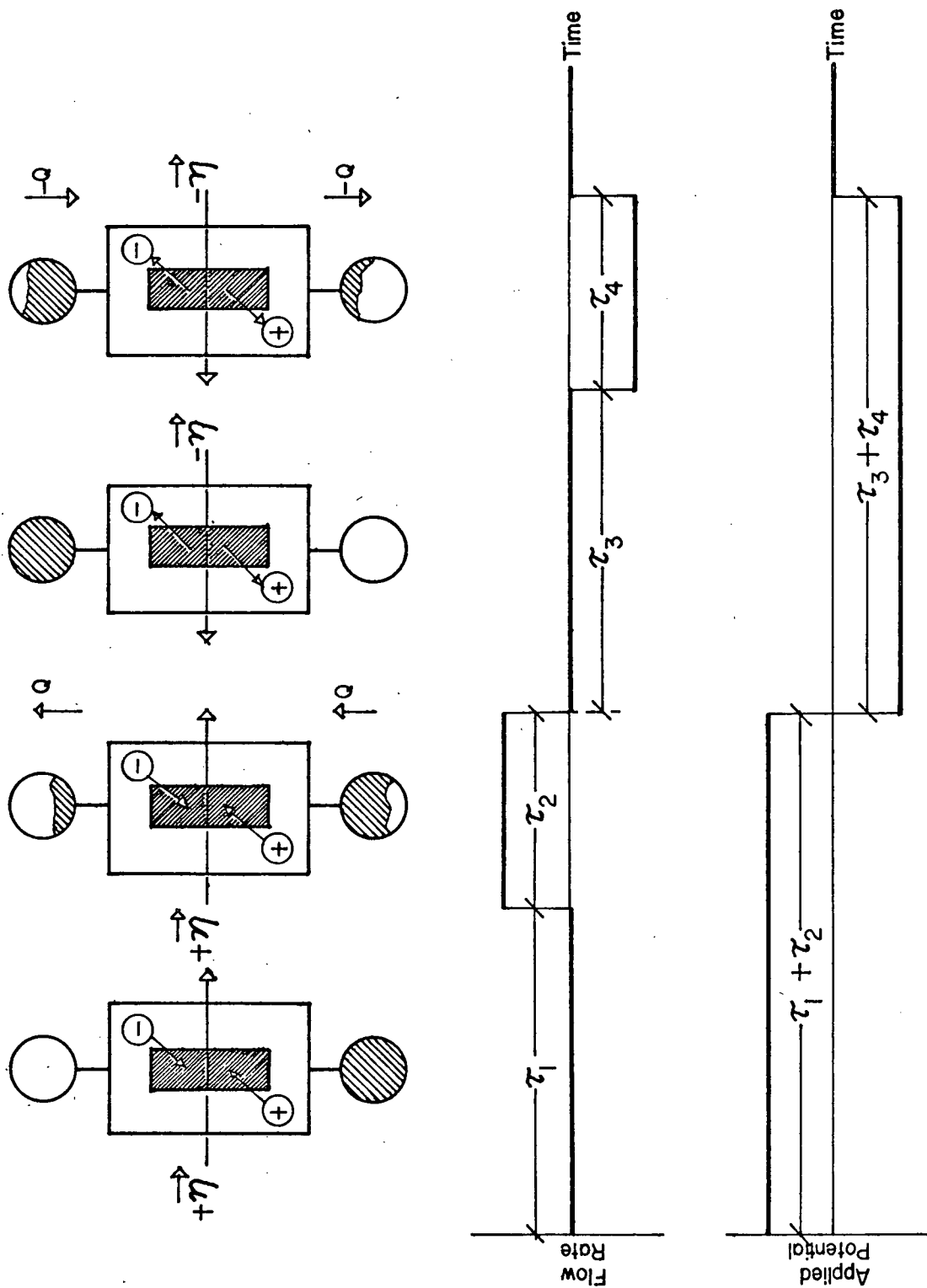
FIGURE 22

Batch operation of cyclic electrodialysis process.

are positioned in such a way that positive polarity is equivalent to solute uptake (i.e. the cationic membranes face the anode). The intrachannel solution is, therefore, depleted during the entire first half-cycle which consists of two parts: a "pause" or no-flow interval (τ_1) followed by a "displacement" interval (τ_2) during which the fluid flows with constant rate (Q) from the lower to the upper reservoir. Displacing fluid entering the bottom of the cell may be fresh feed or "reflux" returning after a previous downward displacement, or a mixture of these. The second half-cycle begins with a polarity reversal ($- \vec{\eta}$) and a simultaneous flow stoppage for another "pause" interval (τ_3). The intrachannel solution receives solute from the membrane stack during the whole period of this second half-cycle, which is concluded by a "displacement" interval (τ_4) during which the solution is returned from the upper to the lower reservoir with flow rate ($- Q$). The displacing fluid entering at the top of the cell may be fresh feed, or a reflux stream of depleted solution obtained during period (τ_2) or a combination of these. In an open system partial reflux must be used to achieve cyclic operation while in a closed system the operation, in some ways, is analogous to total reflux operation of a distillation column.

Initially the solute concentrations in the system are in equilibrium across the membranes and equal everywhere. Each cycle produces depletion of the solution in the upper reservoir and enrichment of the solution in the lower one, and an axial concentration gradient continues to develop in the ED cell until limiting steady-periodic conditions are reached.

In most of the experiments reported here symmetric half cycles with regard to time intervals have been used i.e. $\tau_1 = \tau_3$ and $\tau_2 = \tau_4$.

4.3. Back-to-Back Stack Configuration

Since some, or all, of the fluid leaving the cell during upward displacement is subsequently to be returned as reflux, it is convenient to connect two cells together as shown in Figure 23. This direct coupled back-to-back configuration avoids the necessity of intermediate reflux storage tanks. Also experiments in a batch operation showed that mixing in the end reservoirs lowers separation and a reduction of mixing in the solution external to the stack helps to reduce the effects of internal mixing by reducing the gradients of the travelling fronts. The average separation factor was increased by 30 - 100% when an end reservoir (well mixed) was replaced by a coil tubing (Bass, 1972).

The two cells so connected (Figure 23) are operated electically out-of-phase with each other and, of course, upward displacement in one cell implies downward displacement in the other (with the possible exception of periods when the feed is being introduced or products removed).

This type of configuration can be used in either closed or open system operations. Figure 24 shows how the concentration profiles are predicted to develop during the first few cycles of operation in a closed mode, based on the constant rate model. The model neglects axial diffusion, but quali-tatively it is apparent that axial mixing will tend to smooth out the square-wave profile into a shape more nearly resembling a sine wave.

4.3.1. Open System Operation of a back-to-back configuration

If feed is to be introduced, and products withdrawn, connections must be provided with valves that are timed to open at appropriate moments during the cycle. Since the total volume of the system remains constant, feed must
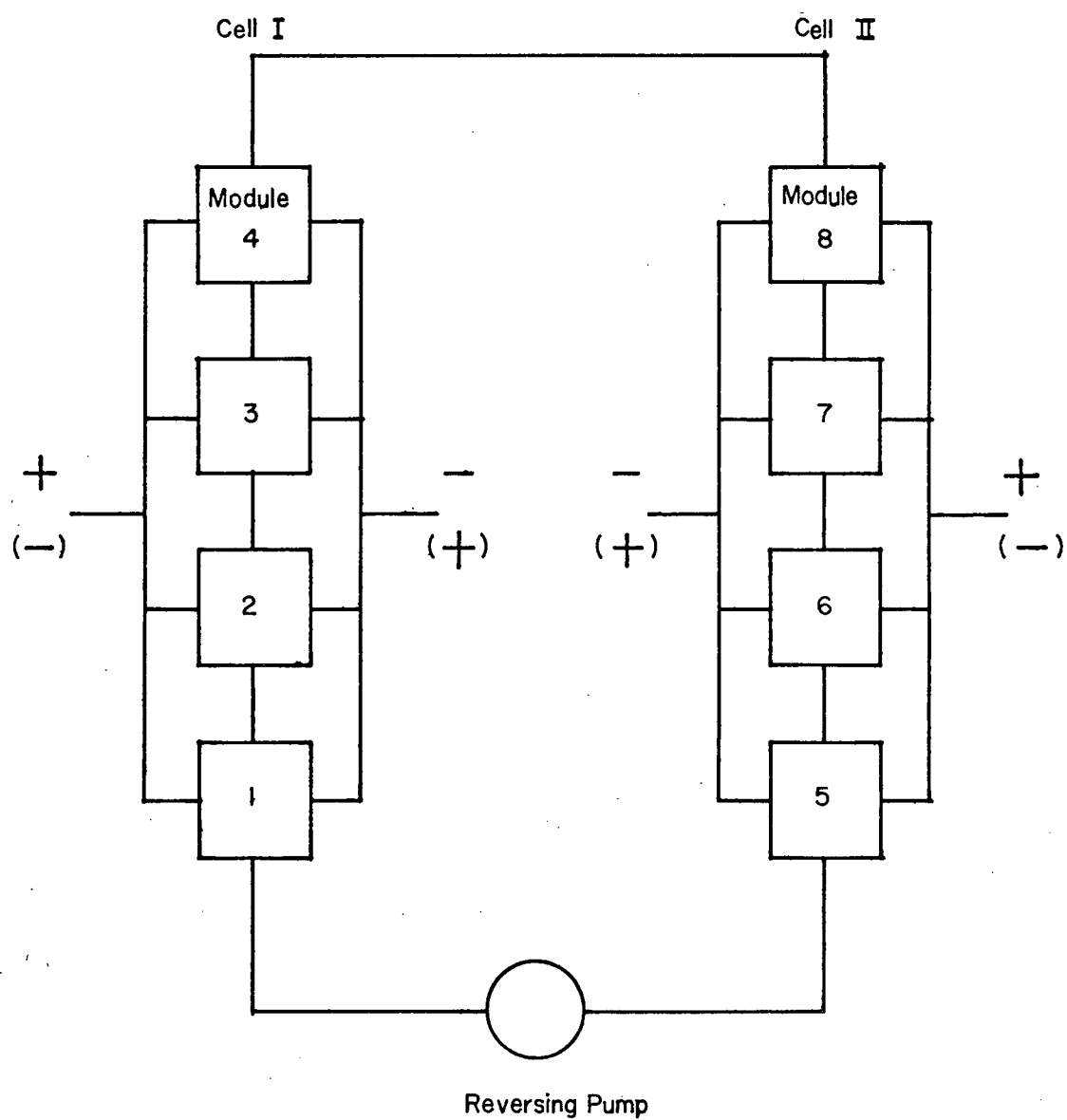
FIGURE 23

Back_to_back operation of two cells.

I   II

Top   Bottom   Top

C_0

t_0

t_1 Pause

t_2 Displace

t_3 Pause

t_4' Displace

t_1' Pause

t_2' Displace

t_3' Pause
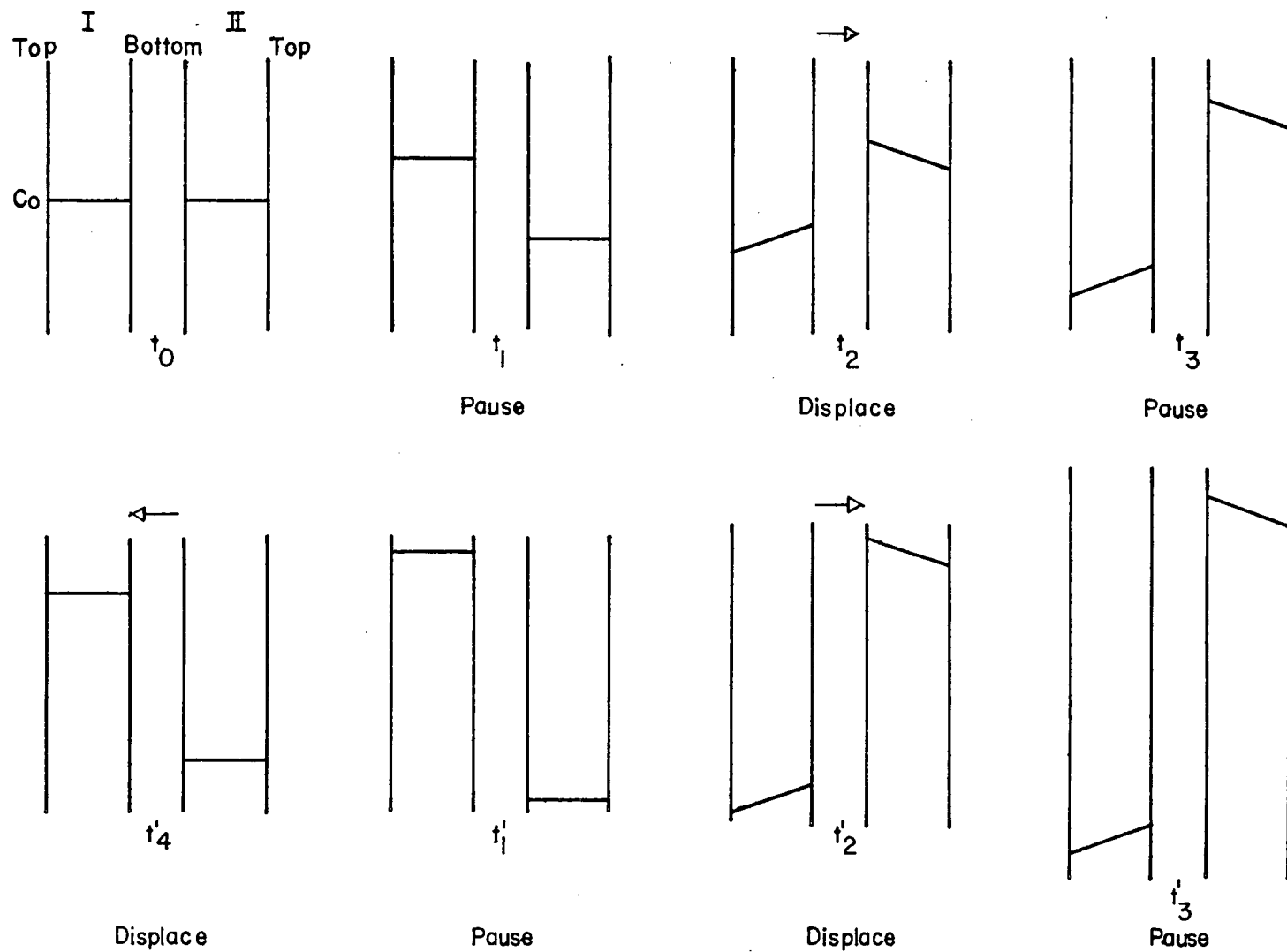
FIGURE 24

Developing concentration profile _ two cells operating back_to_back in a closed system.

be introduced whenever product is withdrawn. For best separation it would seem desirable to take products whenever maxima or minima in the concentration profiles pass the appropriate ports, and to introduce feed at a position where the circulating fluid is close to the feed composition. If the concentration profile around the loop comprising the two cells and their interconnections is approximately sinusoidal then feed introduction ports must be located 90° away from product removal ports.

Regarding the feed location and the feed timing, an open system can be run under either symmetric, semi-symmetric or asymmetric type of operation. In symmetric operation feed is introduced and products removed every half cycle with the feed being introduced to the top and bottom of each cell. In semi-symmetric operation feed is introduced every half cycle, but to one side only of each cell; while in the third mode of operation neither the feed location nor the feed timing is symmetrical, and the feed is introduced only once to one side of each cell every cycle.

Figure 25 represents a symmetric operation with product removal from the mid-points of each cell. It shows the required connections and the valve timing. In symmetric operation each cycle is subdivided into eight intervals t_i (i = 1,2, ... 8). The activity takes place at each time interval as shown in the table of Figure 25 which also shows the polarity of the of the electric field, the condition of the pump (i.e. whether idle or operating and in which direction), it also indicates the state of the various solenoid valves and which of them is energized (open) and which of them is closed during the specific time interval concerned. The developing concentration profile for this mode of operation is shown in Figure 26. Here the amount of feed introduced/cycle is $\frac{1}{3}$ of the total circulating volume.

FIGURE 25

Flow connections and valve timing sequence for symmetric operation.

Top Bottom tTop

I   II

C_0

t_0

t_1
Pause

t_2, t_3
Production

t_4
Circulation

C_0

t_5
Pause

t_6, t_7
Production

t_8
Circulation

t_1'
Pause

FIGURE 26

102
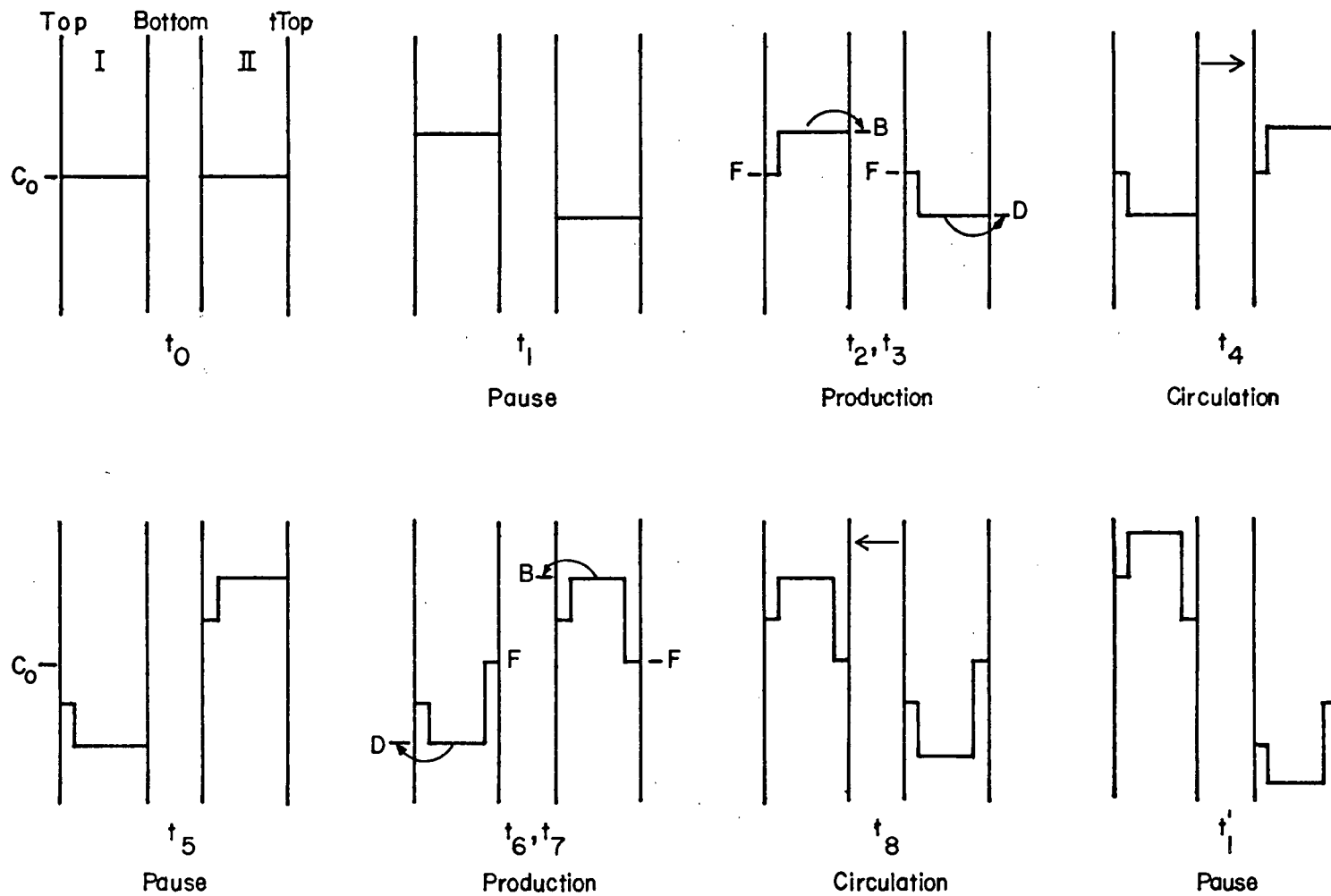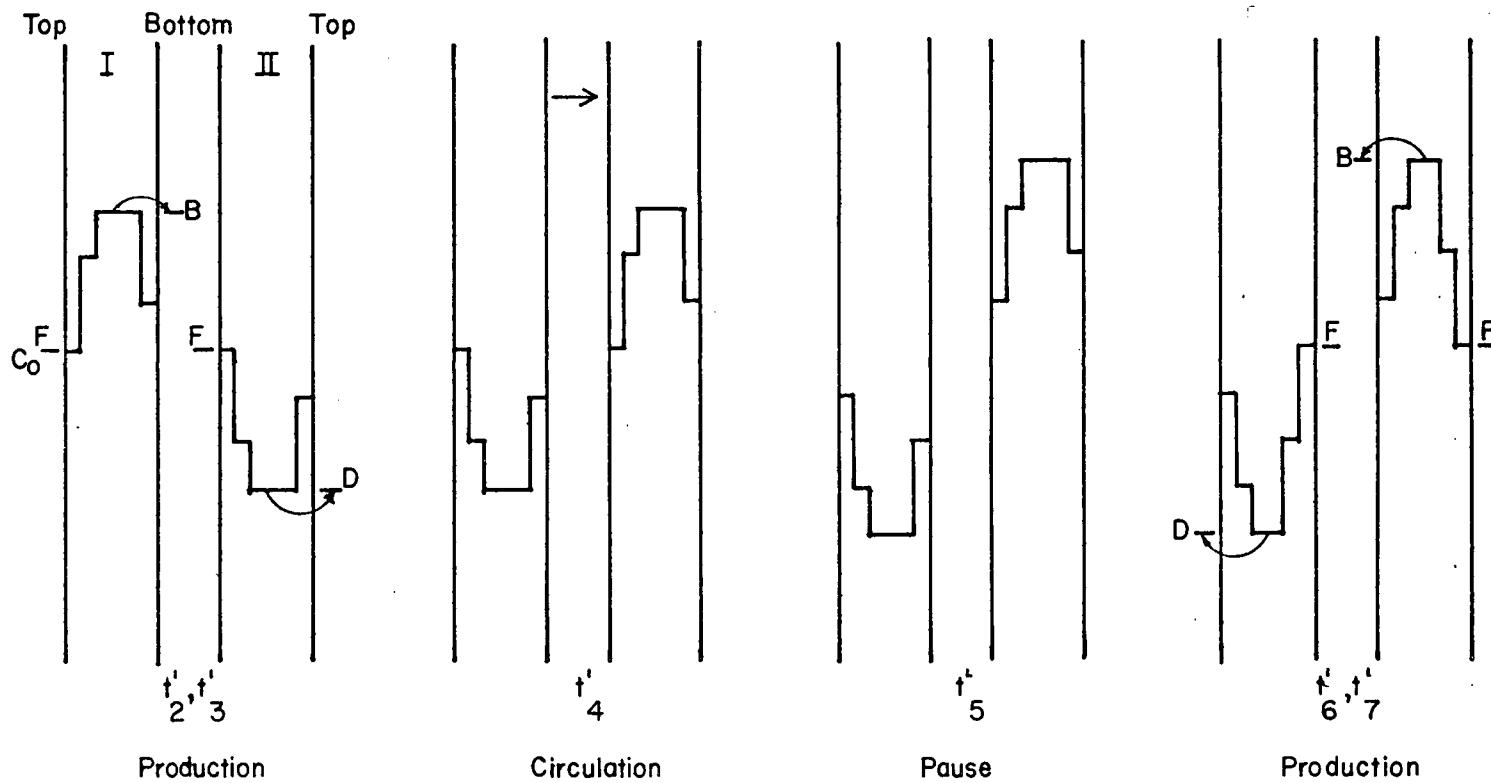
FIGURE 26 — Continued (I) .

Circulation
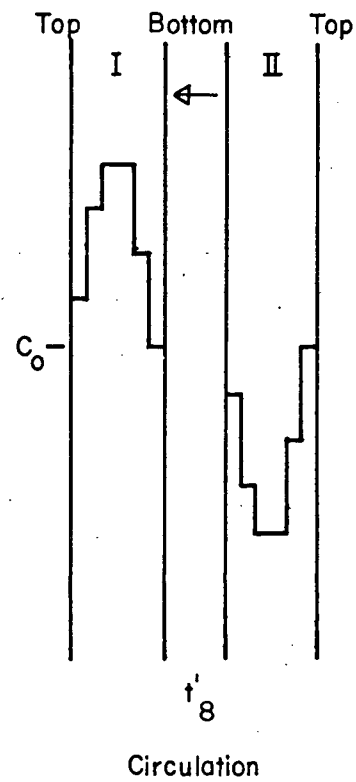
FIGURE 26 _ Continued (2)

FIGURE 26

Developing concentration profile, symmetric operation of an open system.

Figure 26 as well as Figure 28 and 30 ignore axial mixing effects, and

concentration changes during feed admission and displacement have been

omitted for clarity of presentation. The product will undergo

$2 \times \dfrac{\text{total circulating volume}}{\text{total feed volume}}$ cycles of enrichment or depletion before

emerging under this mode of operation. In these Figures vertical axis

indicates concentration level, a horizontal arrow shows circulation of

solution from one cell into another, and the letters F, D, B indicate the

concentration as well as the location in the cell where the feed, F is

introduced or the depleted and enriched products D and B are withdrawn.

Figure 27 represents a semi-symmetric operation with its connections

and valve timing sequence. Here the products are removed alternately from

the top of cell II and the bottom of cell I, while feed is supplied to

the top of cell I and the bottom of cell II. The waveform generated in

Figure 28 is of sawtooth shape, and the efficiency of this operating

cycle will depend on how well this waveform can be maintained under the

influence of axial mixing processes. It would be expected that this method

of operation would be more sensitive to axial mixing than the scheme shown

in Figure 25. In the absence of mixing, both cycles are predicted to give

equal separation (compare Figures 26 and 28).

Figure 29 shows an asymmetric operation. An operating cycle here

consists of six time intervals t_i (i = 1,2 ... 6) that constitute two non-

symmetric half cycles and it needs only 4 valves as indicated in Figure 29.

An asymmetric operation presents a further simplification of the system with-

out affecting its separating capability and results in the same separation

as that predicted by the previous modes of operation (compare Figures 26,

28 and 30).

Time Interval	Item / Operation	VI	V2	V3	V4	V5	V6	V7	Pump P	Vol_tage $\Delta\phi$
t_1	Pause	O	O	O	O	O	O	O	O	+
t_2	B from I	✓	O	O	O	O	O	✓	O	+
t_3	D from II	O	✓	O	✓	O	O	O	O	+
t_4	Circulation	O	O	✓	O	O	O	O	→	+
t_5	Pause	O	O	O	O	O	O	O	O	−
t_6	B from II	O	✓	O	O	O	✓	O	O	−
t_7	D from I	✓	O	O	O	✓	O	O	O	−
t_8	Circulation	O	O	✓	O	O	O	O	←	−

✓ = Valve open
O = Item idle

FIGURE 27

Flow connections and valve timing sequence for semi_symmetric operation.
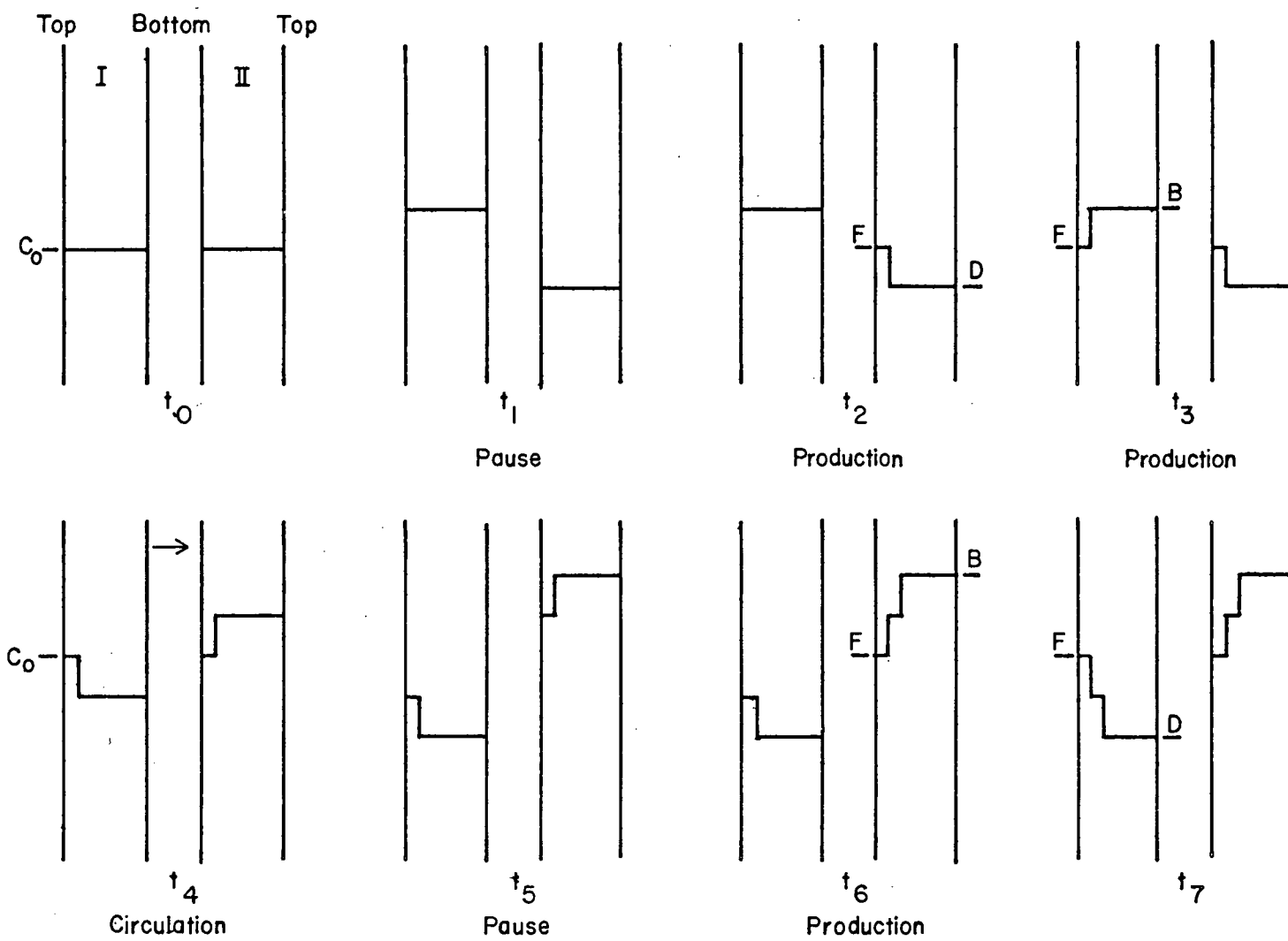
FIGURE 28

FIGURE   28 — Continued (1)

Top   Bottom   Top

I   →   II

C_0

t'_4

t'_5

t'_6 B   F   D

t'_7 F

Circulation   Pause   Production   Production
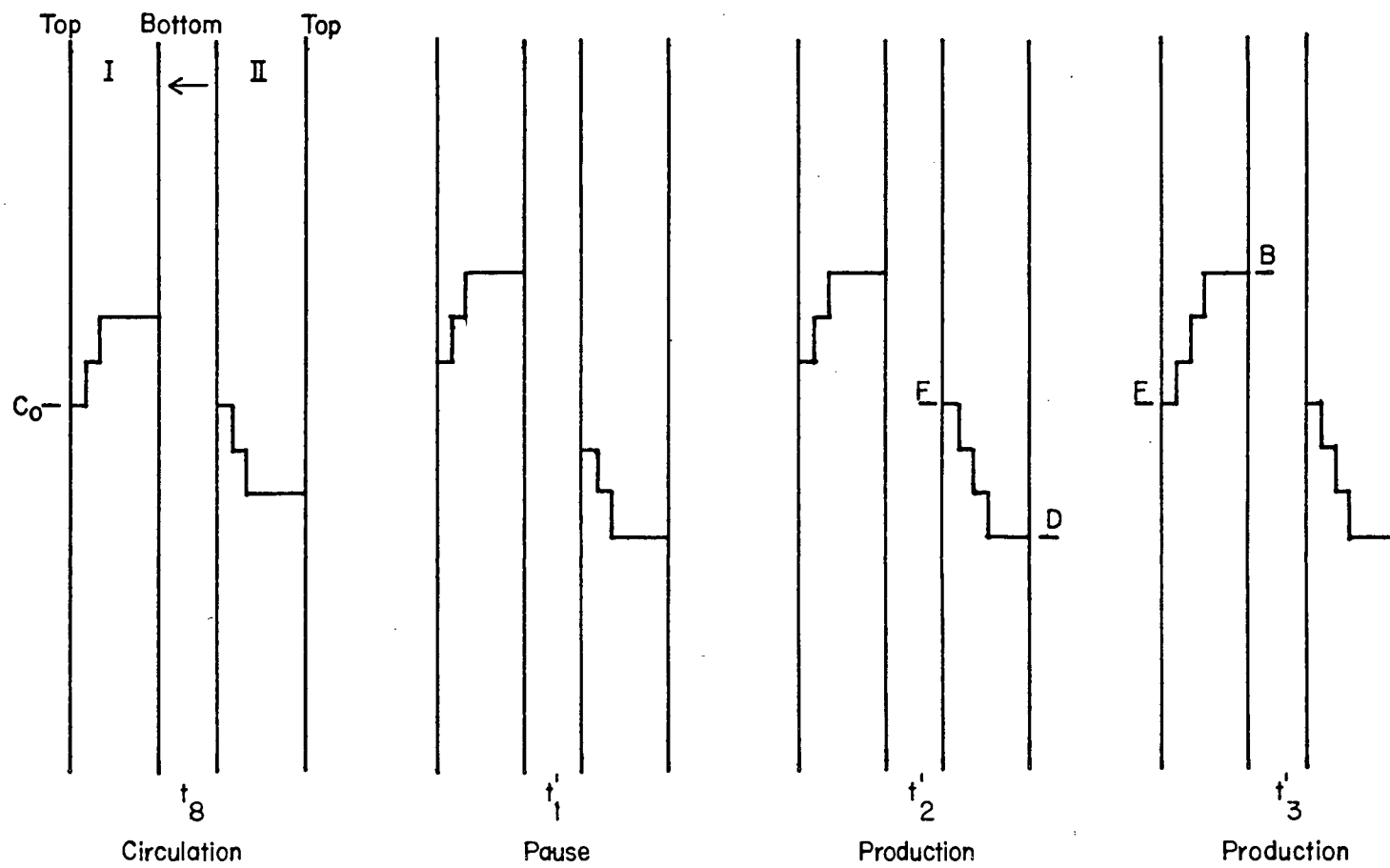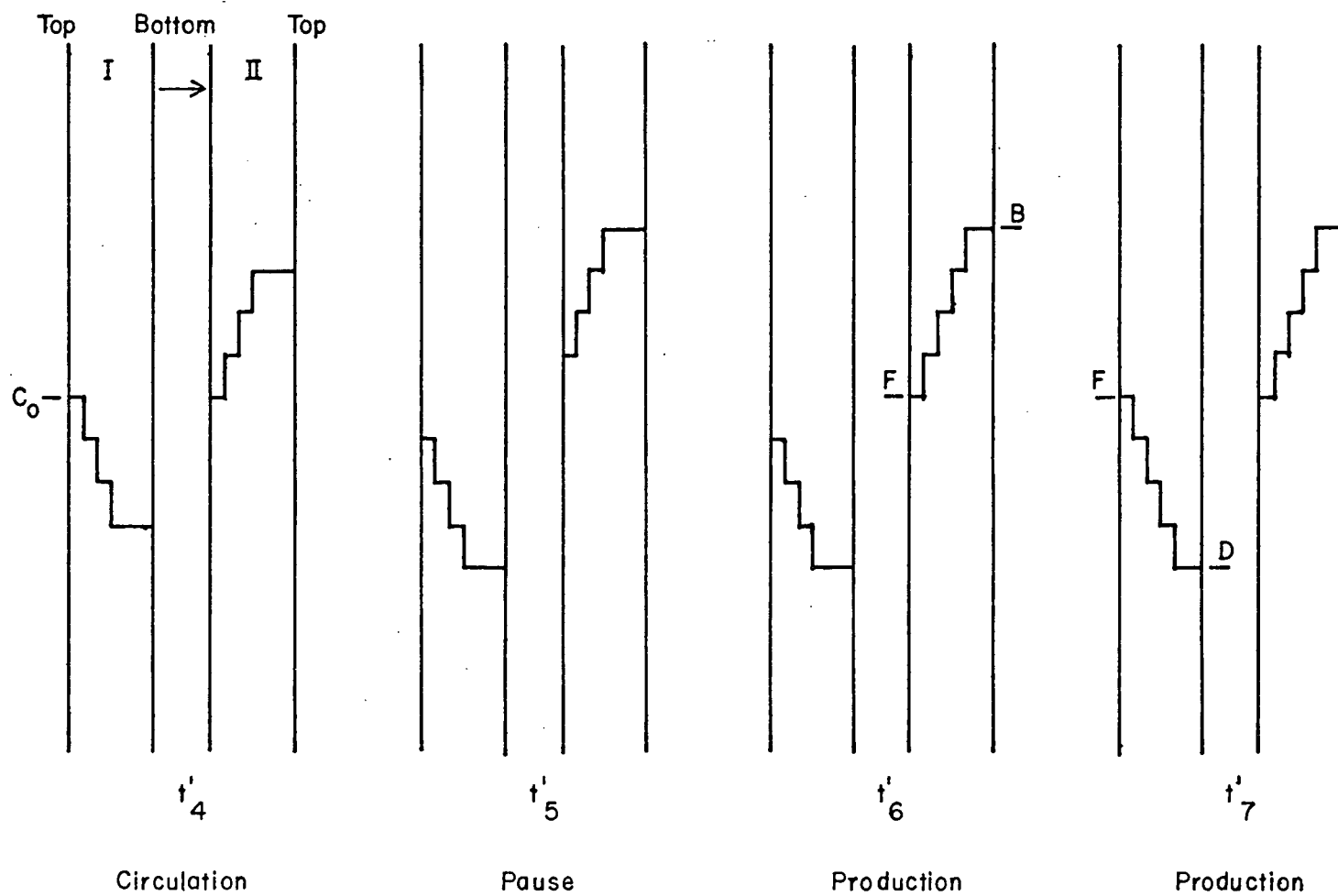
FIGURE 28 _ Continued (2).

109
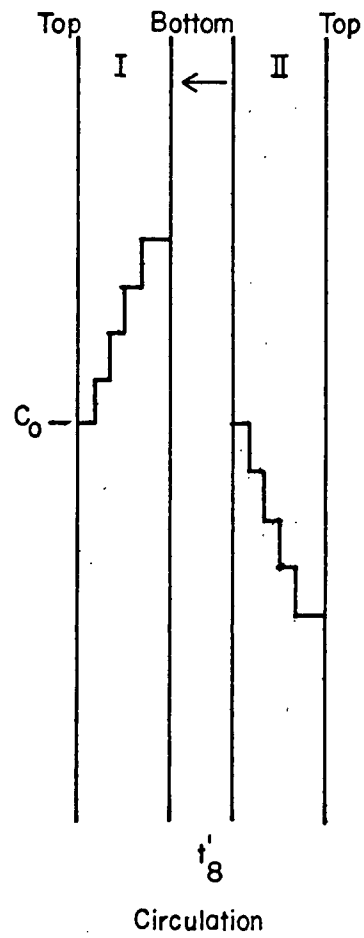
FIGURE 28 _ Continued (3),

FIGURE 28

Developing concentration profile , semi_symmetric operation of an open system .
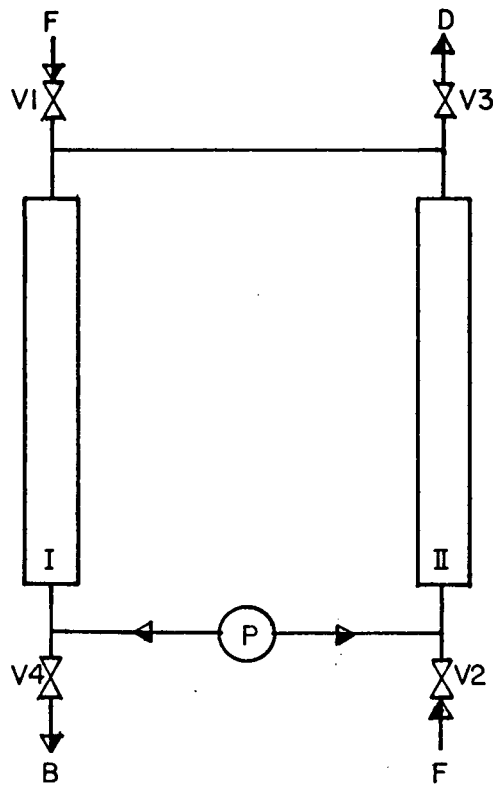
Time Interval	Item Operation	V1	V2	V3	V4	Pump P	Voltage $\Delta\phi$
t_1	Pause	O	O	O	O	O	+
t_2	B from I	✓	O	O	✓	O	+
t_3	D from II	O	✓	✓	O	O	+
t_4	Circulation	O	O	O	O	→	+
t_5	Pause	O	O	O	O	O	−
t_6	Circulation	O	O	O	O	←	−

✓ = Valve open
O = Item idle

FIGURE 29

Flow connections and valve timing sequence for asymmetric operation.

Top   Bottom   Top

I   II

C_0

t_0

t_1

Pause

t_2

Circulation

t_3

Pause

F

F   B

D

t_4, t_5

Production

t_6

Circulation

t'_1

Pause

t'_2

Circulation

FIGURE 30

112
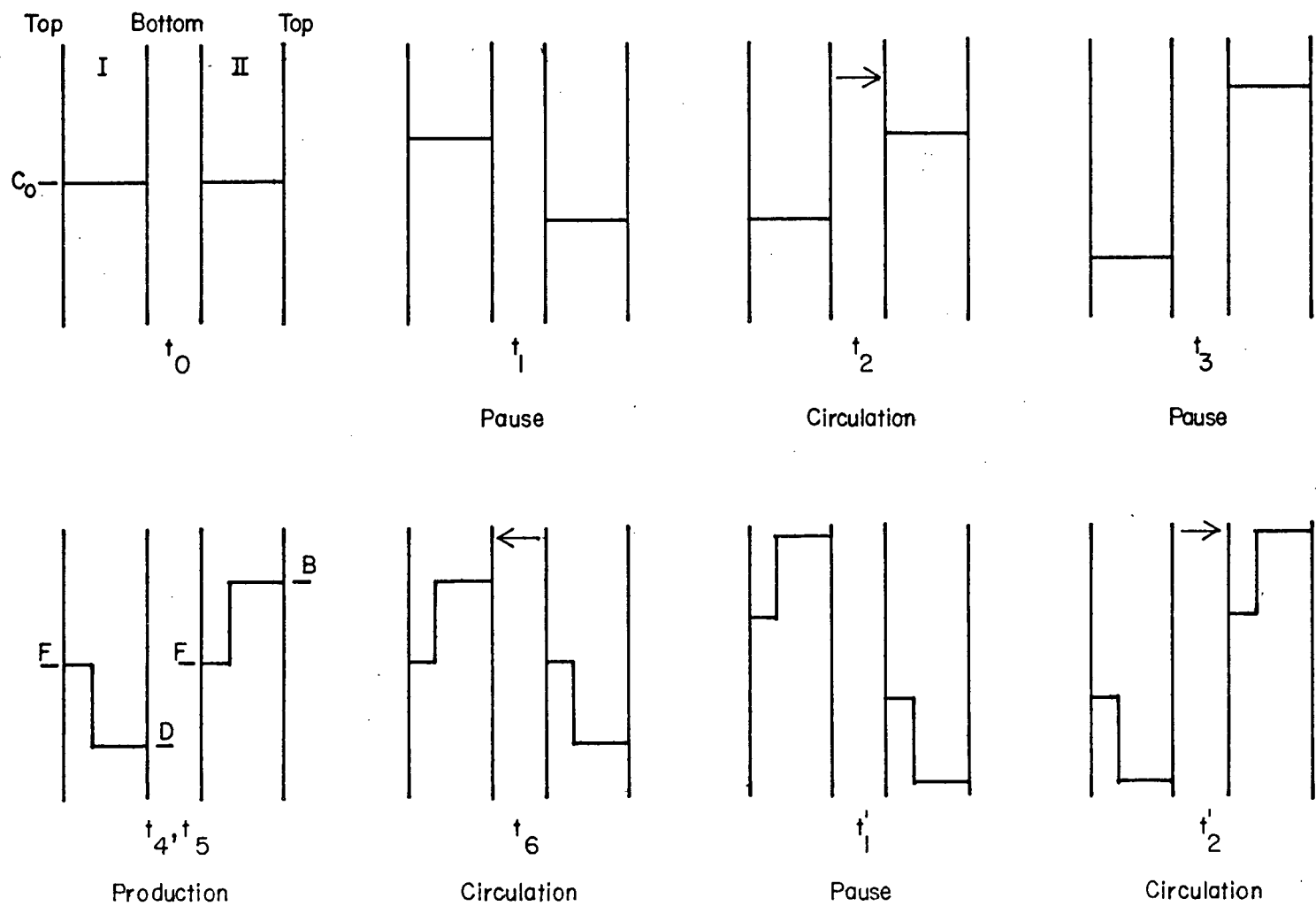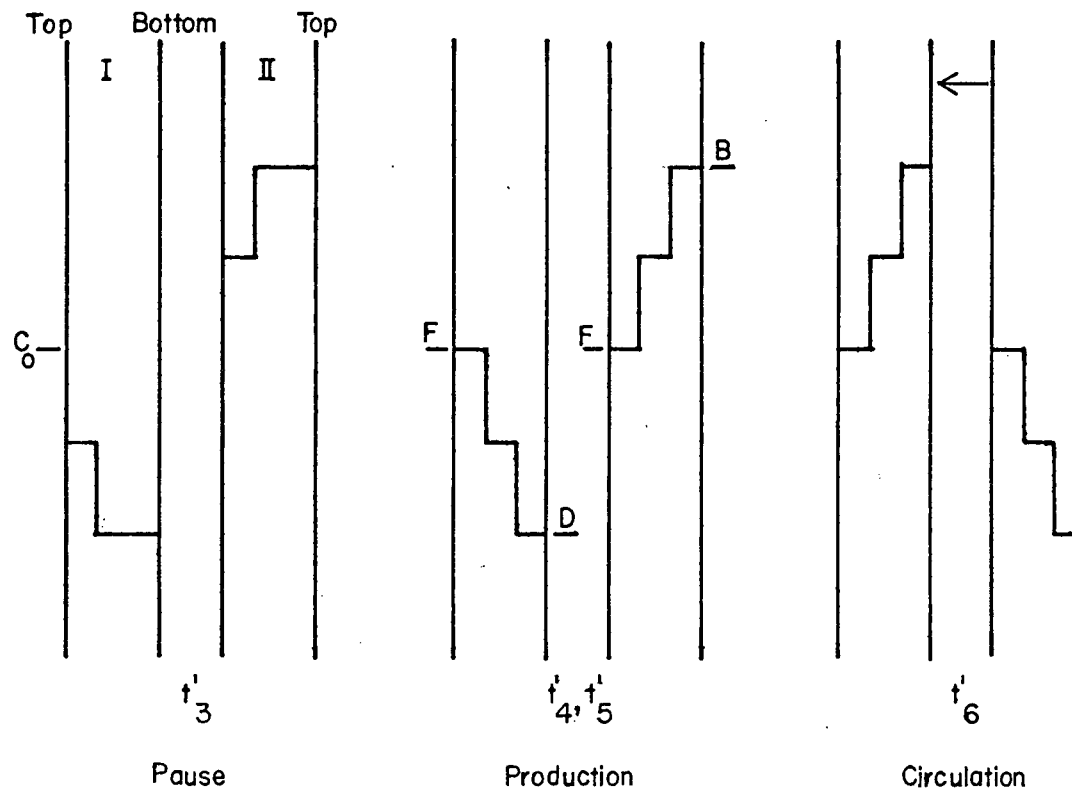
FIGURE 30 - Continued (I)

FIGURE 30 -

Developing concentration profile , asymmetric operation of an open system.

It can be concluded that when axial mixing is ignored all the three modes of operation considered here lead to the same separation. However, as can be seen from Figures 25, 27 and 29 the degree of complexity of the system and the valve economy and timing sequence decreases as the cycle becomes less symmetric.

4.4. Apparatus and Operation

A photograph of the completed unit is shown in Figure 31 which shows the control panel board with its timer, cycle counter, DC motor speed controller, DC power supply, conductivity meters, 4-pen recorder and switches.

The separating unit consists of two columns or cells which are depicted in Figure 32 and are represented by the boxes ED I and ED II in Figure 36 where they are shown connected to the process line, rinse loop, and the electric power supply.

An asymmetric cyclic operation was used here in which the system was open during the first half-cycle and was closed during the second half-cycle (Figure 29). During the first half-cycle the solution in cell II was depleted while that in cell I was enriched. The cycle started with a pause period t_1. This was followed by production periods; t_2, t_3 when the feed was introduced and an enriched product was removed from cell I for the time t_2 and a depleted product was removed from cell II for a period t_3. The first half-cycle was terminated by circulation of the solution from one cell into another. The second half-cycle consists only of a pause period t_5 followed by a circulation period t_6 when the solution was circulated in opposite direction.
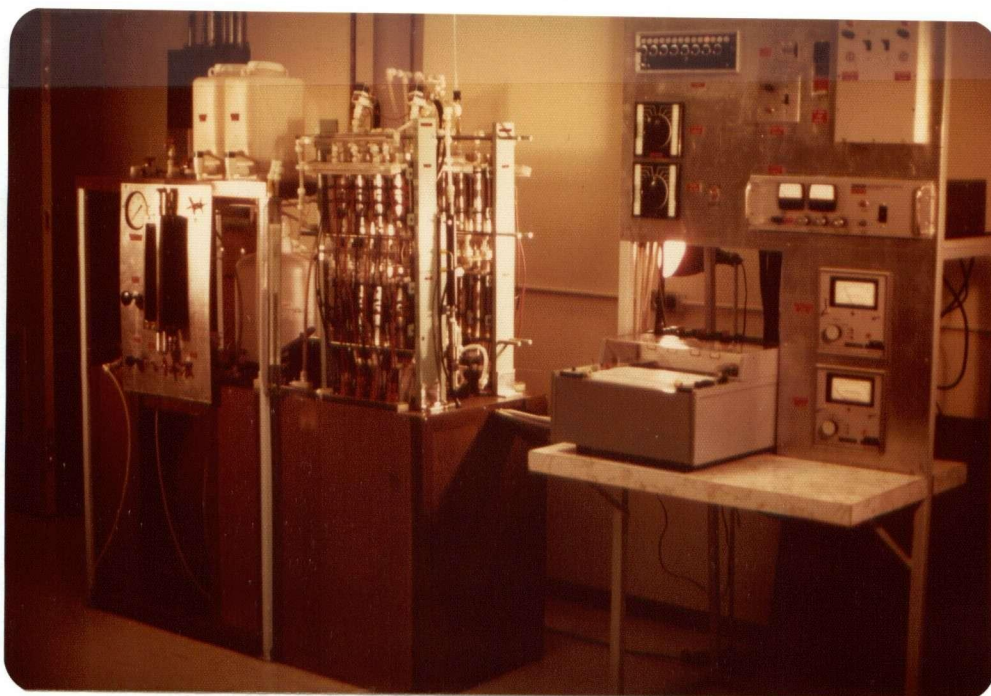
Figure 31   Electrodialysis Unit and Control Equipment
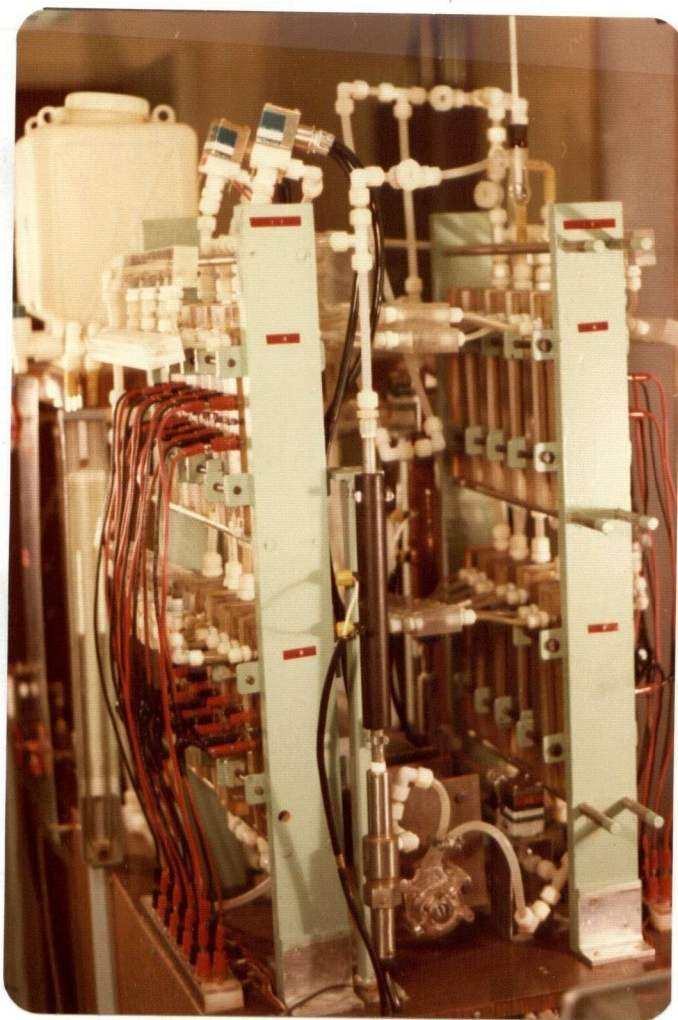
Figure 32   Electrodialysis Cells in Back-to-Back Operation

A block diagram of the experimental test stand is shown in Figure 36. The figure illustrates the way in which feed solution flows through the stack and the auxiliary equipment and it indicates the points at which the conductivities of the effluent streams, the voltage, the amperage were measured and recorded. The feed solution was introduced into the ED cells from a pressurized tank through the process line, which was an open ended line that terminated in the top and bottom products tanks. Four normally closed Dri-solenoid valves [VALCOR, series 51] were included in this line together with a reversible peristatic pump P1 [COLE-PARMER Model 7017] driven by a variable speed DC motor [CENTURY motor type DN, 0.25 HP and BOSTON motor speed controller Ratiotrol model E 25]. The circulating rate of the process solution was set by the motor controller of pump P1; and the flow direction was controlled by the reversing switch SW II.

A separate rinse solution was continually recirculated through the electrode compartments of the ED cells via distributing manifolds by the centrifugal pump P2 (COLE-PARMER model MDX-3, No. 7004-10). The circulating rinse stream served to remove products of electrolysis and any gases evolved at the electrodes were swept out and vented. The electrode wash liquor used was 2000-4000 ppm aqueous solution of sodium chloride and the flow rate was about 0.47 [litre/min] per compartment.

Regulated DC power was supplied to the ED cells from SORENSEN DCR40-10A power supply through the reversing switch SW I. A solid state timer was used to control the sequence of operation, energize the solenoid valves, switch and reverse the polarity of the motor armature, control the polarity of the electric field and give an impulse to an electromechanical counter by the end of each cycle.

4.3.1. Details of an ED Cell Design

A modular construction was used for the ED cells ED I and ED II. Each cell consists of up to eight separate stacks or stages connected together in series hydraulically and in parallel electrically (Figures 23, 32). Each stage as depicted by Figure 33 was built up from eight multilayer sorption membrane assemblies, clamped between plexiglas end-frames in a filter-press type of construction. The end frames held the graphite electrodes and incorporated flow connections for the process stream and the electrode rinse streams (Figure 33). Each assembled stage had an active void volume for the process fluid of 50 cm^3 plus a dead volume of about 5 cm^3.

The construction of one of the individual membrane assemblies is shown in Figures 34, 35. Each unit consisted of the following three components permanently bonded together:

(i) An outer low density polyethylene sealing frame (22.54 cm x 7.62 cm x 0.189 cm) with two key-shaped liquid distribution slots cut into each end.

(ii) A triple-membrane (capacity cell) 16.19 cm x 4.44 cm, composed of a cation selective membrane (AMF C-100 or IONAC MC-3142) and an anion selective membrane (AMF A-100 or IONAC MA-3148) enclosing a core of Whatman No. 1 filter paper (15.56 cm x 4.13 cm).

(iii) A flow channel of polypropylene spacer screen (17.00 cm x 4.60 cm x 0.098 cm) Vexar TP 23, 10 x 10 strands per inch, cut diagonally.

Half of the ion exchange membranes were purchased from American Machine and Foundry Corp., while the rest were obtained from Ionac Chemical Co. and the spacer material was kindly supplied by Du Pont of Canada.
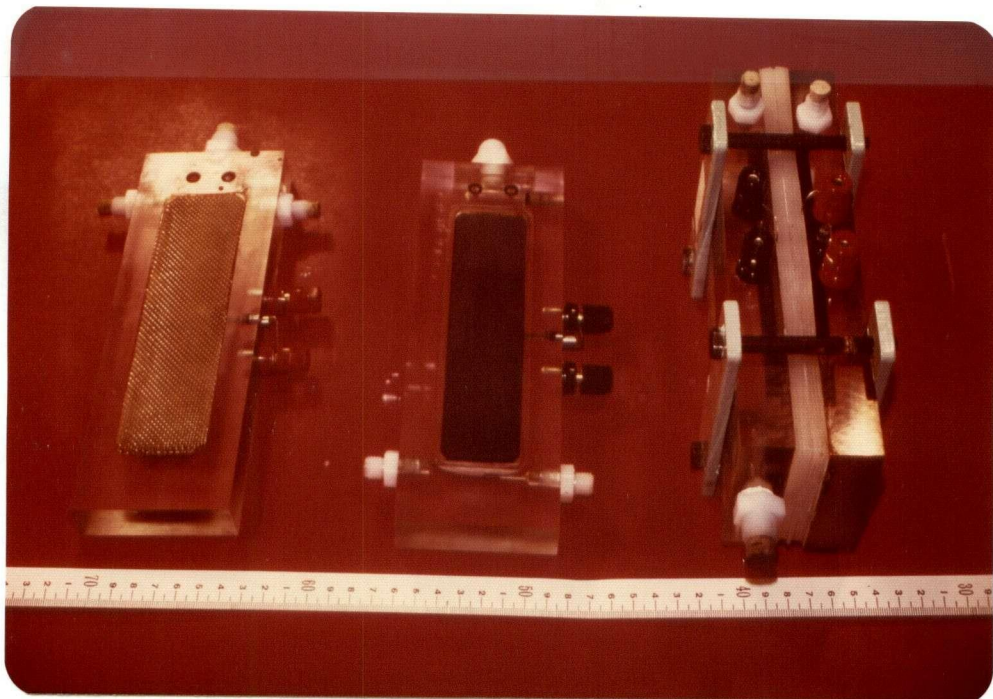
FIGURE 33

A single stage with its two end frames.

FIGURE 34

A triple membrane _ frame _ spacer assembly.

Section at A_A'   Elevation

Anionic
Membrane

Polypropylene
Spacer

Inlet/Outlet
Ports

A

Filter
Paper

Cationic
Membrane

Polyethylene
Frame

A'
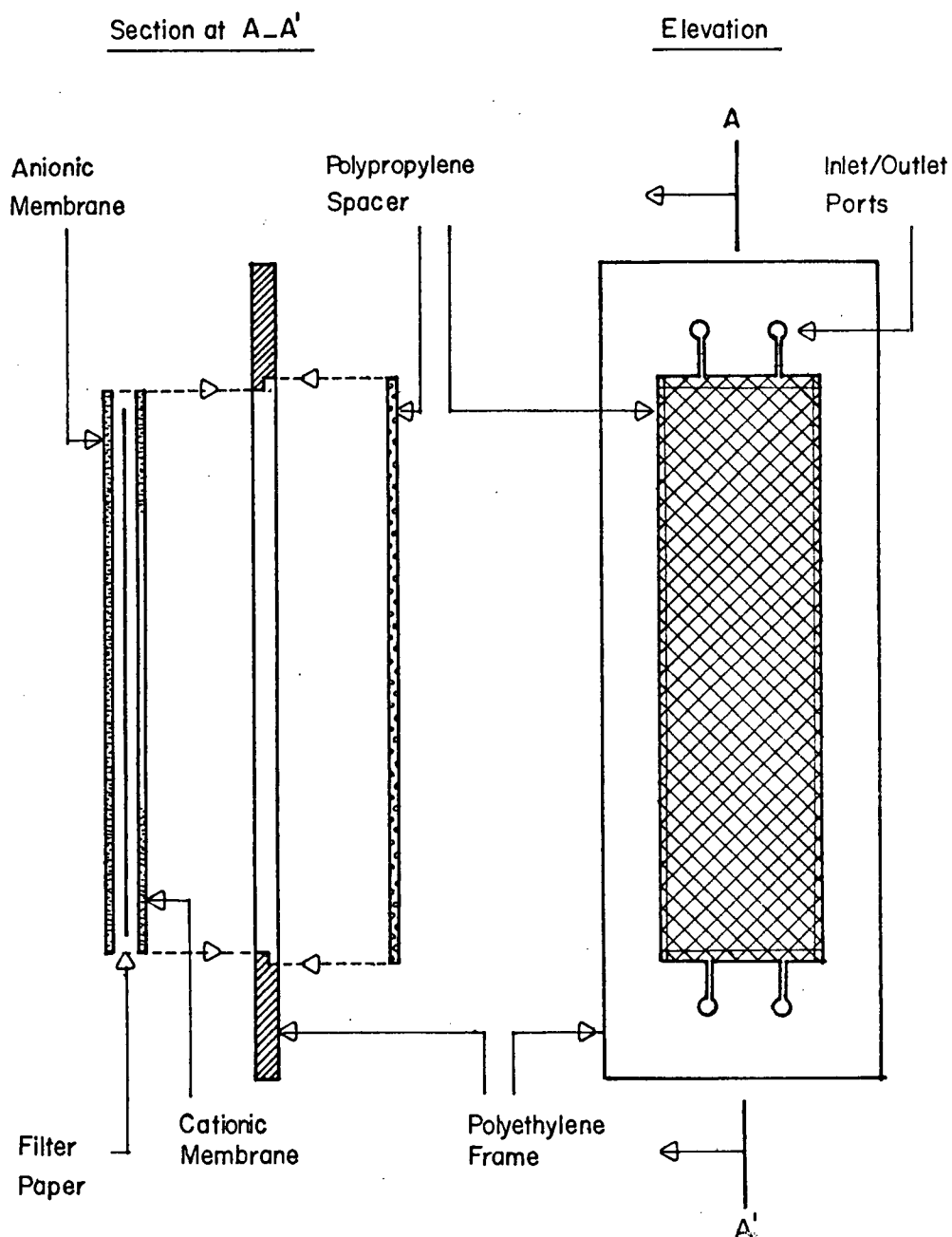
FIGURE 35

Construction of single membrane—spacer assembly for an ED cell
Each stack consisted of eight such assemblies, clamped between end
frames containing electrodes and flow connectors.
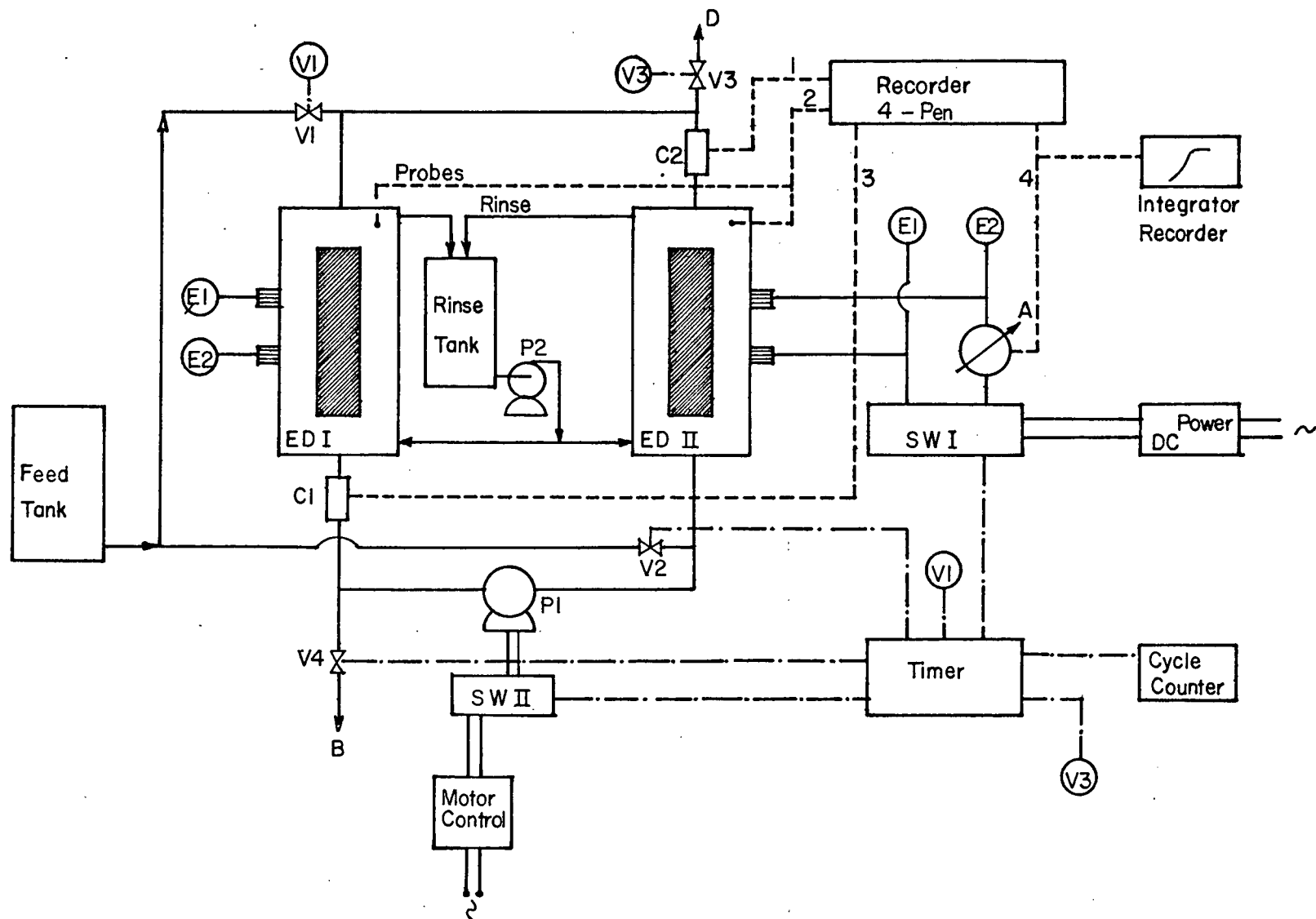
FIGURE 36

Schematic diagram showing solution flows and instrumentation.(Asymmetric operation.)

The membranes were heat sealed along both short sides. The long sides remained open to insert and to remove the filter paper. The polypropylene spacer screen was pressed into the frame by means of a heated jig. Then the triple membrane was tacked at three corners to the frame using a heated bar. A detailed construction procedure is given by Bass (Bass, 1972).

The manufacturer's specifications of the membranes used are given in Table V. Detailed definitions of the parameters and methods for their measurement are found in "Ion Exchange" by Helfferich (1962) and "Test Manual for Permselective Membranes, Research and Development Progress Report #77, Office of Saline Water, U.S. Department of Interior (1964 b).

4.5. Measuring and Recording

4.5.1. Concentrations, Current, Voltage and pH Measurements

(i) Concentrations

The concentrations of the process solution at two points indicated by positions C1, C2 in Figure 33 were continuously measured using epoxy flow-type conductivity cells [BECKMAN, CEL-VDJ] with automatic temperature compensators and direct-reading conductivity meters [BECKMAN, Solu-Meter RA5]. A 0 to 10 (mV) D.C. output signal from the Solu-Meter allowed potentiometric recordering of the concentration in the ranges shown in Table VI.

Accuracy of the type RA5 Solu-Meter indication is within 2% of the scale span. However the accuracy of the electrical output is within 1% of span.

Table V Reported Properties of Ion-Exchange Membranes

Type, Manufacturer and Designation / Property	Cation-Exchange		Anion-Exchange	
	AMF C-100	IONAC MC-3142	AMF A-100	IONAC MA-3142
Backing	Polyethylene		Polyethylene	
Active Group	Sulfonic Acid		Quaternized ammonium	
Area Resistance (ohm-cm^2)	7 (0.6N KCl)	9.1 (0.1N NaCl) 3.4 (1.0N NaCl)	8 (0.6N KCl)	10.1 (0.1N NaCl) 1.7 (1.0N NaCl)
Transference number of counterion (selectivity)[a]:				
(0.5/1.0N KCl or NaCl)	0.90	0.94	0.90	0.90
(0.2/0.1N NaCl)		0.990		0.999
Ion Exchange Capacity (meq/g)	1.3	1.06	1.5	0.96
Approximate thickness (mm)	0.015	0.015	0.018	0.018
Mullen Burst strength (psi)	60	185	50	190
Dimensional Changes on wetting and drying (%)	10-13	< 3	12-15	< 3
Size available	44 in. wide rolls	40 x 120 in.	44 in. wide rolls	40 x 120 in.

(a) Reported from concentration potentials measured between solutions of the two normalities listed.

Table VI

Conductivity and Na Cl Concentration Ranges of BECKMAN
conductivity Cells CEL-VDJ corresponding to a 0-10 [mV]
D.C. Signal from a BECKMAN Solu-Meter RA5.

Cell Constant K [cm^{-1}]	Conductivity [micromhos/cm]	Na Cl Solution Concentration [PPM]
20	0-10,000	0-5,500
50	0-25,000	0-14,800
100	0-50,000	0-30,800

After every run samples of the depleted and enriched products were taken and their concentrations were measured using an epoxy dip Cell [BECKMAN, CEL-VH1-10] together with a conductivity bridge [BECKMAN, Model RC 16B2] with scale multiplier $10^{-2} - 10^{+3}$.

(ii) Current

The current input was measured as a potential drop across a Nichrome resistance wire (14 gauge), shunt A in Figure 36. The shunts were integrated into the electrical manifold which distributed the D.C. power from switch box SW I to the stages. The wiring is shown in Figure 37. The shunt resistances were 50.0 [mΩ] $\pm$ 1.5% for the currents to the individual stages and 25.0 [mΩ] for the total current.

(iii) Voltage

Probe electrodes were prepared from silver wire cable which was hammered into strips approximately 3 mm wide and 0.12 mm thick. The strips were dip coated with contact cement (Weldwood of Canada Limited) and the coating was removed from one side of the tip which was located inside the stack. The probes were inserted between the separating membranes and the stack pack and sealed with silicon grease (Dow Corning). A second selector switch was connected to the probes and to one recorder pen. The circuit was analogous to the one shown in Figure 37; but without shunts.

(iv) pH

Samples for pH-checks were taken for some runs just prior to the experiment and immediately thereafter from the two process products and rinse stream and measured in the usual way (using CORNING digital electrometer model 101).
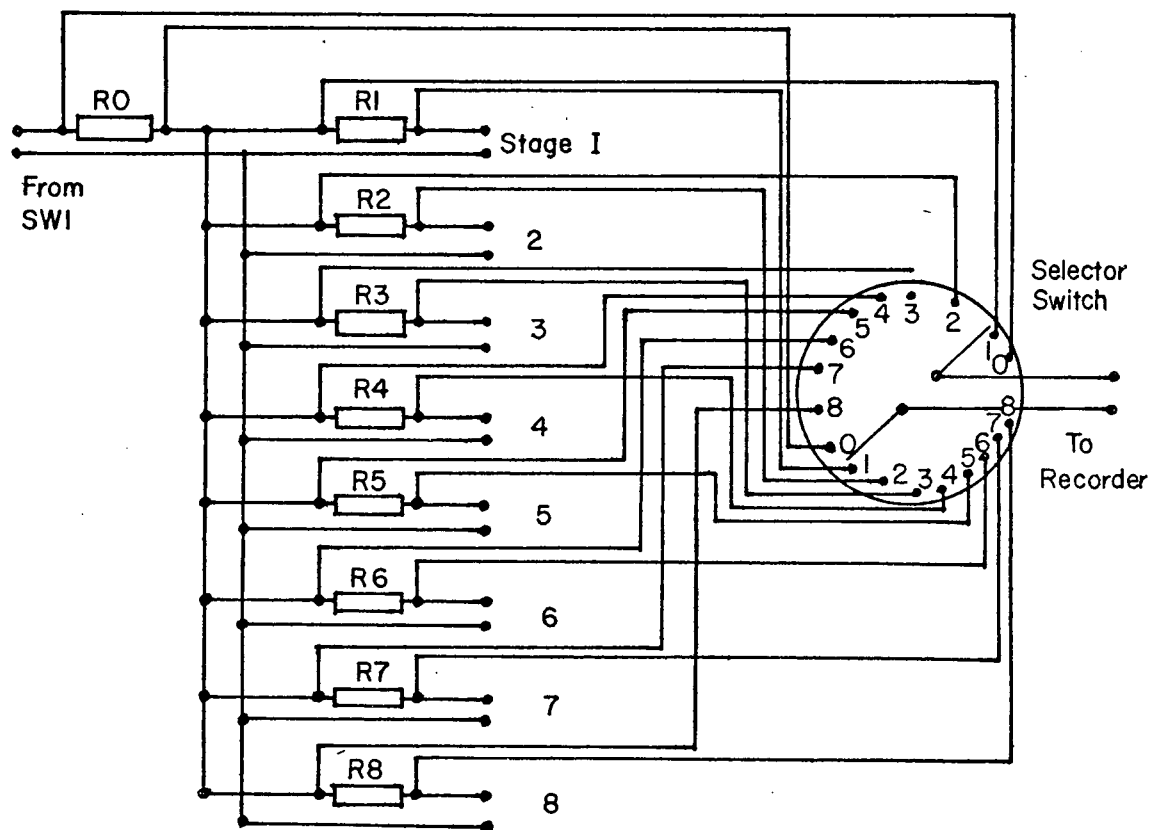
FIGURE 37

Current monitoring circuit.

4.5.2. Recording

A four-channel recorder (WATANABE Multicorder, Model MC6-11 S4H) was used to continuously monitor the current input to the cells, the potential drop across the membrane stack, and the solute concentrations in the bottom and top conductivity cells C1 and C2 (Figure 36).

The stack voltage and the current consumption are measured individually for each stage. However, because of the limited number of pens only one voltage and one current signal are recorded at a time using two selector switches.

The current signal was integrated during several experiments, using a CORNING Recorder 840, to determine the average current consumption.

CHAPTER 5

Experimental Results and Discussion

The primary objectives of the experimental program have been outlined

before (Chapter 4). In the present work altogether 252 runs were made.

These are compiled in the main survey tables (Tables IX-XVI), which show the

operating conditions, production rates and the separation achieved in each run.

These survey tables are followed by group tables and diagrams that illustrate

the effect of single variables under otherwise fixed conditions.

5.1. Data Collection

The collection of raw data during the course of a complete run consisted

of the following consecutive steps:

1. Fill rinse tank with 7.5 liters of fresh rinse liquor (NaCl in

distilled water, with the same concentration as the process stream but not

less than 1000 ppm NaCl).

2. Fill the feed tank with solution of desired concentration (NaCl in

distilled water) and adjust the pressure in the feed tank to about 8 psig.

3. Fill system with the process solution from the pressurized feed tank.

4. Start rinse pump.

5. Set the timer and the peristaltic pump speed and run the system with

power off for few cycles to equilibrate sorption membrane with process solution.

6. Adjust check point of conductivity meters.

7. Select recorder pen ranges and chart speed.

8. Take concentration and pH samples of process and rinse solutions.

9. Set the timer off to bring the equilibrated process solution to

a pause before starting the run.

10. Turn cycle counter back to zero.

11. Set operating conditions (final adjustment of the timer and the applied D.C. voltage).

12. Note down date, operating conditions, variable recorded by each pen and appropriate range, chart speed.

13. Set the timer on and close electric power circuit simultaneously to start the first pause interval in the first cycle.

14. When the system approaches its periodic steady state as indicated by the recorded values of concentrations. Empty the product tanks, measure the volumes and note the cycle number. Discard products obtained in this transition period.

15. Record current and voltage signals at different stations by manipulating selector switches, and mark pen traces accordingly.

16. Write down any observation related to experiment.

17. Terminate run when sufficient products are produced and all information regarding current and voltage signals at the various stations have been obtained.

18. Measure the total amount of products produced and read the total number of cycles to find and record the production rates.

19. Take samples of process and rinse streams to measure pH and con-centrations.

20. Record the measured values.

5.2. Experimental Designation

The experiments reported here fall into two main categories:

(i) Category R which refer to the first set of experiments conducted in two columns each consisted of 4 cells or stages connected together in series hydraulically and in parallel electrically (Tables IX-XI).

(ii) Category M which refers to the second set of experiments performed

in columns with double the length of those used in Category R (Tables XII-XIV).

Each experiment in these categories is designated by either $Rn\alpha$ or $Mn\alpha$ where n is a number which refers to a specific combination of a feed concentration (C_o) and a production rate (P.R.). Three feed concentrations $(C_o \simeq 500, 2000$ and 4000 ppm NaCl) and four production rates (P.R. $\simeq 0.0$, 25, 50 and 100 c.c./cycle) have been used which result in 12 combinations and n assumes the values 1,2, ... 12 as shown in Table VII. α is a letter which represents a specific combination of applied voltage $(\Delta\phi)$ and the pause time (τ). Three voltages $(\Delta\phi = 10, 20$ and 30 volt) and three pause times $(\tau = 15$, 30 and 45 sec.) have been investigated which lead to 9 combinations and α is symbolized by any of the letters A, B, ... I as shown in Table VIII.

5.3. Main Survey Tables

The columns of the main survey tables are (see Tables IX-XVI):

1. EXP Group: This shows the experiment category R or M and the n-value (n = 1, 2, ... 12).

2. Production Rate: of each product (demineralized and concentrated) in c.c./cycle.

3. Feed Concentration: in parts per million NaCl in distilled water.

4. EXP Symbol: the symbol of α in the experimental designation $Rn\alpha$ or $Mn\alpha$.

5. Applied Voltage: the constant voltage supplied by the regulated D.C. power source in volts.

6. Pause Time: in each half cycle in seconds.

7. Brine Concentration:

9. Dialysate Concentration: both measured conductometrically and converted by means of calibration curves into concentrations in parts per million NaCl.

Table VII   Values of n in Experimental Designations
            Rnα and Mnα

Value of n	Operating Parameters	Feed Conc. C_o (ppm)	Production Rate p.p. (c.c./cycle)
1			25
2		2000	0
3			50
4			100
5			25
6		500	0
7			50
8			100
9			25
10		4000	0
11			50
12			100

Table VIII   Values of α in Experimental Designations
             Rnα and Mnα

Operating Parameters α	APPLIED VOLTAGE, $\Delta\phi$ (volt)	PAUSE TIME, τ (sec)
A		30
B	20	45
C		15
D		15
E	30	30
F		45
G		45
H	10	30
I		15

8. <u>Brine Volume:</u>

10. <u>Dialysate Volume:</u> These are the production rates of the two product streams expressed in c.c. per cycle.

11. <u>Separation Factor (ns):</u> Defined as the ratio of brine (bottom product) to dialysate (top product) concentrations

$$ns = \frac{c_B}{c_D}$$

The main survey tables of all successful experiments in category R and M are presented on the following pages. Successful means not interrupted by mechanical, electrical or human failure.

5.4. Parameters and Modes of Operation Investigated

(a) <u>Parameters</u>

The parameters which are studied are:

1. Demineralizing path length.

2. Production rate.

3. Pause time, τ. The total cycle time T is the summation of pause time, τ which is variable, the circulation time t_c which is kept constant and production time t_p which varies between 1.5-6.0 sec depending on the amount of product.

4. Applied voltage, $\Delta\phi$

5. Initial concentration, C_o.

(b) <u>Modes of Operation</u>

The following modes of operation were considered:

6. No-pause operation.

7. No-power during circulation operation.

8. Semi-symmetric operation.

Each of these parameters or modes of operation is analysed separately by forming groups of experiments in which the other parameters are constant.

Table IX Compilation of Experiments with Initial Concentration (Co) of 2000 PPM
Two Columns, Each consists of 4 Cells in Series

1	2	3	4	5	6	7	8	9	10	11
EXP. GROUP	PRODUCTION RATE (C.C./CYCLE)	FEED CONC. (PPM)	EXP. SYMBOL	APPLIED VOLTAGE (VOLT)	PAUSE TIME (SEC)	BRINE		DIALYSATE		SEPARATION FACTOR
						CONC. (PPM)	VOLUME (C.C./CYCLE)	CONC. (PPM)	VOLUME (C.C./CYCLE)	ns
R2	0.0	1950	A		30	3730		212		17.59
			B	20	45	4310		135		31.93
			C		15	3320		415		8.00
		1950	D		15	3450		239		14.44
			E	30	30	4435		133		33.35
			F		45	4800		101		47.52
		1950	G		45	3380		470		7.19
			H	10	30	3020		550		5.49
			I		15	2800		880		3.18
R1	20	1950	A		30	3560	18.80	400	19.83	8.90
			B	20	45	3770	18.19	290	19.80	13.00
			C		15	3310	17.90	580	18.30	5.71
		1950	D		15	3410	17.94	455	18.11	7.49
			E	30	30	3900	17.20	280	19.80	13.93
			F		45	4025	17.73	195	19.86	20.64
		1950	G		45	3300	17.55	735	18.16	4.49
			H	10	30	3010	18.10	820	18.20	3.67
			I		15	2795	18.00	1020	18.13	2.74

Table IX   (Continued)

1	2	3	4	5	6	7	8	9	10	11
EXP. GROUP	PRODUCTION RATE (C.C./CYCLE)	FEED CONC. (PPM)	EXP. SYMBOL	APPLIED VOLTAGE (VOLT)	PAUSE TIME (SEC)	BRINE CONC. (PPM)	BRINE VOLUME (C.C./CYCLE)	DIALYSATE CONC. (PPM)	DIALYSATE VOLUME (C.C./CYCLE)	SEPARATION FACTOR ns
R3	50	1950	A		30	3200	47.38	640	48.30	5.00
			B	20	45	3460	47.41	480	48.62	7.21
			C		15	2850	47.88	990	48.25	2.88
		1950	D		15	3180	47.15	830	49.85	3.83
			E	30	30	3500	47.34	450	49.69	7.78
			F		45	3720	46.46	310	49.83	12.00
		1950	G		45	2780	47.14	1130	48.33	2.46
			H	10	30	2615	47.64	1290	48.14	2.03
			I		15	2370	46.54	1550	48.08	1.53
R4	100	2055	A		30	3050	96.20	1115	98.90	2.74
			B	20	45	3270	96.54	870	98.75	3.76
			C		15	2580	96.23	1545	97.87	1.67
		2055	D		15	2910	96.94	1190	97.11	2.45
			E	30	30	3300	97.83	790	98.10	4.18
			F		45	3615	97.89	515	98.21	7.02
		2055	G		45	2620	97.22	1465	98.50	1.79
			H	10	30	2500	97.15	1590	98.43	1.57
			I		15	2400	96.88	1725	98.13	1.39

Table X Compilation of Experiments with Initial Concentration (Co) of 500 PPM
Two Columns, Each Consists of 4 Cells in Series

1	2	3	4	5	6	7	8	9	10	11
						BRINE		DIALYSATE		SEPARATION FACTOR
EXP. GROUP	PRODUCTION RATE (C.C./CYCLE)	FEED CONC. (PPM)	EXP. SYMBOL	APPLIED VOLTAGE (VOLT)	PAUSE TIME (SEC)	CONC. (PPM)	VOLUME (C.C./CYCLE)	CONC. (PPM)	VOLUME (C.C./CYCLE)	ns
R6	0.0	530	A		30	1447		24.5		59.06
			B	20	45	1915		23.7		80.80
			C		15	1300		28.2		46.10
		530	D		15	1790		24.4		73.36
			E	30	30	1833		19.2		95.47
			F		45					
		530	G		45	1332		86.0		15.49
			H	10	30	1160		101.0		11.49
			I		15	1042		157.0		6.64
R5	20	530	A		30	1070	17.91	31.5	19.14	33.97
			B	20	45	1110	17.19	24.0	19.38	46.25
			C		15	1040	17.94	41.0	19.11	25.37
		530	D		15	1070	17.75	25.0	19.80	42.80
			E	30	30	1125	17.15	20.4	19.79	55.15
			F		45	1150	17.14	16.8	19.82	68.45
		530	G		45	970	17.97	95.0	19.16	10.21
			H	10	30	940	17.95	123.0	19.03	7.64
			I		15	850	17.94	214.0	19.00	3.97

Table X   (Continued)

EXP. GROUP	PRODUCTION RATE (C.C/CYCLE)	FEED CONC. (PPM)	EXP. SYMBOL	APPLIED VOLTAGE (VOLT)	PAUSE TIME (SEC)	BRINE CONC. (PPM)	BRINE VOLUME (C.C./CYCLE)	DIALYSATE CONC. (PPM)	DIALYSATE VOLUME (C.C./CYCLE)	SEPARATION FACTOR ns
R7	50	510	A		30	980	47.43	38	49.14	25.79
			B	20	45	1020	46.15	30	48.30	34.00
			C		15	960	47.87	48	48.10	20.00
		510	D		15	1016	46.17	40	49.63	25.40
			E	30	30	1044	46.14	32	49.89	32.63
			F		45	1055	46.13	27	49.87	39.07
		510	G		45	928	46.96	103	48.04	9.01
			H	10	30	900	47.85	130	49.13	6.92
			I		15	796	47.89	221	48.11	3.60
R8	100	500	A		30	935	96.94	66	97.14	14.17
			B	20	45	950	96.72	57	97.80	16.67
			C		15	915	96.16	103	97.84	8.88
		500	D		15	920	97.80	76	98.28	12.11
			E	30	30	948	96.30	57	96.87	16.63
			F		45	960	96.15	52	98.31	18.46
		500	G		45	852	96.26	153	97.59	5.57
			H	10	30	800	97.40	200	97.72	4.00
			I		15	706	96.03	298	98.17	2.37

Table XI   Compilation of Experiments with Initial Concentration (Co) of 4000 PPM
Two Columns, Each consists of 4 Cells in Series

1	2	3	4	5	6	7	8	9	10	11
EXP. GROUP	PRODUCTION RATE (C.C./CYCLE)	FEED CONC. (PPM)	EXP. SYMBOL	APPLIED VOLTAGE (VOLT)	PAUSE TIME (SEC)	BRINE CONC. (PPM)	BRINE VOLUME (C.C./CYCLE)	DIALYSATE CONC. (PPM)	DIALYSATE VOLUME (C.C./CYCLE)	SEPARATION FACTOR ns
R10	0.0	3670	A	20	30	4980		2080		2.39
			B	20	45	5500		1645		3.34
			E	30	30	5535		1250		4.43
			F	30	45	6210		900		6.90
R9	20	3670	A	20	30	4900	17.73	2475	19.18	1.98
			B	20	45	5400	17.80	2020	19.20	2.67
			E	30	30	5420	18.61	1750	18.72	3.10
			F	30	45	6150	18.13	1350	18.96	4.56
R11	50	3670	A	20	30	4700	47.50	2645	48.75	1.78
			B	20	45	5020	47.24	2280	48.34	2.20
			E	30	30	5300	47.45	2120	48.25	2.50
			F	30	45	5700	46.85	1655	47.95	3.44
R12	100	3720	A	20	30	4520	96.25	2970	98.35	1.52
			B	20	45	4700	96.10	2660	98.35	1.77
			E	30	30	4850	96.74	2540	98.00	1.91
			F	30	45	5330	96.92	2150	98.85	2.48

Table XII Compilation of Experiments with Initial Concentration (Co) of 2000 PPM
Two Columns, Each Consists of 8 Cells in Series

1	2	3	4	5	6	7	8	9	10	11
						BRINE		DIALYSATE		SEPARATION
EXP. GROUP	PRODUCTION RATE (C.C./CYCLE)	FEED CONC. (PPM)	EXP. SYMBOL	APPLIED VOLTAGE (VOLT)	PAUSE TIME (SEC)	CONC. (PPM)	VOLUME (C.C./CYCLE)	CONC. (PPM)	VOLUME (C.C./CYCLE)	FACTOR ns
M2	0.0	2130	A		30	4225		120		35.21
			B	20	45	4300		102		42.16
			C		15	4025		177		22.74
		2120	D		15	4400		85		51.76
			E	30	30	4525		70		64.64
			F		45	4675		57		82.02
		2120	G		45	3900		280		13.93
			H	10	30	3825		380		10.07
			I		15	3650		610		5.98
M1	25	2160	A		30	4000	25.37	196	24.17	20.41
			B	20	45	4075	25.52	148	24.48	27.53
			C		15	3875	25.87	330	24.13	11.74
		2170	D		15	4125	24.67	140	24.50	29.46
			E	30	30	4250	25.00	118	25.00	36.02
			F		45	4350	24.57	94	25.71	46.28
		2170	G		45	3825	25.79	410	24.21	9.33
			H	10	30	36.75	25.88	570	24.13	6.45
			I		15	3375	25.45	840	24.66	4.02

Table XII   (Continued)

1	2	3	4	5	6	7	8	9	10	11
EXP. GROUP	PRODUCTION RATE (C.C./CYCLE)	FEED CONC. (PPM)	EXP. SYMBOL	APPLIED VOLTAGE (VOLT)	PAUSE TIME (SEC)	BRINE		DIALYSATE		SEPARATION FACTOR
						CONC. (PPM)	VOLUME (C.C./CYCLE)	CONC. (PPM)	VOLUME (C.C./CYCLE)	ns
M3	50	2130	A		30	3950	52.14	232	50.48	17.03
			B	20	45	4025	52.55	163	51.76	24.69
			C		15	3775	51.43	470	50.30	8.03
		2120	D		15	4050	50.09	154	50.87	26.30
			E	30	30	4175	50.27	127	52.69	32.87
			F		45	4300	49.12	105	51.68	40.95
		2120	G		45	3725	50.52	550	50.70	6.77
			H	10	30	3400	52.73	810	52.05	4.20
			I		15	3050	50.13	1270	52.39	2.40
M4	100	2100	A		30	3900	101.11	267	99.83	14.61
			B	20	45	4000	98.85	192	96.75	20.83
			C		15	3675	99.09	575	98.86	6.39
		2160	D		15	4025	101.17	180	98.25	22.36
			E	30	30	4125	98.88	145	96.25	28.45
			F		45	4200	99.35	125	98.15	33.60
		2140	G		45	3625	100.00	640	101.18	5.66
			H	10	30	3300	98.17	1100	100.00	3.00
			I		15	2880	98.44	1440	99.88	2.00

Table XIII Compilation of Experiments with Initial Concentration (Co) of 500 PPM
Two Columns, Each Consists of 8 Cells in Series

1	2	3	4	5	6	BRINE 7	BRINE 8	DIALYSATE 9	DIALYSATE 10	11
EXP. GROUP	PRODUCTION RATE (C.C./CYCLE)	FEED CONC. (PPM)	EXP. SYMBOL	APPLIED VOLTAGE (VOLT)	PAUSE TIME (SEC)	CONC. (PPM)	VOLUME (C.C./CYCLE)	CONC. (PPM)	VOLUME (C.C./CYCLE)	SEPARATION FACTOR ns
M6	0.0	550	A		30	1130		16.5		68.48
		550	B	20	45	1200		13.6		88.24
			C		15	1090		20.2		53.96
		550	D		15	1150		15.1		76.16
			E	30	30	1280		12.0		106.67
			F		45					
		530	G		45	1030		33.0		31.21
			H	10	30	1010		44.0		22.95
			I		15	970		75.0		12.93
M5	25	540	A		30	1080	24.20	21.1	25.39	51.18
			B	20	45	1120	24.14	17.1	25.84	65.50
			C		15	1050	24.38	26.3	25.30	39.92
		560	D		15	1090	24.25	19.7	25.25	55.33
			E	30	30	1140	23.84	15.7	25.66	72.61
			F		45	1160	24.13	14.9	25.95	77.85
		530	G		45	1010	25.34	40.0	25.11	25.25
			H	10	30	1000	25.07	53.0	24.78	18.87
			I		15	960	25.62	90.0	24.84	10.67

Table XIII (Continued)

1	2	3	4	5	6	7	8	9	10	11
EXP. GROUP	PRODUCTION RATE (C.C./CYCLE)	FEED CONC. (PPM)	EXP. SYMBOL	APPLIED VOLTAGE (VOLT)	PAUSE TIME (SEC)	BRINE		DIALYSATE		SEPARATION FACTOR ns
						CONC. (PPM)	VOLUME (C.C./CYCLE)	CONC. (PPM)	VOLUME (C.C./CYCLE)	
M7	50	550	A		30	1050	51.82	26.3	49.24	39.92
			B	20	45	1090	50.17	20.2	51.50	53.96
			C		15	1030	51.91	33.0	49.03	31.21
		550	D		15	1070	50.09	24.2	51.00	44.21
			E	30	30	1100	50.77	18.1	51.49	60.77
			F		45	1110	50.50	17.6	51.57	63.07
		530	G		45	1010	50.25	44.0	51.25	22.95
			H	10	30	990	50.94	61.0	49.50	16.23
			I		15	950	50.77	104.0	49.67	9.13
M8	100	540	A		30	1020	99.72	36.0	98.12	28.33
			B	20	45	1050	99.09	26.0	98.18	40.38
			C		15	1010	99.45	48.0	98.79	21.04
		540	D		15	1030	98.50	32.0	99.65	32.19
			E	30	30	1070	97.32	23.0	99.92	46.52
			F		45	1080	97.69	22.3	99.82	48.43
		520	G		45	1000	98.73	55.0	98.55	18.18
			H	10	30	970	98.15	80.0	98.50	12.13
			I		15	890	97.65	139.0	99.15	6.40

Table XIV   Compilation of Experiments with Initial Concentration (Co) of 4000 PPM
Two Columns, Each consists of 8 Cells in Series

1	2	3	4	5	6	7	8	9	10	11
EXP. GROUP	PRODUCTION RATE (C.C./CYCLE)	FEED CONC. (PPM)	EXP. SYMBOL	APPLIED VOLTAGE (VOLT)	PAUSE TIME (SEC)	BRINE		DIALYSATE		SEPARATION FACTOR
						CONC. (PPM)	VOLUME (C.C./CYCLE)	CONC. (PPM)	VOLUME (C.C./CYCLE)	ns
M10	0.0	4100	A		30	7450		550		13.55
			B	20	45	7850		360		21.81
			C		15	7125		820		8.69
		4175	D		15	8100		271		29.89
			E	30	30	8175		194		42.14
			F		45	8300		141		58.87
		4200	G		45	6825		1290		5.29
			H	10	30	6600		1760		3.75
			I		15	6025		2460		2.45
M9	25	4050	A		30	7150	26.28	810	25.47	8.83
			B	20	45	7450	26.00	565	25.00	13.19
			C		15	6800	26.34	1310	25.29	5.19
		4100	D		15	7600	26.50	450	25.82	16.89
			E	30	30	8100	25.17	288	26.48	28.13
			F		45	8150	26.78	218	26.85	37.39
		4175	G		45	6625	25.87	1700	26.65	3.90
			H	10	30	6375	25.09	2240	26.86	2.85
			I		15	5825	25.39	2650	25.84	2.20

Table XIV   (Continued)

EXP. GROUP	PRODUCTION RATE (C.C./CYCLE)	FEED CONC. (PPM)	EXP. SYMBOL	APPLIED VOLTAGE (VOLT)	PAUSE TIME (SEC)	BRINE CONC. (PPM)	BRINE VOLUME (C.C./CYCLE)	DIALYSATE CONC. (PPM)	DIALYSATE VOLUME (C.C./CYCLE)	SEPARATION FACTOR ns
M11	50	4100	A		30	7050	51.23	940	48.84	7.50
		4100	B	20	45	7375	51.39	625	49.61	11.80
		4100	C		15	6775	51.20	1470	49.93	4.61
		4175	D		15	7500	51.86	490	49.14	15.31
		4175	E	30	30	8075	50.15	310	50.15	26.05
		4175	F		45	8125	49.21	239	50.86	34.00
		4200	G		45	6450	50.14	2010	50.64	3.21
		4200	H	10	30	5975	49.70	2490	50.97	2.40
		4200	I		15	5300	49.52	3125	50.85	1.70
M12	100	4050	A		30	6900	101.33	1190	101.50	5.80
		4050	B	20	45	7250	99.75	725	99.50	10.00
		4050	C		15	6650	99.15	1670	101.75	3.98
		4125	D		15	7400	101.75	590	99.15	12.54
		4125	E	30	30	7925	99.11	350	99.11	22.64
		4125	F		45	8100	99.25	283	100.81	28.62
		4200	G		45	6400	99.11	2210	101.58	2.90
		4200	H	10	30	5600	99.41	2800	101.91	2.00
		4200	I		15	5000	99.18	3575	101.73	1.40

1	2	3	4	5	6	7	8	9	10
FEED CONC. (PPM)	EXP.	PRODUCTION RATE (C.C./CYCLE)	APPLIED VOLTAGE (VOLT)	PAUSE TIME (SEC)	BRINE		DIALYSATE		SEPARATION FACTOR
					CONC. (PPM)	VOLUME (C.C./CYCLE)	CONC. (PPM)	VOLUME (C.C./CYCLE)	ns
1980	RR1A	20	20	30	3650	19.72	350	19.52	10.43
	RR1D	20	30	15	3540	19.33	415	19.13	8.53
	RR1E	20	30	30	3850	18.50	233	19.33	16.52
	RR1F	20	30	45	3900	19.60	207	19.70	18.84
	RR3B	50	20	45	3350	49.81	550	48.62	6.09
	RR4F	100	30	45	3325	99.75	555	99.19	5.99
520	RR5A	20	20	30	1050	18.29	28.0	19.11	37.50
	RR5C	20	20	15	995	19.29	35.0	19.18	28.43
	RR5F	20	30	45	1450	17.19	23.4	19.84	61.97
	RR7A	50	20	30	980	49.26	44.0	48.83	22.27
	RR7B	50	20	45	1000	48.88	34.0	49.17	29.41
	RR7C	50	20	15	960	49.66	55.0	49.14	17.45
	RR8F	100	30	45	970	98.29	46.0	98.10	21.09
3725	RR9E	20	30	30	5600	19.35	1650	19.13	3.39
	RR9F	20	30	45	5900	19.95	1440	18.47	4.10
	RR11F	50	30	45	5750	49.86	1530	49.14	3.76

Table XVI   Duplicate Experiments to Test Reproducibility – Group M
Two Columns, Each Consists of 8 Cells in Series

1	2	3	4	5	6	7	8	9	10
FEED CONC. (PPM)	EXP.	PRODUCTION RATE (C.C./CYCLE)	APPLIED VOLTAGE (VOLT)	PAUSE TIME (SEC)	BRINE		DIALYSATE		SEPARATION FACTOR
					CONC. (PPM)	VOLUME (C.C./CYCLE)	CONC. (PPM)	VOLUME (C.C./CYCLE)	ns
2200	MM1B	25	20	45	4150	25.18	133	24.84	31.20
	MM1D	25	30	15	4100	26.86	144	24.66	28.47
	MM1F	25	30	45	4375	25.59	106	24.84	41.27
	MM3C	50	20	15	3950	49.60	415	48.84	9.52
2040	MM4A	100	20	30	3800	102.32	267	99.23	14.23
	MM4E	100	30	30	4150	98.13	129	99.57	32.17
540	MM5C	25	20	15	1040	25.83	28.8	24.64	36.11
	MM7C	50	20	15	1020	51.27	36.0	50.17	28.33
	MM7D	50	30	15	1070	52.78	22.7	50.25	47.14
	MM8B	100	20	45	1040	102.41	27.4	99.86	37.96
	MM8F	100	30	45	1080	102.89	20.3	99.17	53.20
4150	MM9A	25	20	30	7400	25.13	940	24.87	7.87
	MM9E	25	30	30	8350	25.86	271	24.93	30.81
	MM11B	50	20	45	7750	50.21	600	50.82	12.92
4200	MM12C	100	20	15	6600	97.30	1820	99.04	3.63
	MM12D	100	30	15	7600	97.13	650	101.27	11.69
	MM12F	100	30	45	8350	98.17	267	101.48	31.27

Appendix E shows the computer program and calculations for separation factors, amount of salt shifted and a check on material balance for each run and lists tables of printout.

5.4.1. <u>Effect of Demineralizing Path Length</u>

Since the process generates a concentration difference between the solutions at the two ends of the ED cell, the amount of axial dispersion in the stack has a very great effect on the final separation. In all of the runs the concentrations of the two product streams approached limiting values as the dispersive effects of axial mixing and other irreversible processes became equal to the separation produced by cycling.

Increasing the channel length by increasing the number of stages connected in series tends to reduce dispersion. Figures 38, 39 and 40 and Tables XVII, XVIII and XIX show runs in 4-stage columns while Figures 41, 42 and 43 together with Tables XX, XXI and XXII show similar experiments performed in 8-stage columns. By comparing these figures it will be clear that the separation factor reached higher values with increasing channel length in all sets of experiments.

Figures 44-49 and Tables XXIII-XXVIII compare the performance, under the same operating conditions, of a single column consists of 8 stages with that of two short columns each consists of 4 stages which operate in parallel and have the same production rates as the single column. This comparison was made by plotting C_o/C_D versus the reciprocal of the throughput ratio; where C_o is the feed concentration and C_D is the demineralized product concentration. In all runs studied the single column results in a better separation than the two short parallel columns; however, the improvement in separation with the column length was more pronounced at high feed

Table XVII Effect of Production Rate on Separation
            Two Columns Each Consists of 4 Cells in Series
            Initial Concentration Co ≃ 500 PPM
            Exp. Group # R5, R6, R7 and R8

EXP.	GRAPH. SYMBOL	VOLTAGE (VOLT)	PAUSE (SEC) PROD. RATE PER CYCLE	SEPARATION FACTOR ns			
				0.0 (C.C.)	20 (C.C.)	50 (C.C.)	100 (C.C.)
A	◭		30	59.06	33.97 37.50	25.79 22.27	14.17
B	⬒	20	45	80.80	46.25	34.00 29.41	16.67
C	◑		15	46.10	25.37 28.43	20.00 17.45	8.88
D	●		15	73.36	42.80	25.40	12.11
E	▲	30	30	95.47	55.15	32.63	16.63
F	■		45		68.45 61.97	39.07	18.46 21.09
G	☐		45	15.49	10.21	9.01	5.57
H	△	10	30	11.49	7.64	6.92	4.00
I	○		15	6.64	3.97	3.60	2.37
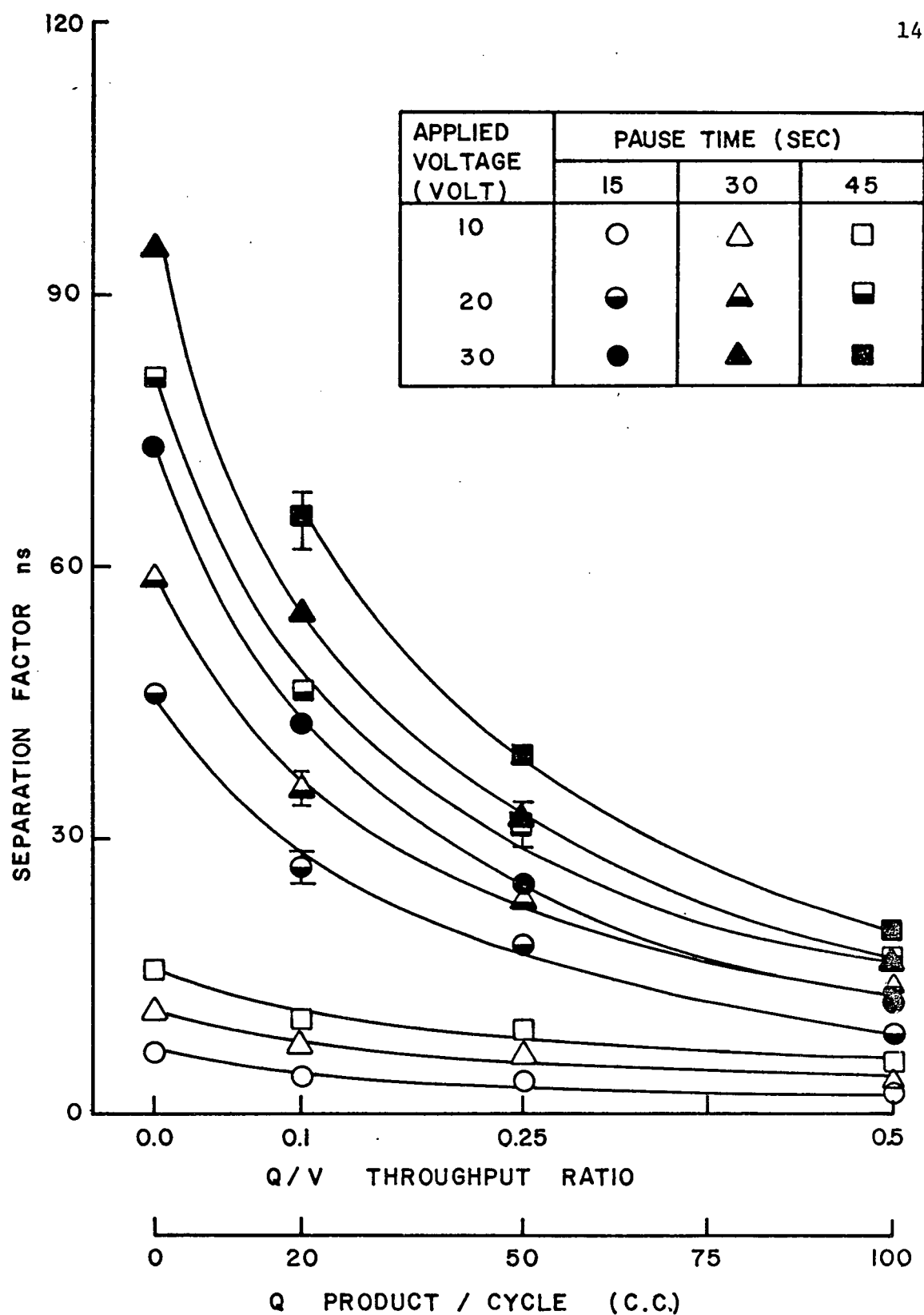
FIGURE 38

Effect of production rate on separation. 4-Cell column; initial conc. $C_0 \cong 500$ PPM.

Table XVIII   Effect of Production Rate on Separation
                Two Columns Each Consists of 4 Cells in Series
                Initial Concentration Co ≃   2000 PPM
                Exp. Group # R1, R2, R3 and R4

EXP.	GRAPH. SYMBOL	PROD. RATE PER CYCLE		SEPARATION FACTOR ns			
		VOLTAGE (VOLT)	PAUSE (SEC)	0.0 (C.C.)	20 (C.C.)	50 (C.C.)	100 (C.C.)
A	◓		30	17.59	8.90 10.43	5.00	2.74
B	▢	20	45	31.93	13.00	7.21 6.09	3.76
C	◒		15	8.00	5.71	2.88	1.67
D	●		15	14.44	7.49 8.53	3.83	2.45
E	▲	30	30	33.35	13.93 16.52	7.78	4.18
F	■		45	47.52	20.64 18.84	12.00	7.02 5.99
G	□		45	7.19	4.49	2.46	1.79
H	△	10	30	5.49	3.67	2.03	1.57
I	○		15	3.18	2.74	1.53	1.39
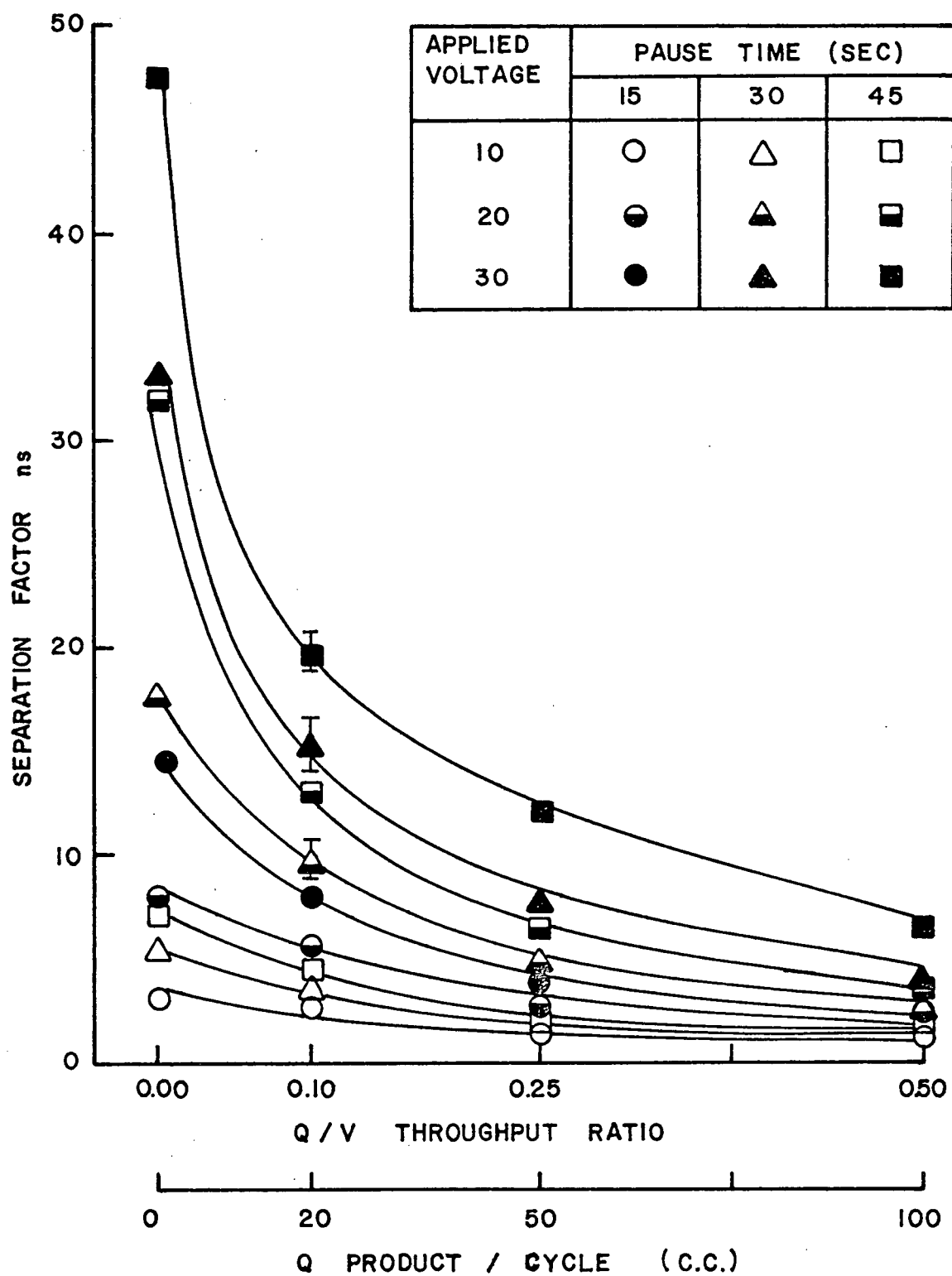
FIGURE 39

Effect of production rate on separation. 4-Cell column; initial conc. $C_0 \simeq 2000$ PPM.

Table XIX   Effect of Production Rate on Separation
Two Columns Each Consists of 4 Cells in Series
Initial Concentration Co $\simeq$ 4000 PPM
Exp. Group # R9, R10, R11 and R12

EXP.	GRAPH. SYMBOL	PROD. RATE PER CYCLE VOLTAGE (VOLT)	PAUSE (SEC)	SEPARATION FACTOR ns			
				0.0 (C.C.)	20 (C.C.)	50 (C.C.)	100 (C.C.)
A	△	20	30	2.39	1.98	1.78	1.52
B	⬓		45	3.34	2.67	2.20	1.77
E	▲	30	30	4.43	3.10 / 3.39	2.50	1.91
F	◼		45	6.90	4.56 / 4.10	3.44 / 3.76	2.48

APPLIED VOLTAGE (VOLT)	PAUSE TIME (SEC)		
	15	30	45
10			
20		△	⬒
30		▲	▣
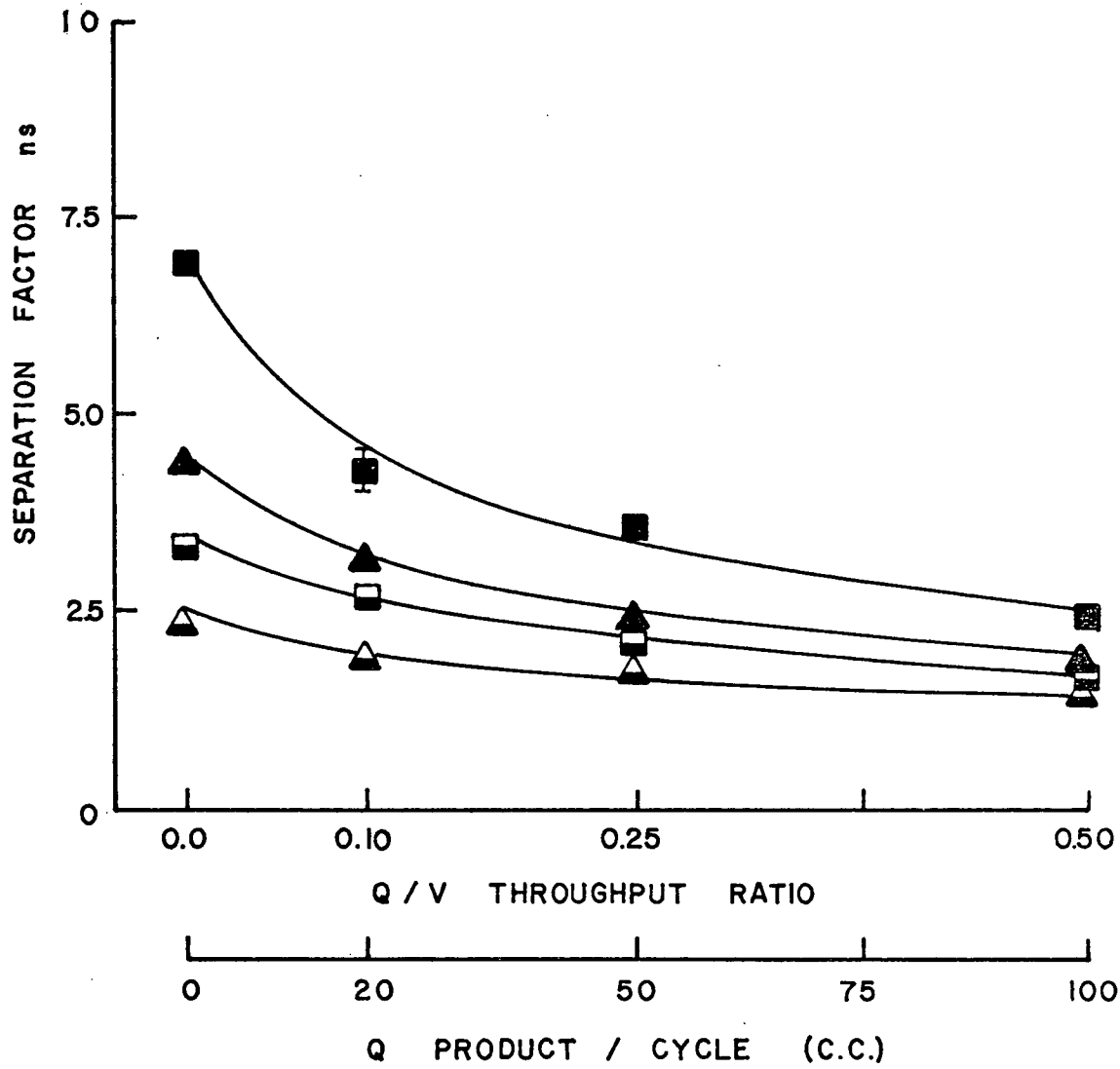
FIGURE 40

Effect of production rate on separation. 4-Cell column; initial conc. $C_0 \cong 4000$ PPM.

Table XX   Effect of Production Rate on Separation
Two Columns Each Consists of 8 Cells in Series
Initial Concentration Co $\simeq$ 500 PPM
Exp. Group # M5, M6, M7 and M8

EXP.	GRAPH. SYMBOL	PROD. RATE PER CYCLE		SEPARATION FACTOR ns			
		VOLTAGE (VOLT)	PAUSE (SEC)	0.0 (C.C.)	25 (C.C.)	50 (C.C.)	100 (C.C.)
A	◭		30	68.48	51.18	39.92	28.33
B	⬒	20	45	88.24	65.50	53.96	40.38 37.96
C	⬓		15	53.96	39.92 36.11	31.21 28.33	21.04
D	●		15	76.16	55.33	44.21 47.14	32.19
E	▲	30	30	106.67	72.61	60.77	46.52
F	▦		45		77.85	63.07	48.43 53.20
G	□		45	31.21	25.25	22.95	18.18
H	△	10	30	22.95	18.87	16.23	12.13
I	○		15	12.93	10.67	9.13	6.40
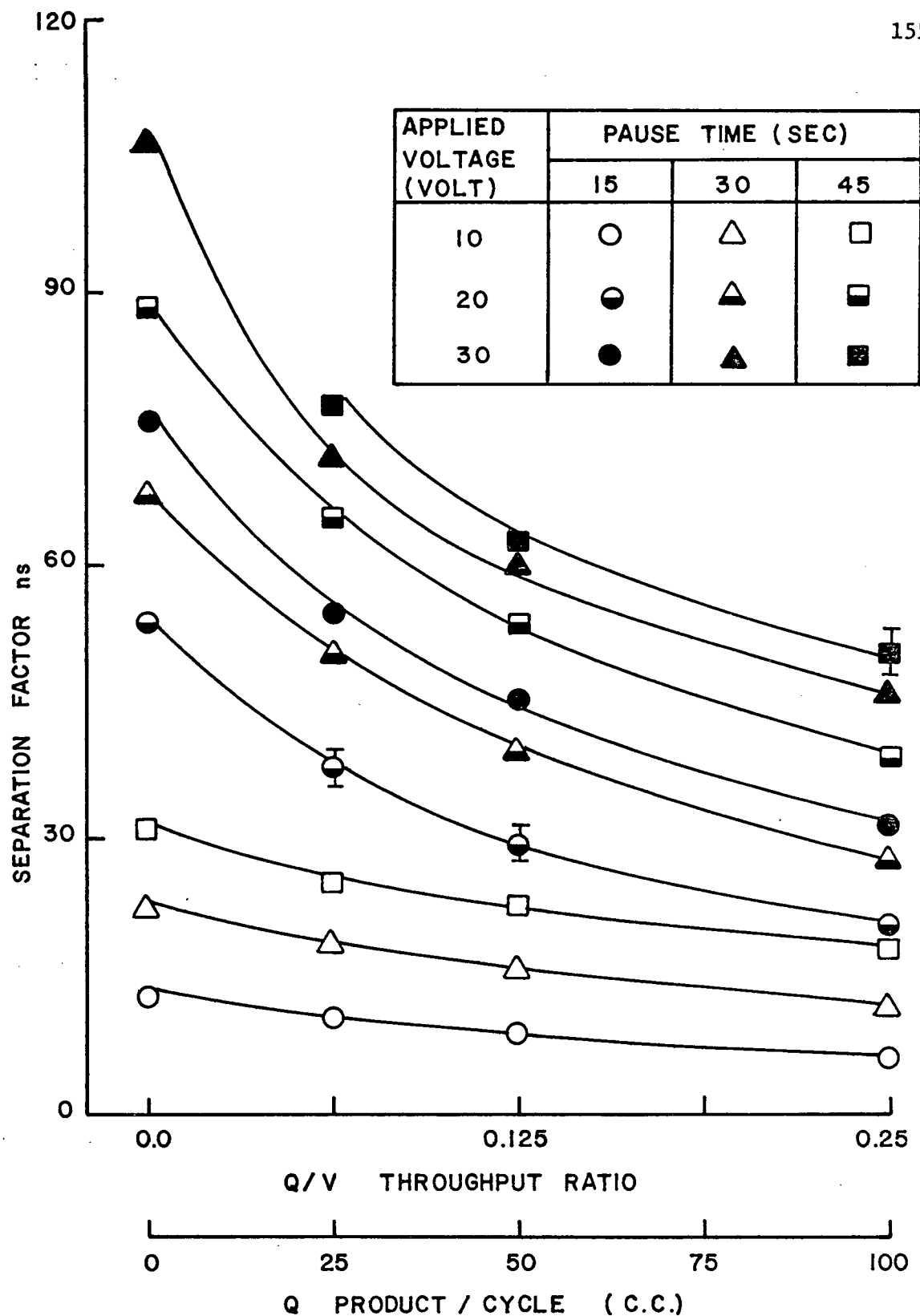
FIGURE 41

Effect of production rate on separation. 8 - Cell cell column ; initial conc. $C_0 \cong 500\,PPM$.

Table XXI   Effect of Production Rate on Separation
             Two Columns Each Consists of 8 Cells in Series
             Initial Concentration Co   ≃ 2000 PPM
             Exp. Group # M1, M2, M3 and M4

EXP.	GRAPH. SYMBOL	PROD. RATE PER CYCLE		SEPARATION FACTOR ns			
		VOLTAGE (VOLT)	PAUSE (SEC)	0.0 (C.C.)	25 (C.C.)	50 (C.C.)	100 (C.C.)
A	◓		30	35.21	20.41	17.03	14.61 14.23
B	⬓	20	45	42.16	27.53 31.20	24.69	20.83
C	◒		15	22.74	11.74	8.03 9.52	6.39
D	●		15	51.76	29.46 28.47	26.30	22.36
E	▲	30	30	64.64	36.02	32.87	28.45 32.17
F	■		45	82.02	46.28 41.27	40.95	33.60
G	☐		45	13.93	9.33	6.77	5.66
H	△	10	30	10.07	6.45	4.20	3.00
I	○		15	5.98	4.02	2.40	2.00
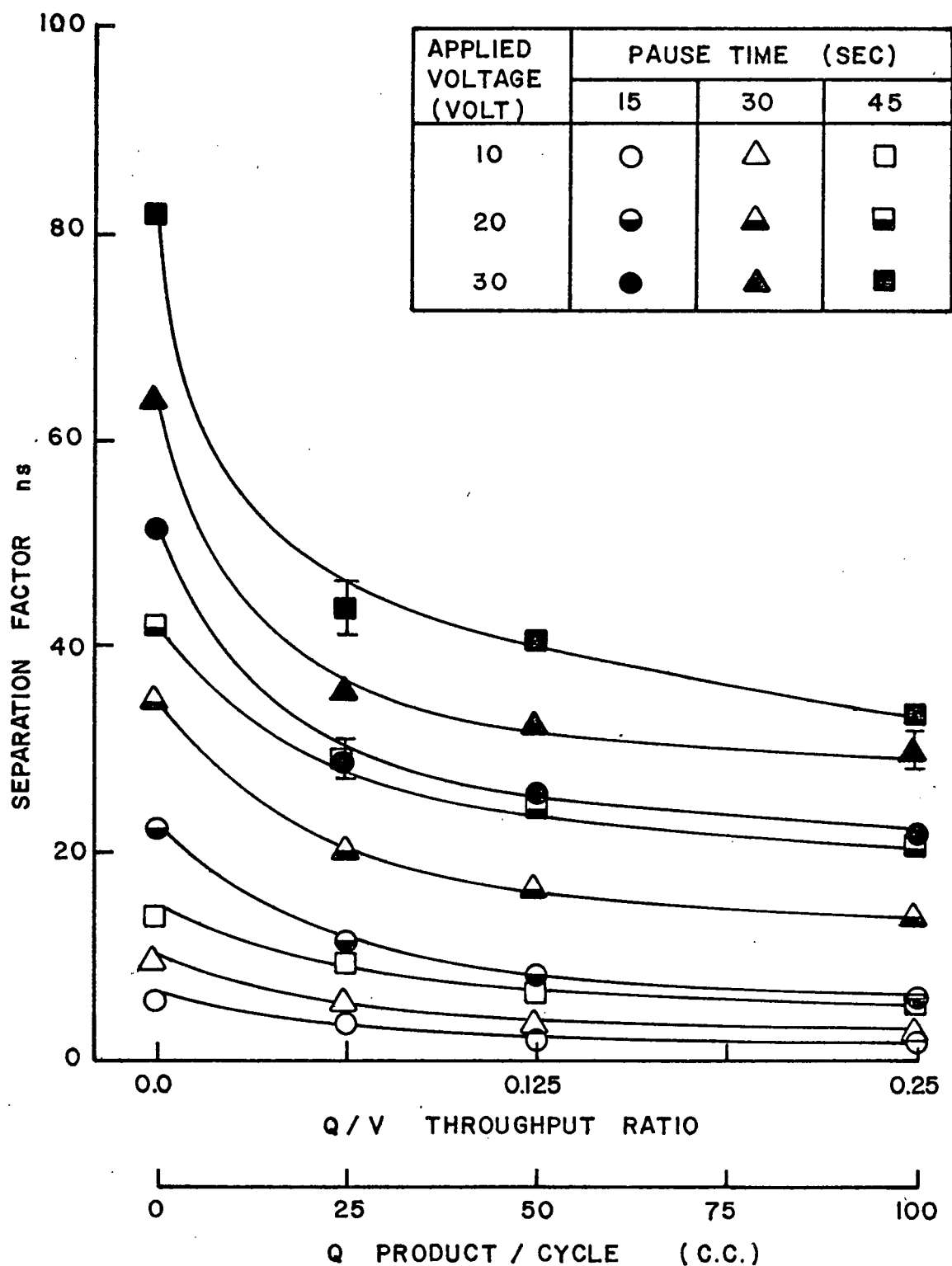
FIGURE 42

Effect of production rate on separation. 8-Cell column ; initial conc. $C_0 \cong 2000$ PPM.

Table XXII Effect of Production Rate on Separation
Two Columns Each Consists of 8 Cells in Series
Initial Concentration Co ≃ 4000 PPM
Exp. Group # M9, M10, M11 and M12

EXP.	GRAPH. SYMBOL	VOLTAGE (VOLT)	PROD. RATE PER CYCLE PAUSE (SEC)	SEPARATION FACTOR ns			
				0.0 (C.C.)	25 (C.C.)	50 (C.C.)	100 (C.C.)
A	◬		30	13.55	8.83 7.87	7.50	5.80
B	⬒	20	45	21.81	13.19	11.80 12.92	10.00
C	⊖		15	8.69	5.19	4.61	3.98 3.63
D	●		15	29.89	16.89	15.31	12.54 11.69
E	▲	30	30	42.14	28.13 30.81	26.05	22.64
F	■		45	58.87	37.39	34.00	28.62 31.27
G	□		45	5.29	3.90	3.21	2.90
H	△	10	30	3.75	2.85	2.40	2.00
I	○		15	2.45	2.20	1.70	1.40
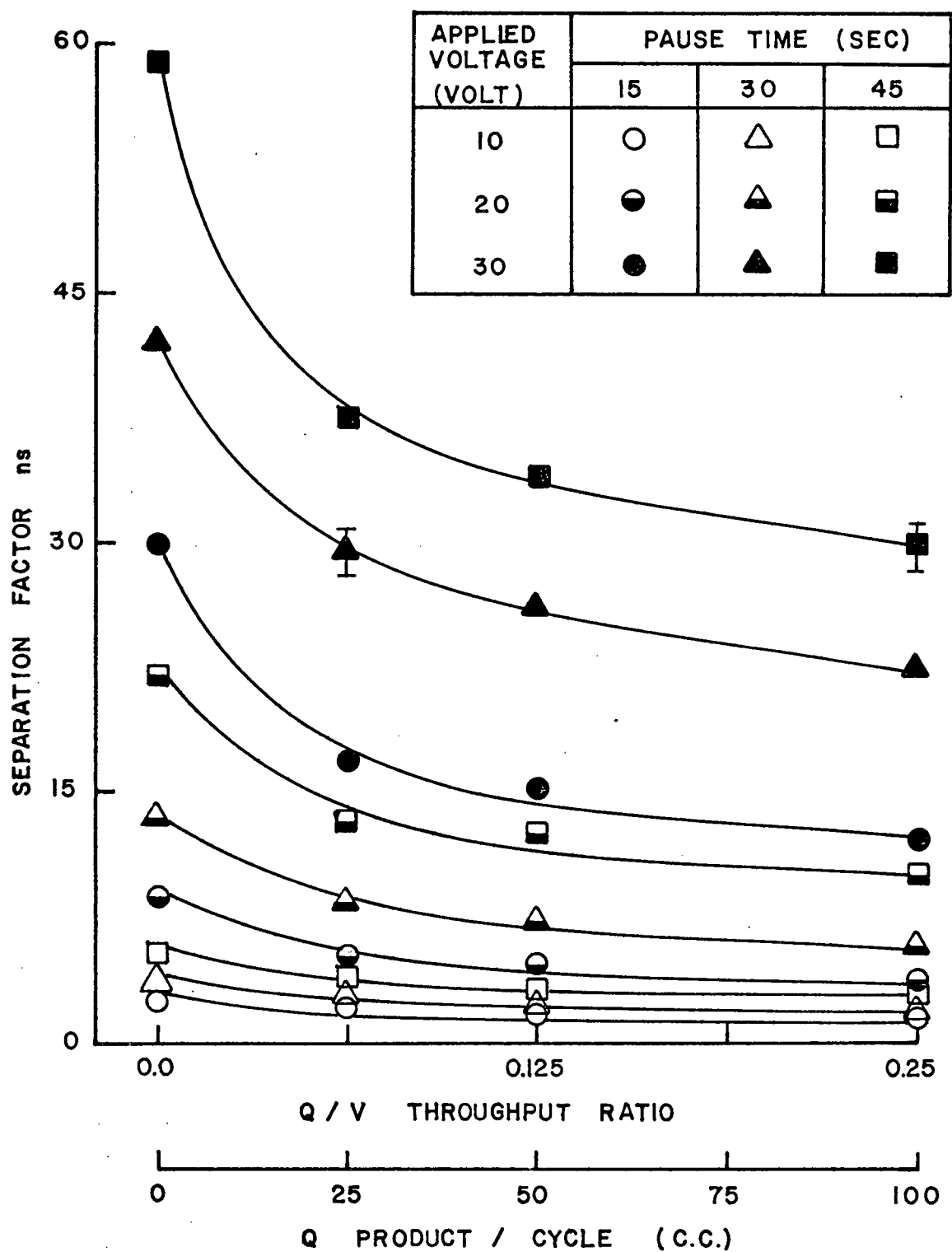
FIGURE 43

Effect of production rate on separation . 8 - Cell column ; initial conc. $C_0 \cong$ 4000PPM.

Table XXIII Effect of Demineralizing Path Length on Separation
$C_o \simeq 500$ ppm; $\Delta\phi = 20$ V

EXP.	GRAPHICAL SYMBOL	PAUSE TIME (SEC)	4-CELL COLUMN		8-CELL COLUMN	
			$\dfrac{1}{\text{THROUGHPUT RATIO}}$	$\dfrac{C_o}{C_D}$	$\dfrac{1}{\text{THROUGHPUT RATIO}}$	$\dfrac{C_o}{C_D}$
8 C			2	4.85	4	11.25
7 C	○ ●	15	4	10.64	8	16.67
5 C			10	12.93	16	20.53
8 A			2	7.58	4	15.00
7 A	△ ▲	30	4	13.42	8	20.91
5 A			10	16.83	16	25.59
8 B			2	8.77	4	20.77
7 B	☐ ◼	45	4	17.00	8	27.23
5 B			10	22.08	16	31.58

Pause Time (Sec)	4 - Cell Column	8 - Cell Column
15	○	●
30	△	▲
45	□	▣
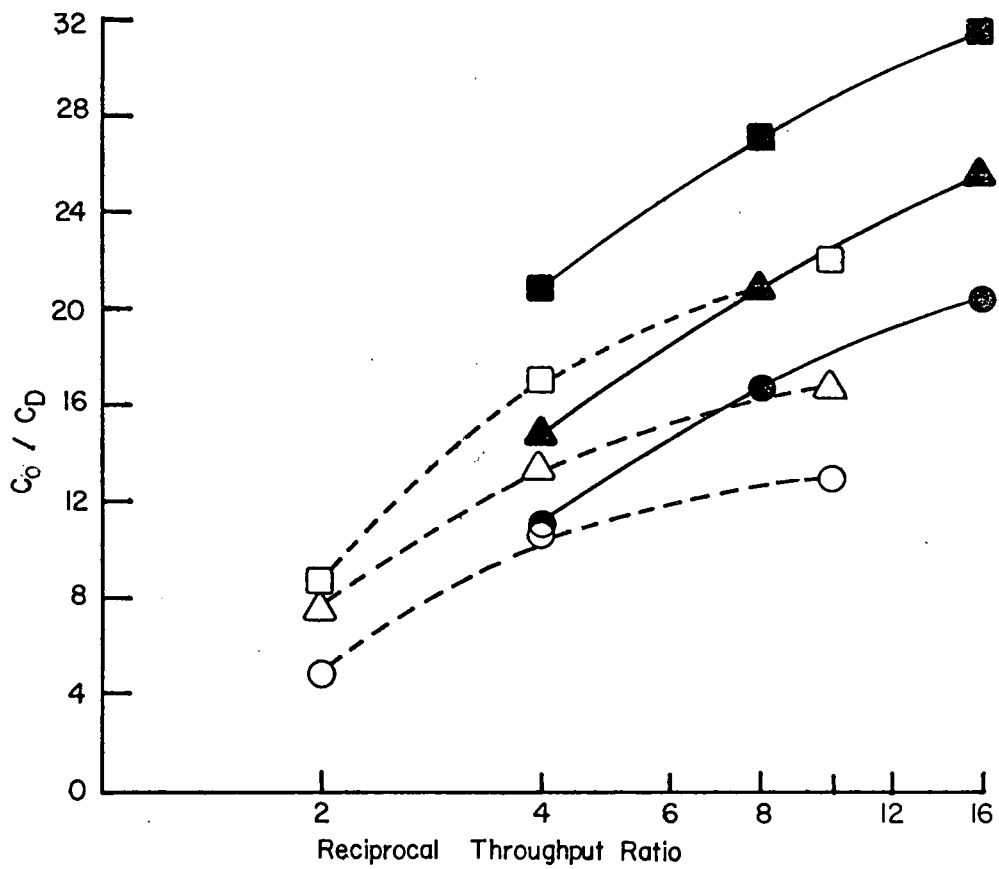
FIGURE 44

Effect of demineralizing path length on separation. $C_0 \approx 500$ PPM, $\Delta \phi = 20$ V.

Table XXIV Effect of Demineralizing Path Length on Separation
$C_o \simeq 500$ ppm; $\Delta\phi = 30$ V

EXP.	GRAPHICAL SYMBOL		PAUSE TIME (SEC)	4-CELL COLUMN		8-CELL COLUMN	
				$\dfrac{1}{\text{THROUGHPUT RATIO}}$	$\dfrac{C_O}{C_D}$	$\dfrac{1}{\text{THROUGHPUT RATIO}}$	$\dfrac{C_O}{C_D}$
8 D				2	6.58	4	16.88
7 D	○	●	15	4	12.75	8	22.73
5 D				10	21.20	16	28.43
8 E				2	8.77	4	23.48
7 E	△	▲	30	4	15.94	8	30.39
5 E				10	25.98	16	35.69
8 F				2	9.62	4	24.22
7 F	□	■	45	4	18.89	8	31.25
5 F				10	31.55	16	37.58

Pause Time (Sec)	4 – Cell Column	8 – Cell Column
15	○	●
30	△	▲
45	▢	▣
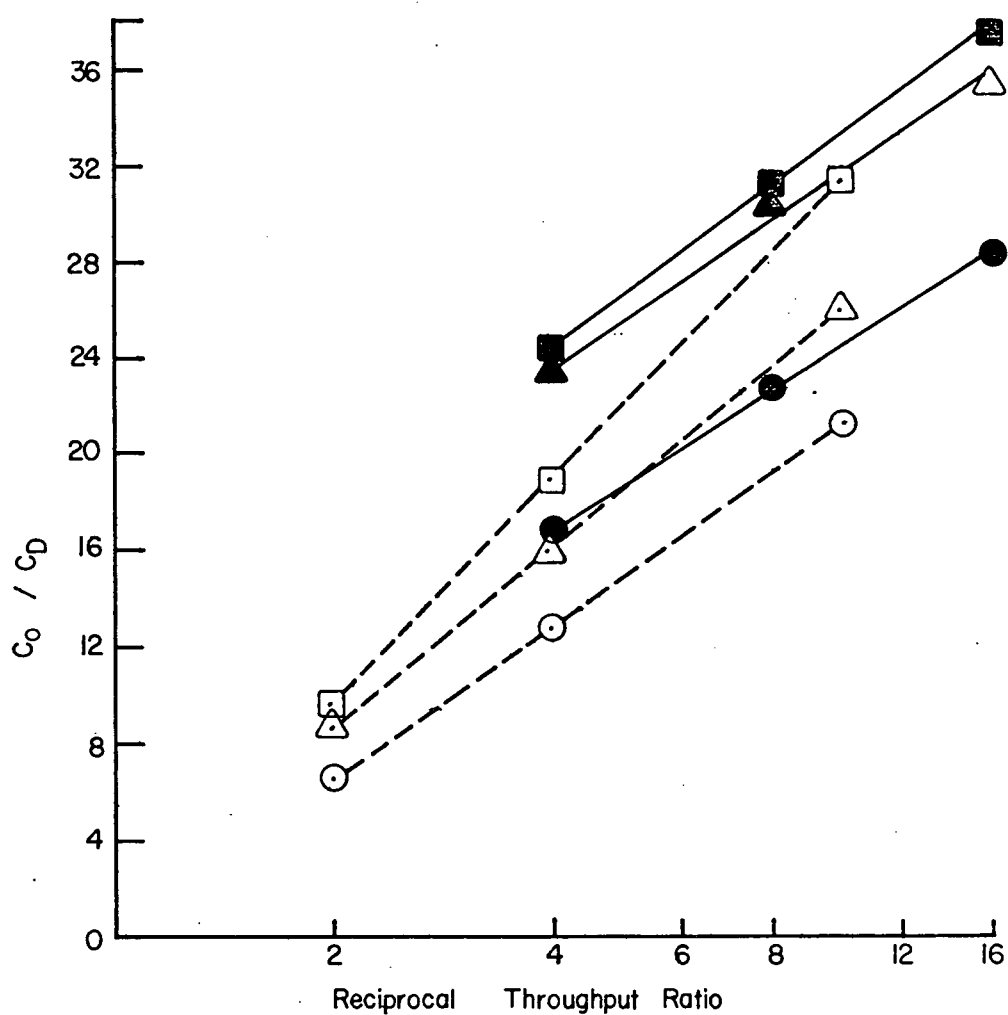
FIGURE 45

Effect of demineralizing path length on separation. $C_0 \approx 500$ PPM, $\Delta\phi = 30$V.

Table XXV   Effect of Demineralizing Path Length on Separation
$C_o \simeq 2000$ ppm; $\Delta\phi = 20$ V

EXP.	GRAPHICAL SYMBOL	PAUSE TIME (SEC)	4-CELL COLUMN		8-CELL COLUMN	
			$\dfrac{1}{\text{THROUGHPUT RATIO}}$	$\dfrac{C_O}{C_D}$	$\dfrac{1}{\text{THROUGHPUT RATIO}}$	$\dfrac{C_O}{C_D}$
4 C			2	1.33	4	3.65
3 C	○ ●	15	4	1.97	8	4.53
1 C			10	3.36	16	6.55
4 A			2	1.84	4	7.87
3 A	△ ▲	30	4	3.05	8	9.18
1 A			10	4.88	16	11.02
4 B			2	2.36	4	10.94
3 B	□ ■	45	4	4.06	8	13.07
1 B			10	6.72	16	14.59

Pause Time (Sec.)	4 – Cell Column	8 – Cell Column
15	○	●
30	△	▲
45	□	▣
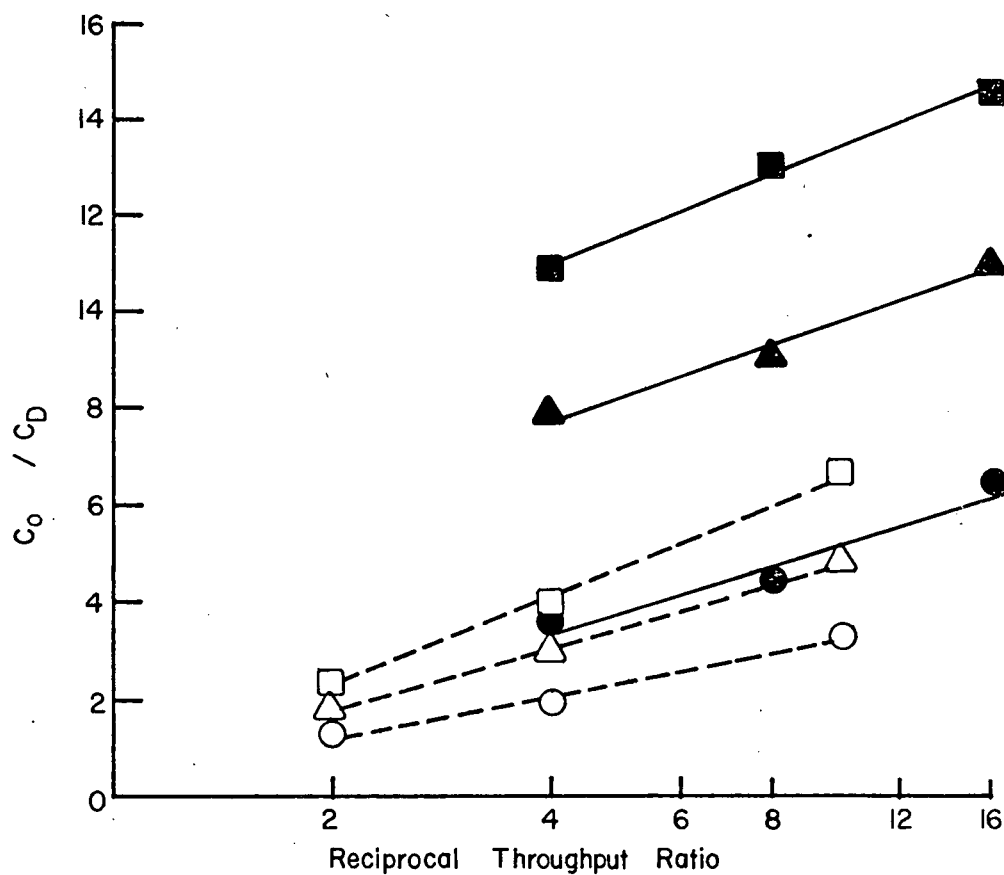
FIGURE 46

Effect of demineralizing path length on separation. $C_0 \approx 2000$ PPM, $\Delta\phi = 20$V.

Table XXVI Effect of Demineralizing Path Length on Separation
$C_o \simeq 2000$ ppm; $\Delta\phi = 30$ V

EXP.	GRAPHICAL SYMBOL	PAUSE TIME (SEC)	4-CELL COLUMN		8-CELL COLUMN	
			$\dfrac{1}{\text{THROUGHPUT RATIO}}$	$\dfrac{C_o}{C_D}$	$\dfrac{1}{\text{THROUGHPUT RATIO}}$	$\dfrac{C_o}{C_D}$
4 D			2	1.73	4	12.00
3 D	○ ●	15	4	2.35	8	13.77
1 D			10	4.29	16	15.50
4 E			2	2.60	4	14.90
3 E	△ ▲	30	4	4.33	8	16.69
1 E			10	6.96	16	18.39
4 F			2	3.99	4	17.28
3 F	□ ■	45	4	6.29	8	20.19
1 F			10	10.00	16	23.09

Pause Time (Sec.)	4 - Cell Column	8 - Cell Column
15	○	●
30	△	▲
45	□	◼
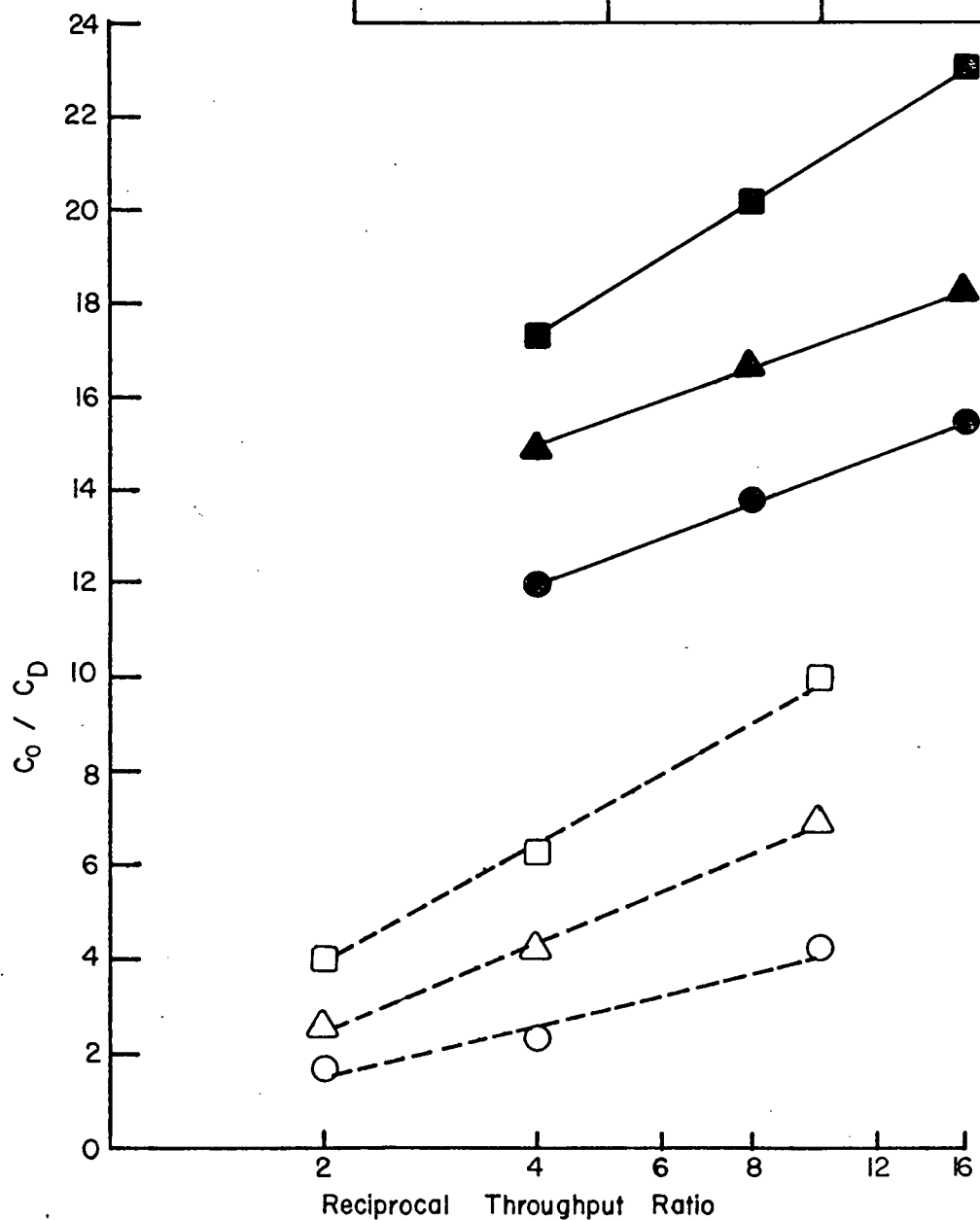
FIGURE 47

Effect of demineralizing path length on separation. $C_0 \approx 2000$ PPM , $\Delta \phi = 30$V.

Table XXVII   Effect of Demineralizing Path Length on Separation
$C_o \simeq 4000$ ppm; $\Delta\phi = 20$ V

EXP.	GRAPHICAL SYMBOL	PAUSE TIME (SEC)	4-CELL COLUMN		8-CELL COLUMN	
			$\dfrac{1}{\text{THROUGHPUT RATIO}}$	$\dfrac{C_o}{C_D}$	$\dfrac{1}{\text{THROUGHPUT RATIO}}$	$\dfrac{C_o}{C_D}$
12 A			2	1.25	4	3.40
11 A	△ ▲	30	4	1.39	8	4.36
9 A			10	1.48	16	5.00
12 B			2	1.40	4	5.59
11 B	☐ ■	45	4	1.61	8	6.56
9 B			10	1.82	16	7.17

Pause Time (Sec.)	4 - Cell Column	8 - Cell Column
30	△	▲
45	☐	■
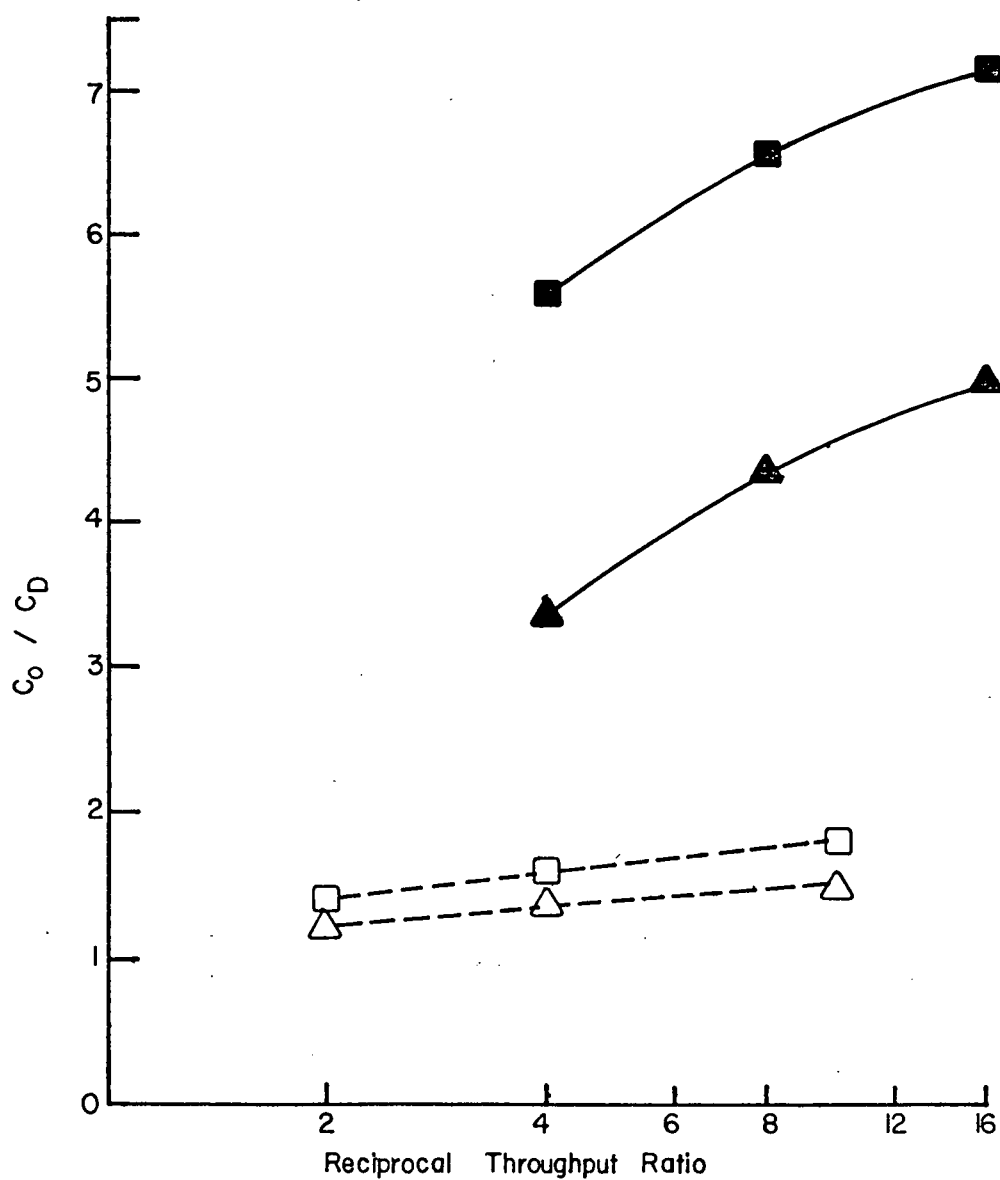
FIGURE 48

Effect of demineralizing path length on separation. $C_0 \approx 4000\,PPM$, $\Delta \phi = 20\,V$

Table XXVIII   Effect of Demineralizing Path Length on Separation

$$C_o \simeq 4000 \text{ ppm;} \quad \Delta\phi = 30 \text{ V}$$

EXP.	GRAPHICAL SYMBOL	PAUSE TIME (SEC)	4-CELL COLUMN		8-CELL COLUMN	
			$\dfrac{1}{\text{THROUGHPUT RATIO}}$	$\dfrac{C_o}{C_D}$	$\dfrac{1}{\text{THROUGHPUT RATIO}}$	$\dfrac{C_o}{C_D}$
12 E			2	1.46	4	11.79
11 E	△ ▲	30	4	1.73	8	13.47
9 E			10	2.10	16	14.24
12 F			2	1.73	4	14.58
11 F	▢ ■	45	4	2.22	8	17.47
9 F			10	2.72	16	18.81

Pause Time (Sec.)	4 – Cell Column	8 – Cell Column
30	△	▲
45	□	■
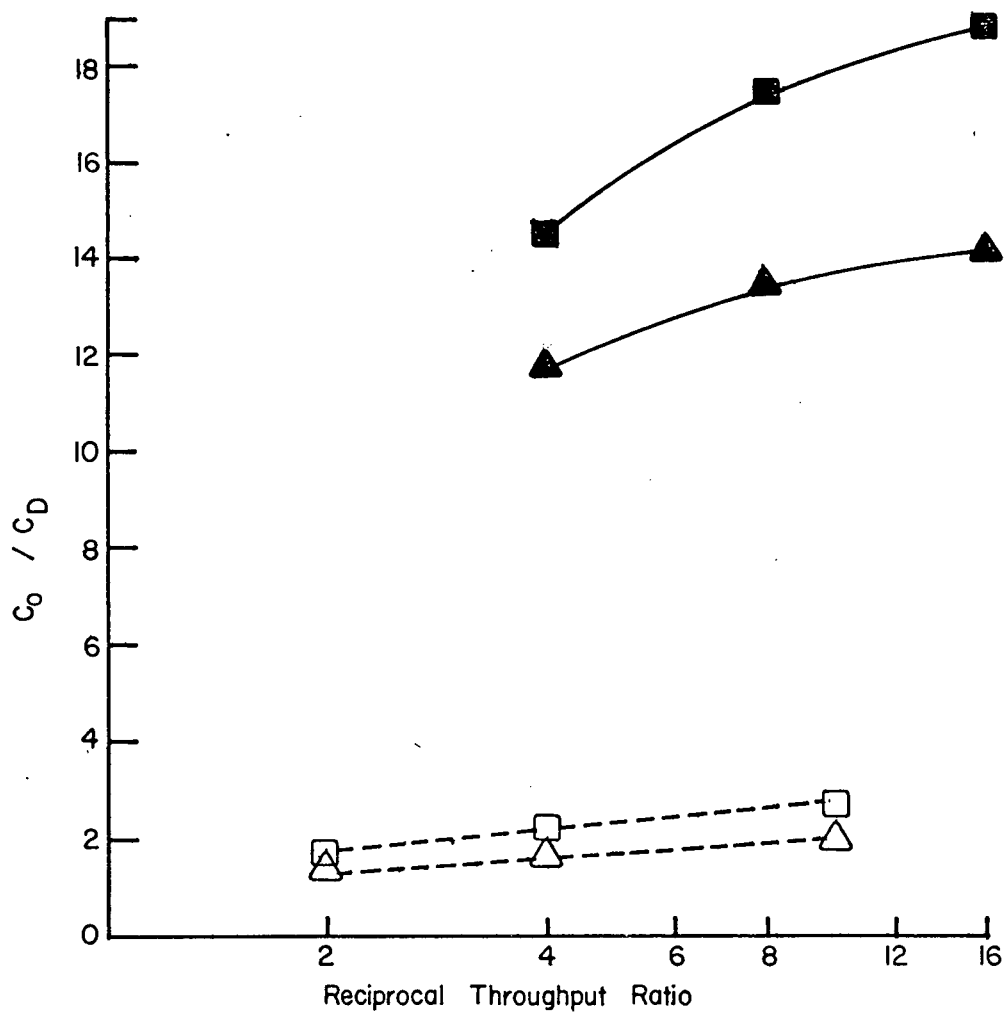
FIGURE 49

Effect of demineralizing path length on separation. $C_0 \approx 4000$ PPM, $\Delta\phi = 30$ V

concentration (compare Figures 44, 45 with Figures 48,49). Figures 44 and 45 indicate that for a feed concentration $C_o \simeq 500$ ppm NaCl an optimum demineralizing path length may lie in the vicinity of 8 stages in series while Figures 46-49 call for longer demineralizing path lengths with the increasing feed concentration.

5.4.2. Effect of Production Rate

As the production rate increases the feed undergoes less cycles in the ED cell before it emerges as products. Thus the amount of separation is reduced as the production rate increases. Figures 38, 41 and Tables XVII, XX show the effect of production rate on the separation factor (ns = $\frac{C_B}{C_D}$) for a series of experiments at a feed concentration (C_o) of about 500 ppm NaCl. The parameters studied were the pause time, τ (at levels of 15, 30 and 45 sec.) and the applied voltage $\Delta\phi$ (at levels of 10, 20 and 30 volt). Figures 39, 42 and Tables XVIII, XXI show similar experiments at feed concentration $C_o \simeq 2000$ ppm NaCl; while Figures 40, 43 together with Tables XIX and XXII indicate experiments with feed concentration $C_o \simeq 4000$ ppm.

All these figures referred to show that there is a strong trade-off between production rate and separation factor. However, useful separation can be obtained at all production rates (provided that higher voltages and/ or longer pause times and demineralizing paths are used with high feed concentration). Figures 41, 42 and 43 show that at an applied voltage ($\Delta\phi$) of 30 V, a pause time (τ) of 45 sec. and a throughput ratio of $\frac{1}{4}$ (i.e. production rate of 100 c.c./cycle), the separation factors for various feed concentrations range between 30 to 50. To fix ideas, most of the commercial ED plants available at present operate with a 2:1 desalination ratio, which means that a feed of 1000 ppm would be desalinated to 500 ppm per path. A mark III stack (Ionics Inc.) which is used in Buckeye ED plant, Ariz.,

has a maximum desalination ratio of slightly better than 2:1. Two stacks are used in series to reduce a brackish water of 2100 ppm total dissolved solids down to 500 ppm. (also refer to Table IV). Most of the health standards (e.g. the United States Public Health Service Standards) require that the total dissolved solids (TDS) content of potable water to be 500 ppm or less; hence with a feed at 2000 ppm NaCl and an equal split of brine and dialysate a separation factor of 7 would be necessary and a separation factor of 15 is required with a feed at 4000 ppm.

5.4.3. Effect of Pause Time

The influence of a pause time (τ) at levels of 15, 30 and 45 sec. was studied under various operating conditions. In all cases, a displacement period of 36 sec. and an average production period of 1.5 sec., 3.0 sec. and 6.0 sec. for production rates of 25 c.c., 50 c.c. and 100 c.c./cycle respectively were used.

Tables XXIX, XXX and XXXI summarize the operating parameters and the final separation factors reached in these experiments, and Figures 50, 51 and 52 directly display the effect of the pause time on separation factor for several groups of experiments performed in 4-stage columns with feed concentrations between 500 ppm and 4000 ppm NaCl. Tables XXXII, XXXIII and XXXIV together with Figures 53, 54 and 55 exhibit results of similar experiments conducted in 8-stage columns.

All these figures show that the separation is improved with a prolonged pause time. However, the effect of pause time can best be examined by considering separation per unit real time obtained with various pause times as shown in Tables XXXV, XXXVI and XXXVII and Figures 56, 57 and 58. In these figures ns/T is plotted vs. pause time (τ), where ns is the separation factor and T is the complete cycle duration in minutes. The results are

Table XXIX Effect of Pause Time on Separation
Two Columns Each Consists of 4 Cells in Series
Initial Concentration Co ≃ 500 PPM
Exp. Group # R5, R7 and R8

EXP. GROUP and PRODUCTION RATE	GRAPH. SYMBOL	PAUSE TIME (SEC) VOLT. (VOLT)	SEPARATION FACTOR ns		
			15	30	45
R5 20 (C.C./cycle)	●	30	42.80	55.15	68.45 61.97
	◒	20	25.37 28.43	33.97 37.50	46.25
	○	10	3.97	7.64	10.21
R7 50 (C.C./cycle)	▲	30	25.40	32.63	39.07
	◮	20	20.00 17.45	25.79 22.27	34.00 29.41
	△	10	3.60	6.92	9.01
R8 100 (C.C./cycle)	■	30	12.11	16.63	18.46 21.09
	◼	20	8.88	14.17	16.67
	□	10	2.37	4.00	5.57
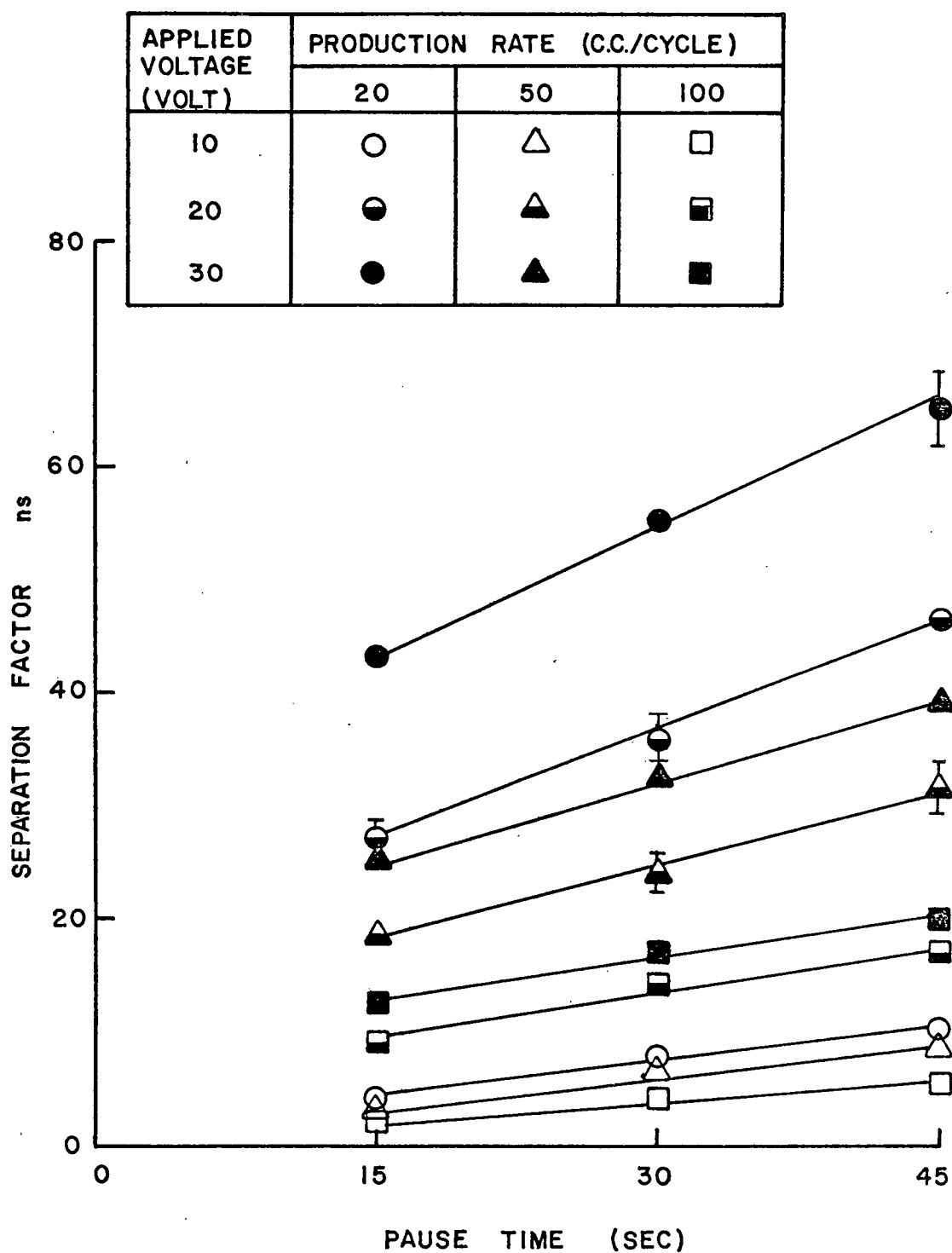
FIGURE 50

Effect of pause time on separation ; 4- Cell column ; initial conc. $C_0 \simeq$ 500 PPM.

Table XXX   Effect of Pause Time on Separation
Two Columns Each Consists of 4 Cells in Series
Initial Concentration Co ≃ 2000 PPM
Exp. Group # R1, R3 and R4

EXP. GROUP and PRODUCTION RATE	GRAPH. SYMBOL	PAUSE TIME (SEC) VOLT. (VOLT)	SEPARATION FACTOR ns		
			15	30	45
R1 20 (C.C./cycle)	●	30	7.49 8.53	13.93 16.52	20.64 18.84
	◐	20	5.71	8.90 10.43	13.00
	○	10	2.74	3.67	4.49
R3 50 (C.C./cycle)	▲	30	3.83	7.78	12.00
	◮	20	2.88	5.00	7.21 6.09
	△	10	1.53	2.03	2.46
R4 100 (C.C./cycle)	■	30	2.45	4.18	7.02 5.99
	▣	20	1.67	2.74	3.76
	□	10	1.39	1.57	1.79

APPLIED VOLTAGE (VOLT)	PRODUCTION RATE (C.C./CYCLE)		
	20	50	100
10	○	△	□
20	◐	▲	◧
30	●	▲	▧
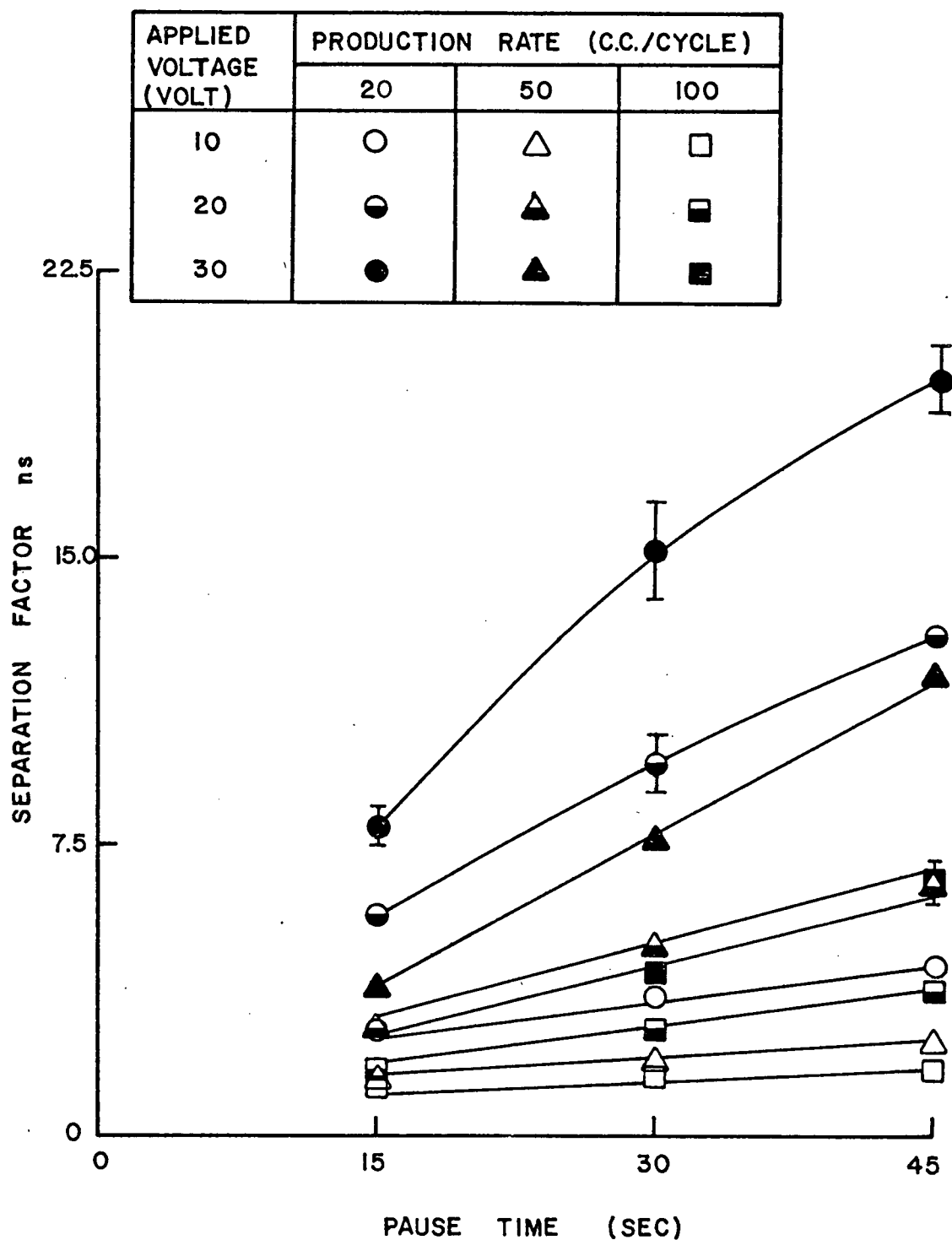
FIGUR 5I

Effect of pause time on separation. 4 - Cell column ; initial conc. $C_0 \approx 2000$ PPM.

Table XXXI Effect of Pause Time on Separation
Two Columns Each Consists of 4 Cells in Series
Initial Concentration Co ≃ 4000 PPM
Exp. Group # R9, R11 and R12

EXP. GROUP and PRODUCTION RATE	GRAPH. SYMBOL	PAUSE TIME (SEC) VOLT. (VOLT)	SEPARATION FACTOR ns	
			30	45
R9 20 (C.C./cycle)	●	30	3.10 3.39	4.56 4.10
	◖	20	1.98	2.67
R11 50 (C.C./cycle)	▲	30	2.50	3.44 3.76
	△	20	1.78	2.20
R12 100 (C.C./cycle)	◼	30	1.91	2.48
	◻	20	1.52	1.77

APPLIED VOLTAGE (VOLT)	PRODUCTION RATE (C.C./CYCLE)		
	20	50	100
20	◑	△	⊟
30	●	▲	⊟
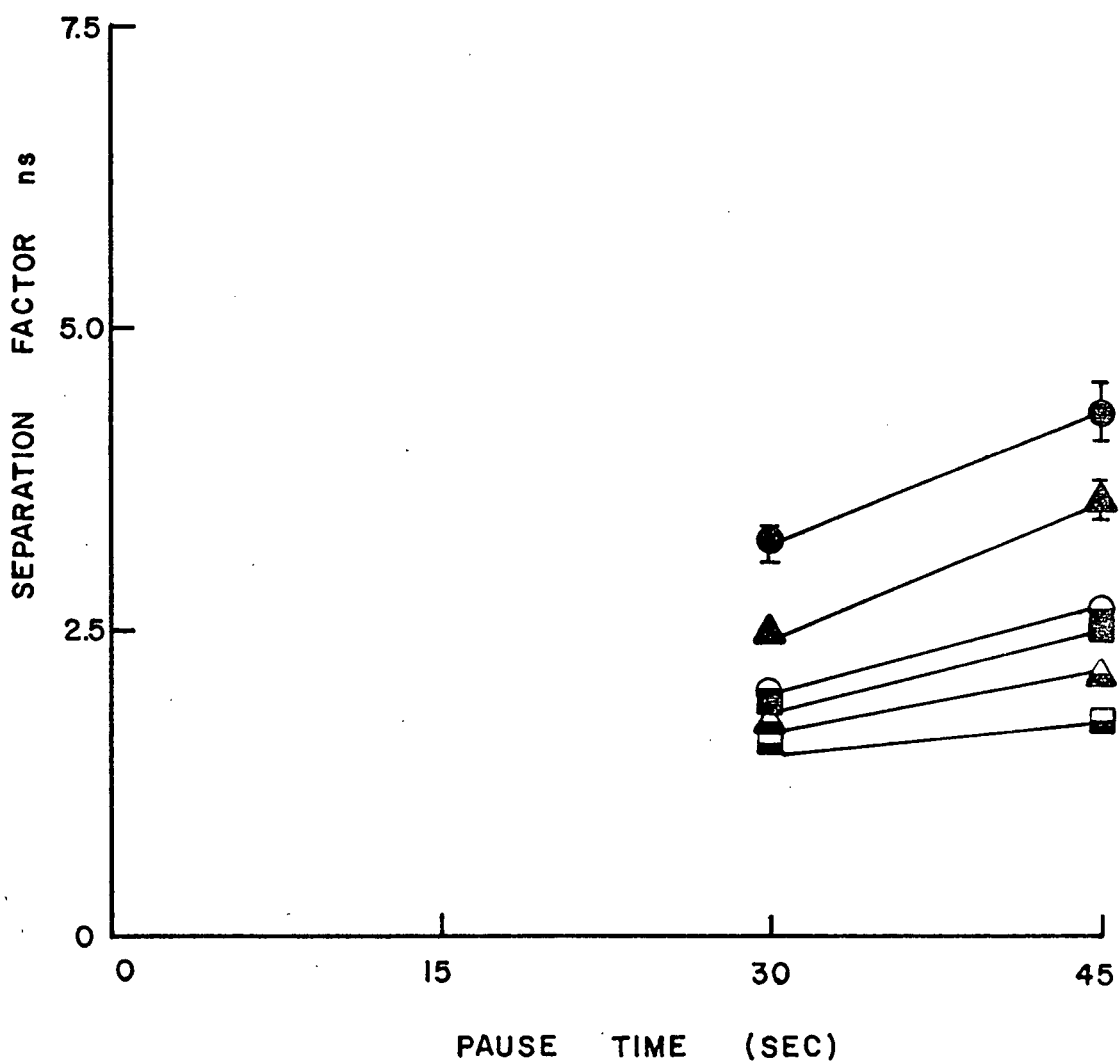
FIGURE 52

Effect of pause time on separation. 4-Cell column ; initial conc. $C_0 \cong 4000$ PPM.

Table XXXII Effect of Pause Time on Separation
Two Columns Each Consists of 8 Cells in Series
Initial Concentration Co ≃ 500 PPM
Exp. Group # M5, M7 and M8

EXP. GROUP and PRODUCTION RATE	GRAPH. SYMBOL	PAUSE TIME (SEC) VOLT. (VOLT)	SEPARATION FACTOR ns		
			15	30	45
M5 25 (C.C./cycle)	●	30	55.33	72.61	77.85
	◒	20	39.92 36.11	51.18	65.50
	○	10	10.67	18.87	25.25
M7 50 (C.C./cycle)	▲	30	44.21 47.14	60.77	63.07
	◭	20	31.21 28.33	39.92	53.96
	△	10	9.13	16.23	22.95
M8 100 (C.C./cycle)	■	30	32.19	46.52	48.43 53.20
	▬	20	21.04	28.33	40.38 37.96
	☐	10	6.40	12.13	18.18
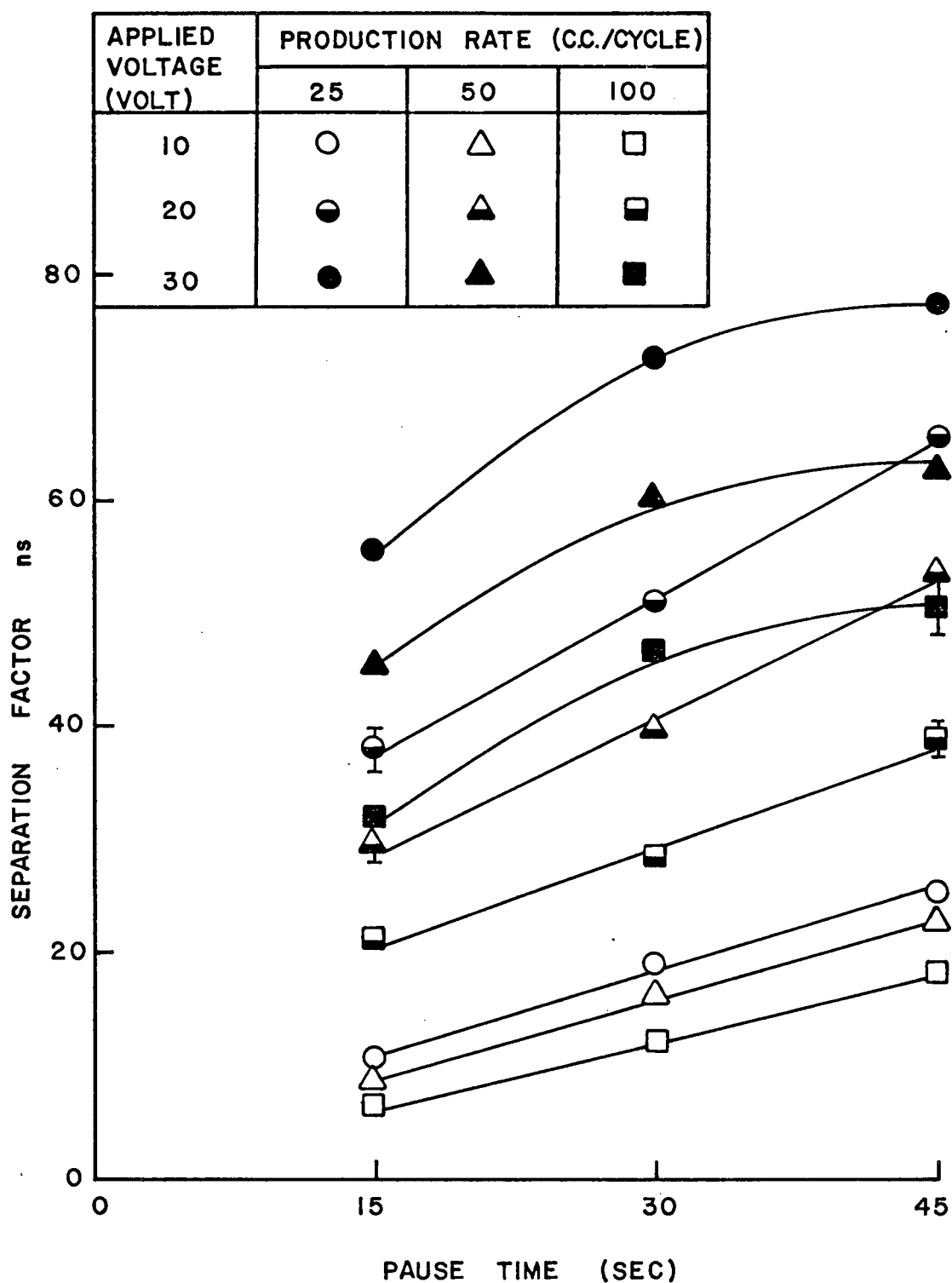
FIGURE 53

Effect of pause time on separation. 8-Cell column; initial conc. $C_0 \triangleq 500\,PPM$.

Table XXXIII Effect of Pause Time on Separation
Two Columns Each Consists of 8 Cells in Series
Initial Concentration Co ≃ 2000 PPM
Exp. Group # M1, M3 and M4

EXP. GROUP and PRODUCTION RATE	GRAPH. SYMBOL	PAUSE TIME (SEC) VOLT. (VOLT)	SEPARATION FACTOR ns		
			15	30	45
M1 25 (C.C./cycle)	●	30	29.46 28.47	36.02	46.28 41.27
	◑	20	11.74	20.41	27.53 31.20
	○	10	4.02	6.45	9.33
M3 50 (C.C./cycle)	▲	30	26.30	32.87	40.95
	◭	20	8.03 9.52	17.03	24.69
	△	10	2.40	4.20	6.77
M4 100 (C.C./cycle)	■	30	22.36	28.45 32.17	33.60
	▢	20	6.39	14.61 14.23	20.83
	▢	10	2.00	3.00	5.66
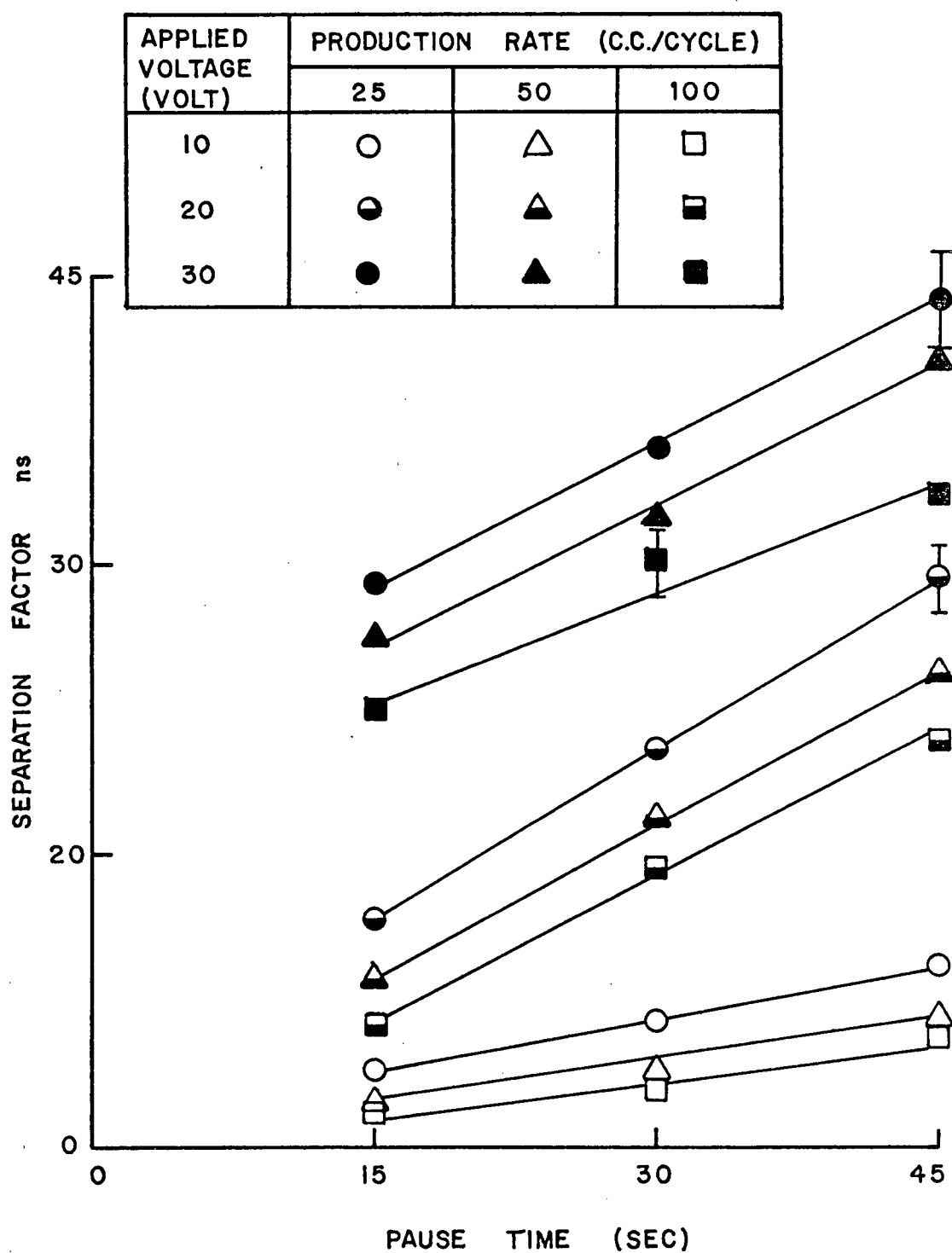
FIGURE 54

Effect of pause time on separation. 8-Cell column ; initial conc. $C_0 \rightleftharpoons 2000$ PPM.

Table XXXIV Effect of Pause Time on Separation
Two Columns Each Consists of 8 Cells in Series
Initial Concentration Co ≃ 4000 PPM
Exp. Group # M9, M11 and M12

EXP. GROUP and PRODUCTION RATE	GRAPH. SYMBOL	PAUSE TIME (SEC) VOLT. (VOLT)	SEPARATION FACTOR ns		
			15	30	45
M9 25 (C.C./cycle)	●	30	16.89	28.13 30.81	37.39
	◒	20	5.19	8.83 7.87	13.19
	○	10	2.20	2.85	3.90
M11 50 (C.C./cycle)	▲	30	15.31	26.05	34.00
	◮	20	4.61	7.50	11.80 12.92
	△	10	1.70	2.40	3.21
M12 100 (C.C./cycle)	■	30	12.54 11.69	22.64	28.62 31.27
	▣	20	3.98 3.63	5.80	10.00
	□	10	1.40	2.00	2.90
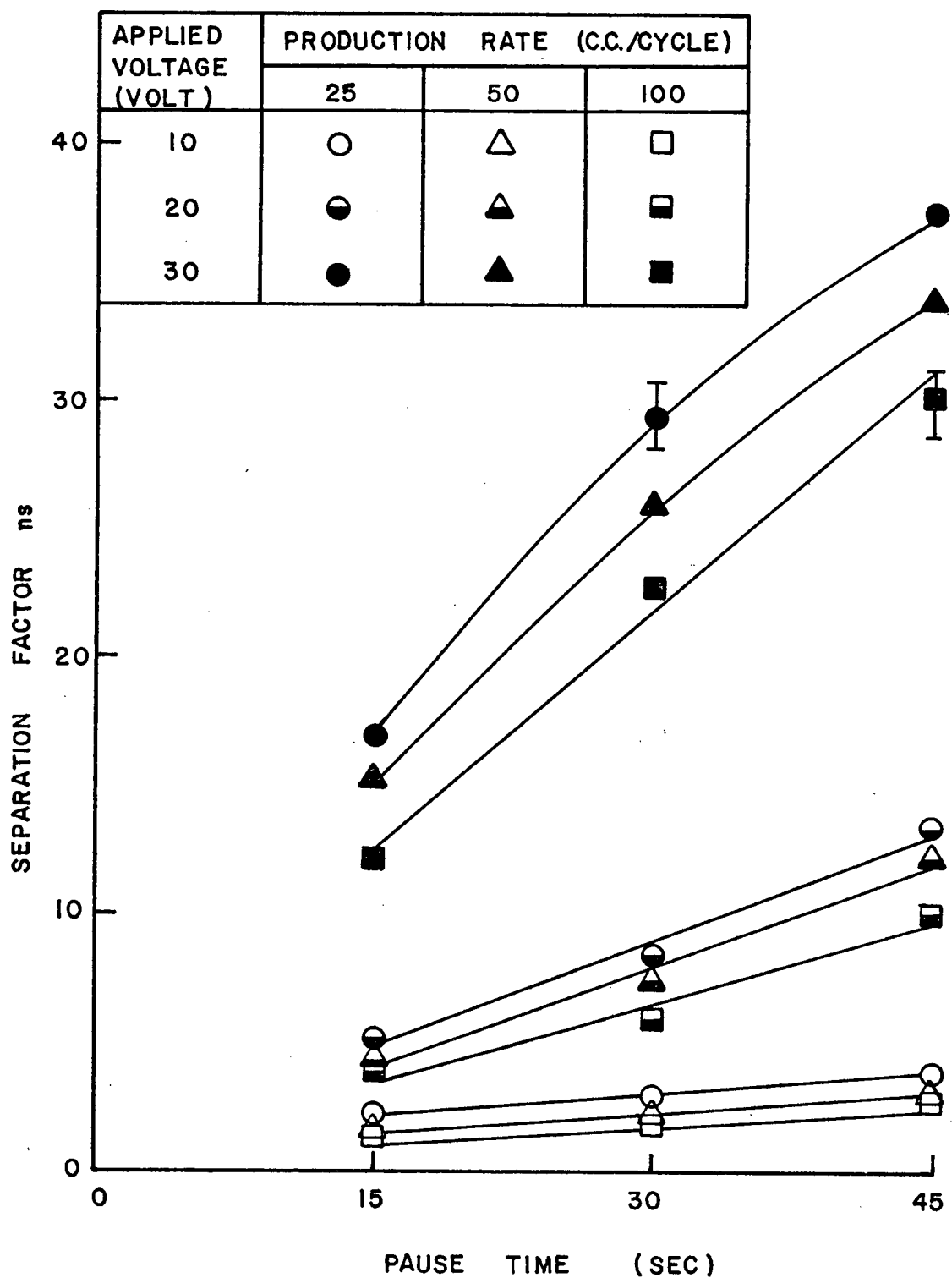
FIGURE 55

Effect of pause time on separation. 8 - Cell column ; initial conc. $C_0 \cong 4000\,PPM.$

Table XXXV   Effect of Pause Time on Separation
$C_o \simeq 500$ ppm;   Group M7

EXP.	GRAPHICAL SYMBOL	PAUSE TIME, τ (SEC)	APPLIED VOLTAGE (VOLT)	CYCLE TIME, T (MIN)	SEPARATION FACTOR ns	$\frac{ns}{T}$ (MIN^{-1})
M7 I	○		10		9.13	5.07
M7 C	◓	15	20	1.8	31.21	17.34
M7 D	●		30		44.21	24.56
M7 H	△		10		16.23	7.06
M7 A	◮	30	20	2.3	39.92	17.36
M7 E	▲		30		60.77	26.42
M7 G	▢		10		22.95	8.20
M7 B	◨	45	20	2.8	53.96	19.27
M7 F	■		30		63.07	22.53

Applied Voltage (Volt)	Pause Time (Sec.)		
	15	30	45
10	○	△	☐
20	◓	◭	◩
30	●	▲	▣
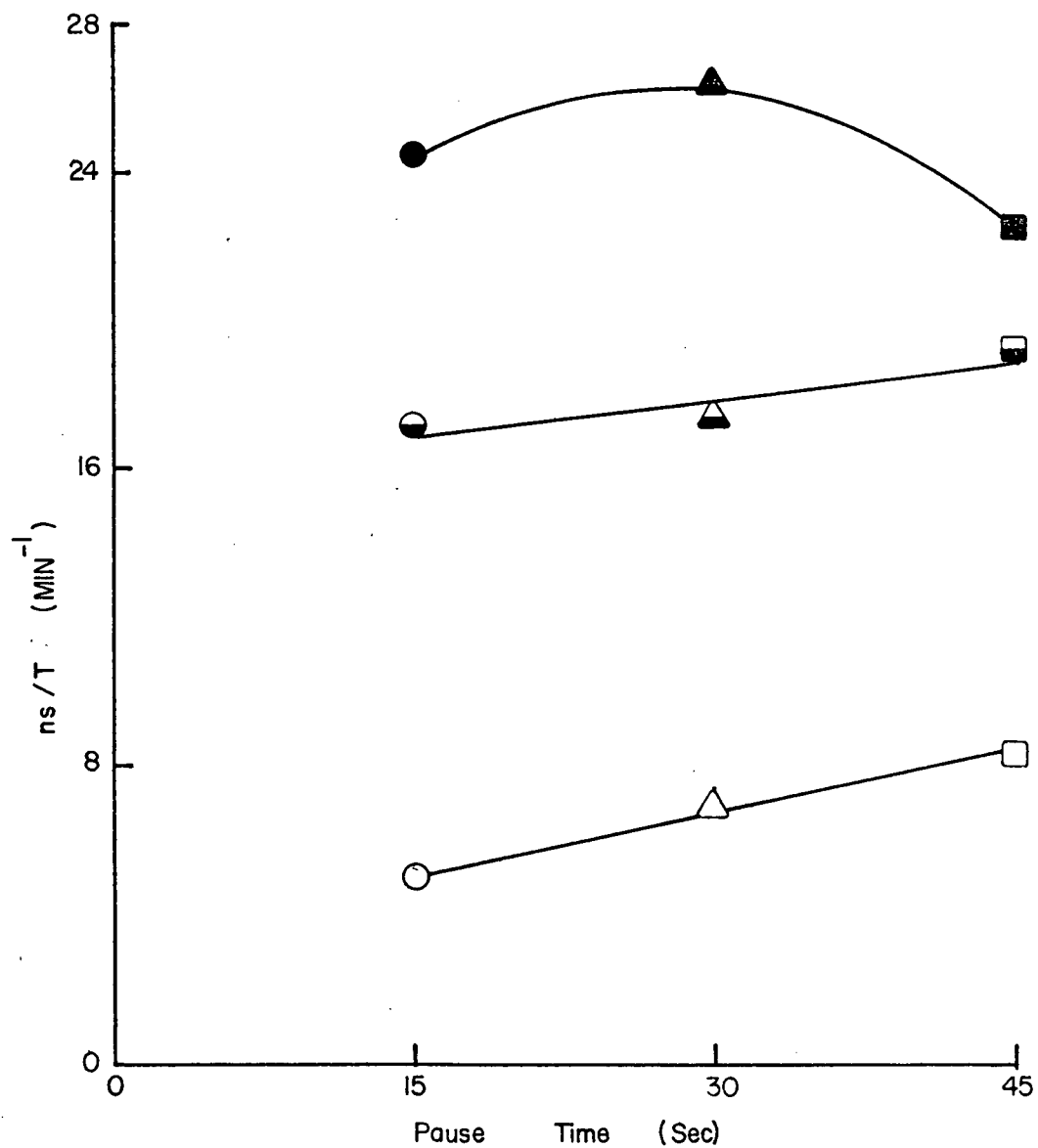
FIGURE   56

Effect of pause time on separation . $C_o \approx 500$ PPM ; Group M 7.

Table XXXVI Effect of Pause Time on Separation
$C_o \simeq 2000$ ppm; Group M3

EXP.	GRAPHICAL SYMBOL	PAUSE TIME, τ (SEC)	APPLIED VOLTAGE (VOLT)	CYCLE TIME, T (MIN)	SEPARATION FACTOR ns	$\dfrac{ns}{T}$ (MIN^{-1})
M3 I	○		10		2.40	1.33
M3 C	◓	15	20	1.8	8.03	4.46
M3 D	●		30		26.30	14.61
M3 H	△		10		4.20	1.83
M3 A	◮	30	20	2.3	17.03	7.40
M3 E	▲		30		32.87	14.29
M3 G	▢		10		6.77	2.42
M3 B	◪	45	20	2.8	24.69	8.82
M3 F	◼		30		40.95	14.63

Applied Voltage (Volt)	Pause Time (Sec.)		
	15	30	45
10	○	△	□
20	◐	◭	▤
30	●	▲	▦
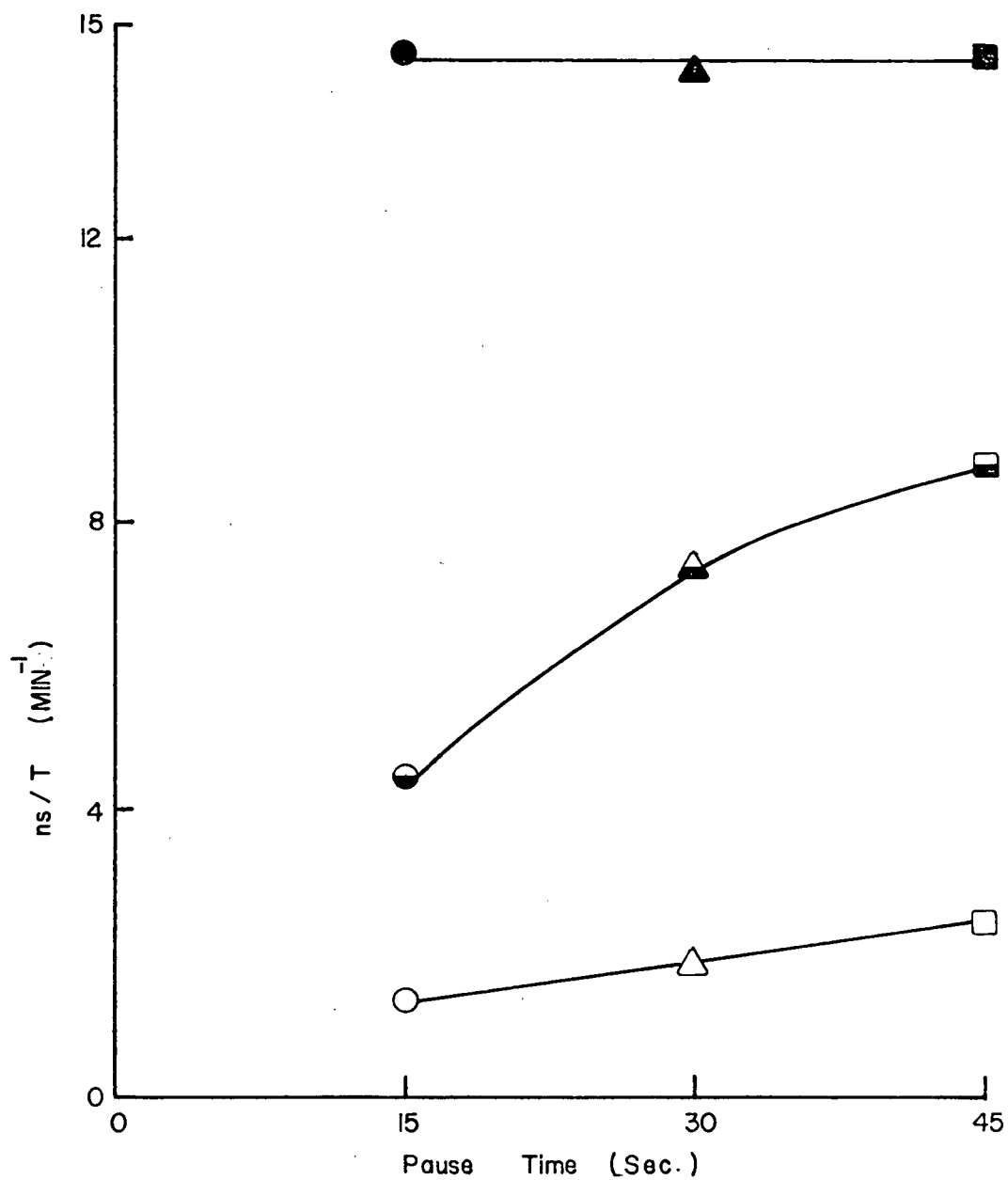
FIGURE 57

Effect of pause time on separation. $C_0 \approx 2000$ PPM ; Group M3 .

Table XXXVII   Effect of Pause Time on Separation
$C_o \simeq 4000$ ppm;   Group M11

EXP.	GRAPHICAL SYMBOL	PAUSE TIME, τ (SEC)	APPLIED VOLTAGE (VOLT)	CYCLE TIME, T (MIN)	SEPARATION FACTOR ns	$\frac{ns}{T}$ (MIN^{-1})
M11 I	○		10		1.70	0.94
M11 C	◑	15	20	1.8	4.61	2.56
M11 D	●		30		15.31	8.51
M11 H	△		10		2.40	1.04
M11 A	◭	30	20	2.3	7.50	3.26
M11 E	▲		30		26.05	11.33
M11 G	☐		10		3.21	1.15
M11 B	◪	45	20	2.8	11.80	4.21
M11 F	◼		30		34.00	12.14

Applied Voltage (Volt)	Pause Time (Sec.)		
	15	30	45
10	○	△	□
20	◐	◭	◒
30	●	▲	▨
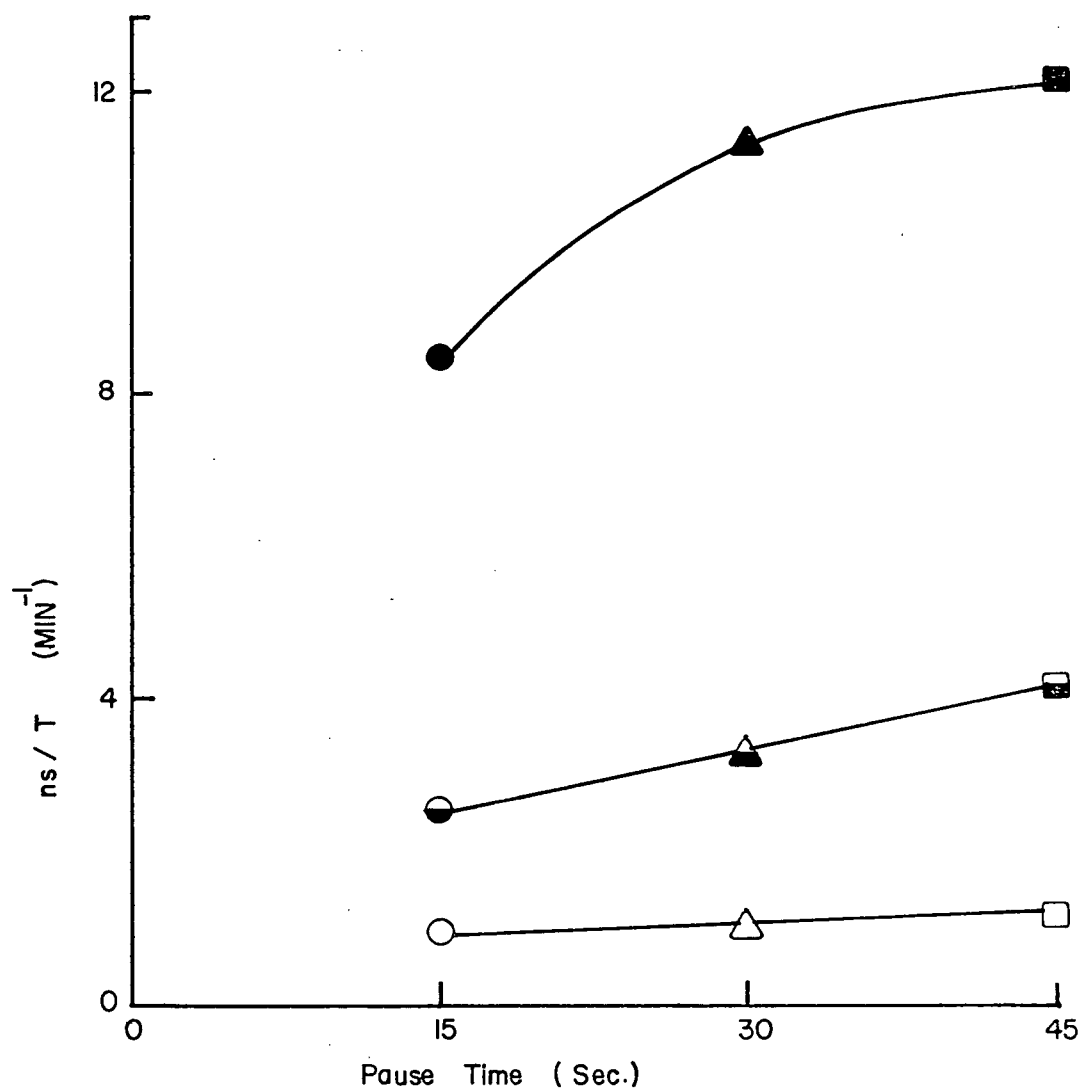
FIGURE 58

Effect of pause time on separation. $C_0 \approx 4000$; Group M II.

summarized as follows:

1. At low voltage ($\Delta\phi$) the separation factor per unit time ns/T varies almost linearly with the pause time τ.

2. As the voltage increases the effect of pause time beyond a certain value becomes less significant and the curve tends to level off.

3. At a further increased voltage the ns/T vs. τ curve goes through a maximum.

4. The maximum pause time that can be utilized without suffering an adverse effect on separation depends on both the applied voltage ($\Delta\phi$) and the feed concentration (C_o). At an applied voltage $\Delta\phi = 30$ V, τ_{max} is about 30 sec for $C_o \simeq 500$ ppm NaCl (Figure 56) and τ_{max} is about 45 sec for $C_o \simeq 2000$ ppm (Figure 57) and a longer pause time can be used for the feed concentration of 4000 ppm NaCl (Figure 58).

5.4.4. <u>Effect of Applied Voltage</u>

The effect of the applied voltage $\Delta\phi$ was investigated in six groups of experiments, each including runs at 10, 20 and 30 V. The other system parameter values are listed in Tables XXXVIII-XLIII which show experiments with feed concentrations of 500, 2000 and 4000 ppm NaCl in 4-stage and 8-stage columns. Figures 59-64 illustrate directly the influence of the applied potential ($\Delta\phi$) on the separation factor (ns).

Increasing the applied voltage improves the separation. The magnitude of this improvement was affected by both the pause time (τ) and the feed concentration (C_o) as shown in Figures 62, 63 and 64. The results are:

1. In experiments with feed concentration $C_o \simeq 500$ ppm NaCl the separation factor (ns) increases almost linearly with the applied voltage; but it levels off at high voltage and long pause time (Figure 62).

Table XXXVIII Effect of Applied Voltage on Separation
Two Columns Each Consists of 4 Cells in Series
Initial Concentration Co ≈ 500 PPM
Exp. Group # R5, R7 and R8

EXP. GROUP and PRODUCTION RATE	GRAPH. SYMBOL	APPLIED VOLTAGE Δφ (VOLT) PAUSE (SEC)	SEPARATION FACTOR ns		
			10	20	30
R5 20 (C.C./cycle)	□	45	10.21	46.25	68.45 61.97
	△	30	7.64	33.97 37.50	55.15
	○	15	3.97	25.37 28.43	42.80
R7 50 (C.C./cycle)	⬓	45	9.01	34.00 29.41	39.07
	◮	30	6.92	25.79 22.27	32.63
	◓	15	3.60	20.00 17.45	25.40
R8 100 (C.C./cycle)	▣	45	5.57	16.67	18.46 21.09
	▲	30	4.00	14.17	16.63
	●	15	2.37	8.88	12.11
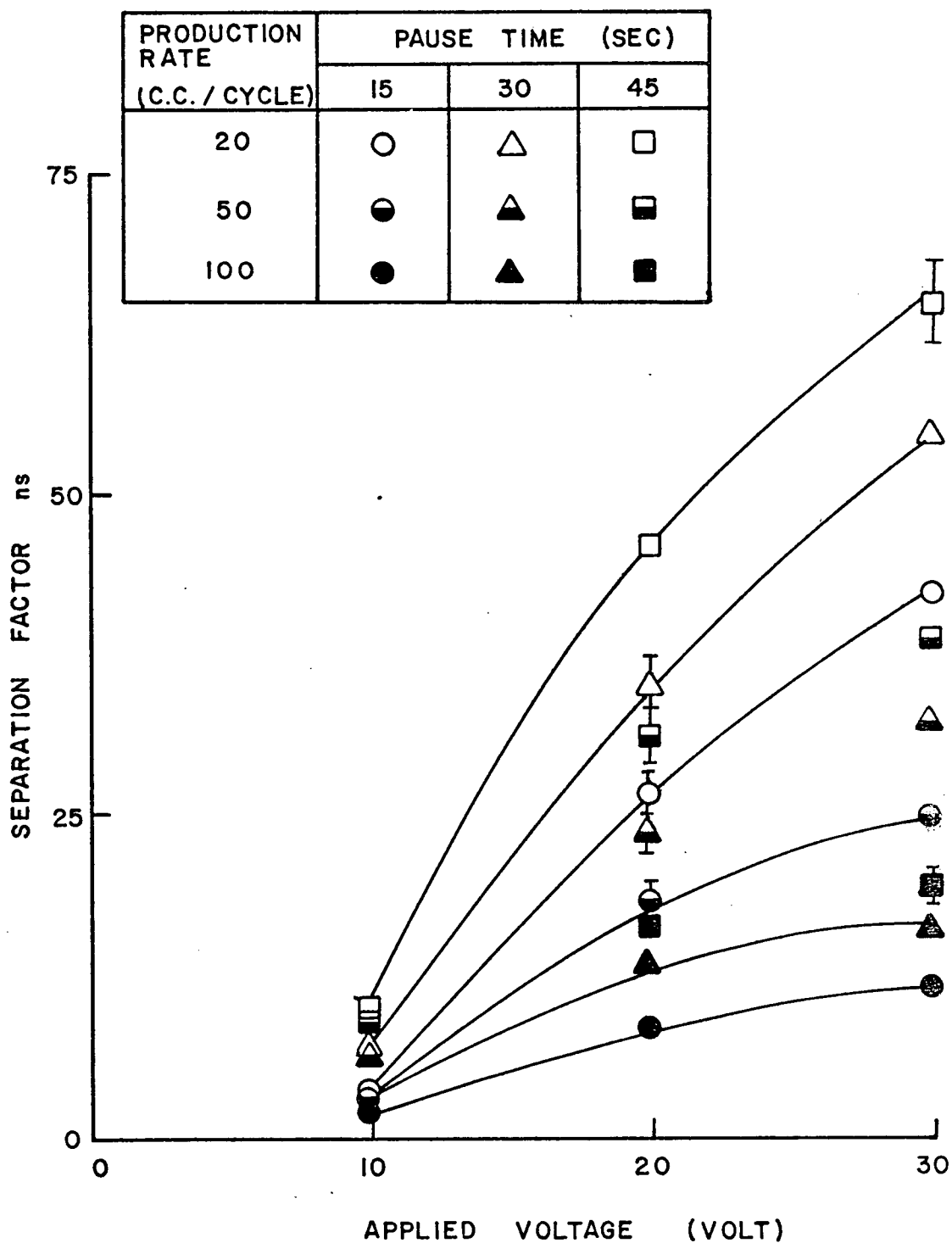
FIGURE 59

Effect of applied voltage on separation. 4-Cell column; initial conc. $C_0 \cong 500$ PPM.

Table XXXIX Effect of Applied Voltage on Separation
Two Columns Each Consists of 4 Cells in Series
Initial Concentration Co ≃ 2000 PPM
Exp. Group # R1, R3 and R4

EXP. GROUP and PRODUCTION RATE	GRAPH. SYMBOL	APPLIED VOLTAGE Δφ (VOLT) PAUSE (SEC)	SEPARATION FACTOR ns 10	20	30
R1 20 (C.C./cycle)	□	45	4.49	13.00	20.64 18.84
	△	30	3.67	8.90 10.43	13.93 16.52
	○	15	2.74	5.71	7.49 8.53
R3 50 (C.C./cycle)	◙	45	2.46	7.21 6.09	12.00
	◮	30	2.03	5.00	7.78
	◓	15	1.53	2.88	3.83
R4 100 (C.C./cycle)	■	45	1.79	3.76	7.02 5.99
	▲	30	1.57	2.74	4.18
	●	15	1.39	1.67	2.45
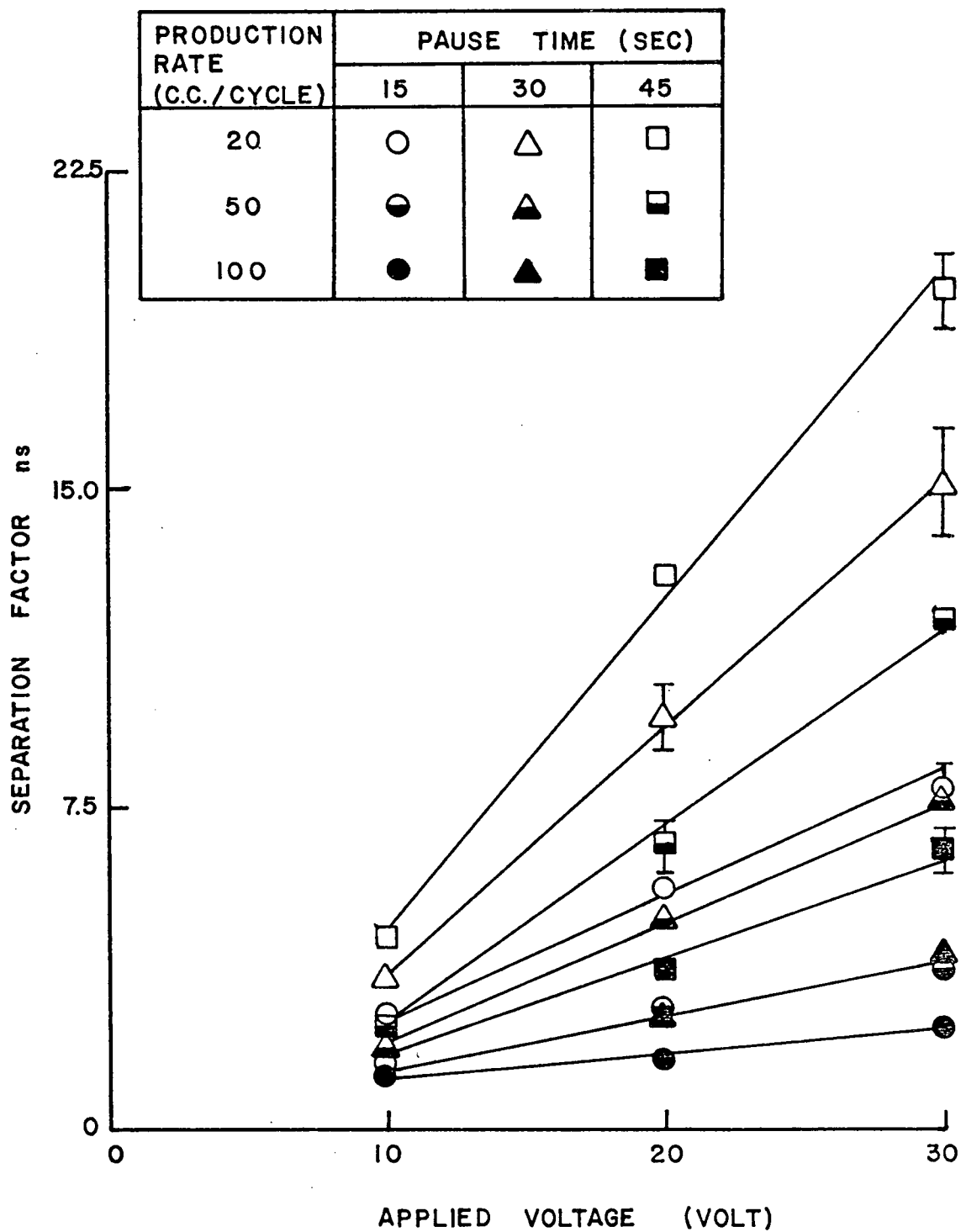
FIGURE 60

Effect of applied voltage on separation . 4 - Cell column ; initial conc. $C_0 \rightleftharpoons$ 2000 PPM .

Table XL   Effect of Applied Voltage on Separation
Two Columns Each Consists of 4 Cells in Series
Initial Concentration Co $\simeq$ 4000 PPM
Exp. Group # R9, R11 and R12

EXP. GROUP and PRODUCTION RATE	GRAPH. SYMBOL	APPLIED VOLTAGE $\Delta\phi$ (VOLT) PAUSE (SEC)	SEPARATION FACTOR ns		
			10	20	30
R9 20 (C.C./cycle)	□	45		2.67	4.56 4.10
	△	30		1.98	3.10 3.39
R11 50 (C.C./cycle)	⬒	45		2.20	3.44 3.76
	◬	30		1.78	2.50
R12 100 (C.C./cycle)	■	45		1.77	2.48
	▲	30		1.52	1.91

PRODUCTION RATE (C.C./CYCLE)	PAUSE TIME (SEC)	
	30	45
20	△	☐
50	◭	◪
100	▲	◼
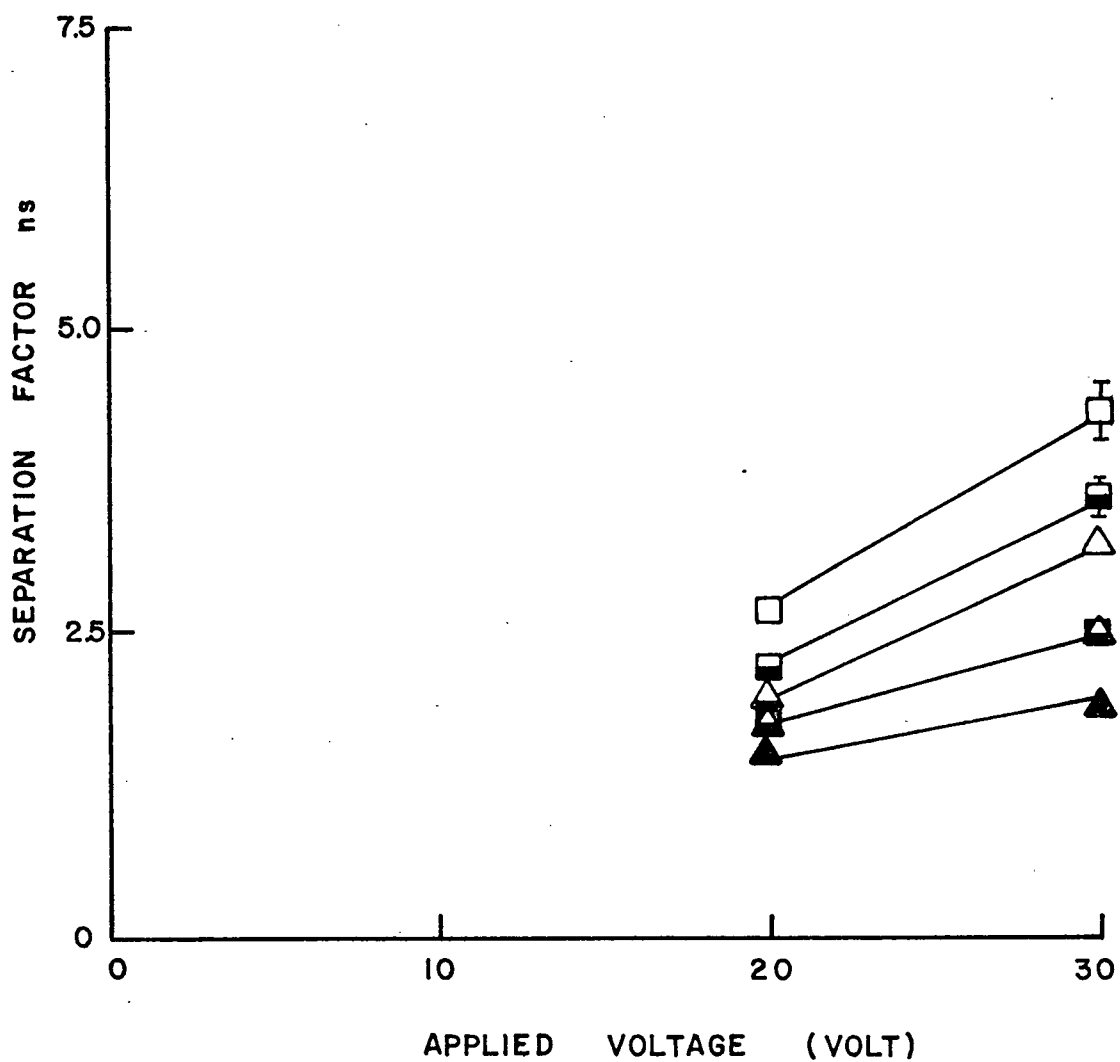
FIGURE 6I

Effect of applied voltage on separation . 4-Cell column ; initial conc. $C_0 \doteq 4000$ PPM.

Table XLI   Effect of Applied Voltage on Separation
            Two Columns Each Consists of 8 Cells in Series
            Initial Concentration Co $\simeq$ 500 PPM
            Exp. Group # M5, M7 and M8

EXP. GROUP and PRODUCTION RATE	GRAPH. SYMBOL	APPLIED VOLTAGE $\Delta\phi$ (VOLT) PAUSE (SEC)	SEPARATION FACTOR ns		
			10	20	30
M5 25 (C.C./cycle)	□	45	25.25	65.50	77.85
	△	30	18.87	51.18	72.61
	○	15	10.67	39.92	55.33
				36.11	
M7 50 (C.C./cycle)	⬓	45	22.95	53.96	63.07
	◓	30	16.23	39.92	60.77
	◓	15	9.13	31.21	44.21
				28.33	47.14
M8 100 (C.C./cycle)	■	45	18.18	40.38	48.43
				37.96	53.20
	▲	30	12.13	28.33	46.52
	●	15	6.40	21.04	32.19

PRODUCTION RATE (C.C./CYCLE)	PAUSE TIME (SEC)		
	15	30	45
25	○	△	☐
50	◓	△	⊟
75	●	▲	■
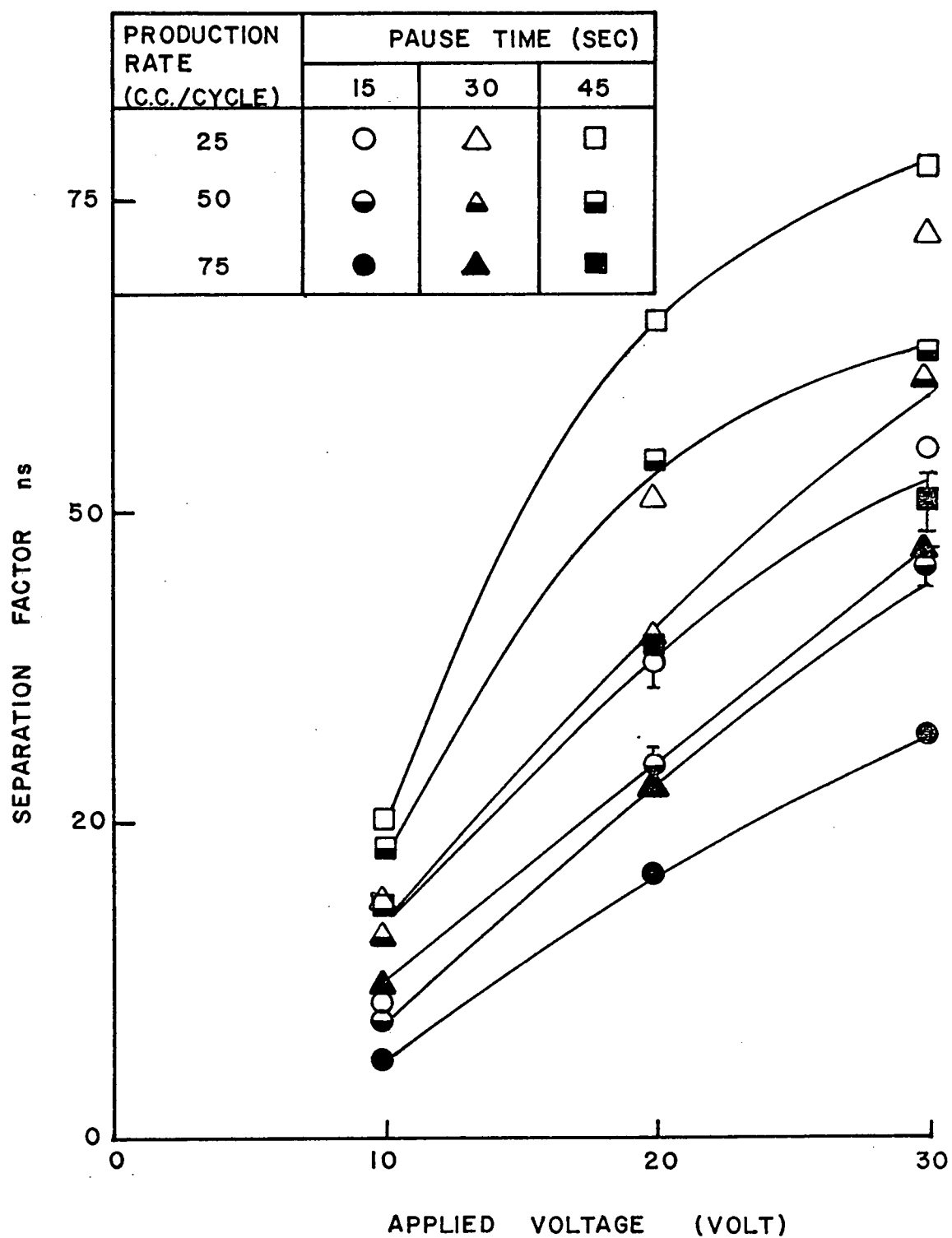
FIGURE 62

Effect of applied voltage on separation . 8-Cell column ; initial conc. $C_0 \simeq 500$ PPM.

Table XLII Effect of Applied Voltage on Separation
Two Columns Each Consists of 8 Cells in Series
Initial Concentration Co $\simeq$ 2000 PPM
Exp. Group # M1, M3 and M4

EXP. GROUP and PRODUCTION RATE	GRAPH. SYMBOL	APPLIED VOLTAGE $\Delta\phi$ (VOLT) PAUSE (SEC)	SEPARATION FACTOR ns		
			10	20	30
M1 25 (C.C./cycle)	□	45	9.33	27.53 31.20	46.28 41.27
	△	30	6.45	20.41	36.02
	○	15	4.02	11.74	29.46 28.47
M3 50 (C.C./cycle)	⬒	45	6.77	24.69	40.95
	⬔	30	4.20	17.03	32.87
	⬓	15	2.40	8.03 9.52	26.30
M4 100 (C.C./cycle)	■	45	5.66	20.83	33.60
	▲	30	3.00	14.61 14.23	28.45 32.17
	●	15	2.00	6.39	22.36
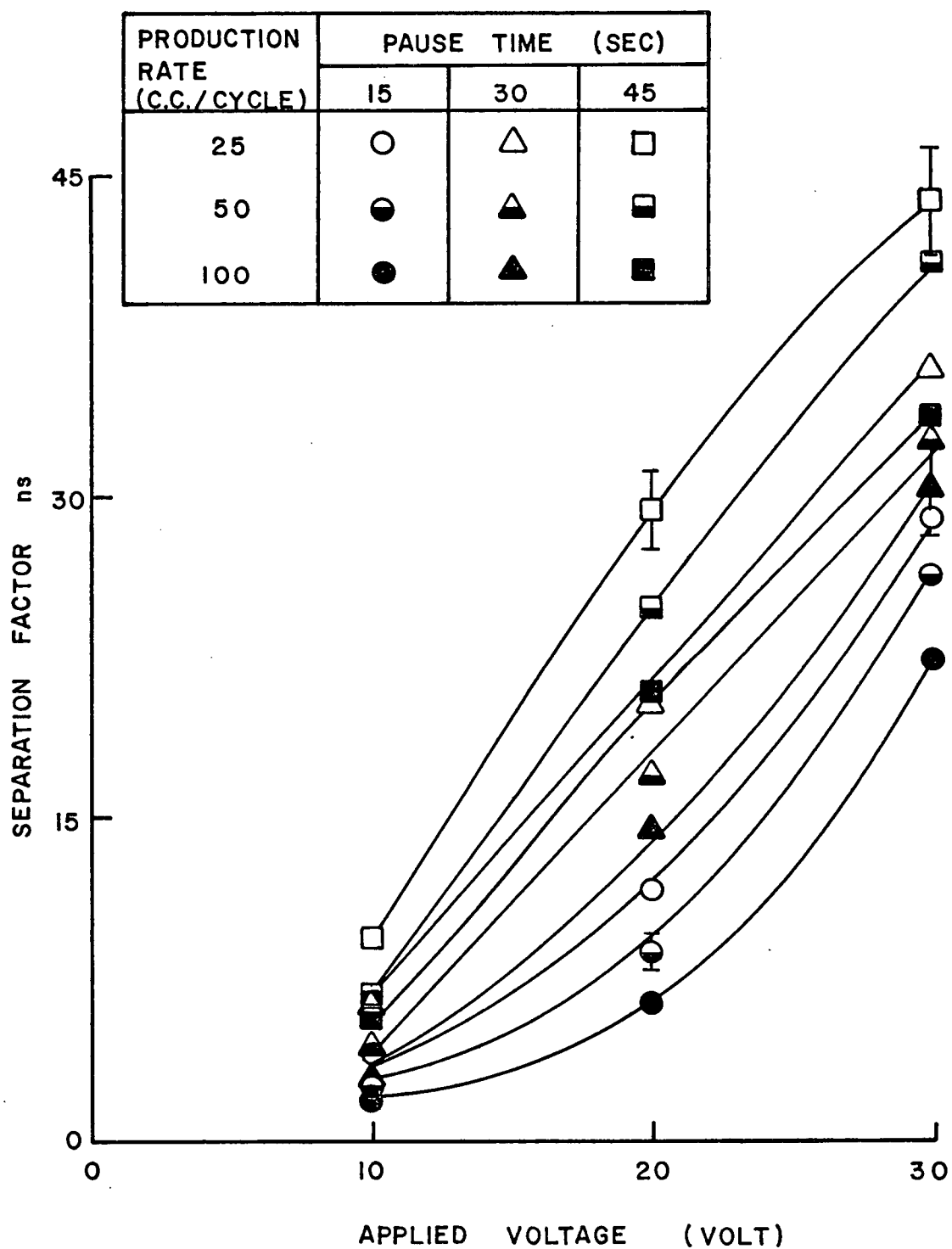
FIGURE 63

Effect of applied voltage on separation. 8- Cell column ; Initial conc. $C_o \cong 2000$ PPM.

Table XLIII   Effect of Applied Voltage on Separation
Two Columns Each Consists of 8 Cells in Series
Initial Concentration Co ≃ 4000 PPM
Exp. Group # M9, M11 and M12

EXP. GROUP and PRODUCTION RATE	GRAPH. SYMBOL	APPLIED VOLTAGE Δφ (VOLT) PAUSE (SEC)	SEPARATION FACTOR ns		
			10	20	30
M9 25 (C.C./cycle)	□	45	3.90	13.19	37.39
	△	30	2.85	8.83	28.13
			.	7.87	30.81
	○	15	2.20	5.19	16.89
M11 50 (C.C./cycle)	⊟	45	3.21	11.80	34.00
				12.92	
	◮	30	2.40	7.50	26.05
	⊖	15	1.70	4.61	15.31
M12 100 (C.C./cycle)	■	45	2.90	10.00	28.62
	▲	30	2.00	5.80	22.64
	●	15	1.40	3.98	12.54
				3.63	11.69
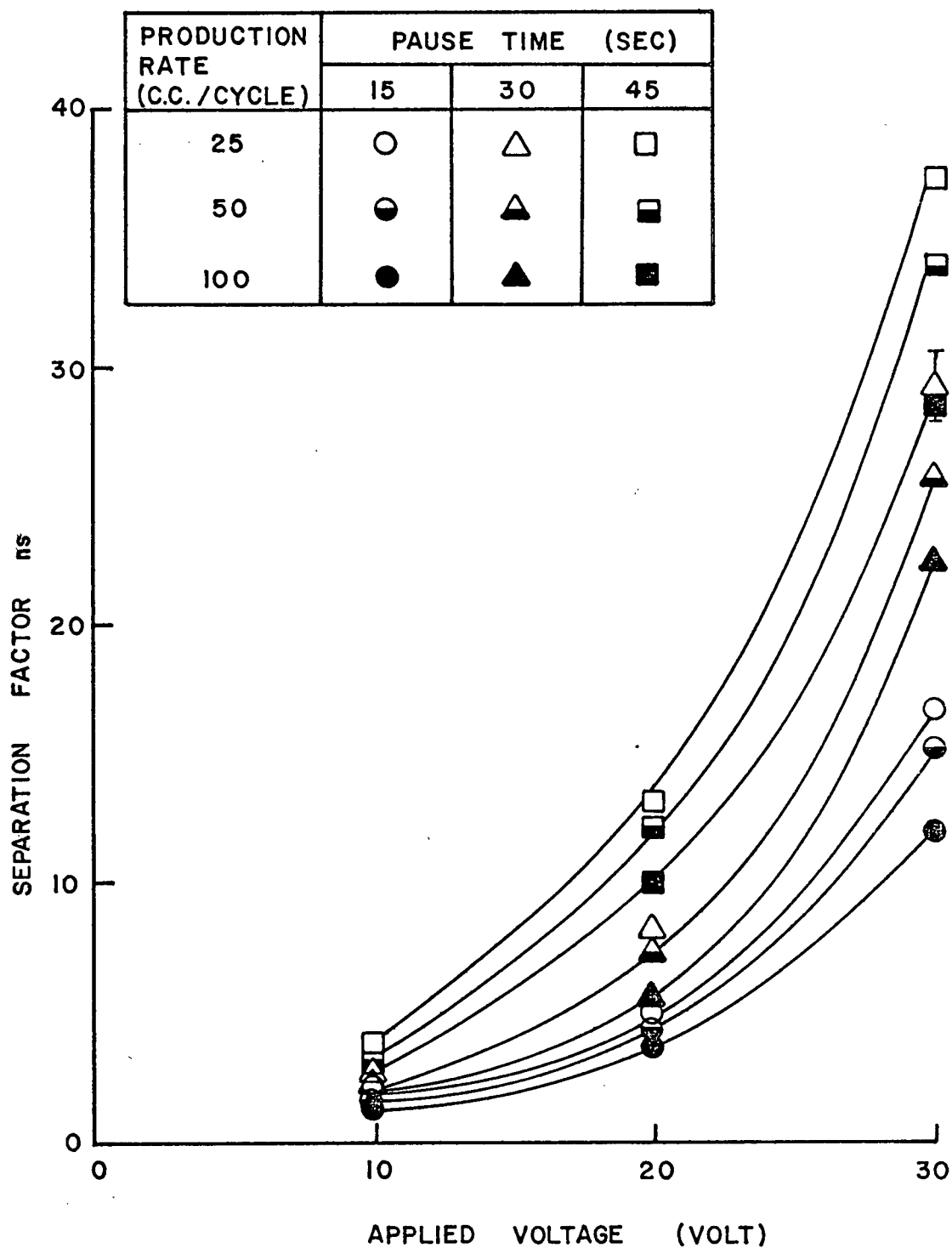
FIGURE 64

Effect of applied voltage on separation . 8- Cell column; initial conc. $C_0 \cong 4000$ PPM.

2. With feed concentrations of 2000 ppm and 4000 ppm NaCl the separation factor is seen to rise more than proportional to the applied voltage.

3. The effect of applied voltage is more pronounced when the feed concentration is high (compare Figures 62 and 64) and/or the pause time is short (refer to Figure 63).

The analysis of the influence of the applied voltage ($\Delta\phi$) is not as straightforward as that of the pause time (τ). Operating at high voltage always results in a higher energy consumption per unit product at a fixed product quality, but at the same time increasing voltage increases the current density and accelerates production rate. Using the method of ohmic analysis, the d.c. power dissipation in a given stack of constant average resistance R at current I is RI^2. The amount of salt shifted, and hence the amount of fresh water produced, are proportional to I. Therefore, the d.c. power dissipation per unit volume of diluate produced is proportional to I. Fixed costs per unit volume of diluate produced, on the other hand, are inversely proportional to I and the optimum current density and the applied voltage can only be determined by the economical evaluation of the plant.

The individual items contributing to the total operating cost of an ED process may be placed in three categories:

(a) costs that vary directly with current density such as the electric energy costs

(b) costs that vary inversely with current density (the fixed charges) such as membrane replacement and amortization of capital investment costs. Less membrane area and lower capital costs are required at high current densities

(c) costs that are invariant with current density such as those for operating and maintenance labor and the cost of pretreatment chemicals.

Figure 65 shows typical variations of these cost items with current density. The cost-optimization method developed by Cowan (1960) expresses the total cost of processing (y) as the sum of three terms:

$$y = aI + \frac{b}{I} + c \tag{102}$$

where a, b and c are taken as constants for a given stack if ohmic analysis applies. This simplified method has been modified by Lacey et al. (1963) and Mattson et al. (1965). By differentiation of Eq. (102) to find minimum product cost, the optimum current is seen to be

$$I_{opt} = (\frac{b}{a})^{\frac{1}{2}} \tag{103}$$

Substituting this value in the equation for the total cost y, it is found that for most economical operation the first two terms are to be equal (power costs = fixed costs).

This optimum condition can almost never be met in conventional electro-dialysis, however, because polarization phenomena set an upper limit to the permissible current densities; and the fixed costs contribute more towards the total cost than they should do under the optimum conditions. Thus the polarization limitation, rather than the results of economic optimization, frequently controls the operating current density and the applied voltage in practical electrodialysis installations.

It can be concluded that when no excessive polarization takes place the high voltage is beneficial and generally results in a more efficient and economical operation of an ED plant.
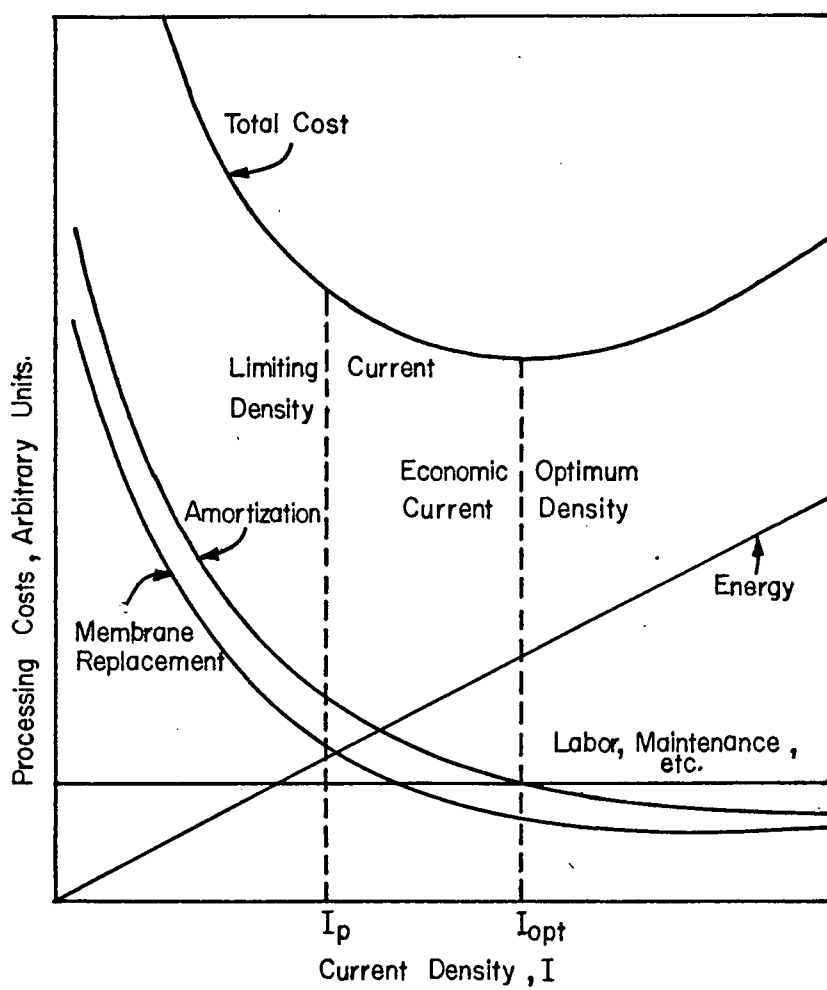
FIGURE 65

Variation of individual cost items making up the total processing cost.

5.4.5. Effect of Initial Concentration

Three groups of experiments were made at initial concentrations C_o of 500, 2000 and 4000 ppm NaCl/H$_2$0. With these experiments the concentration of the rinse solution was 1000, 2000 and 4000 ppm respectively. Tables XLIV, XLV and XLVI summarize the operating conditions of short columns (4 stages in series) at the three feed concentrations and Figures 66, 67 and 68 display the variation of the separation factor with the feed concentration. Tables XLVII, XLVIII and XLIX together with Figures 69, 70 and 71 represent similar groups of experiments performed in longer columns each consisting of 8 stages in series. The results are summarized as follows:

1. In all cases the higher feed concentration had a retarding effect on separation and resulted in a lower separation factor. This is because the higher concentration requires proportionally larger mass transfer rates to achieve the same separation.

2. The effect of the feed concentration C_o on separation factor ns is less pronounced with the longer columns than with the short ones (Compare Figures 66-68 with Figures 69-71). At the same separation factor ns the concentration difference ΔC ($\Delta C = C_B - C_D$) is higher with the higher feed concentration and longer columns are required to diminish the concentration gradient $\frac{\Delta C}{\ell}$ between the column ends and thus to suppress the undesirable axial mixing that developed with the high feed concentration.

5.4.6. No-Pause Operation

The pause time τ was dropped to zero in 7 runs at various feed concentrations to check findings from the previous work in a batch system (Bass, 1972). Table L summarizes the operating conditions and final results and Figure 72 contrasts the separation factors of no-pause operation ($\tau = 0$)

Table XLIV   Effect of Feed Concentration, (Co) on Separation
Two Columns Each Consists of 4 Cells in Series
Production Rate ≃   20 C.C./cycle
Exp. Group # R1, R5 and R9

EXP.	GRAPH. SYMBOL	APPLIED VOLTAGE (VOLT)	INITIAL CONC. (PPM) PAUSE (SEC)	SEPARATION FACTOR ns		
				500	2000	4000
A	△		30	33.97 37.50	8.90 10.43	1.98
B	⊟	20	45	46.25	13.00	2.67
C	◒		15	25.37 28.43	5.71	
D	●		15	42.80	7.49 8.53	
E	▲	30	30	55.15	13.93 16.52	3.10 3.39
F	■		45	68.45 61.97	20.64 18.84	4.56 4.10

APPLIED VOLTAGE (VOLT)	PAUSE TIME (SEC)		
	15	30	45
20	◓	△	◫
30	●	▲	■
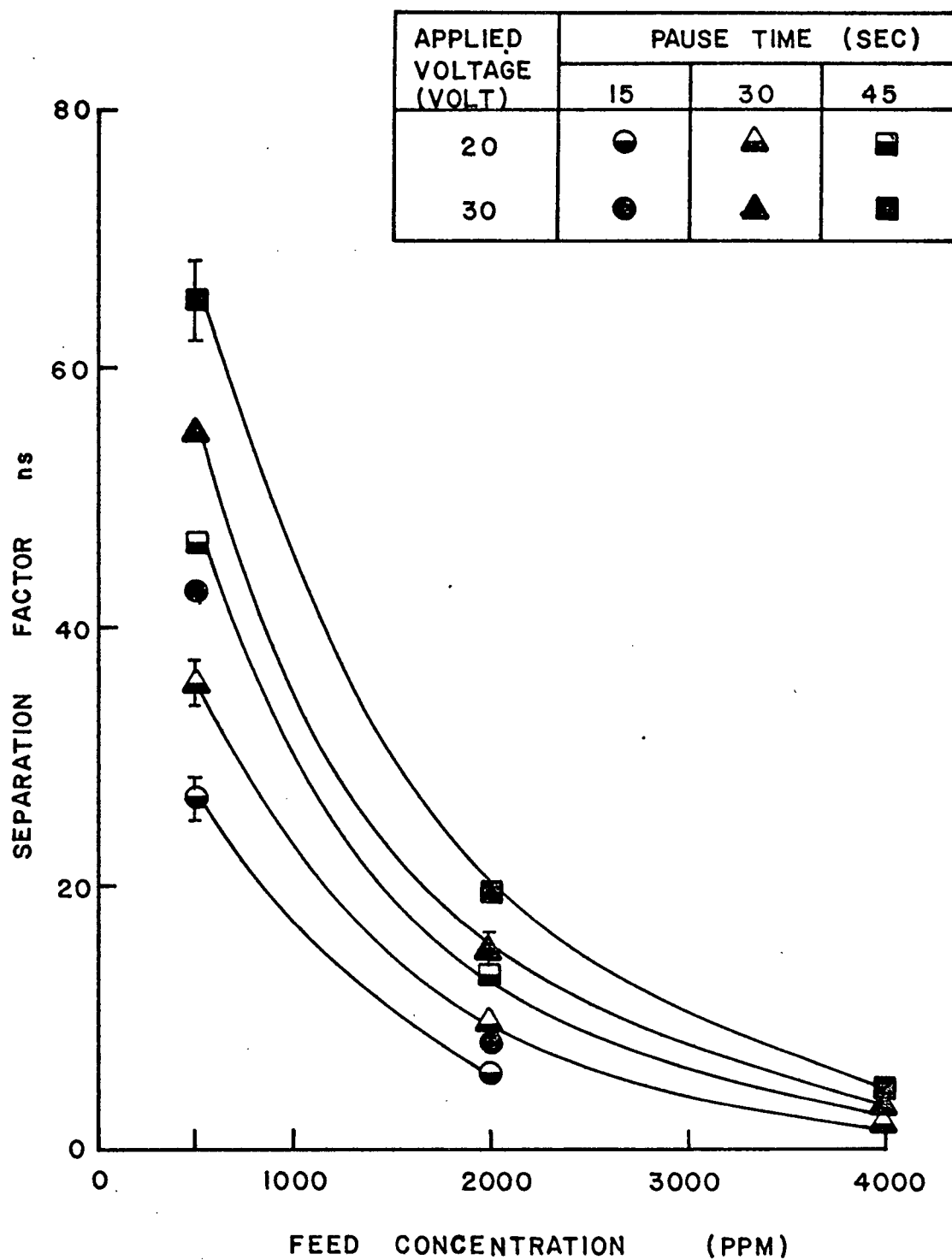
FIGURE 66

Effect of feed concentration (C_0) on separation.
4-Cell column — production rate ≃ 20 C.C./cycle .

Table XLV   Effect of Feed Concentration (Co) on Separation
             Two Columns Each Consists of 4 Cells in Series
             Production Rate ≃ 50 C.C./cycle
             Exp. Group # R3, R7 and R11

EXP.	GRAPH. SYMBOL	APPLIED VOLTAGE (VOLT)	PAUSE (SEC) INITIAL CONC. (PPM)	SEPARATION FACTOR ns 500	2000	4000
A	◬		30	25.79 22.27	5.00	1.78
B	▣	20	45	34.00 29.41	7.21 6.09	2.20
C	◓		15	20.00 17.45	2.88	
D	●		15	25.40	3.83	
E	▲	30	30	32.63	7.78	2.50
F	■		45	39.07	12.00	3.44 3.76
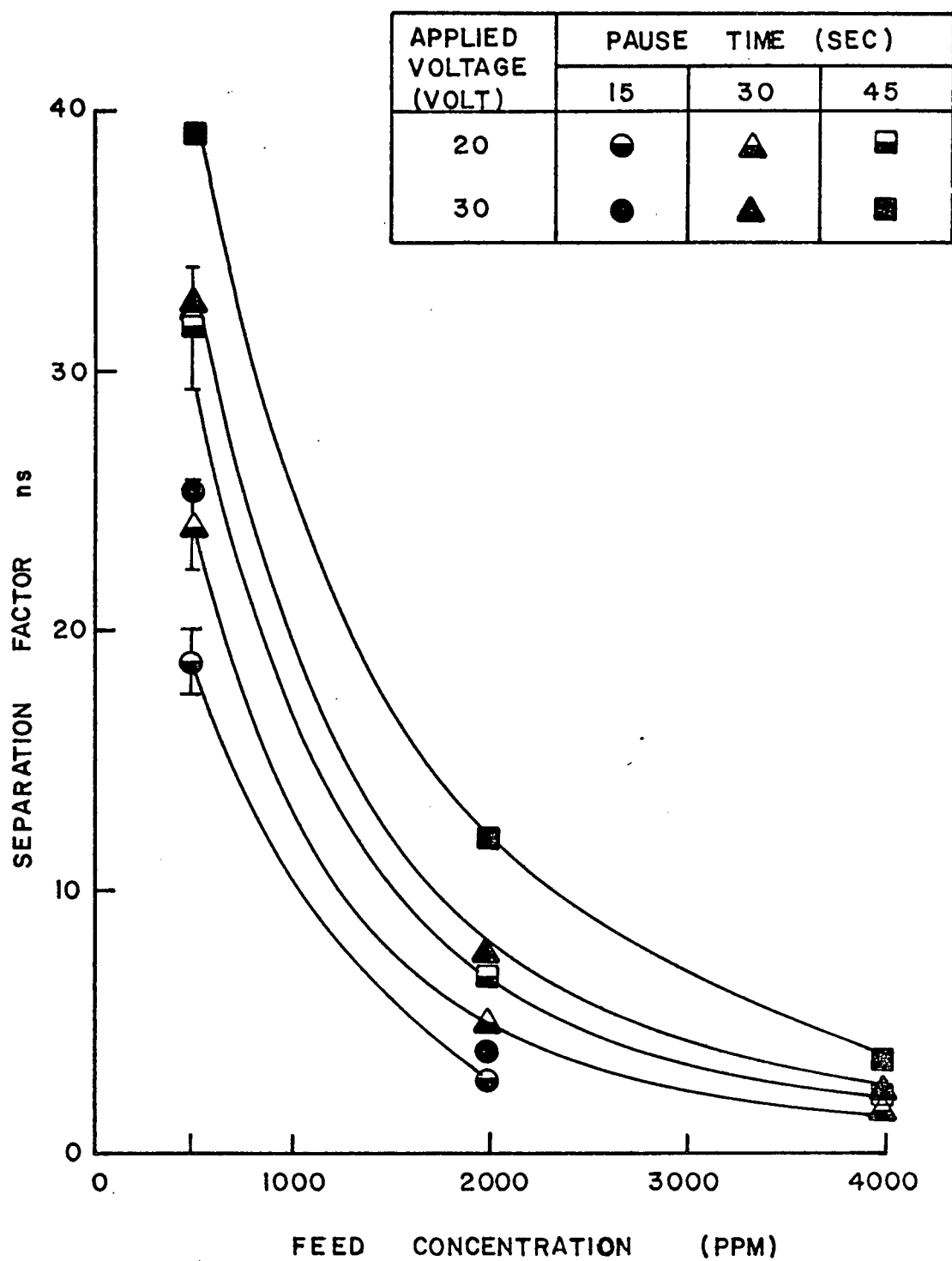
FIGURE 67

Effect of feed concentration (C_0) on separation.
4- Cell column _ production rate $\cong$ 50 C.C./cycle.

Table XLVI Effect of Feed Concentration (Co) on Separation
Two Columns Each Consists of 4 Cells in Series
Production Rate ≃ 100 C.C./cycle
Exp. Group # R4, R8 and R12

EXP.	GRAPH. SYMBOL	APPLIED VOLTAGE (VOLT)	INITIAL CONC. (PPM) PAUSE (SEC)	SEPARATION FACTOR ns		
				500	2000	4000
A	△		30	14.17	2.74	1.52
B	⬒	20	45	16.67	3.76	1.77
C	◓		15	8.88	1.67	
D	●		15	12.11	2.45	
E	▲	30	30	16.63	4.18	1.91
F	■		45	18.46 21.09	7.02 5.99	2.48

APPLIED VOLTAGE (VOLT)	PAUSE	TIME	(SEC)
	15	30	45
20	◓	△	◻
30	●	▲	◼
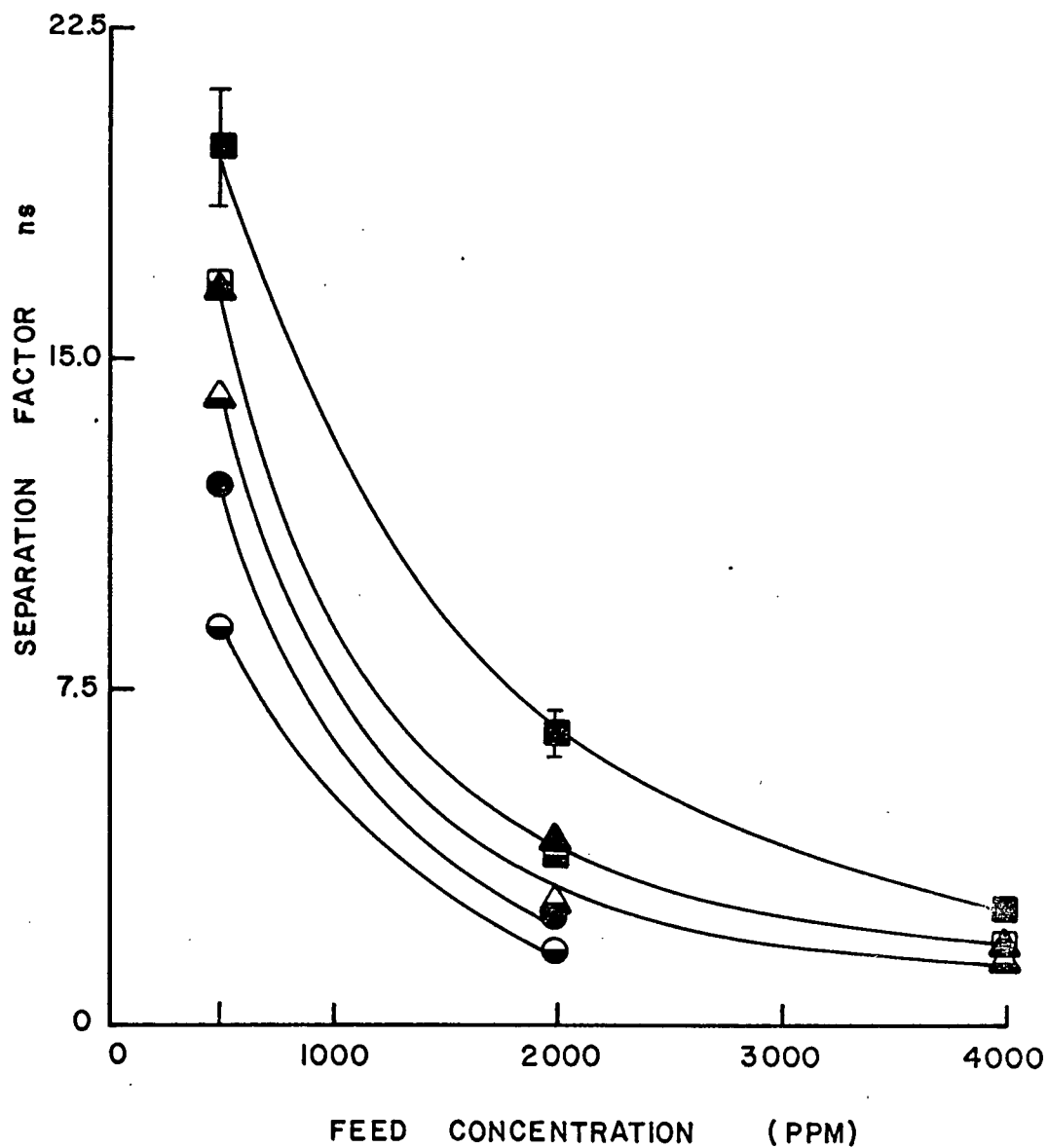
FIGURE 68

Effect of feed concentration (C$_0$) on separation.
4 — Cell column — production rate $\rightleftharpoons$ 100 C.C./cycle.

Table XLVII   Effect of Feed Concentration (Co) on Separation
Two Columns Each Consists of 8 Cells in Series
Production Rate ≃ 25 C.C./cycle
Exp. Group # M1, M5 and M9

EXP.	GRAPH. SYMBOL	APPLIED VOLTAGE (VOLT)	INITIAL CONC. PAUSE (SEC)	(PPM)	SEPARATION FACTOR ns 500	2000	4000
A	◮		30		51.18	20.41	8.83 7.87
B	◪	20	45		65.50	27.53 31.20	13.19
C	◑		15		39.92 36.11	11.74	5.19
D	●		15		55.33	29.46 28.47	16.89
E	▲	30	30		72.61	36.02	28.13 30.81
F	◼		45		77.85	46.28 41.28	37.39
G	▢		45		25.25	9.33	3.90
H	△	10	30		18.87	6.45	2.85
I	○		15		10.67	4.02	2.20

APPLIED VOLTAGE (VOLT)	PAUSE TIME (SEC)		
	15	30	45
10	○	△	□
20	◒	▲	▣
30	●	▲	◼
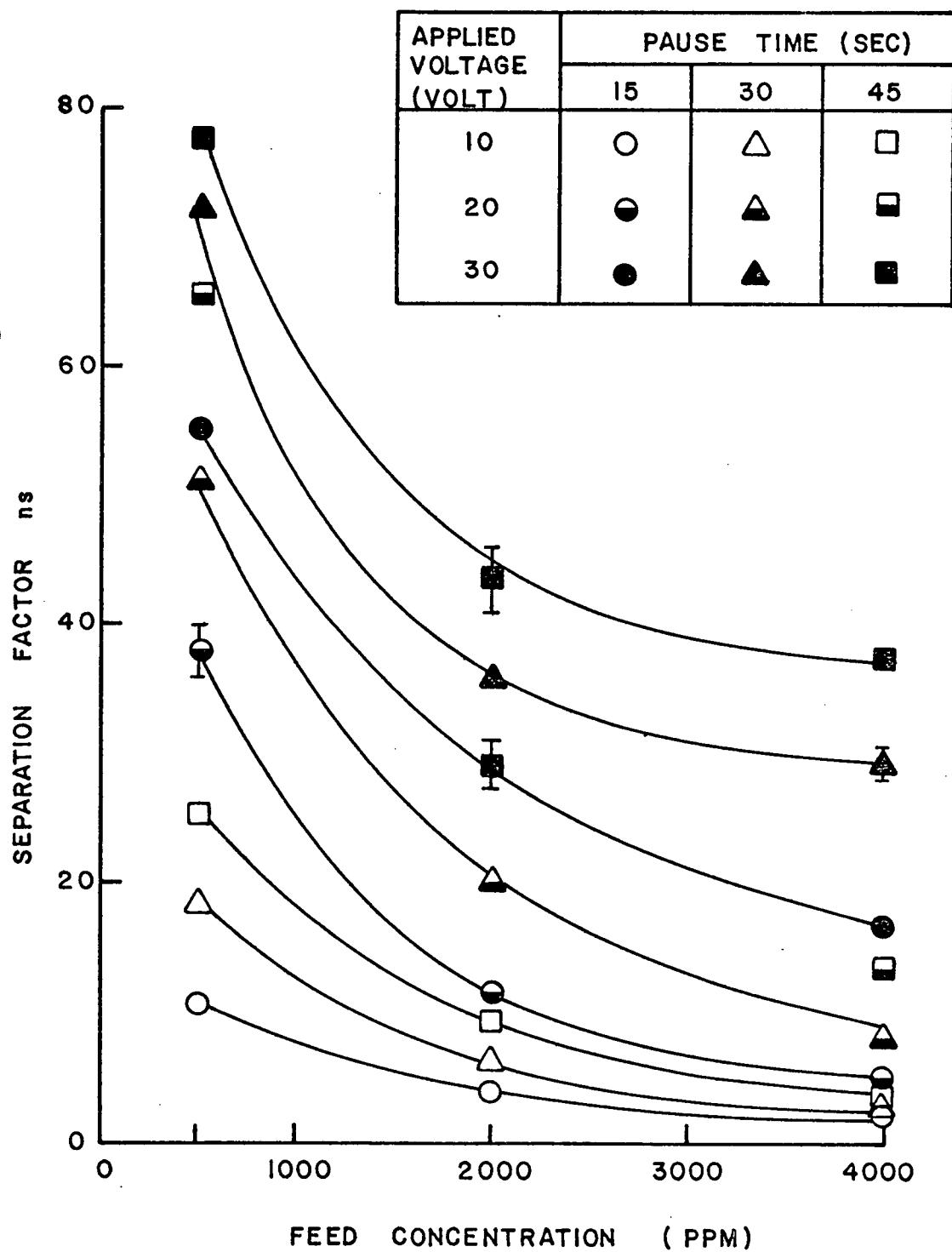
FIGURE 69

Effect of feed concentration (C_0) on separation . 8 - Cell column _ Production rate ≃ 25 C.C./cycle

Table XLVIII   Effect of Feed Concentration (Co) on Separation
Two Columns Each Consists of 8 Cells in Series
Production Rate $\simeq$ 50 C.C./cycle
Exp. Group # M3, M7 and M11

EXP.	GRAPH. SYMBOL	APPLIED VOLTAGE (VOLT)	INITIAL CONC. (PPM) PAUSE (SEC)	SEPARATION FACTOR ns 500	2000	4000
A			30	39.92	17.03	7.50
B		20	45	53.96	24.69	11.80 12.92
C			15	31.21 28.33	8.03 9.52	4.61
D			15	44.21 47.14	26.30	15.31
E		30	30	60.77	32.87	26.05
F			45	63.07	40.95	34.00
G			45	22.95	6.77	3.21
H		10	30	16.23	4.20	2.40
I			15	9.13	2.40	1.70
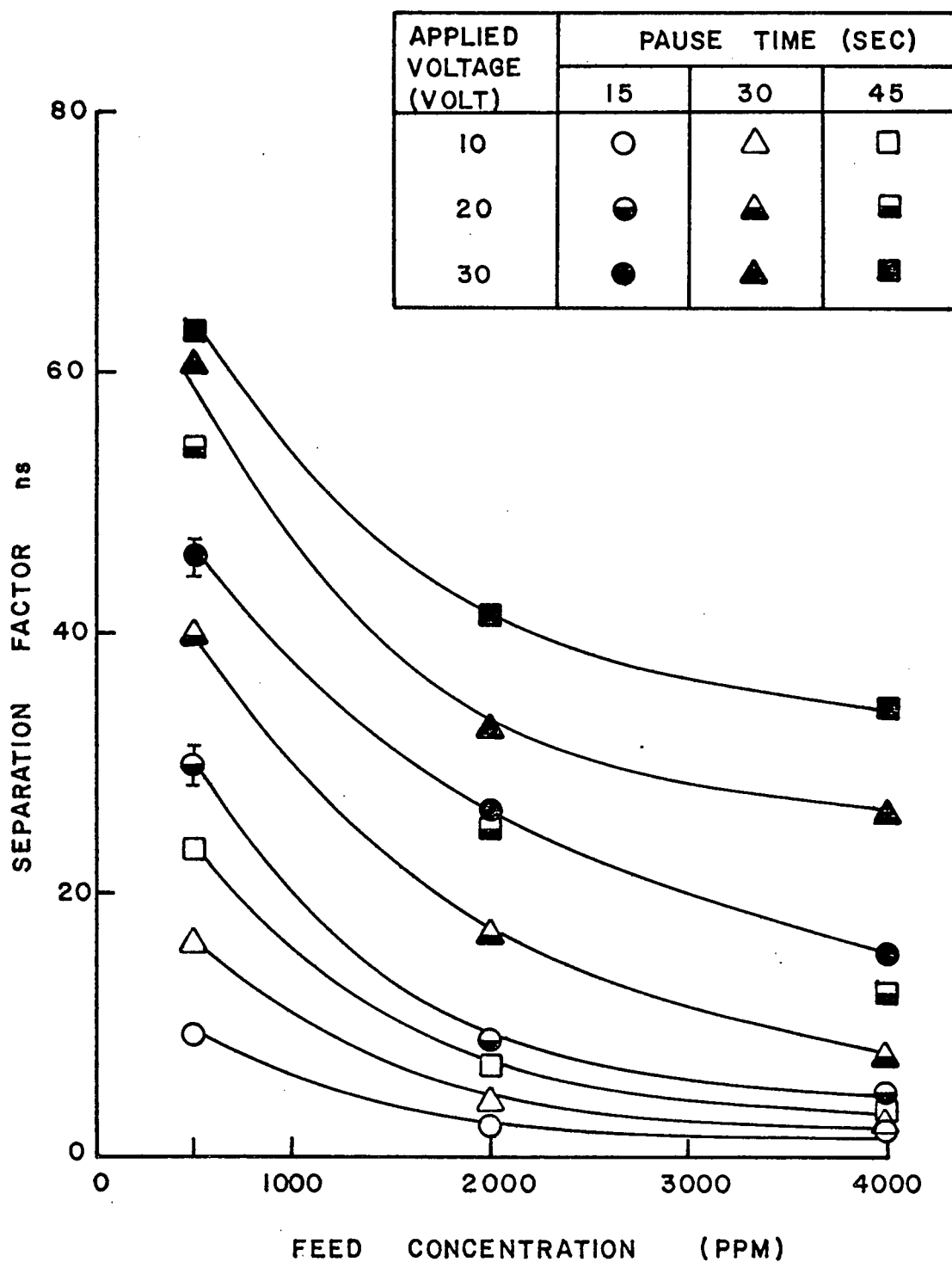
FIGURE 70

Effect of feed concentration (C_0) on separation.
8 - Cell column _ production rate $\cong$ 50 C.C./cycle.

Table XLIX Effect of Feed Concentration (Co) on Separation
            Two Columns Each Consists of 8 Cells in Series
            Production Rate ≈ 100 C.C./cycle
            Exp. Group # M4, M8 and M12

EXP.	GRAPH. SYMBOL	APPLIED VOLTAGE (VOLT)	INITIAL CONC. PAUSE (SEC) (PPM)	SEPARATION FACTOR ns		
				500	2000	4000
A	◓		30	28.33	14.61 14.23	5.80
B	⬒	20	45	40.38 37.96	20.83	10.00
C	◓		15	21.04	6.39	3.98 3.63
D	●		15	32.19	22.36	12.54 11.69
E	▲	30	30	46.52	28.45 32.17	22.64
F	■		45	48.43 53.20	33.60	28.62 31.27
G	□		45	18.18	5.66	2.90
H	△	10	30	12.13	3.00	2.00
I	○		15	6.40	2.00	1.40
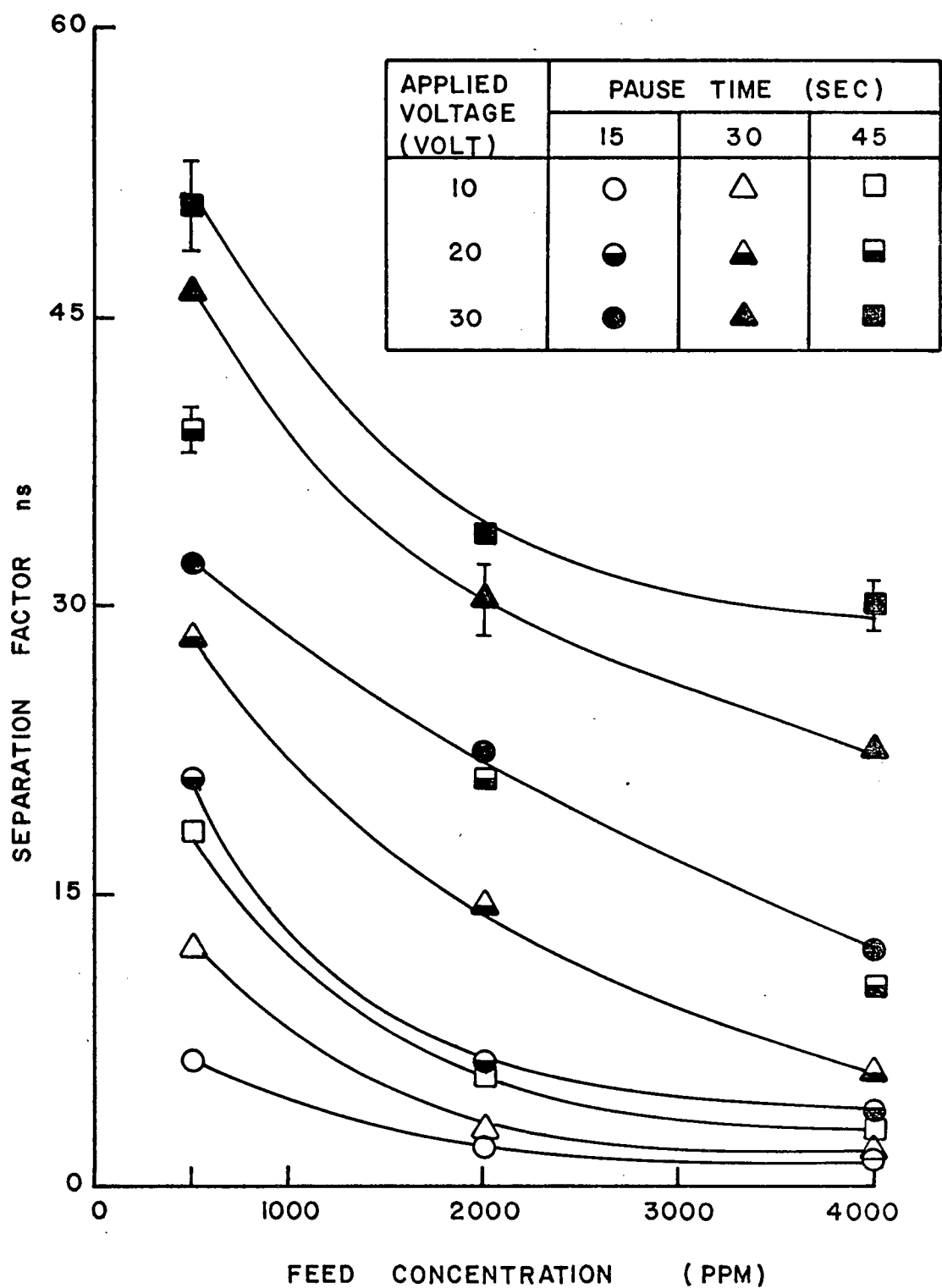
FIGURE 7I

Effect of feed concentration (C_0) on separation.
8 _ Cell column _ production rate ≈ I00 C.C./cycle .

Table L   Comparison of Pause and No-Pause Operations
8-Cell Column
Production Rate $\simeq$ 50 C.C./cycle

EXP.	GRAPH. SYMBOL	FEED CONC. (PPM)	APPLIED VOLTAGE (VOLT)	SEPARATION FACTOR ns			
				PAUSE OPERATION			NO-PAUSE OPERATION
				45 SEC	30 SEC	15 SEC	
M7D	●	500	30	63.07	60.77	47.14 44.21	15.77
M7C	◗		20	53.96	39.92	28.33 31.21	11.91
M3D	▲	2000	30	40.95	32.87	26.30	7.56
M3C	◬		20	24.69	17.03	9.52 8.03	3.56
M3I	△		10	6.77	4.20	2.40	1.60
M11D	■	4000	30	34.00	26.05	15.31	3.13
M11C	⬒		20	12.92 11.80	7.50	4.61	2.16
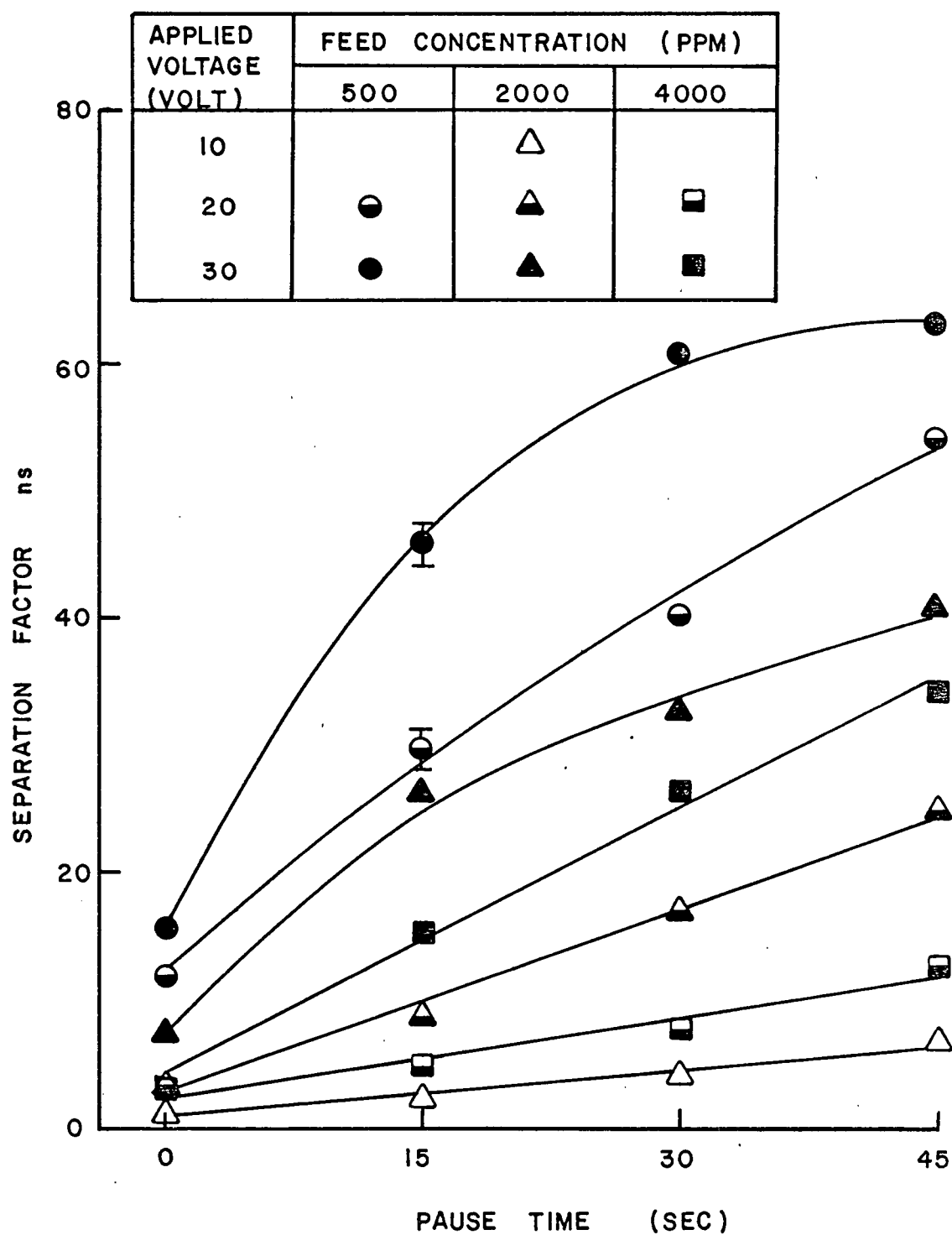
FIGURE 72

Comparison of pause and no_pause operations.
8 — Cell column _ production rate ≏ 50 C.C./cycle.

with the normal or pause-operation (τ = 15, 30 and 45 sec.) under otherwise identical conditions.

One can see that reducing the pause time to zero in all cases studied resulted in a considerably decreased separation. This confirmed the previous findings that flow pauses at the beginning of each half cycle represent important features of the cyclic ED operation.

5.4.7. Pure-Pause Operation

In pure-pause operation the electric power is off during circulation and interphase mass transfer takes place only during pause periods in each cycle. This mode of operation seemed attractive since it could result in large power savings. Table LI lists 12 runs; half of them were conducted with power on during circulation while the other half were performed with pure-pause operation under otherwise identical conditions. Figure 73 displays the separation factor ns achieved by the two modes of operation. The results are:

1. Pure-pause operation saves electric power, but results in poor separation.

2. This effect is more pronounced with short pause time.

5.4.8. Semi-Symmetric Operation

In semi-symmetric operation feed is introduced and products withdrawn every half cycle while in asymmetric operation the system is closed during the first half cycle (refer to Chapter 4). Six experiments were performed under various operating conditions using semi-symmetric operation. Table LII lists the operating conditions and the final separation achieved. These experiments were compared with similar runs under asymmetric operation as

Table LI   Comparison of Pure Pause with Mixed Mode Operations
            8-Cell Columns - PRODUCTION Rate $\simeq$ 50 C.C./cycle
            Initial Concentration (Co) $\simeq$ 2000 PPM

EXP.	GRAPH. SYMBOL	APPLIED VOLTAGE (VOLT)	PAUSE TIME (SEC)	SEPARATION FACTOR ns	
				POWER ON DURING CIRCULATION	POWER OFF DURING CIRCULATION
M3A			30	17.03	4.34
M3B	⬒ ◓	20	45	24.69	7.32
M3C			15	8.03 9.52	2.45
M3D			15	26.30	3.37
M3E	◼ ●	30	30	32.87	7.02
M3F			45	40.95	11.49
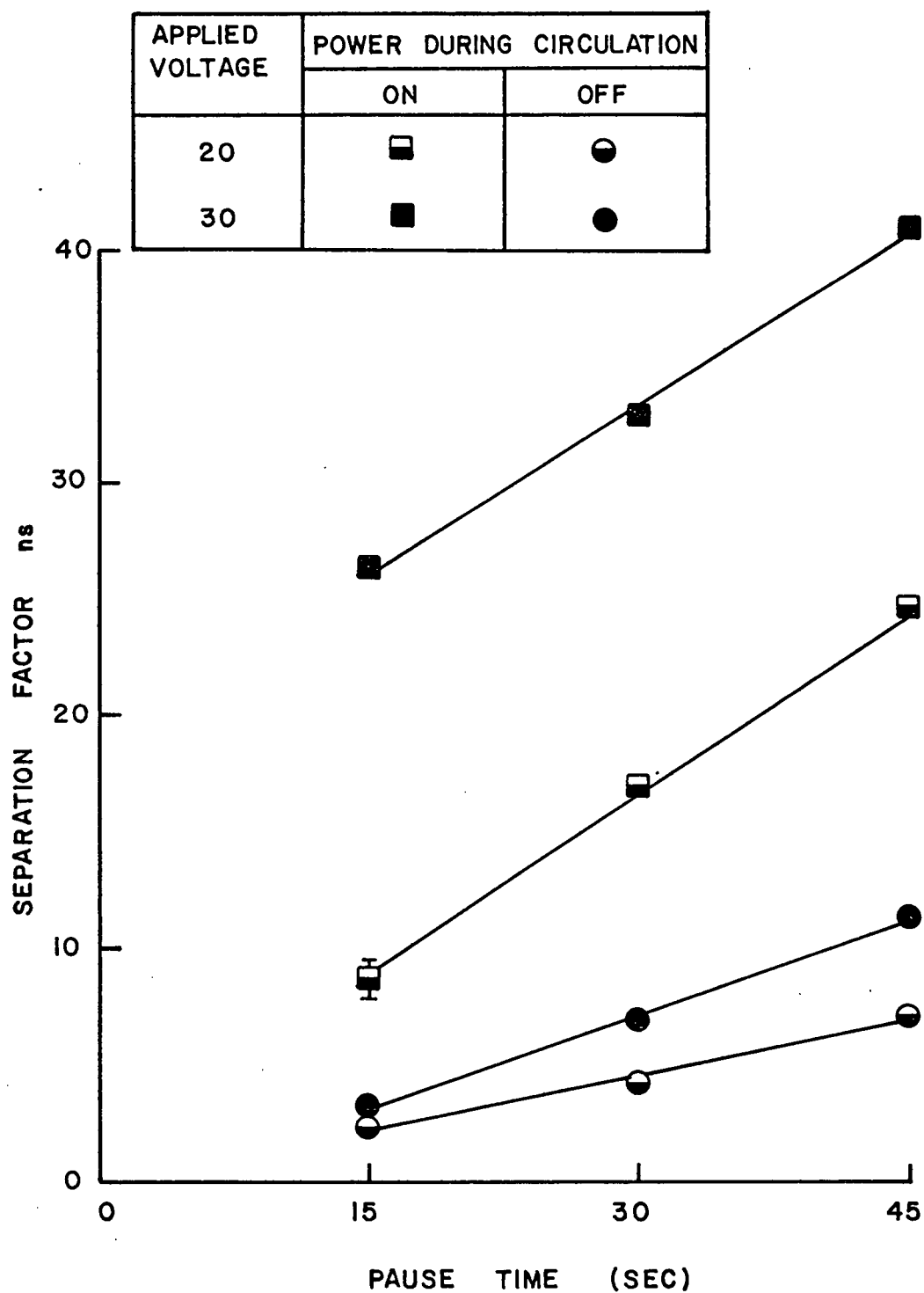
FIGURE 73

Pure pause operation (No. power during circulation).
8 — Cell column _ production rate $\simeq$ 50 C.C./cycle .
Initial concentration $C_0 \simeq$ 2000 PPM .

Table LII Semi-symmetric Operation
Feed Concentration Co ≃ 2000 ppm
Production rate ≃ 100 C.C./Cycle of each product

FEED CONC. (PPM)	EXP.	PRODUCTION RATE (C.C./CYCLE)	APPLIED VOLTAGE (VOLT)	PAUSE TIME (SEC)	BRINE		DIALYSATE		SEPARATION FACTOR ns
					CONC. (PPM)	VOLUME (C.C./CYCLE)	CONC. (PPM)	VOLUME (C.C./CYCLE)	
2080	SS-M4A	100	20	30	3825	98.57	355	101.71	10.77
	SS-M4B			45	3950	100.54	248	99.29	15.93
	SS-M4C			15	3600	99.80	650	99.50	5.54
2110	SS-M4D	100	30	15	3925	97.20	261	103.48	15.04
	SS-M4E			30	4100	98.60	204	101.67	20.10
	SS-M4F			45	4150	99.40	186	102.08	22.31

shown in Table LIII. Figure 74 contrasts the performance of these two modes.

In all cases the semi-symmetric operation results in a lower separation

factor.

Figures 75 and 76 show the ideal developing concentration profiles

predicted for asymmetric and semi-symmetric operation respectively when the

mass transfer takes place during both pause and displacement periods. The

dotted lines in these figures show separately the previous concentration profile

and the change in this profile due to the mass transfer during circulation.

Solid line is the summation of the two dotted lines using the feed concentration

as the zero level. These figures show that when steady state is reached the

two modes of operation should result in the same separation. Table LIV

summarizes Figures 75 and 76 and lists the average product concentrations,

expressed in arbitrary units, which would be expected during the transient

periods and at the periodic steady state.

The low separation achieved with semi-symmetric operation in practice

may be attributed to external mixing outside the active ED region, since a

single port was used to withdraw the depleted and the enriched products

successively during the two half-cycles. Any material from the previous half-

cycle that mixed with the new product would impair separation.

5.5. Comment on pH-Changes

Checks on the pH of both the process and rinse streams showed no

significant changes for most runs. Typical results are listed in Table LV.

The rinse stream remains almost unchanged and only shows a slight fluctuation

in its pH-value while the process solution tends to be a slightly acidic

with a drop in the pH-value of about 0.3 from its initial average value of

5.9. A noticeable exception to this are the experiments with low feed

concentration ($C_o \simeq 500$ ppm) which involve relatively long pause time ($\tau =$

45 sec.) and/or high voltage ($\Delta\phi = 30$ V) as exemplified by experiments M7 F,

Table LIII Comparison of Semi-Symmetric and Asymmetric Operations
8-Cell Column - Production Rate $\simeq$ 100 C.C./Cycle
Feed Concentration Co $\simeq$ 2000 ppm

EXP.	GRAPHICAL SYMBOL	APPLIED VOLTAGE (VOLT)	PAUSE TIME (SEC)	SEPARATION FACTOR ns	
				SEMI-SYMMETRIC OPERATION	ASYMMETRIC OPERATION
M4 A			30	10.77	14.61 14.23
M4 B		20	45	15.93	20.83
M4 C			15	5.54	6.39
M4 D			15	15.04	22.36
M4 E		30	30	20.10	28.45 32.17
M4 F			45	22.31	33.60
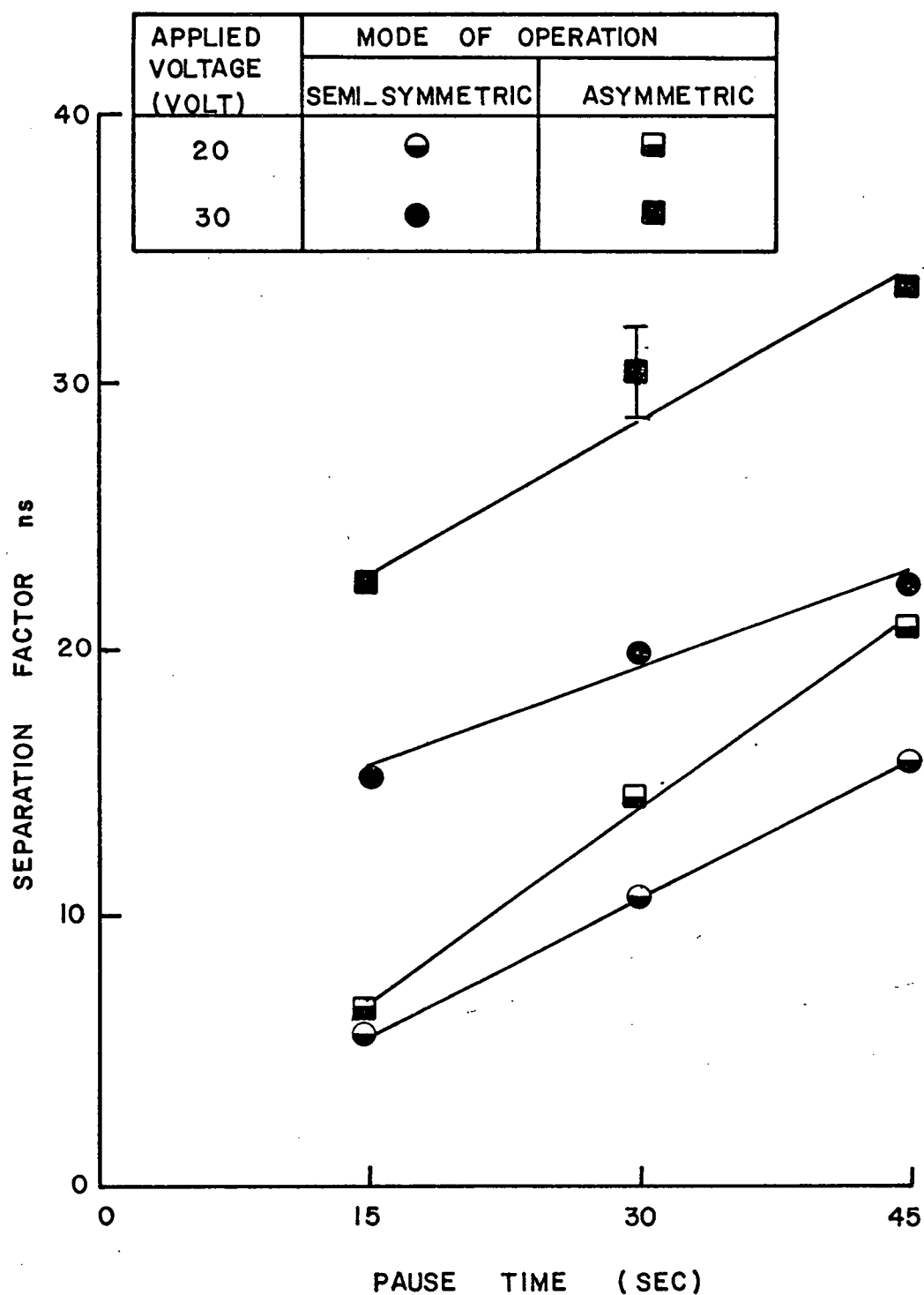
FIGURE 74

Comparison of semi symmetric and asymmetric operations.
8- Cell column_ production rate $\approx$ 100 C.C./cycle .
Feed concentration $C_0 \approx$ 2000 PPM .

FIGURE 75

FIGURE 75 — Continued I

t_1^{iii}

Pause
3rd cycle

t_2^{iii}

t_3^{iii}
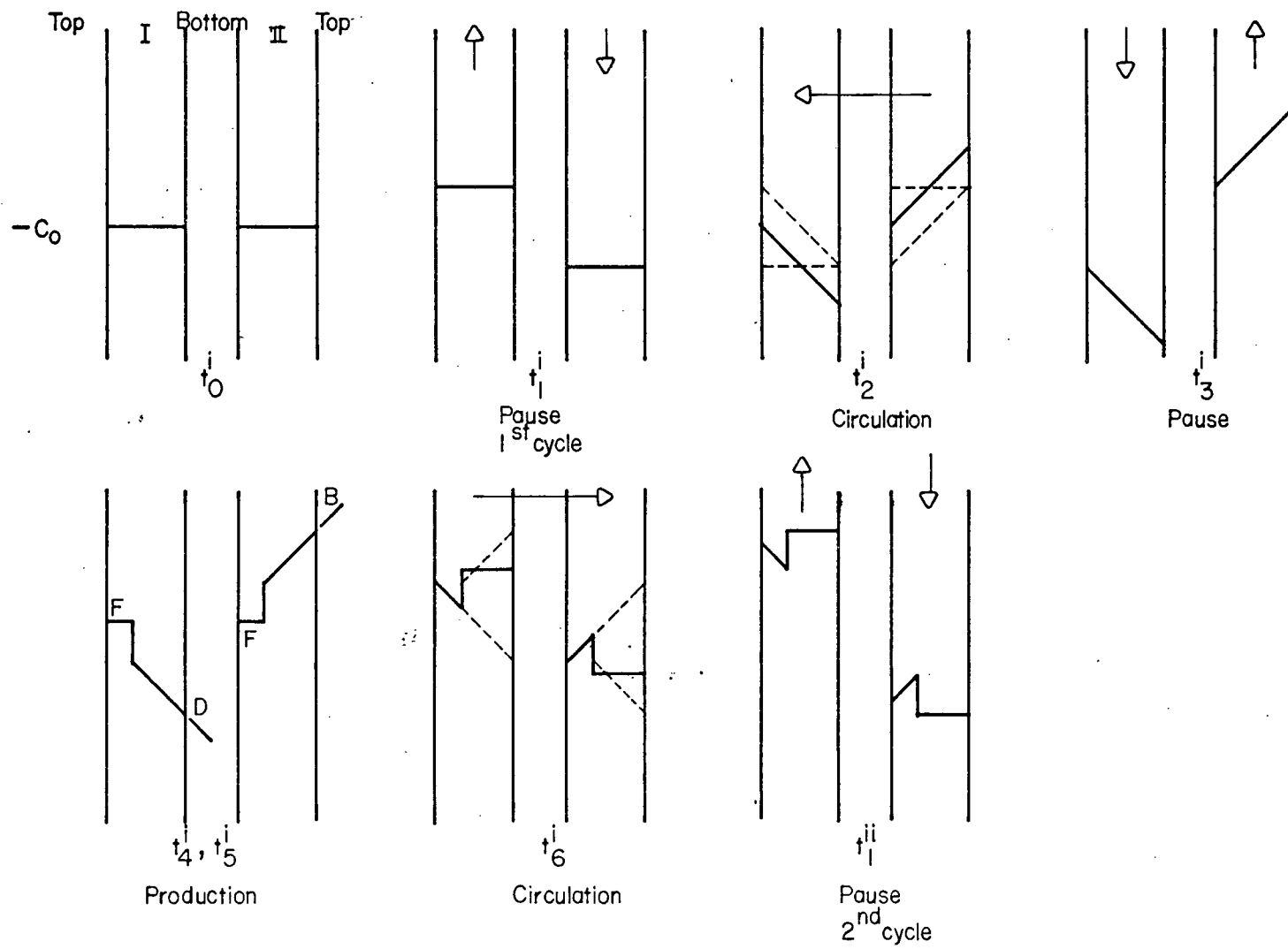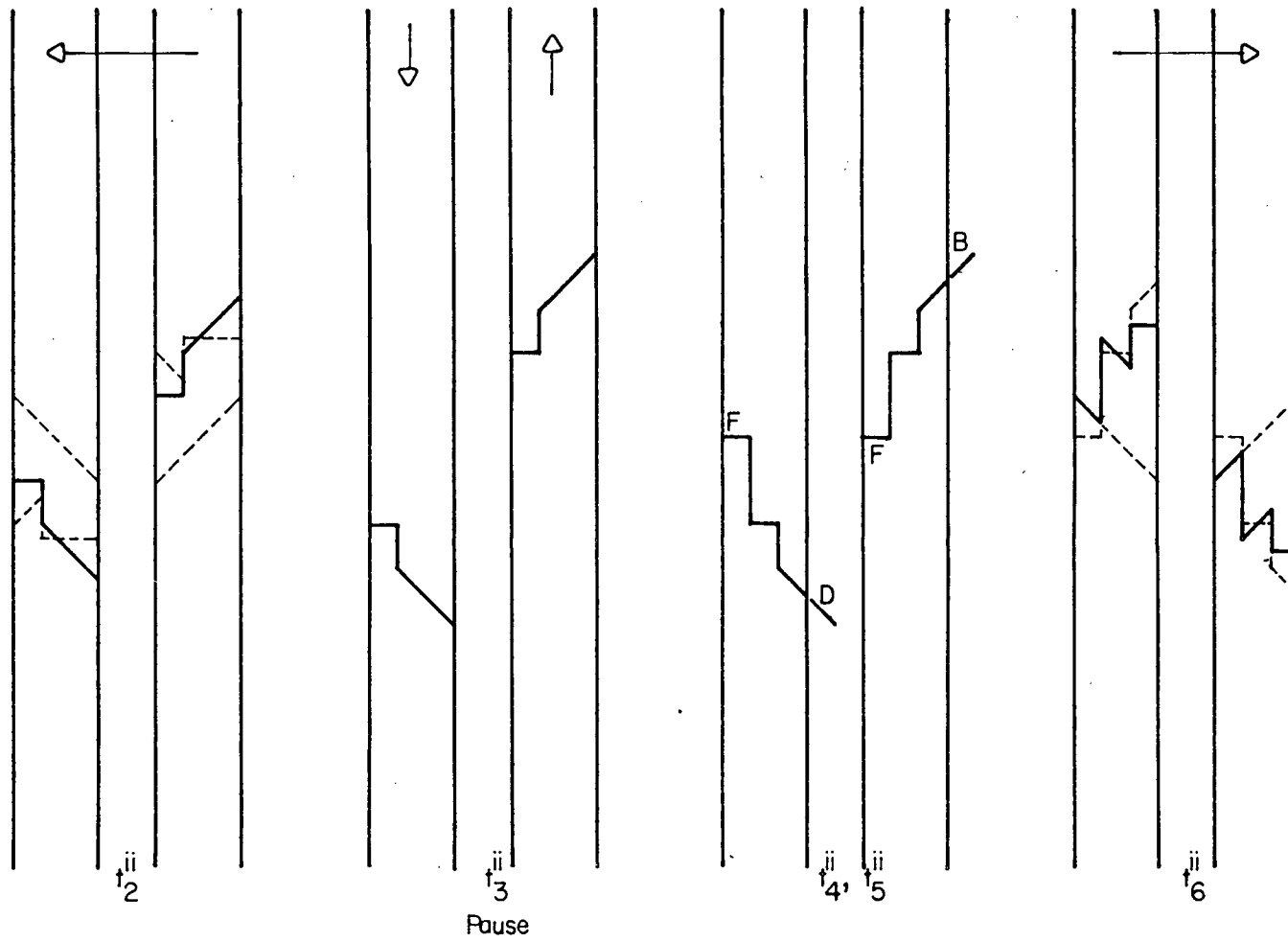
Pause

t_4^{iii}, t_5^{iii}
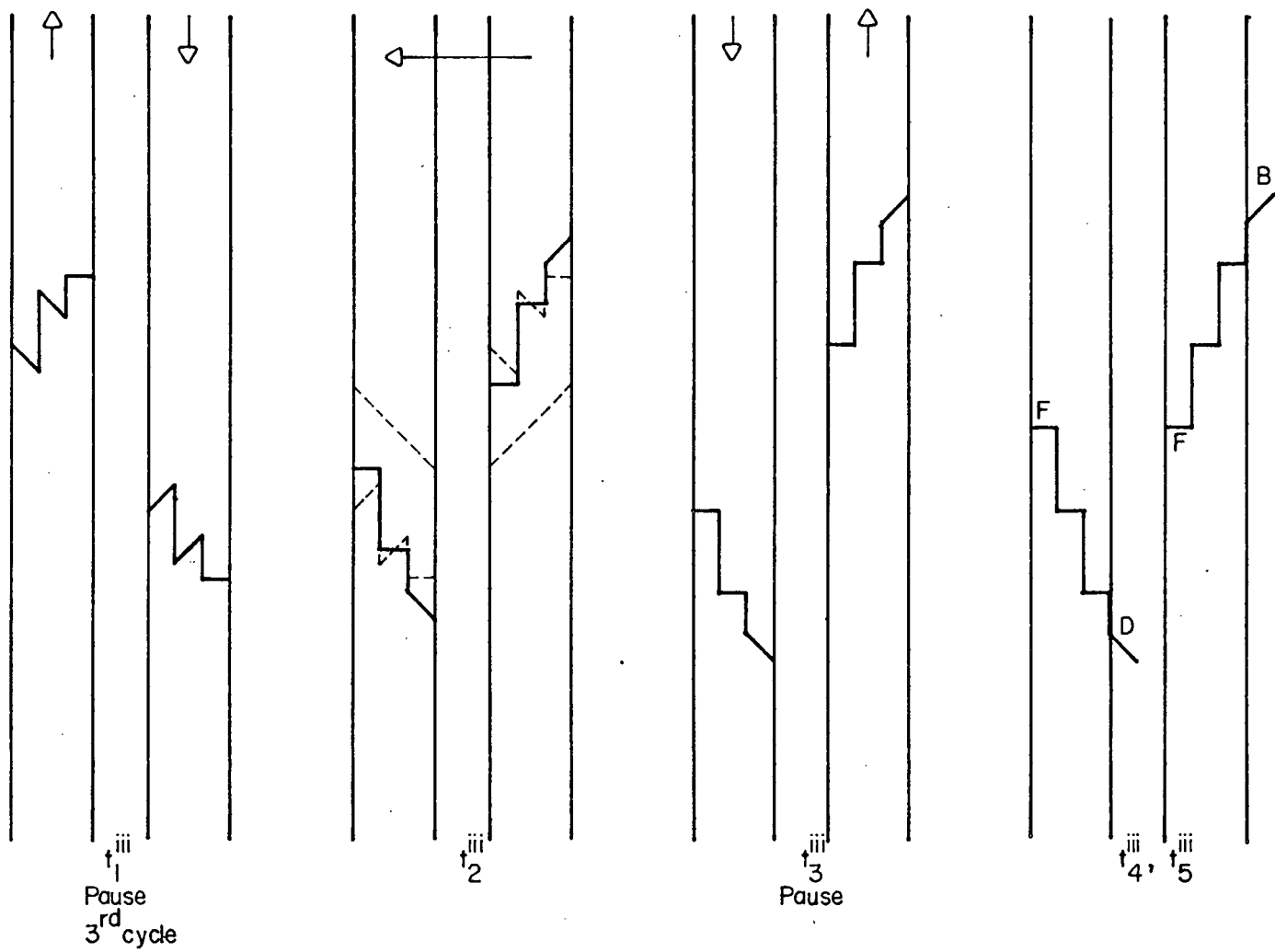
FIGURE 75 — Continued 2

232
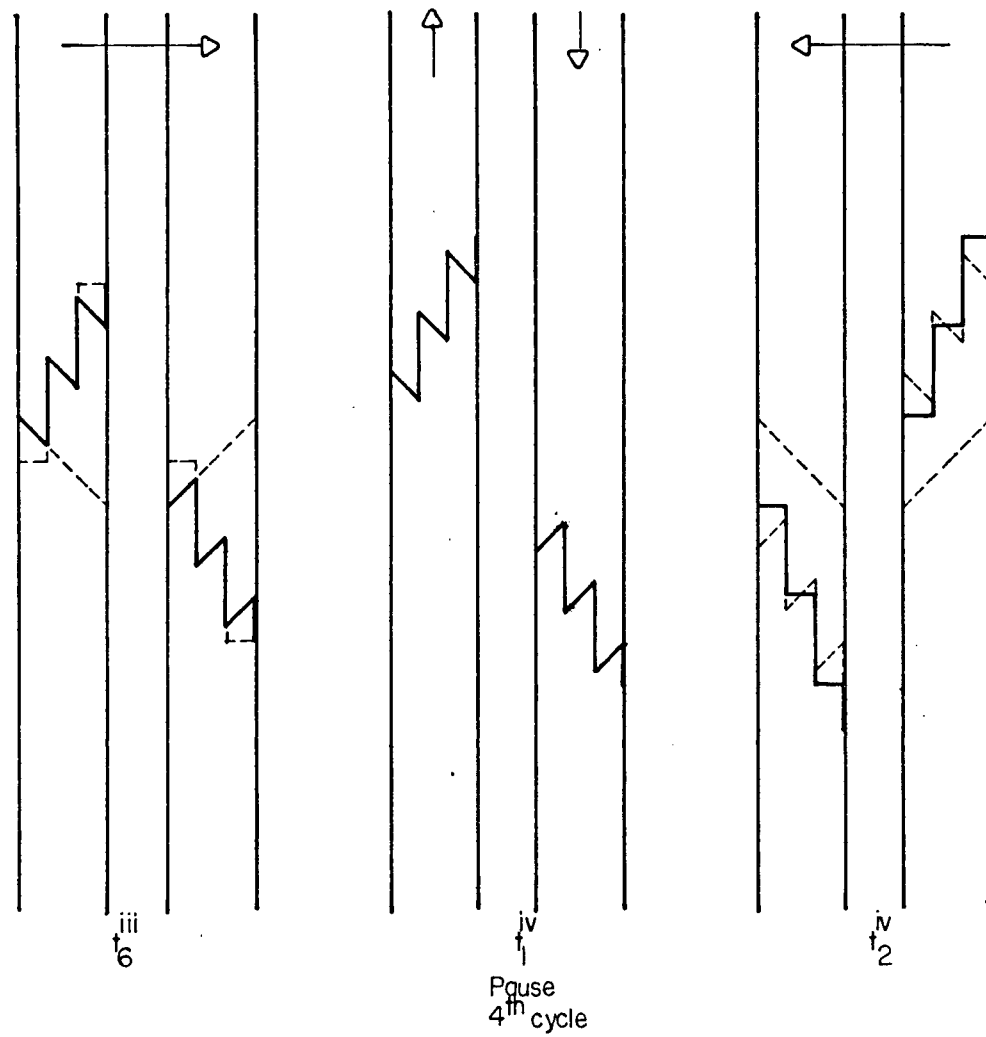
FIGURE 75 — Continued 3
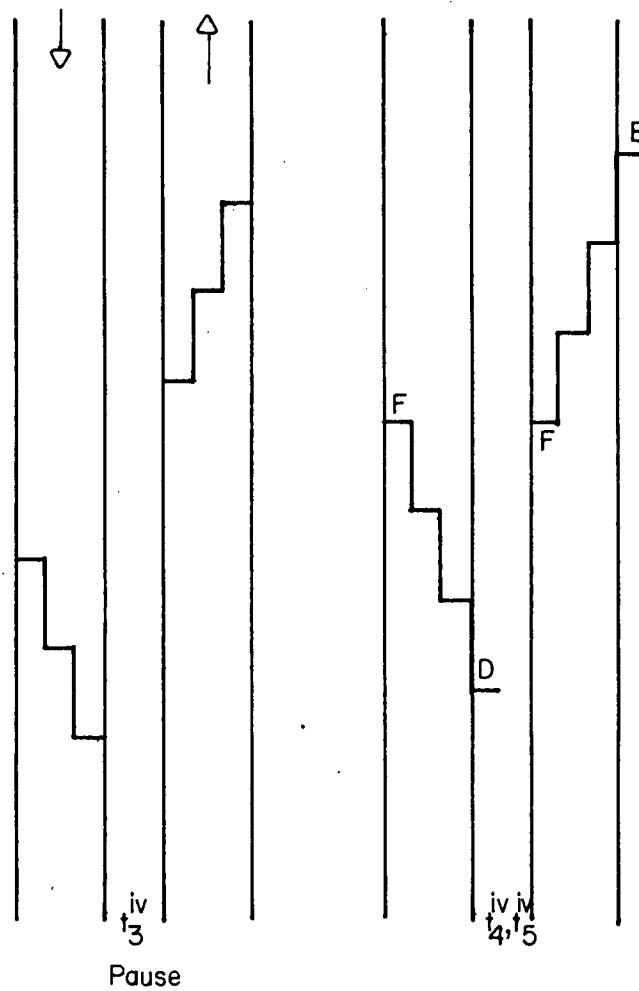
FIGURE 75

FIGURE 75 – Continued 4 .

Developing concentration profile; asymmetric operation of an open system with mass transfer during both pause and displacement periods . Dialysate product = brine product = 1/3 cell volume / cycle .

FIGURE 76

t^i_8

t^{ii}_1

Pause
2nd cycle

t^{ii}_2 t^{ii}_3

t^{II}_4
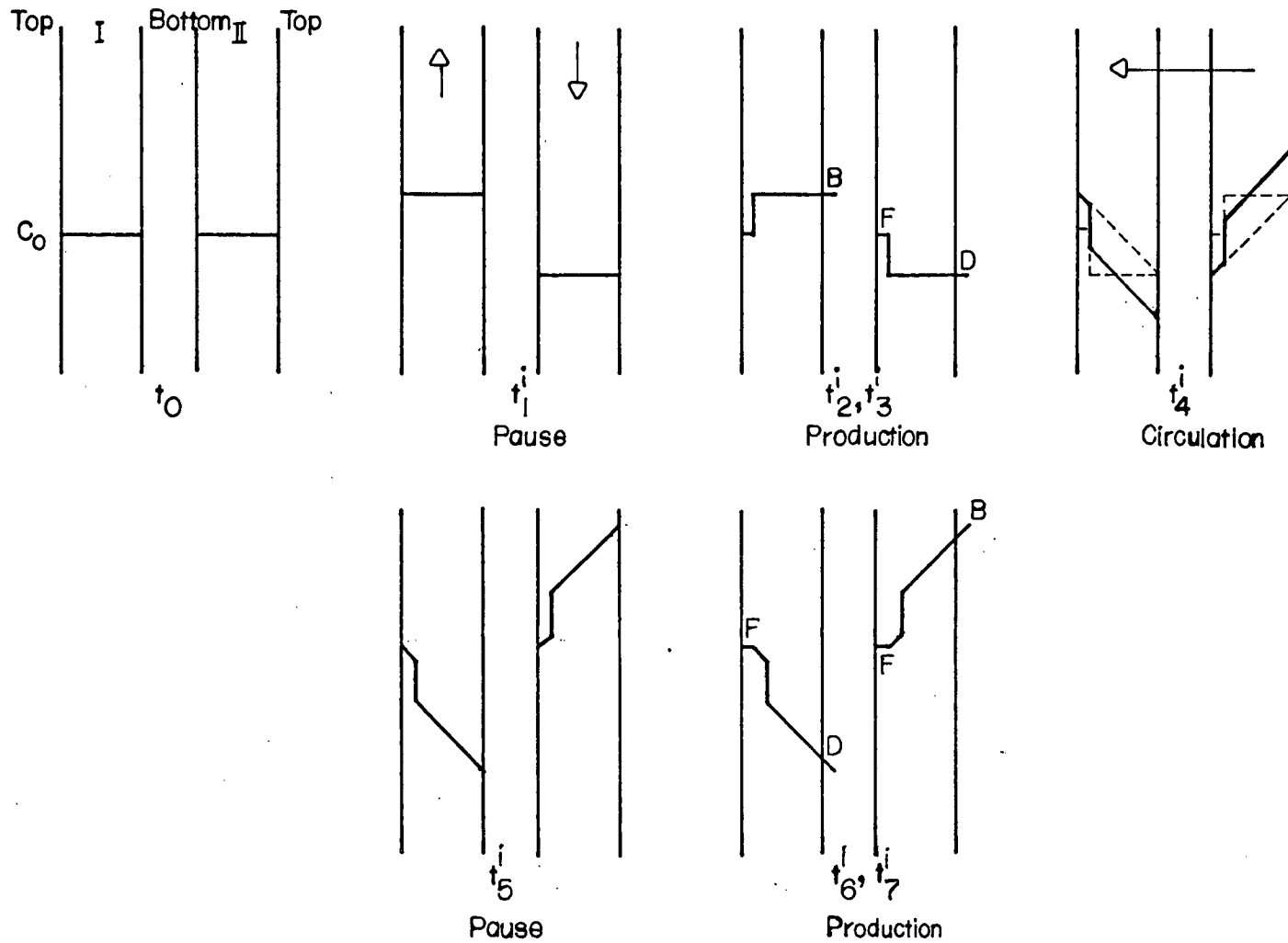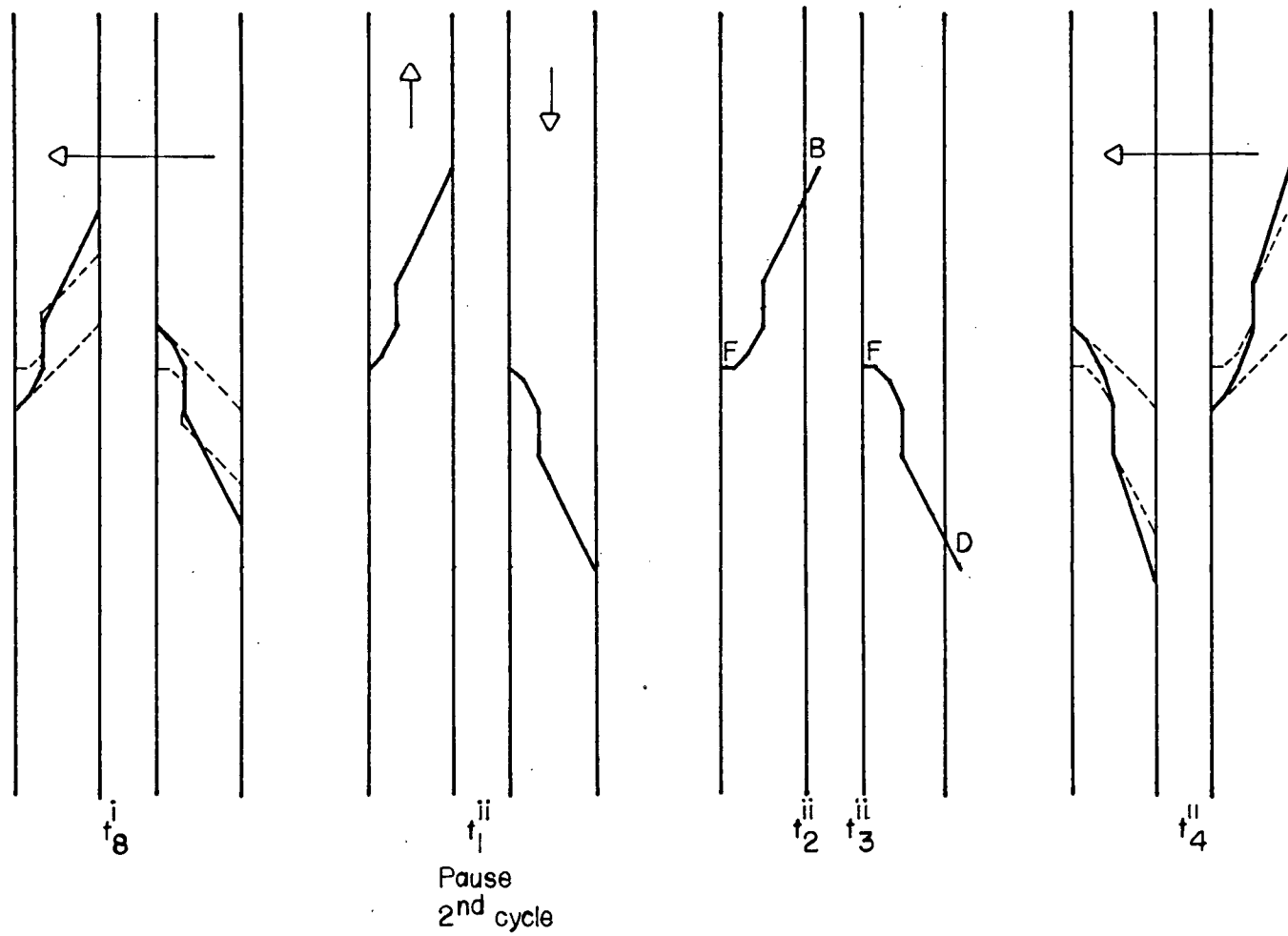
FIGURE 76 — Continued I
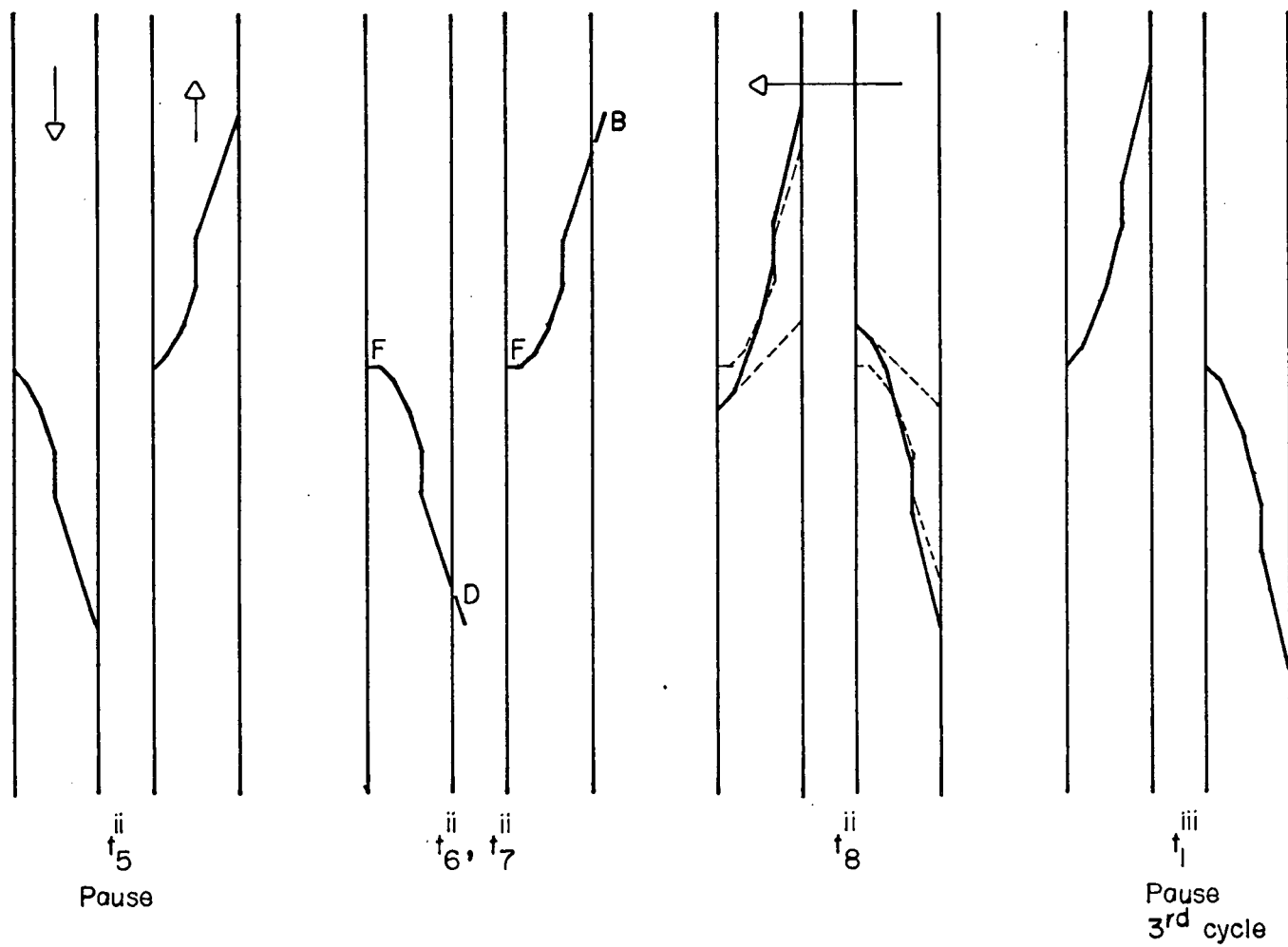
FIGURE 76 — Continued 2
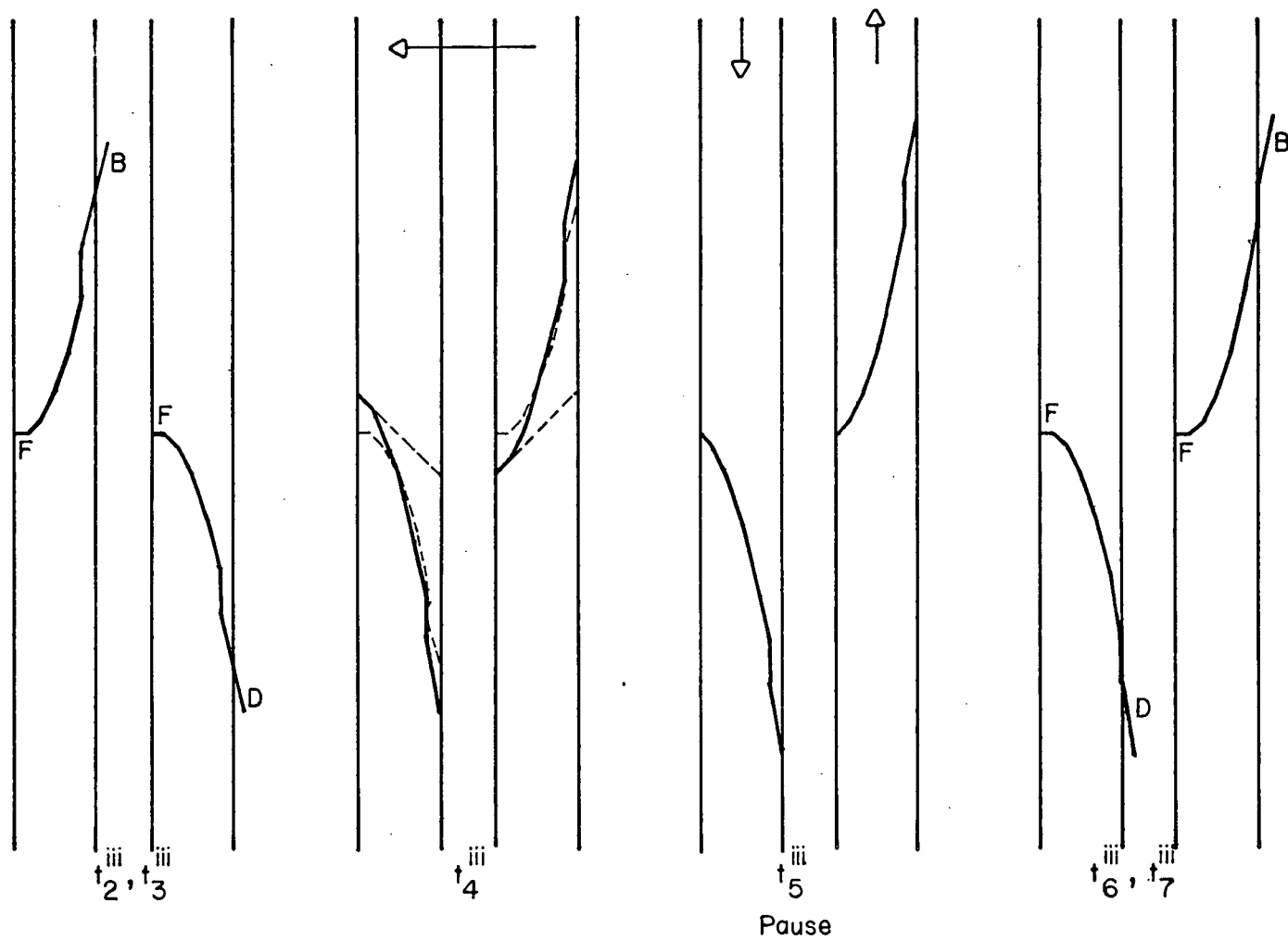
FIGURE 76 — Continued 3
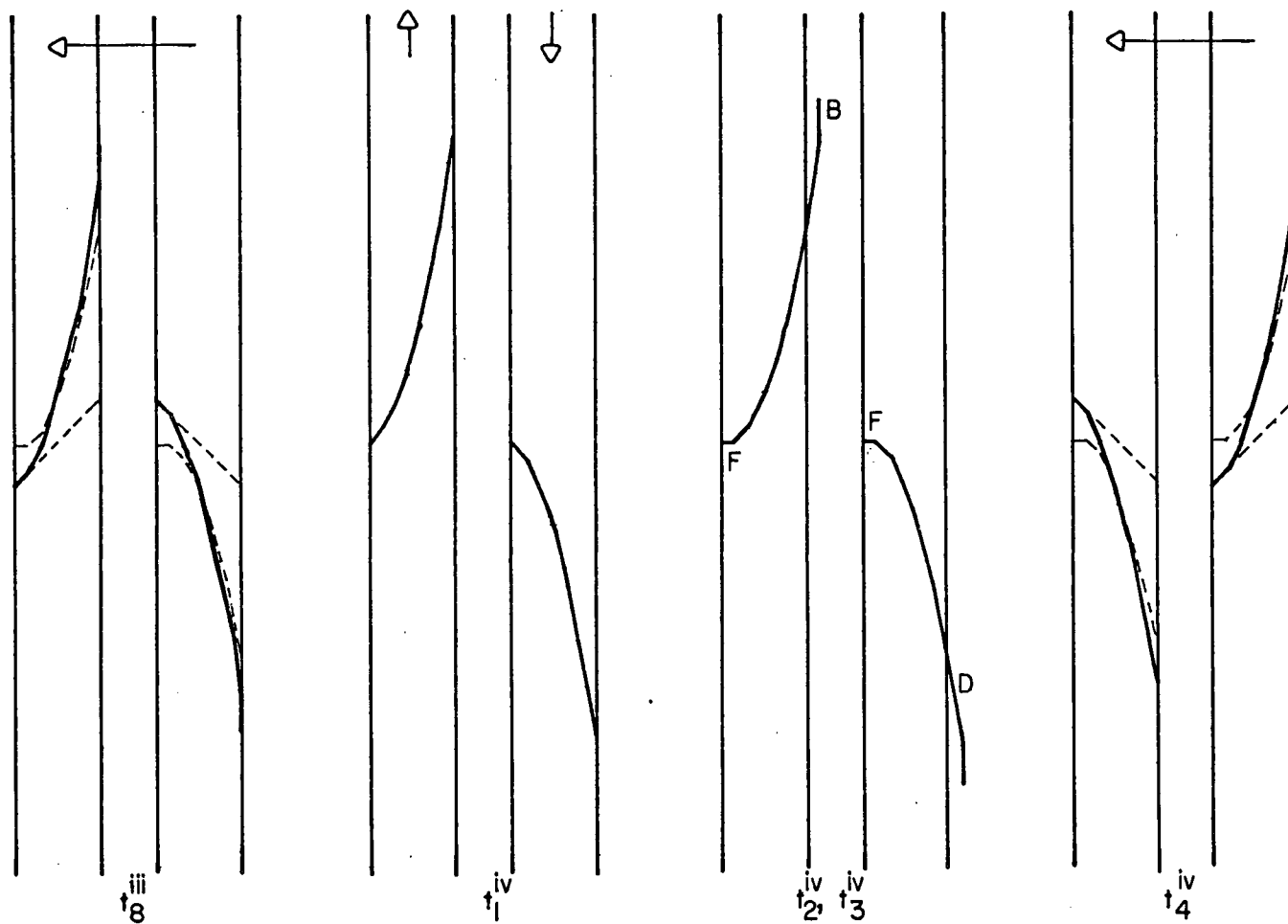
Pause , 4th Cycle

FIGURE 76 — Continued 4.
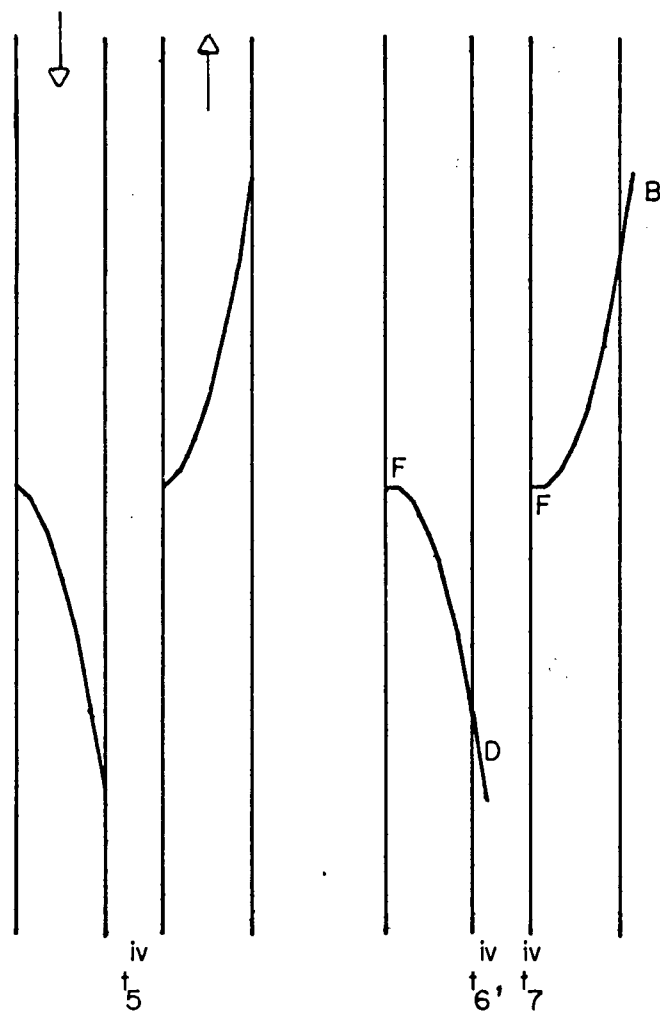
FIGURE 76 - Continued 5

FIGURE 76

Developing concentration profile ; semi_symmetric operation of an open system with mass transfer during both pause and displacement periods. Dialysate product = brine product = 1/3 cell volume / cycle.

Table LIV Average products concentrations in arbitrary units obtained under semi-symmetric and asymmetric operations

CYCLE NUMBER	FIRST HALF-CYCLE	SECOND HALF-CYCLE	SEMI-SYMMETRIC OPERATION		ASYMMETRIC OPERATION	
			ENRICHED PRODUCT C_B	DEPLETED PRODUCT C_D	ENRICHED PRODUCT C_B	DEPLETED PRODUCT C_D
1	✓		Co + 3	Co − 3	−	−
1		✓	Co + 8.5	Co − 8.5	Co + 8	Co − 8
2	✓		Co + 13	Co − 13	−	−
2		✓	Co + 16.5	Co − 16.5	Co + 12	Co − 12
3	✓		Co + 19	Co − 19	−	−
3		✓	Co + 20.5	Co − 20.5	Co + 16	Co − 16
4	✓		Co + 18	Co − 18	−	−
4		✓	Co + 18	Co − 18	Co + 18	Co − 18
5	✓		Repeat	Repeat	Repeat	Repeat
5		✓				

Table LV   pH-Changes for Some ED Runs at
various feed concentrations and operating
conditions

EXP.	FEED CONC. Co (ppm)	PROCESS pH		RINSE pH	
		Initial	Final	Initial	Final
M3 A	2000	5.7	5.4	5.7	5.4
M3 F		5.6	5.0	5.6	5.7
M3 E		5.8	5.3	5.8	5.6
M3 H		5.6	5.4	5.6	5.7
M7 A	500	5.7	5.3	6.1	5.9'
M7 B		6.2	5.0	5.8	5.6
M7 E		5.6	4.6	6.0	5.8
M7 F		5.8	4.2	5.7	5.8
M7 G		6.1	5.6	5.8	6.0
M7 H		6.2	6.0	6.1	6.1
M11 A	4000	5.9	5.7	5.9	5.6
M11 B		6.2	6.0	6.2	5.9
M11 F		5.7	5.3	5.7	5.8
M11 I		6.1	6.0	6.1	6.2

M7 B and M7 E (refer to Table LV).

5.6. Temperature Measurements

The initial and final temperatures of the process stream for several

runs under various operating conditions were measured using an inserted

mercury thermometer. An average temperature rise of 3-5°C from its initial

value of 23-25°C was observed in most cases.

5.7. Pressure Drop Measurements

The pressure drop across an 8-stage ED column was measured at various

flow rates using a mercury manometer. Measured values are listed in Table

LVI and a plot of ΔP (mm Hg) vs. flow rate (c.c./sec) is displayed in

Figure 77. Most of the runs in the present work involve a flow rate of about

16.7 c.c./sec. The mean hydraulic radius of the flow channel was about 2.76

x 10^{-2} cm which gives rise to a Reynolds number of about 760.

5.8. Probe Voltage, Apparent Resistance and Current Consumption

In all experiments described here the applied voltage supplied by the

D.C. power source was held constant during each half cycle. The voltage

drop across the stack (as measured by probe electrodes) was primarily a

function of this applied potential, but it is generally below the applied

voltage due to resistance in the connectors, rinse solution and electric

overpotentials as shown in Table LVII and Figure 78.

Both the stack voltage (probe voltage) and the current consumption vary

systematically during the cycle and along the demineralization path. Typical

examples of these fluctuations are shown in Figures 79 and 80 for the voltage

Table LVI   Pressure Drop Measurements
            8-Stage ED Stack
            Time Period t_6 = 63.5 sec

MANOMETER READING (mm Hg)	VOLUME (C.C.)	FLOW RATE (C.C./SEC)
8	84	1.32
20	169	2.66
35	266	4.19
51	355	5.59
69	495	7.80
89	577	9.09
102	658	10.36
129	760	11.97
198	940	14.80
247	1107	17.43
296	1210	19.06
331	1328	20.91
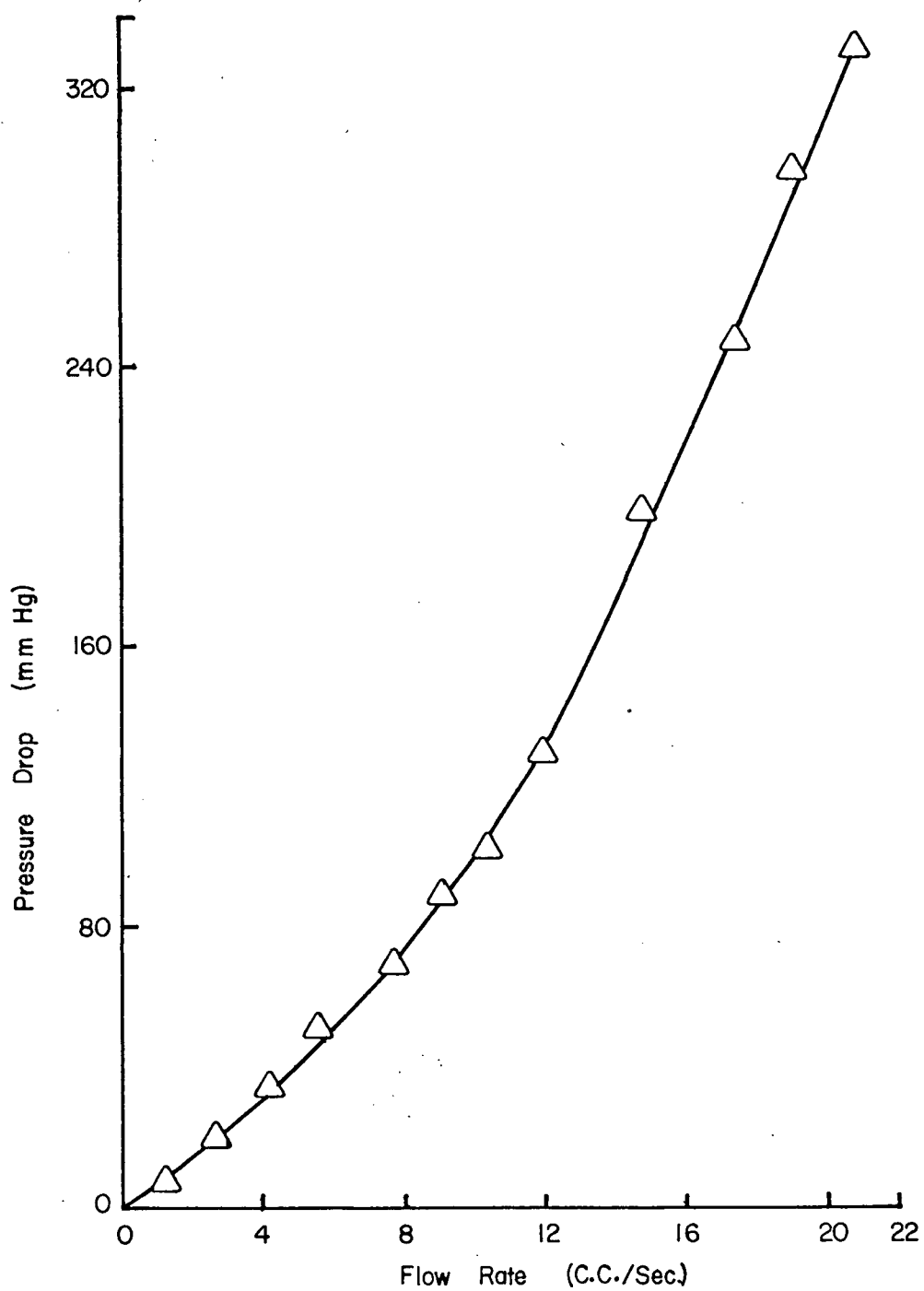
FIGURE 77

Pressure drop vs. flow rate. 8-Stage ED stack.

Table LVII Average Probe Voltage (Stack Voltage) over
a complete cycle for various feed concentration
and applied voltages. Pause time τ = 45 sec
Exp. Group # M3, M7 and M11

EXP. GROUP	GRAPH. SYMBOL	FEED CONC. (ppm) APPLIED VOLTAGE (VOLT)	AVERAGE PROBE VOLTAGE (VOLT)		
			10	20	30
M7	▲	500	8.95	18.00	27.25
M3	●	2000	8.60	17.15	25.50
M11	▢	4000	8.25	16.65	24.85
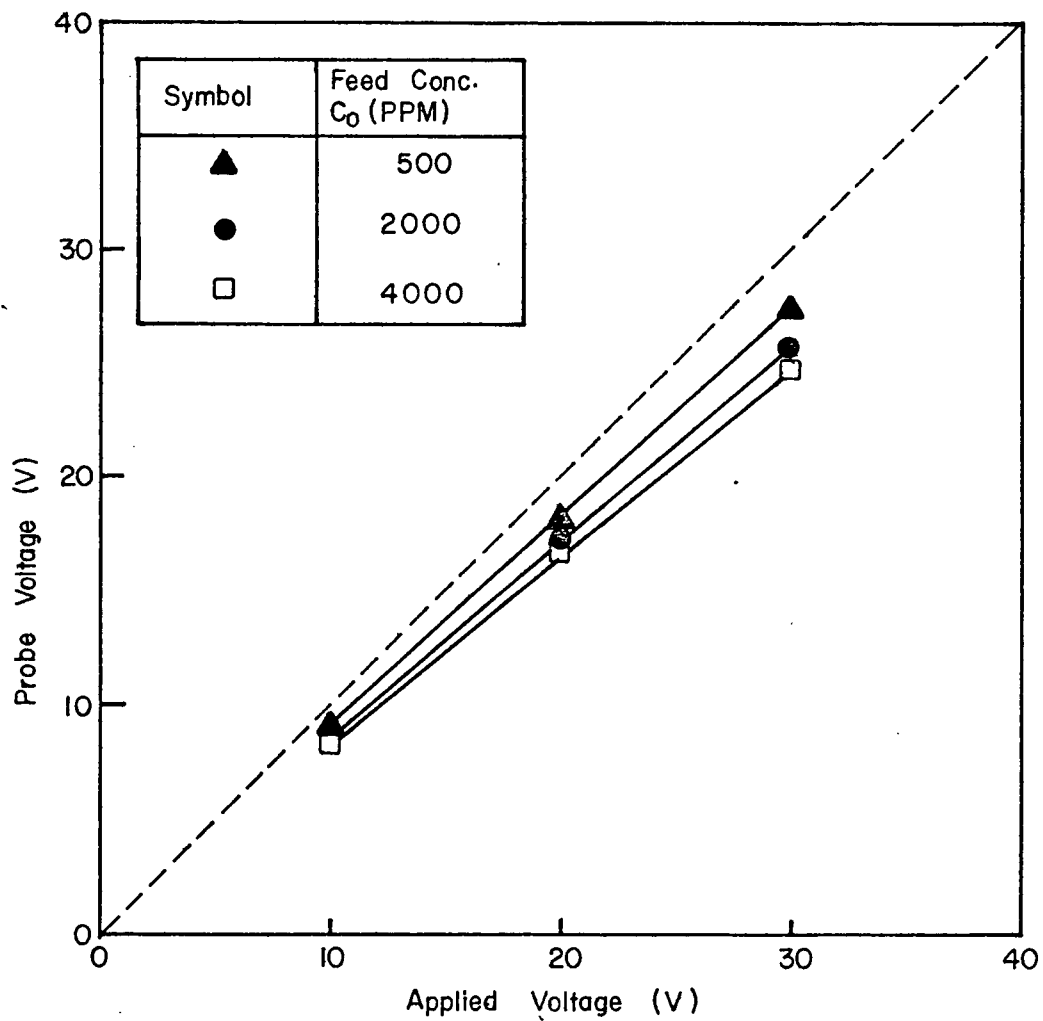
FIGURE 78

Average stack voltage (probe voltage) vs. applied voltage for various feed concentrations. Pause time $\mathcal{T}$ = 45 sec. , EXP group M3, M7 & M II.

Feed | End

Product | End

30V   20   10   0   10   20   30V
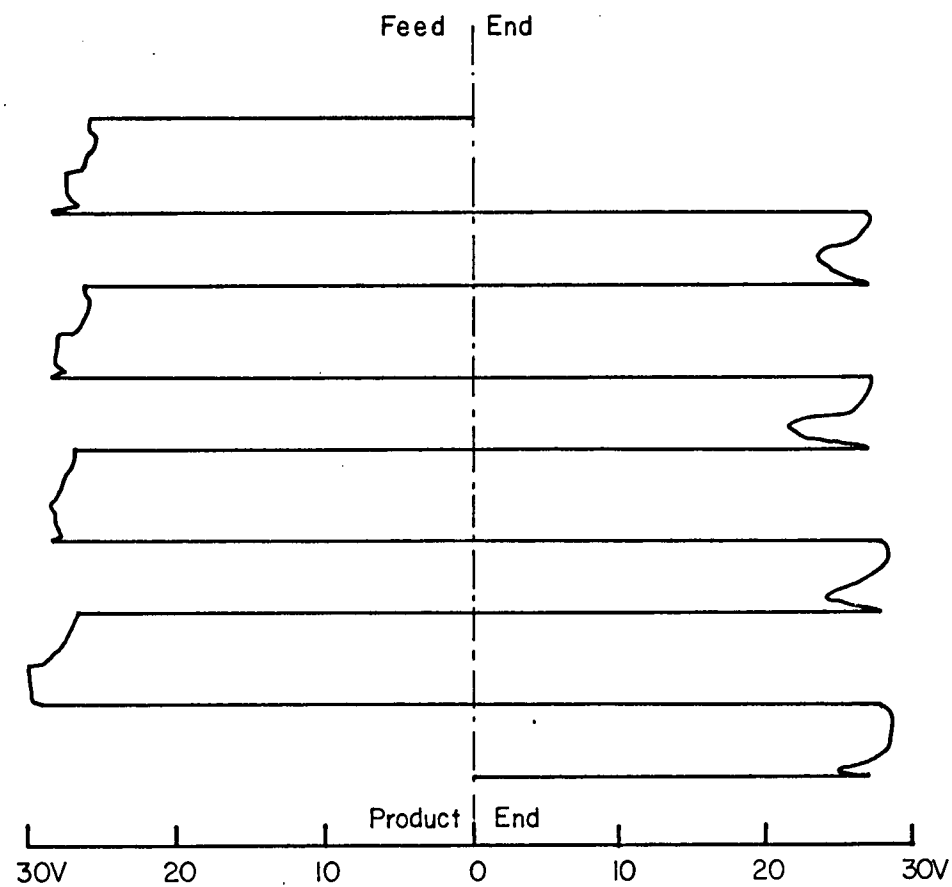
FIGURE 79

Traces of probe voltage recording during a cycle at four points along the demineralizing path. EXP. M7F .

Feed   End

Product   End

750 mA	500	250	0	250	500	750 mA
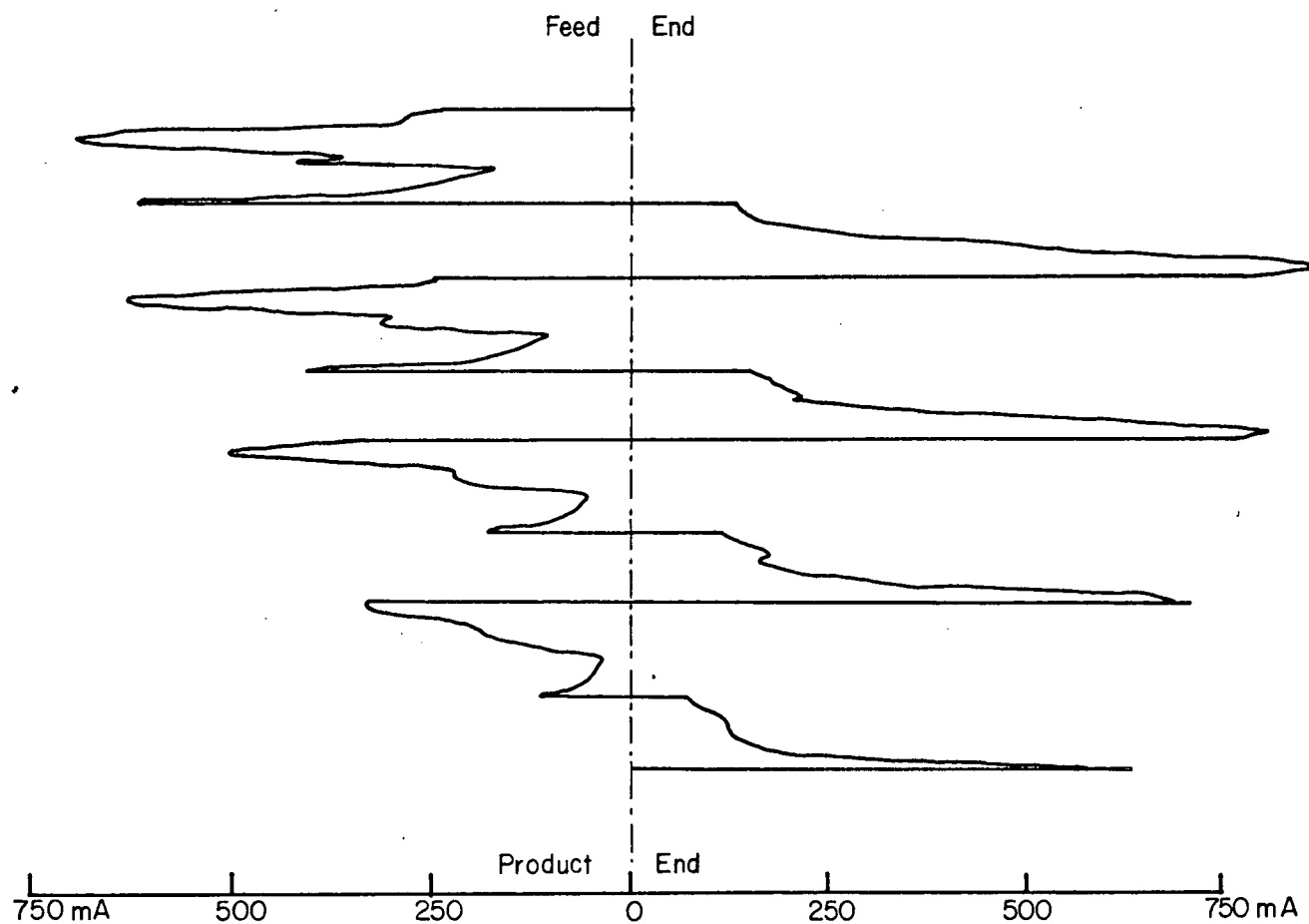
FIGURE 80

Traces of current recording during a cycle at different points along the demineralizing path. EXP M7F.
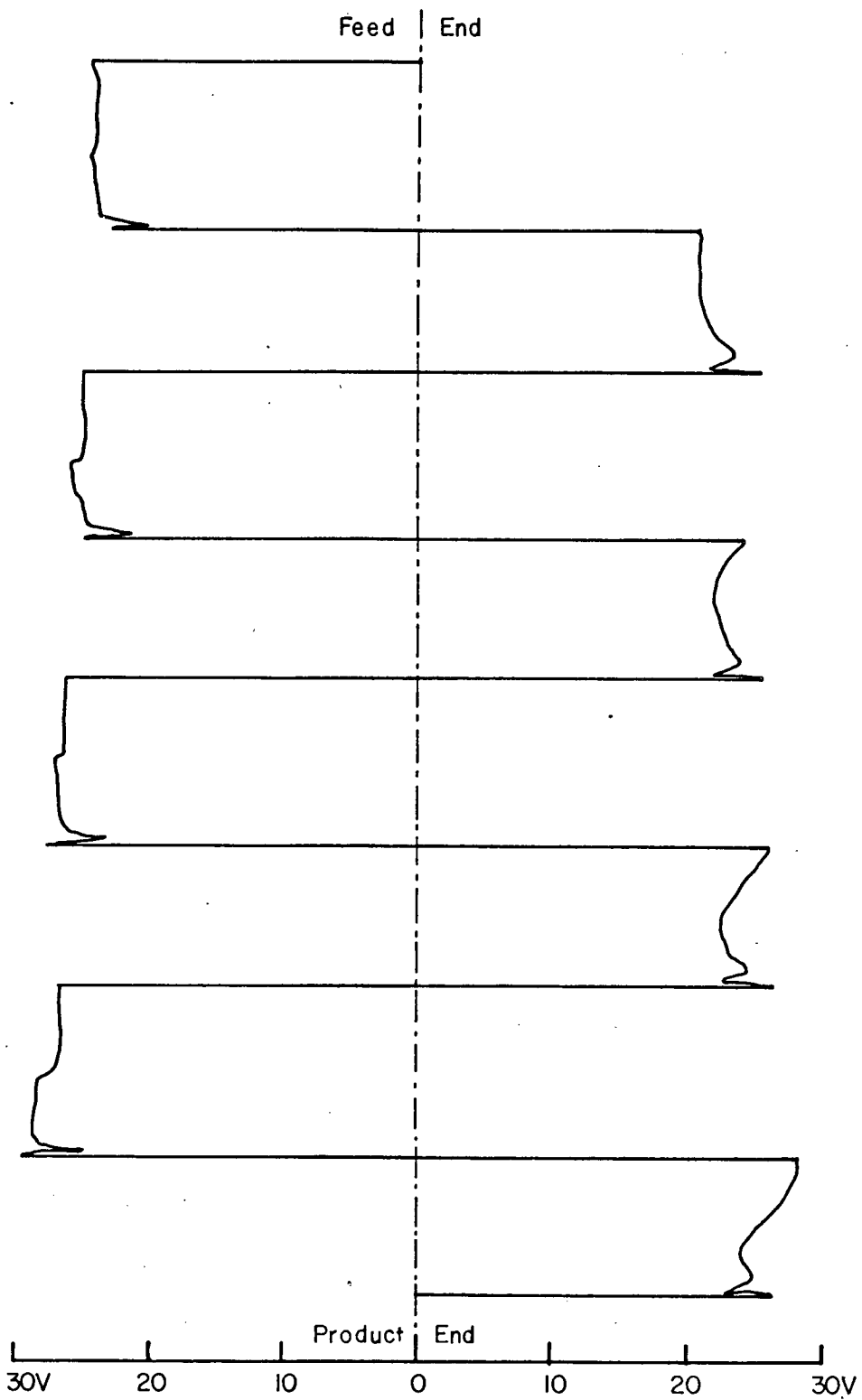
Feed | End

Product | End

30V   20   10   0   10   20   30V

FIGURE 81

Traces of probe voltage recording during a cycle at four points along the demineralizing path EXP. M II F.
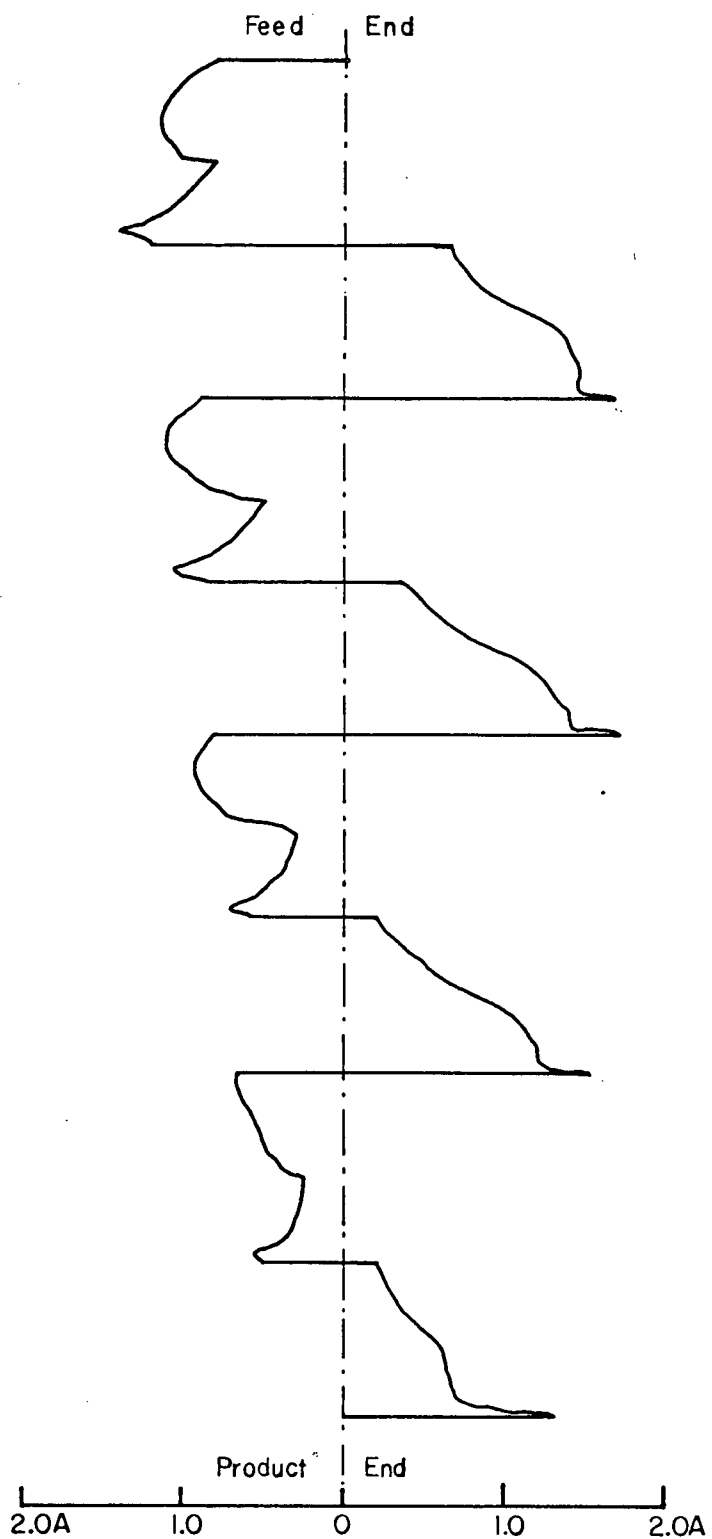
FIGURE 82

Traces of current recording during a cycle at four points along the demineralizing path EXP. M II F .

and current respectively at the feed concentration $C_o \simeq 500$ ppm. Figures 81 and 82 display similar variations of stack voltage and current consumption during the cycle and along the demineralization path for the feed concentration $C_o \simeq 4000$ ppm. Average values of these variations along the demineralization path are indicated in Table LVIII and Figure 83 for the stack voltage and in Tables LIX and LX and Figures 84 and 85 for the current consumption.

The current consumption decreases with increasing separation, thus it drops along the demineralization path as we move from the feed end towards the product end (refer to Figure 84) and it increases with increasing feed concentration (refer to Figure 85). The main influence causing the wide variations in the current was the depletion of solute in either the flow channels or the capacity cells towards the end of each half cycle. The stack voltage, as shown in Figure 83, approaches the applied voltage as the current consumption drops due to either a high separation or a low feed concentration.

Tables LXI, LXII and LXIII show variations of probe voltage, current, apparent resistance and power consumption along the demineralization path for various runs with the applied voltage at level of 10, 20 and 30 volt and feed concentrations C_o of 500, 2000 and 4000 ppm NaCl.

Table LXIV and Figure 86 show the variation of average stack resistance with feed concentration. The average stack resistance decreases with increasing feed concentration and with decreasing applied voltage. Table LXV and Figure 87 show the variation of stack resistance along the demineralization path during the depletion half cycle. The resistance increases as the process stream becomes more depleted towards the product end.

Table LVIII   Variation of probe voltage along the demineralization
              path during the depletion half cycle for various
              feed concentrations. $\Delta\phi$ = 30 V
              Exp. M7F and M11F

EXP.	GRAPH. SYMBOL	FEED CONC. (PPM)	STAGE NUMBER / APPLIED VOLTAGE (VOLT)	PROBE VOLTAGE/APPL. VOLT.			
				4 FEED END	3	2	1 PROD. END
M7 F	▲	500	30	0.883	0.917	0.943	0.960
M11 F	☐	4000	30	0.787	0.850	0.883	0.917

Symbol	Feed Conc· C_O (PPM.)
▲	500
☐	4000
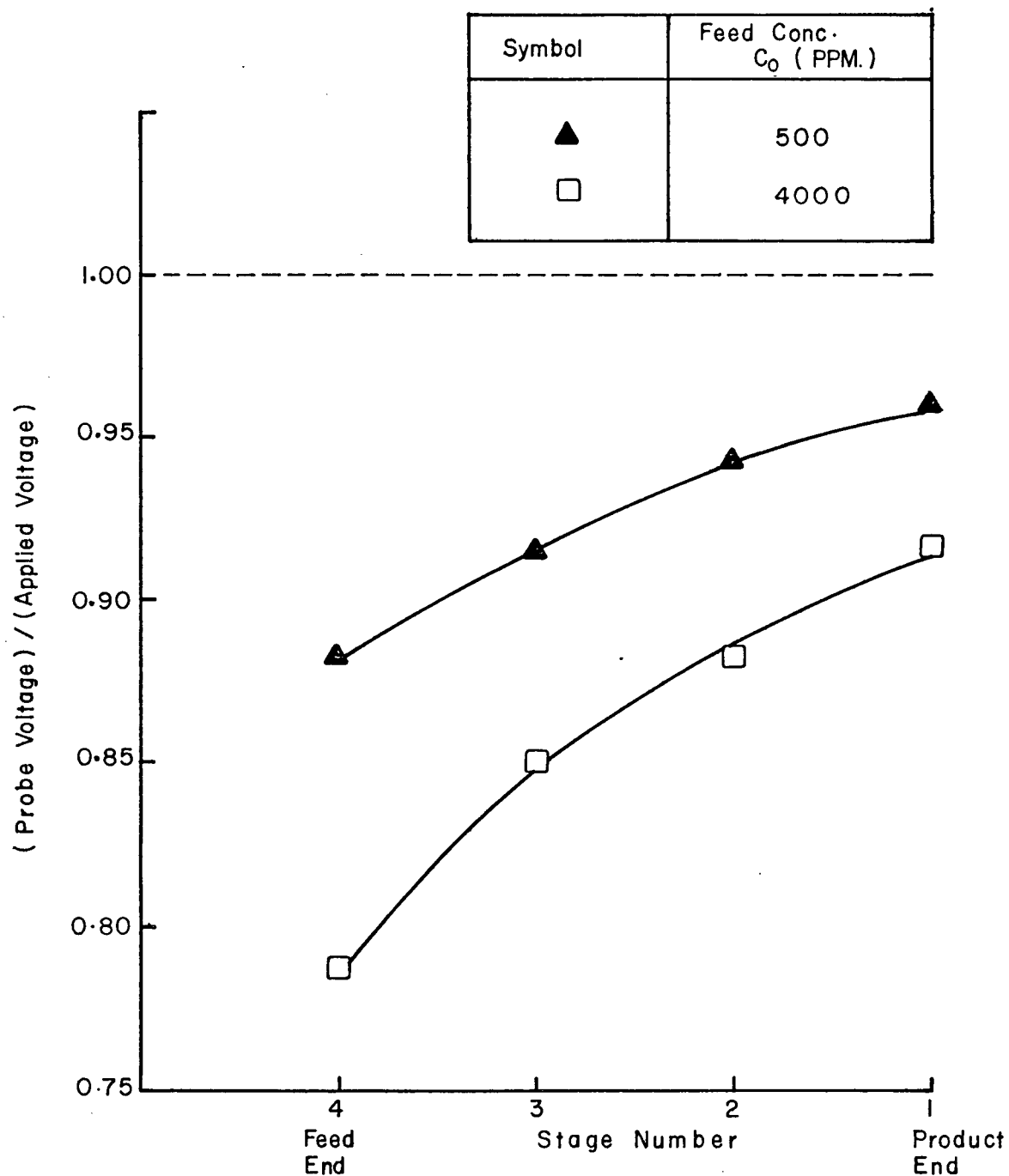
FIGURE 83

Variation of stack voltage (probe voltage) alonge the demineralizing path for various feed concentrations. EXP. M7F & M II F.

Table LIX   Variation of current consumption along the demineralization
            path during the depletion half cycle at various applied
            voltages.   Co ≃ 2000 ppm
            Exp. M3 B, M3 F and M3 G

EXP.	GRAPH. SYMBOL	STAGE NUMBER / APPLIED VOLTAGE (VOLT)	CURRENT CONSUMPTION (mA)			
			4 FEED-END	·3	2	1 PROD-END
M3 G	△	10	167	161	150	109
M3 B	●	20	323	273	192	126
M3 F	☐	30	463	347	232	153
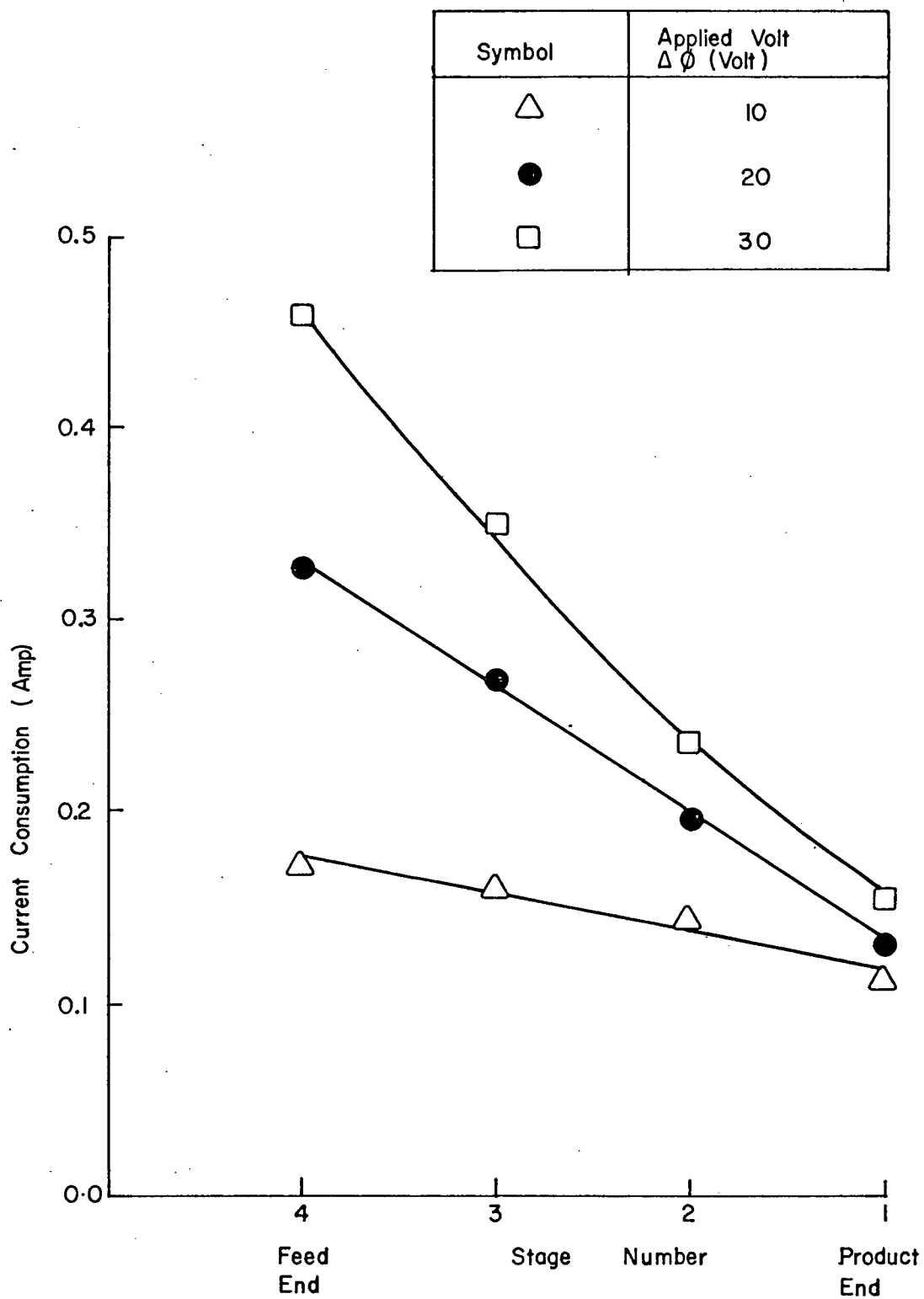
FIGURE 84

Variation of current consumption along the demineralization path at various applied voltages. $C_0 \approx$ 2000 PPM , EXP. M3 B , M3 F & M3 G

Table LX Variation of current consumption along the demineralization
path during the depletion half cycle at various feed
concentrations. $\Delta\phi$ = 30 V
Exp. M3 F, M7F and M11 F

EXP.	GRAPH. SYMBOL	STAGE NUMBER / FEED CONC. (PPM)	CURRENT CONSUMPTION (mA)			
			4 FEED-END	3	2	1 PROD-END
M7 F	△	500	225	105	55	29
M3 F	●	2000	463	347	232	153
M11 F	□	4000	1050	640	409	288
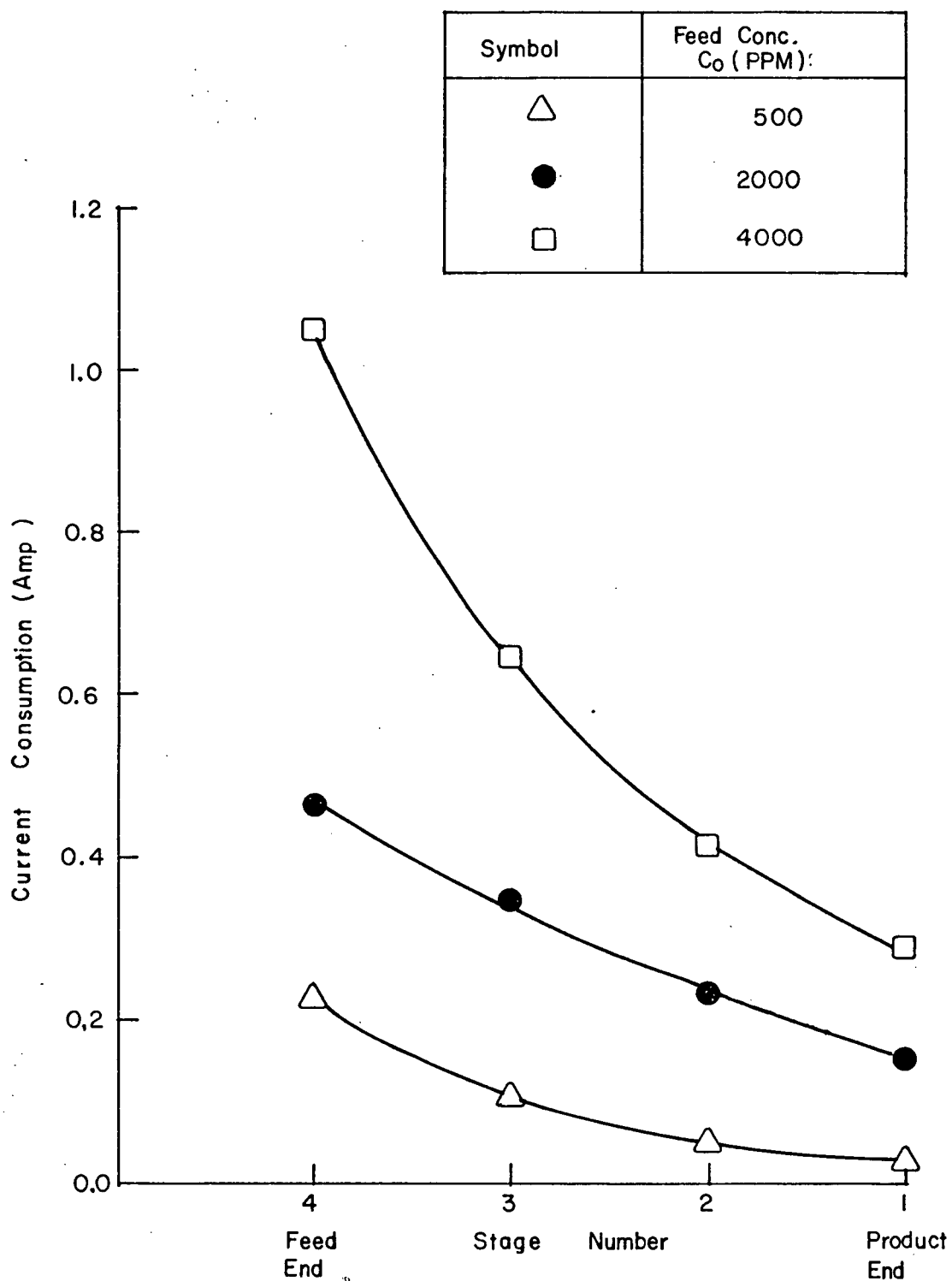
FIGURE 85

Variation of current consumption along the demineralization path at various feed concentrations. $\Delta\phi$ = 30 V , E X P M3F, M7F & M 11 F.

Table LXI Variation of probe voltage, current, resistance and power consumption along the demineralizing path. Co ≈ 500 ppm, Exp. M7 B, M7 F and M7 G

EXP.	APPLIED VOLTAGE (VOLT)	STAGE NUMBER / VARIABLE	ENRICHMENT HALF CYCLE					DEPLETION HALF CYCLE				
			1	2	3	4	AVERAGE VALUES	1	2	3	4	AVERAGE VALUES
M7 B	20	Probe Voltage (Volt)	18.5	17.9	17.3	16.8	17.6	19.1	18.8	18.1	17.5	18.4
		Current (mA)	31	56	97	167	88	21	40	76	158	74
		Apparent Resistance (Ω)	596.8	319.6	178.4	100.6	298.9	909.5	470.0	238.1	110.8	432.1
		Power (Watt)	0.57	1.00	1.68	2.81	1.52	0.40	0.75	1.38	2.77	1.33
M7 F	30	Probe Voltage (Volt)	28.3	27.3	26.0	25.0	26.7	28.8	28.3	27.5	26.5	27.8
		Current (mA)	43	77	132	232	121	29	55	105	225	104
		Apparent Resistance (Ω)	658.1	354.5	197.0	107.8	329.4	993.1	514.5	261.9	117.8	471.8
		Power (Watt)	1.22	2.10	3.43	5.80	3.14	0.84	1.56	2.89	5.96	2.81
M7 G	10	Probe Voltage (Volt)	9.1	8.9	8.6	8.4	8.8	9.5	9.3	9.0	8.7	9.1
		Current (mA)	25	47	74	84	58	18	37	57	81	48
		Apparent Resistance (Ω)	364.0	189.4	116.2	100.0	192.4	527.8	251.4	157.9	107.4	261.1
		Power (Watt)	0.23	0.42	0.64	0.71	0.50	0.17	0.34	0.51	0.70	0.43

Table LXII Variation of probe voltage, current, resistance and power consumption along
the demineralizing path. Co ≃ 2000 ppm, Exp. M3 B, M3 F and M3 G

EXP.	APPLIED VOLTAGE (VOLT)	STAGE NUMBER / VARIABLE	ENRICHMENT HALF CYCLE					DEPLETION HALF CYCLE				
			1	2	3	4	AVERAGE VALUES	1	2	3	4	AVERAGE VALUES
M3 B	20	Probe Voltage (Volt)	18.0	17.3	16.3	15.4	16.8	18.7	18.0	17.1	16.3	17.5
		Current (mA)	167	228	324	352	268	126	192	273	323	229
		Apparent Resistance (Ω)	107.8	75.9	50.3	43.7	69.4	148.4	93.8	62.6	50.4	88.8
		Power (Watt)	3.01	3.94	5.28	5.42	4.41	2.36	3.46	4.67	5.26	3.94
M3 F	30	Probe Voltage (Volt)	27.0	25.8	24.4	22.4	24.9	28.0	27.0	25.5	24.0	26.1
		Current (mA)	197	278	371	510	339	153	232	347	463	299
		Apparent Resistance (Ω)	137.1	92.8	65.8	43.9	84.9	183.0	116.4	73.5	51.8	106.2
		Power (Watt)	5.32	7.17	9.05	11.42	8.24	4.28	6.26	8.85	11.11	7.63
M3 G	10	Probe Voltage (Volt)	9.0	8.6	8.2	7.8	8.4	9.3	9.0	8.6	8.2	8.8
		Current (mA)	139	192	210	220	190	109	150	161	167	147
		Apparent Resistance (Ω)	64.7	44.8	39.0	35.5	46.0	85.3	60.0	53.4	49.1	62.0
		Power (Watt)	1.25	1.65	1.72	1.72	1.59	1.01	1.35	1.38	1.37	1.28

Table LXIII Variation of probe voltage, current, resistance and power consumption along
the demineralizing path. Co ≃ 4000 ppm, Exp. M11 B, M11 F and M11 G

EXP.	APPLIED VOLTAGE (VOLT)	STAGE NUMBER / VARIABLE	ENRICHMENT HALF CYCLE					DEPLETION HALF CYCLE				
			1	2	3	4	AVERAGE VALUES	1	2	3	4	AVERAGE VALUES
M11 B	20	Probe Voltage (Volt)	17.3	16.3	15.6	15.0	16.1	18.3	17.6	16.7	16.0	17.2
		Current (mA)	517	639	759	880	699	393	500	685	833	603
		Apparent Resistance (Ω)	33.5	25.5	20.6	17.0	24.2	46.6	35.2	24.4	19.2	31.4
		Power (Watt)	8.94	10.42	11.84	13.20	11.10	7.19	8.80	11.44	13.33	10.19
M11 F	30	Probe Voltage (Volt)	26.0	24.5	23.2	21.7	23.9	27.5	26.5	25.5	23.6	25.8
		Current (mA)	391	540	711	1097	685	288	409	640	1050	597
		Apparent Resistance (Ω)	66.5	45.4	32.6	19.8	41.1	95.5	64.8	39.8	22.48	55.6
		Power (Watt)	10.17	13.23	16.50	23.80	15.93	7.92	10.84	16.32	24.78	14.97
M11 G	10	Probe Voltage (Volt)	8.5	8.1	7.7	7.5	8.0	8.9	8.6	8.4	8.1	8.5
		Current (mA)	347	443	460	469	430	323	383	403	460	392
		Apparent Resistance (Ω)	24.5	18.3	16.7	16.0	18.9	27.6	22.5	20.8	17.6	22.1
		Power (Watt)	2.95	3.59	3.54	3.52	3.40	2.87	3.29	3.39	3.73	3.32

Table LXIV Effect of Initial Concentration on the equivalent
            resistance of ED stack
            Exp. Group M7, M3 and M11

EXP.	GRAPH. SYMBOL	APPLIED VOLTAGE (VOLT) / FEED CONC. (ppm)	EQUIVALENT STACK RESISTANCE (ohm)		
			500	2000	4000
Mn G	O	10	46.48	14.82	5.39
Mn B	▲	20	60.78	18.79	7.00
Mn F	□	30	65.54	21.29	10.47
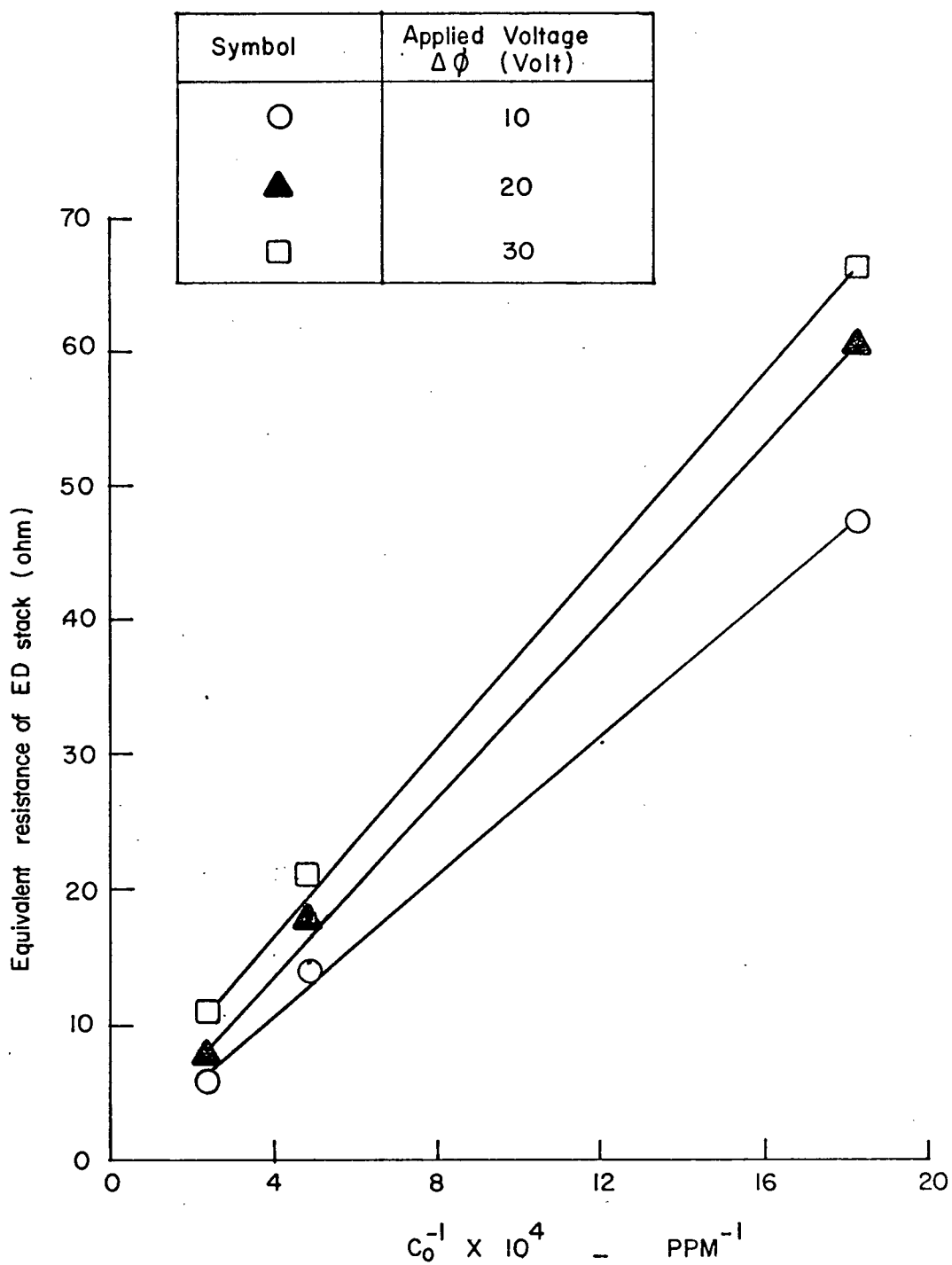
FIGURE 86

Effect of initial concentration on equivalent resistance of ED stack

Table LXV Variation of ED Stack Resistance along the demineralization path during the depletion half cycle at various applied voltages. Co ≃ 500 ppm Exp. M7 B, M7 F and M7 G

EXP.	GRAPH. SYMBOL	STAGE NUMBER / APPLIED VOLTAGE (VOLT)	RESISTANCE, $R = \Delta\phi/I$ (Ω)			
			4 FEED-END	3	2	1 PROD-END
M7 G	▲	10	107.4	157.9	251.4	527.8
M7 B	●	20	110.8	238.1	470.0	909.5
M7 F	□	30	117.8	261.9	514.5	993.1
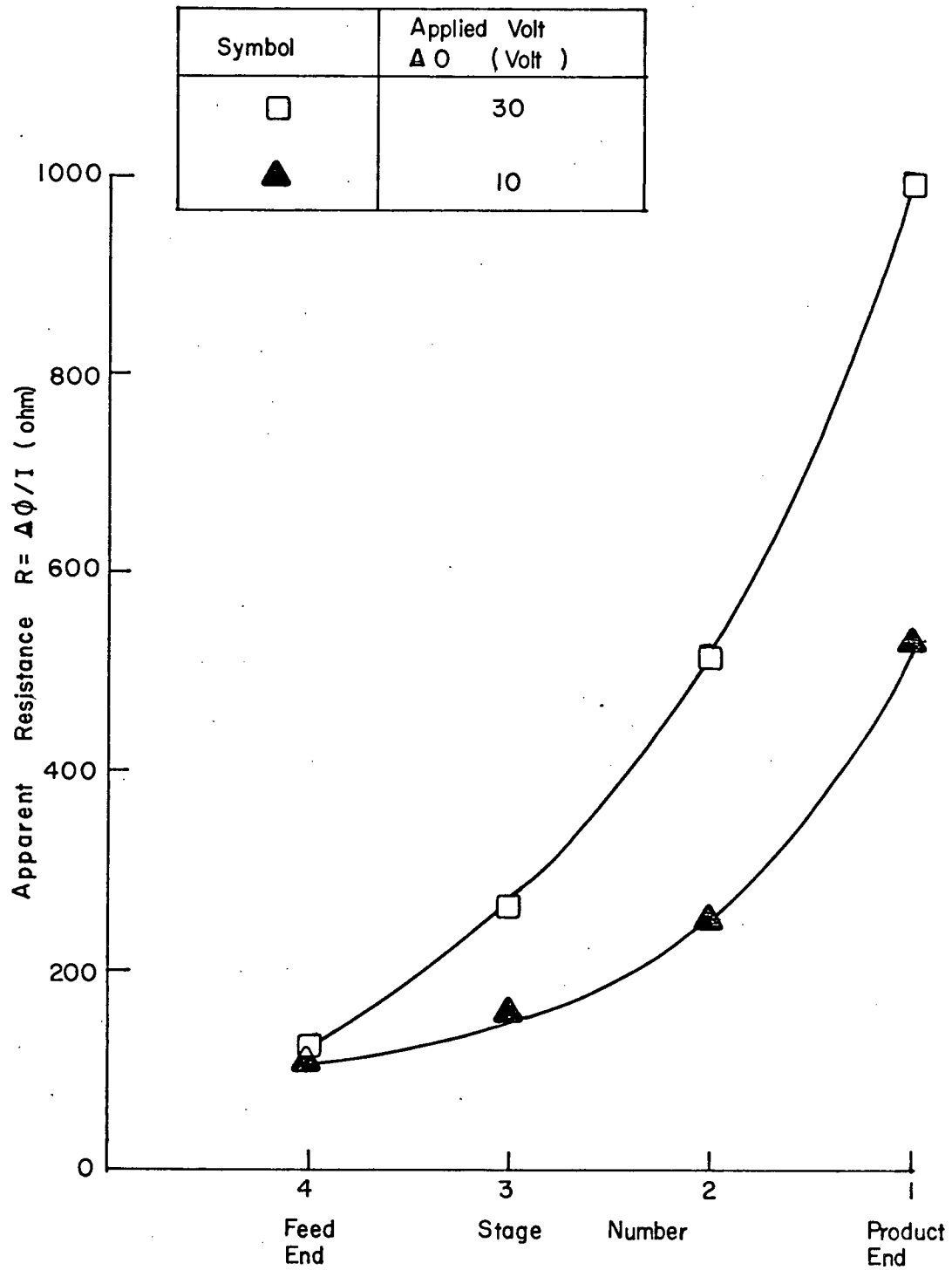
FIGURE 87

Variation of stack resistance along the demineralizing path during the depletion half cycle. $C_0 \approx 500$ PPM; EXP M7F & M7G

Figure 88 displays the plot of the stage apparent resistance ($R = \Delta\phi/I$) on logarithmic scale vs. the stage position along the demineralization path during the depletion half cycle. The plots are fitted by straight lines which suggest that the apparent resistance of an ED stack may be expressed by an empirical relation of the form:

$$\ln R_{\ell} = C_1 + C_2\ell \tag{104}$$

where R_{ℓ} is the local resistance at distance ℓ from the feed inlet and C_1 and C_2 are constants. If we are concerned only with the average value of the stage resistance then we have

$$\ell = n\ell' \tag{105}$$

where ℓ' is a single stage length and n is the stage number ($n = 1$ at feed end). Substitute Eq. (105) into Eq. (104):

$$\ln R_n = C_1 + C_3 n \tag{106}$$

where R_n is the average resistance of stage number n.

Figure 89 shows the variation of the average stage resistance with the stage position on a semi-logarithmic scale when the feed concentration $C_o \simeq 2000$ ppm and applied voltage was at levels of 10, 20 and 30 V. Various points under the same operating conditions are fitted by straight lines. The slope of these lines increases with increasing applied voltage and when these lines are extrapolated they tend to merge into a single point (a pole). For feed concentration $C_o \simeq 2000$ ppm the pole lies at the point P (0.70, 45) (refer to Figure 89). For this case Eq. (106) can be written as

$$\ln R_n = \ln 45 + C_3 (n - 0.70) \tag{107}$$

The value of C_3 can be obtained from the slope of the lines in Figure 89
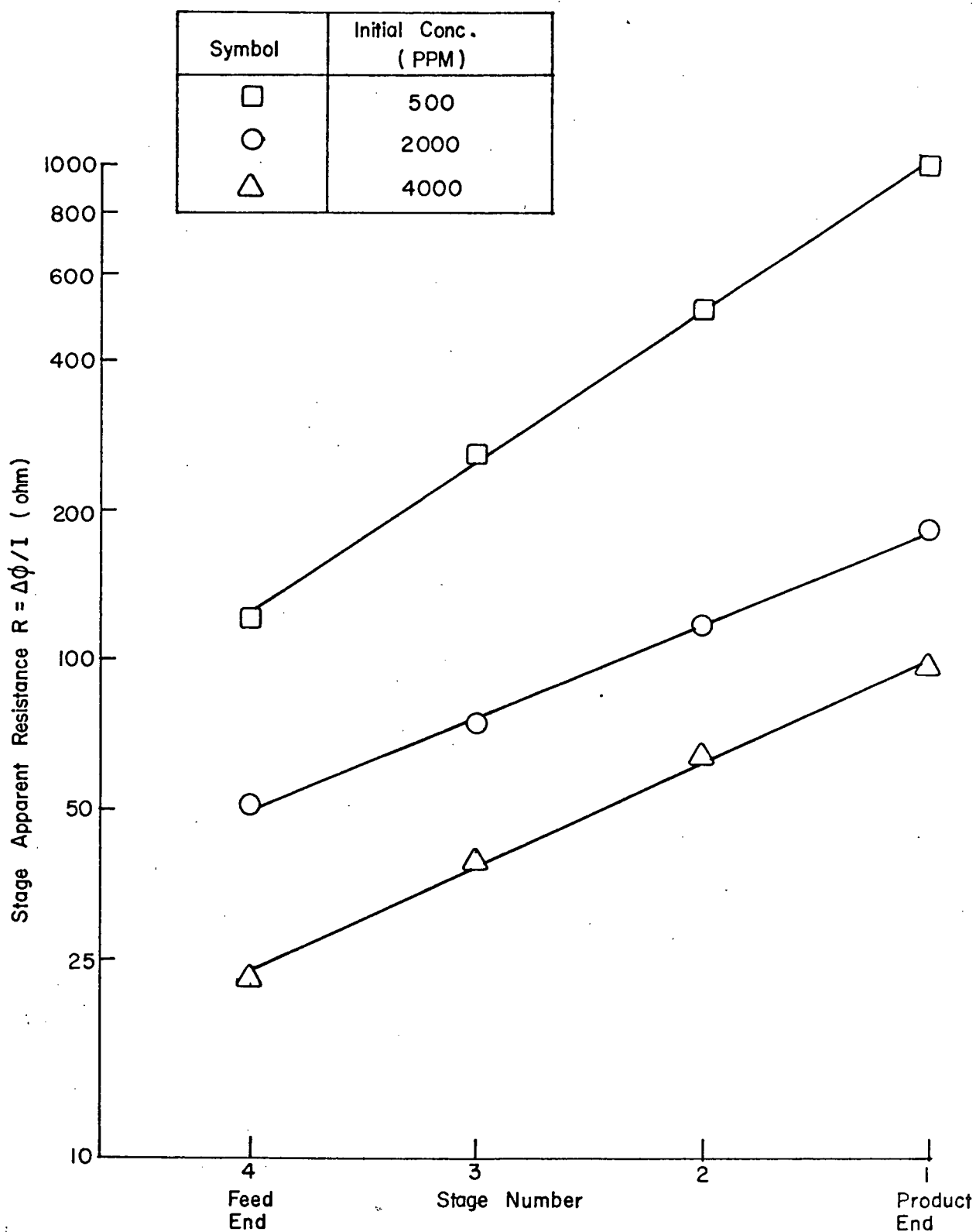
FIGURE 88

Variation of apparent ED stack resistance along the demineralizing path during the depletion half cycle using a semi_log scale.

$\Delta \phi$ =30 V ; EXP. M3F, M7F & M11F (refer to Tables LXI_LXIII)

Symbol	Applied Voltage (Volt)
△	30
○	20
□	IO
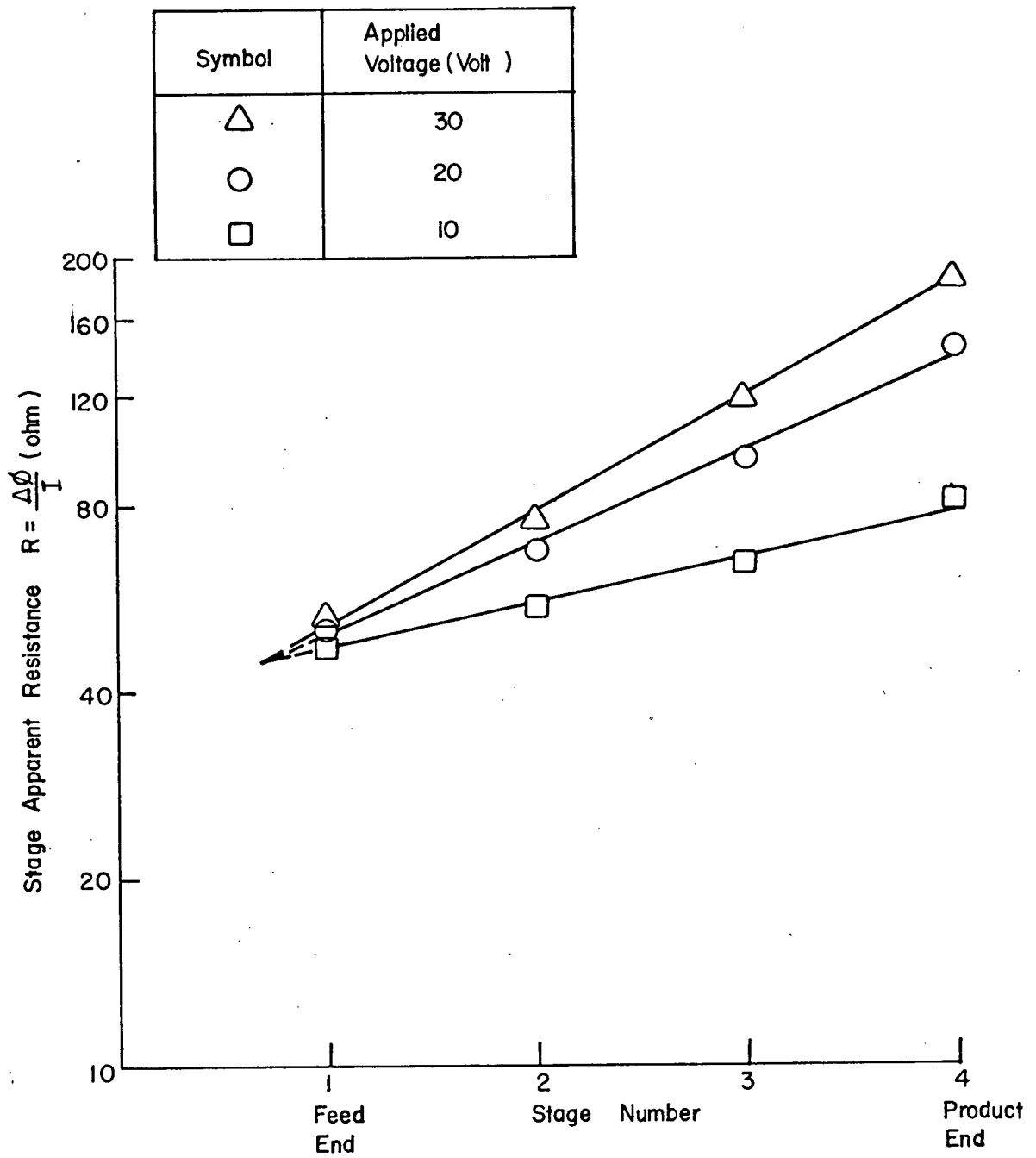
FIGURE 89
Variation of apparent ED stack resistance along the demineralization path
using a semi_log scale. $C_0 \approx$ 2000 PPM ; EXP. M3B , M3F & M3G .
(refer to Table LXII)

as follows:

$$C_3 \simeq 0.43 \quad ; \quad \text{for } \Delta\phi = 30 \text{ V}$$

$$C_3 \simeq 0.34 \quad ; \quad \text{for } \Delta\phi = 20 \text{ V}$$

$$\text{and } C_3 \simeq 0.17 \quad ; \quad \text{for } \Delta\phi = 10 \text{ V}$$

Similarly the parameters C_1 and C_3 in the expirical Eq. (106) can be determined for the other feed concentrations under various operating conditions.

5.9. Voltage Efficiency

Voltage efficiency may be defined as the fraction of the applied voltage that is utilized in separation (probe voltage).

$$\eta_v = \frac{\Delta\phi - \Delta\phi_{con} - \Delta\phi_{el}}{\Delta\phi} \cdot * \ 100 \qquad (108)$$

where

$\Delta\phi$ = applied voltage

$\Delta\phi_{con}$ = voltage drop in the connectors

$\Delta\phi_{el}$ = voltage drop due to the rinse solution and electrode overpotentials

Table LXVI lists voltage efficiency for several runs under various operating conditions. The voltage efficiency ranges between 82.50 and 90.83%.

5.10. Current density and efficiency

In the present work the current density, i, varies between 1.00 and 10.82 mA/cm^2. Low current density corresponds to operation with a low feed concentration and a small applied voltage.

The true current efficiency, η_I, is defined by Eq. B.7 as

Table LXVI Voltage Efficiency

EXP.	APPLIED VOLTAGE (VOLT)	UTILIZED VOLTAGE (VOLT)	VOLTAGE EFFICIENCY %
M3 B	20	17.15	85.75
M3 F	30	25.50	85.00
M3 G	10	8.30	83.00
M7 B	20	18.00	90.00
M7 F	30	27.25	90.83
M7 G	10	8.95	89.50
M11 B	20	16.65	83.25
M11 F	30	24.85	82.83
M11 G	10	8.25	82.50

$$\eta_I = \eta_s \eta_m \eta_w \qquad \text{(B.7.)}$$

When the selectivity of the membrane is 0.90 the true current efficiency, η_I is usually about 80%. The current utilization factor or the overall current efficiency, $\bar{\eta}_I$ can be defined as

$$\bar{\eta}_I = \frac{\text{actual amount of salt transported}}{\text{theoretical amount of salt transported}} * 100 \qquad (109)$$

where the theoretical amount of salt transported in g-equivalent is given by

$$V\Delta C = \frac{I \cdot t \cdot 10^6 \cdot M}{ZF} \qquad (110)$$

where

V = the volume of fluid demineralized during time t in a flow channel (c.c.)

ΔC = change in fluid concentration (ppm)

I = current passed (amp)

t = duration of the current passage (sec)

Z = valence (g-equiv./g-mole)

F = Faraday's constant = 96500 (coulomb/g-equiv.)

M = Molecular weight of solute = 58.44 (g/g-mole)

The overall current efficiency as defined above includes the true current efficiency, η_I together with any inefficiencies in the process such as dispersive effects, diffusion under concentration gradient and internal and external leakage if any exist.

The overall current efficiency, $\bar{\eta}_I$, was evaluated for several runs under various operating conditions as shown in Table LXVII. The overall current efficiency ranges between 26 and 32% in most cases; runs with high feed concentration resulted in lower values. Previous work in the closed

Table LXVII Overall Current Efficiency

EXP.	APPROX. FEED CONC (ppm)	CURRENT (Amp)	OVERALL CURRENT EFFICIENCY %
M4 A	2000	3.98	26.26
M4 D	2000	5.10	27.19
M4 G	2000	2.70	26.35
M8 C	500	1.30	26.63
M8 I	500	0.85	31.57
M12 E	4000	10.26	20.98
M12 G	4000	6.58	15.16

system indicated an overall current efficiency between 20 and 40 for the first cycle, decreasing rapidly for subsequent cycles, and tending to zero as the separation approached steady periodic state.

The overall current efficiency could be improved by utilizing a more efficient unsymmetric power wave with a short regeneration step compared with the demineralizing step and by using a longer demineralizing path. Also as most of the useful separation takes place during pause periods decreasing circulation time may result in an increased current efficiency.

5.11. Comments on Stack Resistance Models

Four experiments under various operating conditions have been used to test the non-ohmic model. The following simplified equation (Eq. 51) was used to predict the apparent resistance of an ED stage at the product end.

$$R_p = \frac{2RT}{Fi} [(\bar{t} - t_c) \ln \frac{ns + k}{1 - k}]$$

$$+ \frac{2FD}{(\bar{t} - t)\Lambda i} \ln \frac{1 + k/ns}{1 - k}$$

$$+ \frac{\Delta - 2\delta}{C_D \Lambda_D} + \frac{\Delta - 2\delta}{C_C \Lambda_C} + \rho_a + \rho_c \tag{51}$$

where

R_p is the resistance per unit area (ohm-cm^2)

R is the gas law constant

     = 8.3144 (Joule-gmole^{-1} - °K^{-1})

T = the absolute temperature (°K)

F = Faraday's constant (Coulomb/g.equiv)

i = current density (A/cm^2)

$\bar{t}, t$ = transport numbers of counter-ions in membrane and solution respectively

t_c = transport number of co-ions in the membrane

Λ = equivalent solution conductance (mho.cm^2/gmole)

D = diffusivity (cm^2/sec)

ns   = separation factor   = $\dfrac{C_B}{C_D}$

k   = ratio of the operating to limiting current density

Δ = flow channel thickness (cm)

δ = diffusion layer thickness (cm)

ρ_a, ρ_c = the anion and cation membrane resistance per unit area

(ohm – cm^2)

System Data and Assumptions

Room temperature = 25°C = 298°K

Molecular weight of NaCl = 58.44

Equivalent conductance of aqueous sodium chloride solution, Λ, is given by Table LXVIII and Figure 90.

Diffusivity of aqueous sodium chloride, D, is given by Table LXVIII and Figure 91.

$\Delta - 2\delta \simeq \Delta$

Electrode area = 61.23 cm^2

Spacer thickness = 0.098 cm

Exposed area of spacer = 0.50

Membrane selectivity = 90%

$(\bar{t} - t_c)$	= 0.90
$(\bar{t} - t)_{av}$	= 0.45
$\rho_a + \rho_c$	= 19.2 Ω-cm^2
k	= 0.80

Table LXVIII   Equivalent Conductance and Diffusivity
of aqueous sodium chloride solutions[*]

CONC. of NaCl (ppm)	EQUIVALENT CONDUCTANCE, Λ (mho $-$ cm^2/gmole)	DIFFUSIVITY D x 10^5 cm^2/sec
0	126.45	
100	125.60	1.599
500	122.89	1.585
2000	117.57	1.535
4000	113.47	1.494
8000	108.96	1.481

* Saline Water Conversion Engineering Data Book, Second Edition,
U.S. Office of Saline Water, November, 1971.
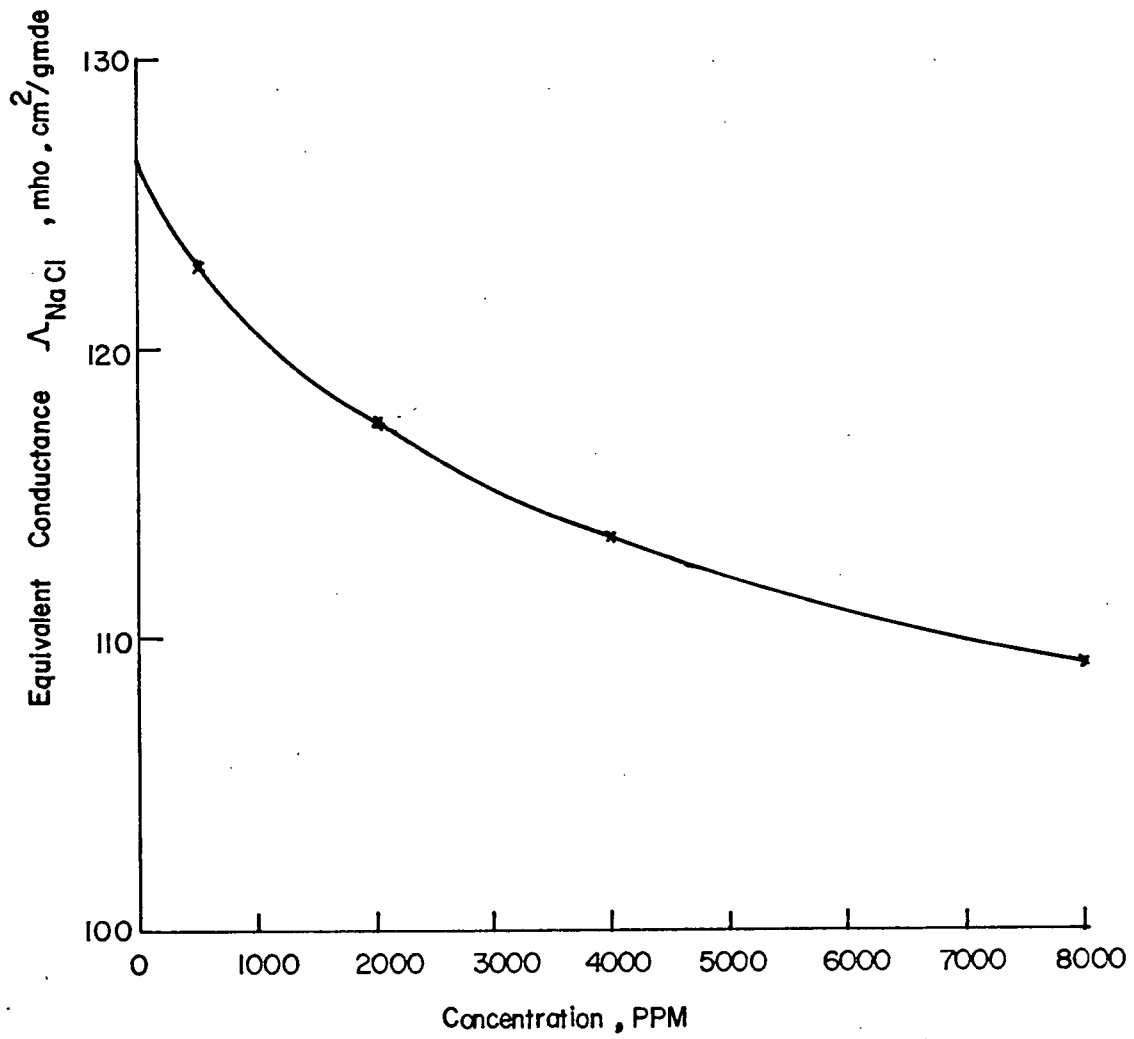
FIGURE 90

Equivalent conductance of aqueous sodium chloride solutions at 25° c .
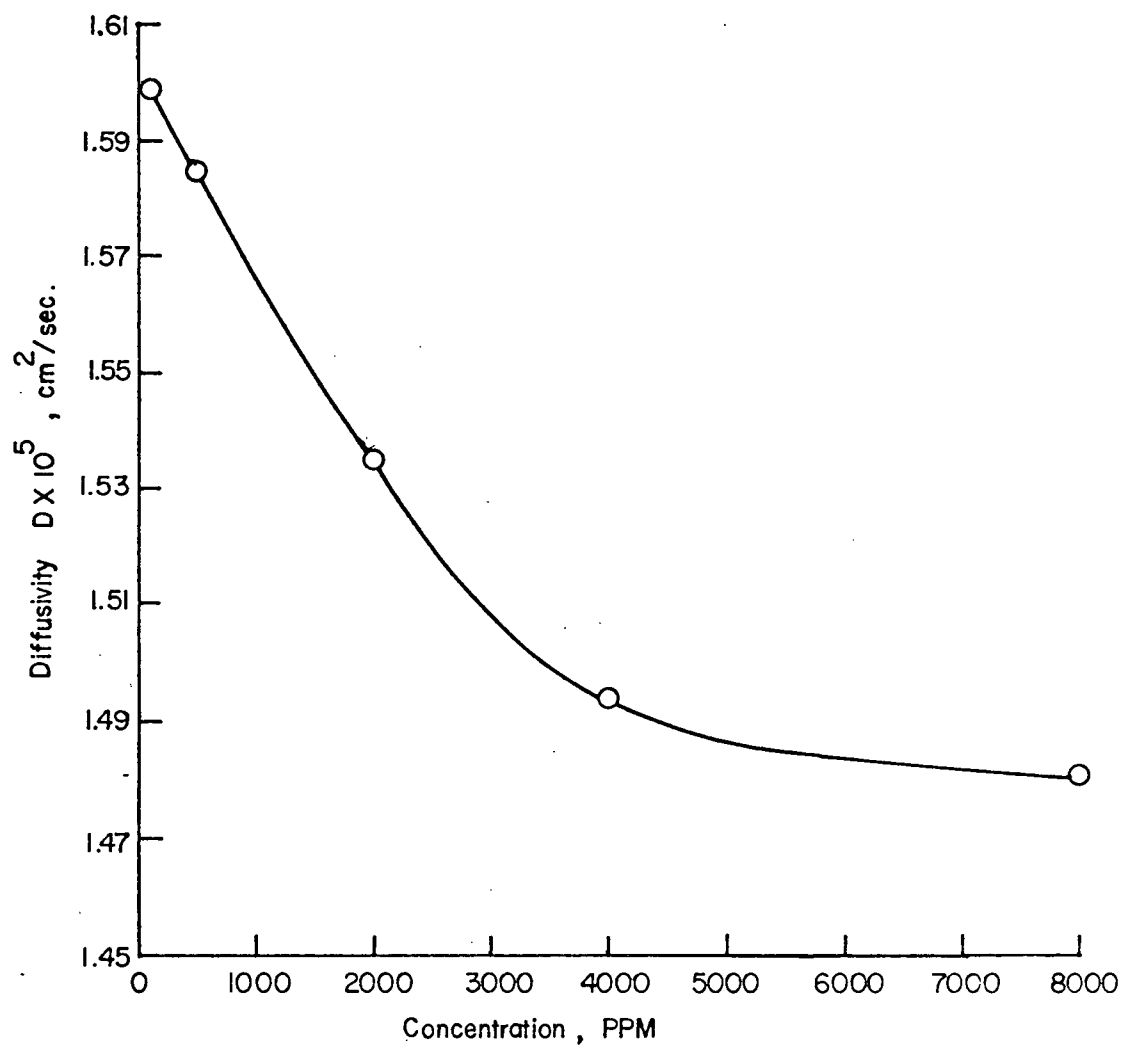
FIGURE 9I

Diffusivity of aqueous sodium chloride solutions at 25°c.

Sample of Calculations

EXP M3F   ; C_o = 2120 ppm

C_D = 105 ppm   ; Λ_D = 125.6 mho. cm^2/gmole

                    D = 1.599 x 10^{-5} cm^2/sec

C_B = 4300 ppm ; Λ_C = 113 mho. cm^2/gmole

ns = 40.95   ; i_{av} = 2.858 mA/cm^2

1st term (membrane potential term)

$$R_{\phi,m} = \frac{(2)(8.3144)(298)(0.9)}{(96500)(2.858)10^{-3}} \ln \frac{40.95 + 0.8}{0.2} = 86.37 \ \Omega - cm^2$$

2nd term (diffusion layer resistance term)

$$R_\delta = \frac{(2)(96500)(1.599) 10^{-5}}{(2.858)(0.45)(125.6)10^{-3}} \ln \frac{1 + 0.0195}{0.2} = 31.12 \ \Omega - cm^2$$

3rd term (membrane resistance term)

$$R_m \qquad\qquad\qquad\qquad\qquad\qquad = 38.40 \ \Omega - cm^2$$

4th term (depleted solution resistance term)

$$R_d = \frac{(0.098)(58.44)10^6}{(0.5)(105)(125.6)} \qquad = 868.58 \ \Omega - cm^2$$

5th term (enriched solution resistance term)

$$R_e = \frac{(11.45) 10^6}{(4300)(113)} \qquad\qquad = 23.57 \ \Omega - cm^2$$

The apparent resistance per unit area of a cell pair, R_p is given by

$$R_p = R_{\phi,m} + R_\delta + R_m + R_d + R_e \qquad = 1048.04 \ \Omega - cm^2$$

The predicted stage resistance is given by

$$R_s = \frac{(1048.04)(8)}{(61.23)} \qquad\qquad = 136.93 \ \Omega$$

$$\text{Measured stage resistance} \quad = \quad 160.05 \; \Omega$$

$$\text{the percentage error} \quad = \quad \frac{136.93 - 160.05}{160.05} \quad = \quad -14.44\%$$

Table LXIX lists values of predicted and measured resistances for several experiments and breaks down the total predicted resistance into its main resistive elements and it also indicates the contribution of each element towards the overall value. Figure 92 displays the discrepancy between predicted and measured values of an ED stage resistance. The discrepancy may be attributed to the assumed values used in the calculation or to the simplifying assumptions involved in the model or to both of them.

From Table LXIX it can be seen that the membrane potential term together with the diffusion layer resistance contribute about 20% while the bulk solutions contribute about 80% towards the overall resistance value. These findings also indicate that ohmic model can be used satisfactorily to predict the stack resistance.

The basic equation of ohmic analysis is given as

$$R_p \; = \; \frac{K_1}{\bar{C}} + K_2 - K_3 \bar{C} \tag{52}$$

where K_1, K_2 and K_3 are constants for a given system and $\bar{C}$ is the local average concentration.

Measured stage resistances in several runs were plotted vs. the reciprocal of the average concentration as shown in Figure 93 and Table LXX. The plot was fitted by a straight line. The model constants were determined from the slope and intercept of the graph as follows:

$$K_1 \; \simeq \; 216484$$

$$K_2 \; \simeq \; 191.34$$

$$\text{and} \quad K_3 \; \simeq \; 0.0$$

EXP. RESISTIVE ELEMENT	M3 F 2000 ppm		M3 B 2000 ppm		M7 G 500 ppm		M11 F 4000 ppm	
	VALUE Ω	% age of R_s	VALUE Ω	% age of R_s	VALUE Ω	% age of R_s	VALUE Ω	% age of R_s
Membrane Potential	11.29	8.24	12.23	12.37	82.18	20.41	5.62	8.67
Membrane Resistance	5.02	3.66	5.02	5.07	5.02	1.25	5.02	7.75
Diffusion Layer Resistance	4.07	2.97	4.91	4.97	33.30	8.27	2.11	3.26
Depleted Bulk Sol. Resistance	113.48	82.88	73.45	74.27	269.96	67.02	50.34	77.71
Enriched Bulk Sol. Resistance	3.08	2.25	3.28	3.32	12.29	3.05	1.69	2.61
Predicted total Resistance Value	136.93	100	98.90	100	402.74	100	64.78	100
Measured Resistance Value	160.05		128.1		445.90		81.00	
Discrepancy as % Age	- 14.44		- 22.80		- 9.68		- 20.03	

FIGURE 92

Discrepency between predicted and measured value of an ED stage .

Table LXX Values of local average concentration, $\bar{C}$
and measured stage resistance

EXP.	PRODUCT CONC (ppm)		LOCAL AVERAGE CONC. (ppm)	STAGE RESISTANCE (Ω)
	C_B	C_D		
M3 B	4025	163	313	128
M3 F	4300	105	205	160
M3 G	3725	550	958	75
M7 B	1090	20.2	40	753
M7 F	1110	17.6	35	826
M11 B	7375	625	1152	40
M11 F	8125	239	464	81
M11 G	6450	2010	3065	26
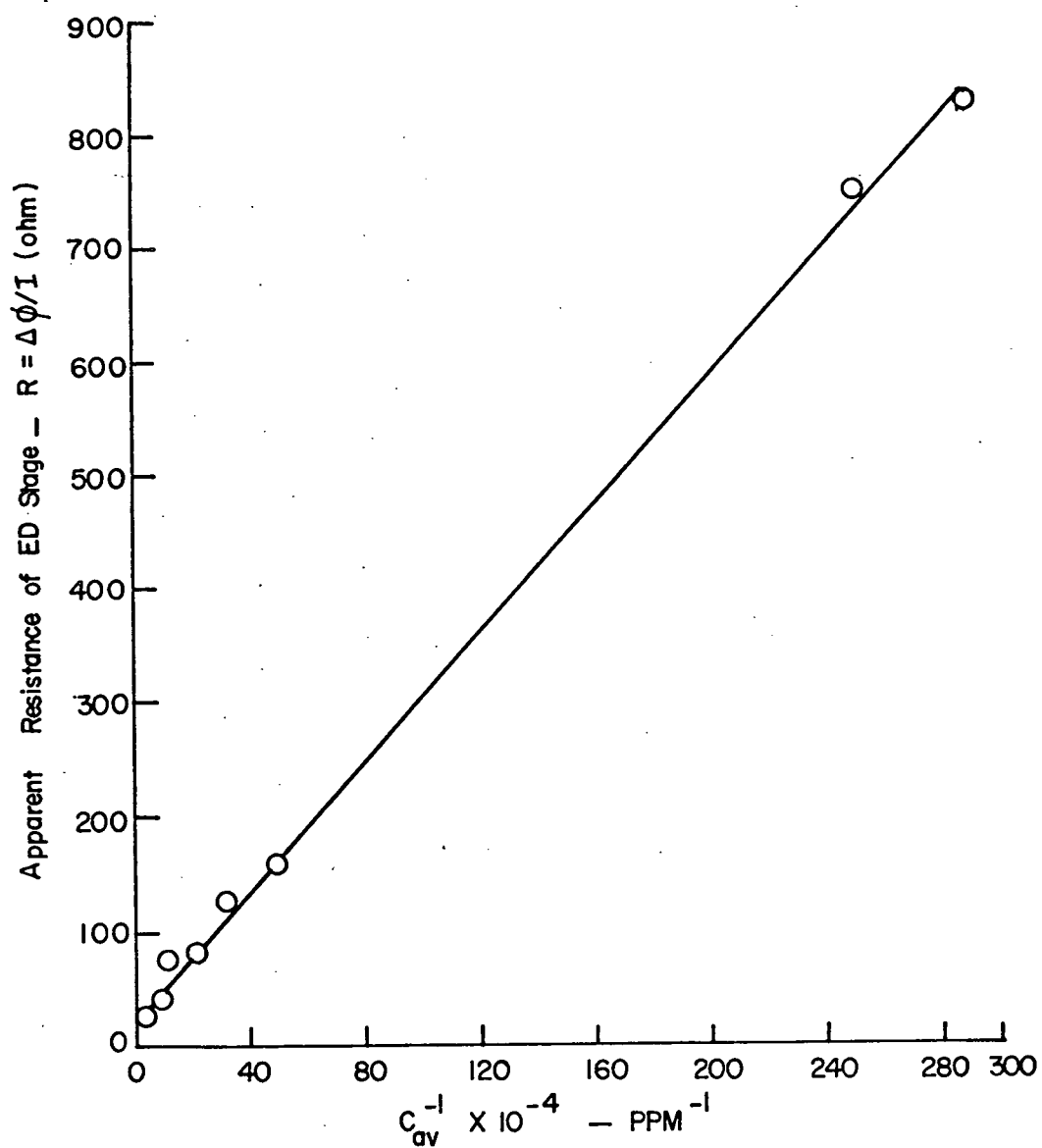
FIGURE 93

Variation of apparent resistance of an ED stage with the reciprocal of the average product concentrations.

5.12 Comparison with Previous Work in Closed System

(i) Separation

Bass (1972) reported some experiments performed in a batch-recirculation mode of operation in which a 90% demineralized product was intermittently replaced by fresh feed every eight cycles. Experiments under this mode of operation resulted in a separation factor of 16 with a feed concentration $C_o = 1250$ ppm, applied voltage $\Delta\phi = 10$ V, pause time $\tau = 10$ sec, displaced volume $\delta = 2/3$ the active volume and a throughput ratio of about 0.075. In the present work experiments with $\Delta\phi = 20$ V, $\tau = 15$ sec result in a separation factor of 20 at a throughput ratio of 0.25 which is the same magnitude of separation per unit power consumption as in the previous case.

However, the previous work does not show any consistent effect of initial concentration, C_o on the final separation.

(ii) Resistance and Current Consumption

The initial resistance and current consumption in the closed system were generally of the same magnitude as in the present work and they exhibit the same trend of variation along the demineralizing path.

(iii) Analysis of Axial Dispersion

The axial dispersion in the ED cells has been determined previously using the step response method. The resulting F-diagrams did not suggest excessive channelling or by-passing. From the slope of response curve it was estimated that the system corresponds to about 50 effective mixing stages. In the spacer used in both works there are 10 x 10 strands per inch and there are about 55 holes along the flowpath in the ED cell.

(iv) Effect of Pause Time

The previous work in the batch operation showed that flow pauses at the beginning of each half cycle represent important features of the cyclic process operation. This is in line with the findings in the present work.

5.13 Reproducibility

Several of the runs under different operating conditions were repeated to test the reproducibility of the results. Table LXXI lists the duplicate experiments and compares them with the initial ones conducted in 4-stage columns. Table LXXII makes the same comparison for experiments performed in 8-stage columns. In both cases the reproducibility of the results are considered as quite satisfactory.

Table LXXI Reproducibility – GROUP R
Two Columns Each Consists
of 4 Cells in Series

EXP.	SEPARATION FACTOR ns		DISCREPANCY AS PERCENTAGE OF (ns) Av.
	OLD	NEW	
R1 A	8.90	10.43	+ 15.83
R1 D	7.49	8.53	+ 12.98
R1 E	13.93	16.52	+ 17.01
R1 F	20.64	18.84	– 9.12
R3 B	7.21	6.09	– 16.84
R4 F	7.02	5.99	– 15.83
R5 A	33.97	37.50	+ 9.88
R5 C	25.37	28.43	+ 11.38
R5 F	68.45	61.97	– 9.94
R7 A	25.79	22.27	– 14.65
R7 B	34.00	29.41	– 14.48
R7 C	20.00	17.45	– 13.62
R8 F	18.46	21.09	+ 13.30
R9 E	3.10	3.39	+ 8.94
R9 F	4.56	4.10	– 10.62
R11 F	3.44	3.76	+ 8.89

Table LXXII   Reproducibility – Group M
              Two Columns Each Consists
              of 8 Cells in Series

EXP.	SEPARATION FACTOR ns		DISCREPANCY AS PERCENTAGE OF (ns) Av.
	OLD	NEW	
M1 B	27.53	31.20	+ 12.50
M1 D	29.46	28.47	− 3.42
M1 F	46.28	41.27	− 11.44
M3 C	8.03	9.52	+ 16.98
M4 A	14.61	14.23	− 2.64
M4 E	28.45	32.17	+ 12.27
M5 C	39.92	36.11	− 10.02
M7 C	31.21	28.33	− 9.67
M7 D	44.21	47.14	+ 6.41
M8 B	40.38	37.96	− 6.18
M8 F	48.43	53.20	+ 9.39
M9 A	8.83	7.87	− 11.50
M9 E	28.13	30.81	+ 9.09
M11 B	11.80	12.92	+ 9.06
M12 C	3.98	3.63	− 9.20
M12 D	12.54	11.69	− 7.02
M12 F	28.62	31.27	+ 8.85

CHAPTER 6

Conclusions and Recommendations

The present work has proven the feasibility of continuous cyclic

electrodialysis for desalination of brackish waters. The conventional

electrodialysis demineralizing process competes mainly with distillation and

it appears to be more attractive economically than distillation for low

salinity waters (with concentrations of up to about 10,000 ppm dissolved

salt). However, conventional electrodialysis is subject to excessive

polarization, fouling and scale formation on ion-exchange membranes, and

generally requires expensive materials for electrodes. Cyclic electrodialysis

promises to overcome these problems by the reversed polarity technique.

In the present work no excessive polarization was noticed in

most of the runs (up to the maximum voltage applied of 30 volts)

and inexpensive graphite electrodes proved to be satisfactory over a

reasonably long period of time. The process resulted in a separation factor

$(ns = C_B/C_D)$ up to 50 at a throughput ratio of 0.25 which is equivalent to

a desalination ratio (defined as C_o/C_D) of about 25 compared with the

desalination ratio per path of about 2 in most commercial plants currently in

operation.

The primary objectives of the experimental program undertaken were

to explore the possible region of application of cyclic operation in an

open electrodialysis system, to screen system parameters, and to determine

their relative importance. The following design and operating parameters have been investigated:

a) Design Parameters

    (i) Demineralization path length

    (ii) Semi-symmetric and asymmetric modes of operation

    (iii) Pause and no-pause operations

    (iv) Pure-pause operation with power off during circulation

b) Operating Parameters

    (v) Production rate with throughput ratio varying from 0.0625 to 0.50.

    (vi) Applied voltage $\Delta\phi$ at levels of 10, 20 and 30 volt.

    (vii) Pause time τ at levels of 15, 30 and 45 sec.

    (viii) Feed concentration C_o at levels of 500, 2000 and 4000 ppm

The results of the study can be summarized in the following:

1. Despite the strong trade-off between production rate and separation, the separation factor ranged from 30 (for 4000 ppm feed) to 50 (for 500 ppm feed) at the highest production rate used (100 c.c./cycle).

2. The pause time proved to be an important operating parameter. Decreasing the pause time below 15 sec. resulted in considerably lower separation.

3. The maximum pause time that can be utilized without an adverse effect on separation depends on both the applied voltage $\Delta\phi$ and the feed concentration C_o. At an applied voltage $\Delta\phi = 30$ V; τ_{max} was about 30 sec. for $C_o \simeq 500$ ppm and it was about 45 sec. for $C_o \simeq 2000$ ppm.

4. In all cases increasing the applied voltage improves the separation. The separation factor increases at least proportionally with the applied

voltage. The effect of applied voltage was more pronounced when the feed concentration was high and/or the pause time was short.

5. With the feed concentration $C_o \simeq 500$ ppm the optimum conditions are thought to be: a demineralizing path length in the vicinity of 8 stages in series, an applied voltage in the range 20-30 volt and a pause time of about 30 sec. An increase of pause time above 30 sec. had a deleterious effect on separation, presumably because of polarization.

6. As the feed concentration C_o increases the separation decreases. Higher feed concentration calls for a longer demineralizing path, higher voltage and longer pause time.

7. Pure-pause operation saves electric power at the expense of poor separation.

8. Variations in the methods of feed introduction and product withdrawal, such as symmetric, semi-symmetric and asymmetric operations, were investigated theoretically (Chapter 4). When axial mixing is ignored all these modes predict the same final separation as shown by the graphical solutions. However, the degree of complexity of the system, the number of valves and the number of subdivisions in the timing sequence decrease as the operation becomes less symmetric.

9. When semi-symmetric and asymmetric operations were compared experimentally under otherwise identical conditions the former resulted in lower separation. This may be attributed mainly to the external mixing outside the active demineralizing area.

10. The experimental results are generally highly reproducible.

11. Cyclic electrodialysis in an open system has been fully demonstrated. The process looks promising and it deserves further study along the

following lines:

a) The present work has been limited by the following design
parameters:

(i) A demineralizing path of maximum length of 8 stages in
series

(ii) A D.C. power supply of 400 watts (a maximum applied
voltage of about 30 volts)

(iii) A maximum time interval of about 50 sec.

To explore fully the whole operating domain at feed concentration C_o
higher than 500 ppm all these parameters need to be relaxed by modifying
the process design.

b) The feed concentration should be extended to the range C_o =
10,000 – 15,000 ppm.

c) Other operating procedures should be investigated. In particular
it is proposed to disconnect the electric power from the ED stacks during
part of the displacement. Also, the system may be run in semi-batch operation
with feed introduction and product withdrawal once every several cycles.
Different voltage waves other than the present rectangular wave can be
applied such as triangular wave and unsymmetric wave with different magnitude
and duration in the two half cycles. This may result in a better power
economy.

d) The proposed stack resistance model predicts quite accurately the
resistance of the experimental stacks under the operating conditions used here.
An extension of the constant-rate model based on the stack resistance could
form a basis for a more refined representation.

e)   A scale-up and an optimization study of the system are essential for evaluation of the process economics and its comparison on a commercial scale with other competitive processes.

f)   Other solutes should be investigated, both in binary and in multicomponent mixtures.

g)   By using cation and anion exchange membranes selectively permeable for univalent ions only, the system can be used to separate monovalent ions from divalent and other ions.

NOMENCLATURE

a	=	membrane area	cm^2
$a_\pm$	=	ionic activity of cation (+) or anion (-)	$\dfrac{g-mole}{litre}$
a_1	=	rate constant during dilution half cycle	sec^{-1}
a_2	=	rate constant during enrichment half cycle	sec^{-1}
A	=	membrane area	cm^2
C	=	solute concentration	$\dfrac{g-mole}{litre}$ or ppm
C_1, C_2, C_3	=	constant	
D	=	diffusion coefficient	cm^2/sec
e	=	potential drop per cell pair	volt
E	=	potential drop	volt
f	=	the fraction desalted	
F	=	Faraday's constant or flow rate of process stream	A.sec/g-equiv. litre/sec.
i	=	current density	mA/cm^2
I	=	current	A
$\vec{j}$	=	ionic flux vector	$(g-mole)/(cm^2)(sec)$
k	=	electrical conductivity or the ratio between operating and limiting current density	mho/cm

			Typical Unit
$k_1, k_2 \ldots$	=	constant	
K	=	rate constant or cell constant	cm^{-1}
K_1, K_2, K_2	=	constant	
ℓ	=	channel length	cm
ℓ'	=	a single stage length	cm
L	=	phenomenological coefficient	
m	=	length of the membrane or the demineralizing path	cm
n	=	number of cycles or number of membrane pairs or width of membrane	
ns	=	separation factor	cm
N	=	normality of solution	g-equiv.litre
p	=	$\exp\left(- a_1 \dfrac{T}{2}\right)$ or permselectivity of ion exchange membrane or membrane area utilizing factor	
q	=	$\exp\left(- a_2 \dfrac{T}{2}\right)$	
Q	=	flow rate	cm^3/sec
$\vec{Q}$	=	heat flow vector	
r	=	dimensionless ratio of spacer thickness in the concentrate and the diluate compartments	
R	=	areal resistance or the gas law constant	ohm cm^2 (joules)/(°K)(mole)
t	=	transport number or temperature	°C
T	=	cycle time or absolute temperature	sec °K
u_+	=	ionic mobility	$(cm^2)/(volt)(sec)$
U	=	total chemical potential	

Typical Unit

v	=	displacement velocity	cm/sec
$\vec{v}$	=	velocity vector	cm/sec
V	=	volume	cm^3
w	=	water transport number	
x	=	distance co-ordinate	cm
y	=	lateral distance co-ordinate	cm
z	=	valence of charged species or direction of flow	(g-equiv)/(g-mole)

Greek Symbols

α	=	fraction of half cycle	
β	=	fraction of half cycle	
γ	=	phase lag	
$\gamma_{\pm}$	=	the mean ionic activity coefficient	
δ	=	thickness of Nernst layer or diffusion layer	cm
Δ	=	compartment thickness	cm
ε	=	fractional void volume of packing	
η	=	efficiency	
$\vec{\eta}$	=	electric field vector	volt/cm
Λ	=	equivalent conductance	$(mho)(cm^2)/(g\text{-}equiv)$
ν	=	partial molar volume	$cm^3/mole$
$\nu_{\pm}$	=	stoichiometric coefficients for electrolyte $M_{\nu_+} X_{\nu_-}$	
ρ	=	electrical resistivity	ohm-cm
ρ	=	$(1 - \varepsilon)/\varepsilon$ = ratio of volume of packing to void volume	
τ	=	pause time or tranference number of water	sec

		Typical Unit
$\Delta\phi$	= applied electric potential	volt
$\Delta\phi_{Don}$	= Donnan potential	volt
∇	= divergence operator or gradient operator	

Subscripts

1,2 ...	refer to positions across a cell pair or to the number of time interval during a cycle; (τ_1, τ_2)
+	for positively charged species; (t_+)
-	for negatively charged species; (t_-)
a	for anion-exchange membrane; (t_a) or an average value; (C_a)
b	brine product; (C_b)
B	brine (enriched) product; (C_B)
c	cation-exchange membrane; (t_c) or concentrate product; (C_c) or concentration polarization; (η_c)
d	dialysate (depleted) product; (C_d)
d_1, d_2	Donnan terms; (E_{d_1}, E_{d_2})
D	dialysate (depleted) product; (C_D)
e	enriched product; (C_e) or electrode; (η_e)
f	fluid or mobile phase; (C_f)
F	Faraday; (η_F)
H	Henderson term; (E_H)
i	refers to inlet; (C_{di})
I	current; (η_I)
j	co-ion; (C_j)

k	counter-ion; (C_k) or species k; $(\vec{J}_k)$
ℓ	refers to local value at distance ℓ from the feed inlet; (R_ℓ)
m	manifold; (n_m) or membrane; (E_m) or membrane solution interface; (C_m)
n	stage number; (R_n)
o	refers to initial state; (C_o)
p	cell pair; (R_p)
R	resistance; (n_R)
S	solid or stationary phase; (C_s) or permselectively; (n_s)
T	total; (E_T) or top (demineralized) product; (C_T) or temperature; $(\nabla_T U)$
w	water transport; (n_w)
π	unit area per cell pair; (R_π)
ν	refers to the average concentration of salt; (Λ_ν)
∞	refers to infinite dilution; (Λ_∞)

Superscripts

$-$	= refers to property in membrane; $(\bar{C}_k, \bar{C}_j)$ or to negatively charged species; (t_a^-)
$+$	= refers to positively charged species; (t_c^+)

REFERENCES

Acrivos, A., Ind. Eng. Chem., 48, 703 (1956).

Aris, R., Ind. Eng. Chem. Fundam., 8, 603 (1969).

Asawa, T., et al., "Proc. 4th Intern. Symp. Fresh Water Sea", Vol. 3, p. 143, Heidelberg, 1973.

Bass, D., "A Cyclic Electrodialysis Process - Investigation of Closed Systems", Ph.D. Thesis, University of British Columbia, 1972.

Bass, D. and D.W. Thompson, "Proc. 4th Intern. Symp. Fresh Water Sea", Vol. 3, p. 269. Heidelberg, 1973.

Belfort, G. and G.A. Guter, "U.S. Off. Saline Water Res. Dev. Rep. 459 (1968)".

Belfort, G. and G.A. Guter, Desalination, 10, 221 (1972).

Bell, W.E., et al., "U.S. Off. Saline Water Res. Dev. Rep. 536 (1970)".

Bockris, J. O'M. and A.K.N. Reddy, Ed., "Modern Electrochemistry," Plenum Press, New York, 4th ed., 1973.

Bradley, C.C., Science [2] 138, 489 (1962).

Bradley, P.H., et al., "U.S. Off. Saline Water Res. Dev. Rep. 597 (1970)".

Calvit, B.W. and J.J. Sloan, "Proc. First Intern. Symp. on Water Desalination", Vol. 2, p. 11, Washington, D.C., Oct. 3-9, 1965.

Chapman, T.W., "Lectures in Transport Phenomena", A.I.Ch.E. Continuing Education Series 4, 90 (1969).

Chen, H.T. and F.B. Hill, Separ. Sci., 6, 411 (1971).

Chen, H.T., J.L. Rak, J.D. Stokes and F.B. Hill, Amer. Instit. Chem. Eng. J., 18, 356 (1972).

Chiolle, A., L. Credali and P. Parrini, "Proc. 4th Intern. Symp. Fresh Water Sea", Vol. 3, p. 81, Heidelberg, 1973.

Cooke, B.A., Electrochem. Acta, 3, 307; 4, 179; 5, 216 (1961).

Cooke, B.A., "Proc. First Intern. Symp. on Water Desalination", Vol. 1, p. 219, Washington, D.C., Oct. 3-9, 1965.

Cowan, D.A. and J.G. Brown, Ind. Eng. Chem., 51, 1445 (1959).

Cowan, D.A., Advances in Chem. Ser., 27, 224, American Chemical Society, Washington, D.C., 1960.

Craig, L.C., and D. Craig, "Technique of organic Chemistry", Vol. 3, A. Weissberger, Ed., Wiley-Intersci., New York, 1956.

Davis, T.A. and G.F. Brockman, "Physiochemical Aspects of Electromembrane Processes", in "Industrial Processing with membranes", R.E. Lacey and S. Loeb, Eds., Wiley-Intersci., New York, 1972.

Deming and P. Kollsman, U.S. Pat. 2, 872, 407 (1959).

Foo, S.C. and R.G. Rice, A.I.Ch.E.J., 21 (6), 1149 (1975).

Foo, S.C. and R.G. Rice, A.I.Ch.E.J., to be published.

Friedlander, H.Z. and R.N. Rickles, Anal. Chem., 37, 27A (1966).

Furukawa, D.H., "U.S. Off. Saline Water Res. Dev. Rep. 285 (1968)".

Gregory, R.A. and N.H. Sweed, Chem. Eng. J., 1, 207 (1970).

Gregory, R.A. and N.H. Sweed, Chem. Eng. J., 4, 139 (1972).

Gupta, R. and N.H. Sweed, "Nonequilibrium Theory of Parametric Pumping", A.I.Ch.E. National Meeting, Minneapolis, Aug. 24 (1972).

Helfferich, F., Ed., "Ion-Exchange", Chapter 8, McGraw-Hill Book Co., New York, 1962.

Hills, G.J., et al., Proc. Roy. Soc. (London), A 262, 246 (1961).

Hoek, van C., U.S. Pat. 2, 735, 812 (1956).

Huffman, E.L., "U.S. Off. Saline Water Res. Dev. Rep. 439 (1969)".

Hwang, Sun-Tank and Kammermeyer, K., "Membranes in Separation", Wiley-Intersci, New York, 1975.

Israel Patent 13, 242, Mar. 23, 1961.

Kellogg, M.W. Company, "Saline Water Conversion Engineering Data Book", Washington, D.C., 1965, Supplement 1, 1966.

Kobus, E.J.M. and P.M. Heertjes, Desalination, 10, 383 (1972).

Korngold, E., et al., Desalination, 8, 195 (1970).

Kuhn, A.T., Ed., "Industrial Electrochemical Processes", Elsevier Publishing Co., Amsterdam, 1971.

Lacey, R.E., "U.S. Off. Saline Water Res. Dev. Rep. 80 (1963)".

Lacey, R.E., "U.S. Off. Saline Water Res. Dev. Rep. 135 (1965)".

Lacey, R.E., Ed., "Membrane Processes for Industry", Southern Research Instit., Birmingham, Ala., 1966.

Lacey, R.E., Desalination, 2, 387 (1967).

Lacey, R.E., "U.S. Off. Saline Water Res. Dev. Rep. 398 (1968)".

Lacey, R.E., E.W. Lang and E.L. Huffman, Advances in Chem. Ser., 38, 168, American Chemical Society, Washington, D.C., 1963.

Lacey, R.E. and E.W. Lang, "U.S. Off. Saline Water Res. Dev. Rep. 106 (1964)".

Lang, E.W. and F.L. Huffman, "U.S. Off. Saline Water Res. Dev. Rep. 439 (1969)".

Laskorin, B.N., et al., "Proc. 4th Intern. Symp. Fresh Water Sea", Vol. 3, p. 99, Heidelberg, 1973.

Lynch, M.A. and M.S. Mintz, J. Am. Water, 64, 711 (1972).

McDermott, J., Ed., "Industrial Membranes Design and Applications", Noyes Data Cor., New Jersey, 1972.

Malherbe P. Le. and W.G.B. Mandersloot in "Demineralization by Electrodialysis", Chapter 2, J.R. Wilson, Ed., Butterworth, London, 1960.

Mandersloot, W.G.B. and R.E. Hicks, Ind. Eng. Chem. Proc. Des. Dev., 4, 304 (1966).

Mangan, G.F., J.M. Shackelford and K.A. Kase, "U.S. Off. Saline Water Res. Dev. Rep. 83 (1963)".

Mason, E.A. and T.A. Kirkham, Chem. Eng. Progr. Symp. Series, 55 (24), 173 (1959).

Mattson, M.E., L.L. Snedden and J.E. Gugeler, "Proc. First Intern. Symp. on Water Desalination", Vol. 3, p. 265, Washington, D.C., Oct. 3-9, 1965.

Matz, R.C., C. Forgacs and S. Perlmutter, U.S. Pat. 3, 029, 196 (1962).

Matz, R.C., "Proc. Interregional Seminar Economic Appl. Water Desal.," New York, 22 Sept., 1965.

Mintz, M.S. and E.W. Lang, "Study of Electrogravitational Separation", Southern Research Instit. Rep. 7374-1650-I (1965).

Murphy, G.W., Electrochem. Soc., $\underline{97}$, 405 (1950).

Nernst, W., Z. Physik Chem. (Leipzig), $\underline{47}$, 52 (1904).

O'Shaughnessy, F., "Desalting Plant Inventory Rep. $\underline{4}$ (1973)", ed. by the U.S. Off. Saline Water.

OSW (1963), "Saline Water Conversion Report for 1962", U.S. Off. Saline Water, Washington, D.C.

OSW (1964 a), "Saline Water Conversion Report for 1963", U.S. Off. Saline Water, Washington, D.C.

OSW (1964 b), "Test Manual for Permselective Membranes", U.S. Off. Saline Water Res. Dev. Rep. $\underline{77}$ (1964).

OSW (1968), "U.S. Off. Saline Water Res. Dev. Rep. $\underline{325}$ (1968)".

Patrick, R.R., J.T. Schrodt and R.I. Kermode, Separ. Sci., $\underline{7}$, 331 (1972).

Pepper, K.W., H.M. Paisley and M.A. Young, J. Chem. Soc., 4097 (1953).

Pigford, R.L., B. Baker III and D.E. Blum, Ind. Eng. Chem. Fundam., $\underline{8}$, 144 (1969 a).

Pigford, R.L., B. Baker III and D.E. Blum, Ind. Eng. Chem. Fundam., $\underline{8}$, 848 (1969 b).

Popkin, R., Ed., "Desalination Water for the World's Future", Frederick A. Praeger Publishers, New York, 1968.

Redman, R., "U.S. Off. Saline Water Res. Dev. Rep. $\underline{683}$ (1971)".

Rhee, H.K. and N.R. Amundson, Ind. Eng. Chem., $\underline{9}$, 303 (1970).

Rice, R.G., Ind. Eng. Chem. Fundam., $\underline{12}$ (4), 406 (1973).

Rickles, R.N., Ed., "Membranes Technology and Economics", Noyes Develop. Corp., New Jersey, 1967.

Roberts, E.J., U.S. Pat. 2, 799, 638 (1957).

Rosenberg, N.W. and C.E. Tirrel, Ind. Eng. Chem., $\underline{49}$, 780 (1957).

Sabadell, J.E. and N.H. Sweed, Separ. Sci., $\underline{5}$ (3), 171 (1970).

Shaffer, L.H. and M.S. Mintz, "Electrodialysis", in "Principles of desalination", K.E. Spiegler, Ed., Acad. Press, New York, 1966.

Smith, J.D. and J.L. Eisenman, Eds., "Electrodialysis in Advanced Waste Treatment", U.S. Dept. of the Interior, 1967.

Solan, A. and Y. Winograd, Phys. Fluids, 12, 1372 (1969).

Solt, G.S., "Proc. First Intern. Symp. on Water Desalination", Vol 1, p. 13, Washington, D.C., Oct. 3-9, 1965.

Solt, G.S., "Electrodialysis" in: "Industrial Electrochemical Processes", A. Kuhn, Ed., Elsevier Publ. Co., Amsterdam, 1971.

Sonin, A.A. and R.F. Probstein, Desalination, 5, 293 (1968).

Sonin, A.A. and R.F. Probstein, "U.S. Off. Saline Water Res. Dev. Rep. 375 (1968)".

Spiegler, K.S., Ed., "Salt-Water Purification", John Wiley and Sons, New York, 1962.

Spiegler, K.S., Advanc. Chem. Ser., 38, 179 (1963).

Spiegler, K.S., Ed., "Principles of Desalination", Acad. Press, New York, 1966 a.

Spiegler, K.S., Interim Rept. 4, U.S. Off. Saline Water, 13 (1966).

Spiegler, K.S., Desalination, 9, 367 (1971).

Sporn, P., Ed., "Fresh Water from Saline Waters", Pergamon Press, Oxford, 1966.

Sweed, N.H., in: "Progress in Separation and Purification", Vol. 4, pp. 171-240, Wiley-Intersci, New York, 1971.

Sweed, N.H. and R.A. Gregory, A.I.Ch.E.J., 17, 171 (1971).

Sweed, N.H., in: "Recent Developments in Separation Science", Vol. 1, Chemical Rubber Co., Cleveland, 1972.

Thangappan, et al., Ind. Eng. Chem. Prod. Res. Dev., 9 (4), 563 (1970).

Thompson, D.W. and B.D. Bowen, Ind. Eng. Chem., 11, 415 (1972).

Thompson, D.W., D. Bass and M.E. Abu-Goukh, Can. J. Chem. Eng., 52, 479 (1974).

Tuwiner, S.B., Ed., "Diffusion and Membrane Technology", Reinhold, New York, 1962.

Tye, F.L., Trans. Inst. Chem. Eng. (London), 41 (1963).

United Nations, "First Desalination Plant Operation Survey Rept. No. E.69.11. B. 17 (1969); Second Rept. No. E.73.11. A. 10 (1973).

U.S. Bureau of Reclamation and Office of Saline Water, "Desalting Handbook for Planners", 1st. ed. May 1972, 2nd ed. Nov. 1972.

Vetter, K.J., Ed., "Electrochemical Kinetics, Theory and Experimental Aspects", translated by Bruckenstein, S. and Howard, B., Acad. Press. New York, 1967.

Wankat, P.C., Separ. Sci., $\underline{9}$ (2), 85 (1974).

Watanabe, T., et al., Nippon Kaisui Gakkai-Shi, $\underline{26}$, 83 (1972); C.A. $\underline{78}$ (1973), No. 163, 886.

Weiner, S.A., P.M. Rapier and W.K. Baker, Ind. Eng. Chem. Proc. Design Dev., $\underline{3}$ (2), 126 (1964).

Wiechers, S.G., U.S. Pat. 2, 676, 144 (1954).

Wilhelm, R.H., A.W. Rice and A.R. Bendelius, Ind. Eng. Chem. Fundam., $\underline{5}$, 141 (1966 a).

Wilhelm, R.H., in: "Interacellular Transport, Symp. of the International Society for Cell Biology", Vol. 5, p. 199, K.B. Warren, Ed., Acad. Press, New York, 1966 b.

Wilhelm, R.H. and N.H. Sweed, Science, $\underline{159}$, 522 (1968 a).

Wilhelm, R.H., A.W. Rice, R.W. Rolke and N.H. Sweed, Ind. Eng. Chem. Fundam., $\underline{7}$, 337 (1968 b).

Wilson, J.R., Ed., "Demineralization by Electrodialysis", Butterworth, London, 1960.

Zajic, J.E., "Water Pollution Disposal and Reuse", Vol. 2, Marcel Dekker, Inc., New York, 1971.

Appendix A

Electrode System

A.1. Electrode Materials

Various materials for electrodes are in use, for example, graphite and stainless steel, which are gradually attacked in oxidizing conditions and must be replaced. Platinum-coated metals (e.g. titanium, tantalum, or zirconium), with a high level of corrosion resistance and a life of several years, are now frequently used, especially as anodes. Oxides of some metals such as lead and ruthenium have proven to be sufficiently conductive and insoluble in acids to be used as coating for anodes (Thangappan, et al., 1970). Magnetite electrodes have been used for anodes in electrodialysis, but this material is very fragile (Davis and Brockman, 1972).

A.2. Electrode Reactions

Throughout the diluting and concentrating cells of an electrodialysis stack, and in the intervening membranes, electrical conduction is ionic. At the electrodes, however, the mechanism of electrical conduction changes abruptly from ionic to electronic. The technology of electrode reactions is highly developed in many respects, but there is still considerable controversy concerning mechanisms and the relative importance of competing reactions that occur at the electrodes (Davis and Brockman, 1972).

The cathode or negatively changed electrode is the source of electrons, and at the cathode, the electrons must be transferred from the external circuit to ions in the solution. The following are typical reactions by which this transfer of charge may be accomplished:

$$M^{+x} + xe^- \rightarrow M^\circ \qquad \text{metal deposition} \qquad (A.1.)$$

$$O_2 + 2H_2O + 4e^- \rightarrow 4OH^- \qquad \text{reduction of gaseous oxygen} \qquad (A.2.)$$

$$2H^+ + 2e^- \rightarrow H_2 \text{ (acidic solution)} \qquad \text{evolution of gaseous} \qquad (A.3.)$$

$$2H_2O + 2e^- \rightarrow H_2 + 2OH^- \text{ (basic solution)} \quad \text{hydrogen} \qquad (A.4.)$$
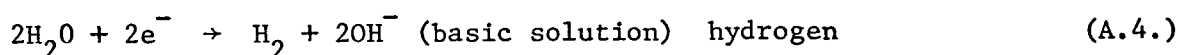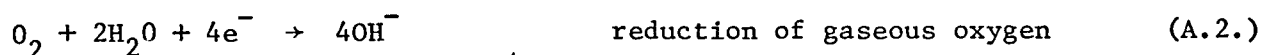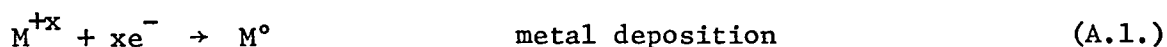
Metal-deposition reactions are useful in processes such as electroplating and the recovery of spent pickle liquor. Reactions in which gaseous oxygen is reduced are important in fuel cells. The principal cations present in typical brine are much less readily discharged than hydrogen ion, and the net result of this is that the cathode reaction is almost invariably the cathodic half of the water electrolysis reaction:

$$2H_2O + 2e^- \rightarrow H_2 + 2OH^- \qquad E_o = 0 \qquad (A.5.)$$
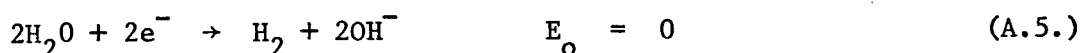
There is usually almost no deterioration of the cathode, and almost any conductor that is compatible with the rest of the system can be used as a cathode. Carbon steel is a commonly used cathode material. Heavy metal ions such as copper and iron may plate out on the cathode, and, in addition, the shift in pH caused by the cathode reaction may cause the precipitation of a variety of substances that may foul the system. The principal problems are apt to be due to $CaCO_3$, $Mg(OH)_2$, and $Fe(OH)_3$.

Depending on the composition of the solution, pH, anode composition, and current density, one or more of the following reactions may occur at the anode:

$$M° \rightarrow M^{+x} + xe^- ; \qquad \text{metal dissolution} \qquad (A.6.)$$

$$M° + xOH^- \rightarrow M(OH)_x + xe^- \qquad \text{oxidation of electrode} \qquad (A.7.)$$

$$2M° + 2xOH^- \rightarrow M_2O_x + xH_2O + 2xe^- \qquad (A.8.)$$

$$H_2 \rightarrow 2H^+ + 2e^- \qquad \text{oxidation of gaseous hydrogen} \qquad (A.9.)$$

$$2H_2O \rightarrow O_2 + 4H^+ + 4e^- \text{ (acidic solutions)} \qquad \text{evolution of} \qquad (A.10.)$$

$$4OH^- \rightarrow O_2 + 2H_2O + 4e^- \text{ (basic solutions)} \qquad \text{gaseous oxygen} \qquad (A.11).$$

$$2Cl^- \rightarrow Cl_2 + 2e^- , \qquad \text{evolution of gaseous chlorine} \qquad (A.12).$$
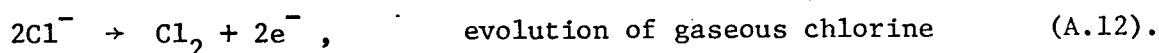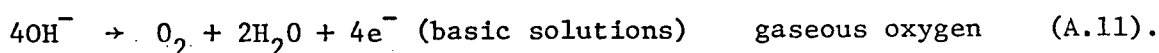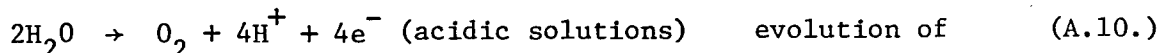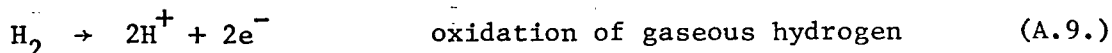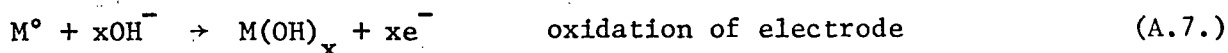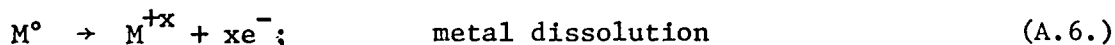
Oxidation of gaseous hydrogen is an important reaction in fuel-cell operation.

Metal dissolution results in destruction of the electrode. When the anode

is oxidized, hydroxyl ions are consumed. Unless provision is made for

removing the companion hydrogen ions or supplying hydroxyl ions, the electrode

solution will become acidic. Most metal oxides and hydroxides are soluble

in acidic solutions.

$$M_2O_x + 2xH^+ \rightarrow 2M^{+x} + xH_2O \qquad (A.13.)$$

or

$$M(OH)_x + xH^+ \rightarrow M^{+x} + xH_2O \qquad (A.14.)$$

The net result is the dissolution of electrode metal.

Reactions in which gaseous oxygen or chlorine is evolved are commonly

encountered in electrodialysis when noble metal anodes are used. In a

typical naturally occurring brine such as seawater chloride ions may be

oxidized at the anode to produce hypochlorite:

$$Cl^- + 2OH^- - 2e^- \rightarrow OCl^- + H_2O \qquad E_o = 0.94 \text{ volt} \qquad (A.15.)$$

Or, in acidic media chlorine gas will be released,

$$Cl^- - e^- \rightarrow \tfrac{1}{2} Cl_2 \text{ (g)} \qquad E_o = 1.35 \text{ volt} \qquad (A.16.)$$

A portion of the chloride oxidized at the anode will be carried out of the cell in the anode rinse stream (anolyte), and a portion may escape as chlorine gas. Chlorine remaining in the solution will eventually form an equilibrium mixture according to

$$Cl_2 + H_2O = HCl + HOCl \tag{A.17.}$$

In many situations, and most particularly in a high-sulfate, low-chloride water, we will find that the anode reaction discharges oxygen from the water with the simultaneous production of hydrogen ions:

$$H_2O - 2e^- \rightarrow \tfrac{1}{2}O_2 + 2H^+ \qquad E_o = 1.23 \text{ volts} \tag{A.18.}$$

Typical brackish water contains significant amounts of both chloride and sulfate, and frequently both chlorine and oxygen are evolved simultaneously. We cannot predict the relative amounts of each with any degree of success because the reactions are principally controlled by electrode kinetics rather than by any considerations of electrode potential. Any or all of the reactions listed above, or further reactions that produce even more highly oxidized products, such as ClO_4^-, may occur, depending on local current densities and the nature of the electrode surface. If noble metal electrodes are not used, the anode reaction will also include the oxidative products of the electrodes. Iron or steel anodes, for example, will produce iron oxides in various degrees, and carbon anodes will produce carbon dioxide.

The electrode reactions necessarily associated with electrodialysis operation introduce two problems: first, added power must be supplied to provide the electrode reaction energy; second, the products of the electrode reactions may be harmful to the electrodialysis stack or may interfere with

the continued operation of the system. The first of these may be minimized

easily by increasing the number of cells per electrode pairs as will be

discussed in process efficiency section; the second is more complicated

and there is no single simple solution.

We can expect that the chlorine or other oxidizing materials formed

at the anode may cause rapid deterioration of the stack components; and

the alkaline cathode material, if allowed to enter the stack, is obviously

likely to produce precipitation. Because of this it is usual to provide

for hydraulic isolation of the two electrode stream compartments at the

ends of the dialysis stacks. Frequently isolation of these streams plus

a high rate of flushing with feed water is all that is attempted by way

of controlling the possible harmful effects of the electrode reaction

products.

The use of sodium bisulfite in the anode rinse stream, to avoid the

formation of chlorine, has been described by Wiechers (1954). The

catholyte basicity can be controlled by the addition of inorganic acids

to the cathode stream. Several more nearly closed systems have also been

tried or proposed. In principle we could circulate sodium sulfate or

sulfuric acid in the anolyte-catholyte system and limit the reactions to

oxygen and hydrogen generation. If this were all that happened, electrolyte

volume could be maintained by adding very small quantities of pure water from

time to time or by reacting the two gases. An even more subtle approach has

been suggested by Roberts (1957), who has patented the circulation of a

redox solution between the two compartments. The oxidation at the anode and

the reduction at the cathode theoretically balance each other in this case.

Unfortunately, none of these "closed" schemes work too well in practice

because it is difficult to confine a given ion to a particular stream. Either the materials in the electrode stream tend to diffuse into the remainder of the cell or vice versa, and in either case problems of oxidation, pH shift, and fouling inevitably arise.

A.3. Electrode Polarization Effect on power Consumption

The energy consumed by the processes occurring at the electrodes depends upon a number of factors, including the electrode materials, the reactions involved, the concentrations of the ions, the applied current density and the solution velocity. A detailed discussion of electrode polarization is given by Vetter (1967) and by Bockris and Reddy (1973).

The passage of current through each of the electrode compartments involve three steps:

(1) The transfer of ions from the bulk of the solution to the surface of the electrode.

(2) The electrochemical reaction at the electrode.

(3) The formation of the final products of the reaction and their removal from the electrode surface.

Three overpotentials are involved:

(i) Concentration overpotential

When the current is flowing, the ions that discharge migrate towards the electrode and cause a concentration gradient across the thin diffusion layer at the electrode surface. This phenomenon is exactly analogous to the concentration gradient that occurs at the ion exchange membranes. The concentration gradient leads to a change in electrode potential of

$$\eta_{con} = \frac{RT}{F} \ln \frac{C_{bulk}}{C_{surface}} \qquad \text{(A.19.)}$$

(ii) Chemical overpotential

The chemical overpotential, η_{chem}, is defined to be that potential in excess of the discharge potential for the given reaction which must be applied to the cell in order to maintain a finite rate of discharge. Chemical overpotential occurs as a result of steps (2) and (3) above. The value of η_{chem} for the electrode reaction is given by Tafel's Formula:

$$\eta_{chem} = a + \frac{RT}{\alpha' F} \ln i \qquad (A.20.)$$

where

$\alpha' \simeq \frac{1}{2}$ and a = constant (depends on nature of cathode).

(iii) Ohmic overpotential

The ohmic overpotential, η_{ohm}, consists of two parts, namely the voltage drop which occurs in the bulk solution of constant concentration plus the voltage drop across the diffusion layer where the concentration gradient varies linearly with the current density

$$\eta_{ohm} = \eta_{sol} + \eta_\delta$$
$$= i R_{ohm} \qquad (A.21.)$$

where R_{ohm} consists of two series resistances,

$$R_{ohm} = R_{sol} + R_\delta \qquad (A.22.)$$

R_{sol} can be evaluated in terms of the mean resistivity of the bulk solution,

$$R_{sol} = \frac{\rho_{mean} y}{Ap} \qquad (A.23.)$$

where

ρ_{mean} = the mean restivity of the electrode solution, $\Omega - cm$

y = bulk solution thickness, cm

Ap = active membrane area, cm^2

R_δ may be evaluated by specifying the resistivity at any point within the diffusion layer as a function $\rho(x,z)$ and by computing the double integral of this function as discussed in Section 3.1.1.

$$\frac{1}{R_\delta} = \frac{1}{\ell} \int_{z=0}^{\ell} \left[\int_{x=0}^{\delta} \rho(x,z)dx \right]^{-1} dz \qquad (A.24.)$$

Thus, the electrode polarization potential, E_e, can be evaluated by summing these separate components.

A.4. Electrode Flow System

The two electrode compartments present in each multimembrane stack are usually supplied with rinse solution from a separate recirculating hydraulic system. In passing through the cell catholyte becomes basic and anolyte becomes acidic, when these are mixed they partially neutralize one another.

Provision should be made in electrode system for discharge of the electrode gases, and a small discharge of electrode solution is required to prevent buildup of ions produced by electrode reactions. A feed-and-bleed system as shown in Figure A.1, is frequently employed.
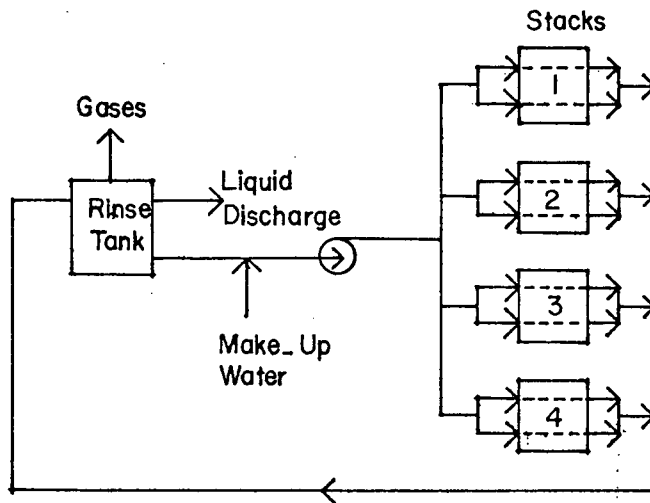
FIGURE A_I

Electrode system flow sheet .

Appendix B

The Current Efficiency

The total current efficiency, η_I, is related to the Faraday efficiency, η_F by the relation

$$\eta_I = \eta_F \cdot \eta_w \qquad (B.1.)$$

where η_w is the water transfer term.

The Faraday efficiency, η_F, is defined as the ratio of the salt shifted to the theoretical current requirement

$$\eta_F = \frac{(\text{equivalent of salt transported})}{(\text{Faradays of electricity passed})(\text{number of membrane pairs employed})}$$

$$= \frac{F \, \Delta N \, Fp}{In} \qquad (B.2.)$$

where

$\quad$ F = Faraday's constant, 96500 A/(sec)(equivalent)

$\quad \Delta N$ = change in product stream normality, equiv/liter

$\quad$ Fp = flow rate of the product stream, liter/sec

$\quad$ I = total current passed through the stack, A

$\quad$ n = number of membrane pairs used

Faraday efficiency, η_F, as defined by Eq.(B.2.) depends on both the actual membrane used and the amount of leakage current that a particular stack design may permit and it expresses the performance of the process w.r.t. the current. It is often determined by an inexact method (apparent values) for brine and dialystate streams independently:

313

$$\eta_D = \frac{F_D (D_1 - D_2)_F}{nI} \tag{B.3.}$$

$$\eta_B = \frac{F_B (B_2 - B_1)_F}{nI} \tag{B.4.}$$

where

η_D, η_B = apparent Faraday efficiencies based on the dialystate and brine streams respectively

F_D, F_B = dialystate and brine efflux rates respectively, ml/sec.

D_1, B_1 = dialystate and brine influent concentrations respectively equiv/ml

D_2, B_2 = dialystate and brine effluent concentrations respectively

The influent and effluent flow rates of a single stream are not identical because of:

(a) water transfer by osmosis and electro-osmosis

(b) a minor volume change resulting from the salt displacement

The true Faraday efficiency, η_F, is defined by:

$$\eta_D = \eta_F (1 - 18 w D_1) \tag{B.5.}$$

$$\eta_B = \eta_F (1 - 18 w B_1) \tag{B.6.}$$

where

w = moles of water transported per equivalent of salt transfer;

$w = w^a + w^c$, where w^a, w^c are water transport numbers ($\simeq$ hydration number of ions) e.g. for NaCl, $w^a = 4$, $w^c = 8$.

Determination of η_D and η_B enable both η_F and w to be calculated (Wilson, 1960).

The factors that may contribute towards low current efficiency in an electrodialysis stack are mechanical and electrochemical ones:

(1)   Imperfect selectivity of membranes or deterioration of membranes. The fact that the membranes are not perfectly selective means that more than the theoretical current must be passed.

(2)   Electrical leakage by stray current and parallel current paths through the stack manifold.

(3)   Short-circuiting of membrane packs.

(4)   Internal and external water leakage. A large water transfer may accompany the current flow across the membrane due to osmosis and electro-osmosis, which results in loss of product water. Also there may be hydraulic leakages between cells and/or external leakages.

(5)   Back diffusion of electrolytes.

(6)   Severe polarization effects or unwanted ion transfer. At sufficiently high current densities or low salt concentrations, the H^+ and OH^- ions normally present in water will begin to participate in the current-carrying process.

Assuming that obvious problems, such as external parallel current paths through bolts and containers, gross leaks between the product and waste compartments, and water splitting, have been properly taken care of, we can express an over all current efficiency, η_I, as the product of these efficiencies:

$$\eta_I = \eta_s \eta_m \eta_w = \eta_F \eta_w \tag{B.7.}$$

where

η_s: takes care of effects due to the permselectivity of the individual membranes

η_m: accounts for the effects of current leakage through the manifold

η_w: is the result of water transport through the membranes.

The quantities η_s, η_m and η_w are all defined in such a way that ideally they approach 1.0.

(i) Permselectivity efficiency, η_s

The permselectivity efficiency, η_s, is defined as

$$\eta_s = \frac{n_c t_- Pc + n_a t_+ Pa}{n_c t_- + n_a t_+} \tag{B.8.}$$

where

n_c, n_a are numbers of cation and anion-permeable membranes

t_+, t_- are transport numbers in solution of cation and anion respectively

Pc, Pa are permselectivity of cation and anion-permeable membranes respectively

$$Pc = \frac{\bar{t}_+ - t_+}{1 - t_+} = \frac{\bar{t}_+ - t_+}{t_-}$$

$$Pa = \frac{\bar{t}_- - t_-}{1 - t_-} = \frac{\bar{t}_- - t_-}{t_+} \tag{B.9.}$$

where $\bar{t}_+$, $\bar{t}_-$ refer to transport numbers of counter-ions in membranes. When $n_c = n_a$, Eq. (B.8.) reduces to:

$$\eta_s = t_- Pc + t_+ Pa$$

$$= (\bar{t}_+ + \bar{t}_-) - 1 = 1 - (t_-^c + t_+^a) \tag{B.10.}$$

where

t_-^c = anion transport number in the cation-permeable membrane

t_+^a = cation transport number in the anion-permeable membrane

$- (t_-^c + t_+^a)$ is imperfect selectivity factor or penetration of co-ions into a membrane.

If $t_- = t_+ = 0.5$, then η_s will be equal to the average permselectivity

$$\eta_s = (\frac{Pa + Pc}{2})$$

(B.11.)

(ii) Electrical Leakage and Short-circuiting term, η_m

The partial short-circuiting of a membrane stack by conduction through manifolds and stray parallel current paths consume power without producing any useful results, thus reduce the effective current efficiency.

Because of the inherent engineering design of electrodialysis units, each concentration stream within the stack is connected, via conduits, to all other concentration streams. The same applies for the dilution streams. Since the concentration stream is more conductive to electricity than the dilute stream, it would be expected that a high fraction of non-productive-leakage current would flow through the concentration stream.

Leakage current calculations have been developed by Wilson (1960) and Mandersloot and Hicks (1966) and presented by Belfort and Guter (1968).

Usually the effect of current leakage through the manifold is a reduction in efficiency of less than 5%. Belfort and Guter (1968) in their study of Webster and Buckeye electrodialysis plants showed that current leakage has only minor effect. The leakage current for a given design can be estimated by assembling a sample stack with insulating sheets of plastic in place of the membranes, thereby interrupting the electrical field, but not the liquid flow. The normal operating voltage is then applied and the current measured is regarded as being that due to leakage through the entire

internal and external liquid flow path of the stack.

(iii) Water transfer term, n_w

Some water is transported through the membranes along with the electrolytes due to electro-osmosis. The amount of electro-osmotic water transport varies with membrane type, ionic species, and concentration of solution. When the feed is of low salinity or when moderate quantities of salt are removed from brackish water, transport is seldom a problem. However, in more concentrated solutions or in systems involving a high degree of desalination, water transfer can have important effects on the current utilization in the process.

A large transfer of water will:

(a) require the use of additional current to meet the desalted-product quality specifications.

(b) reduce the quality of product obtainable from a given amount of feed to the dilute stream.

The effect of water transport on the current efficiency is given by:

$$n_w = 1 - \frac{n\tau_w \, (0.018) \, m_i}{n_s} \qquad\qquad \text{(B.12.)}$$

where

m_i = the molality of the feed water

τ_w = transference number of water defined as the number of moles water transferred per Faraday

n = number of membrane pairs.

Appendix C

Nernst Idealized Model of Wall Layers

C.1. The Flow Field in an Electrodialysis Cell

In almost all electromembrane processes the solutions to be treated flow between parallel planar ion-exchange membranes. The flow channels are filled with spacer materials that cause complex flow patterns. The velocity of the solutions past the membranes and through the spacer materials results in relatively good mixing of the solution in the center portions of the flow channels, but the mixing is less near the surfaces of the membranes, where the solution is almost static.

C.2. Nernst Model

The complex hydraulic pattern in an electrodialysis cell is approximated by the simplified Nernst model. This is an idealized model (Nernst, 1904) based on the following assumptions:

- there are layers adjacent to the membranes in which the solutions are completely static or in laminar flow.

- the solution in the bulk (i.e. between the wall layers) is thoroughly mixed so that the concentration of electrolyte at any point in this zone is the same as that at any other point.

- there is no change of either the thickness of the wall layers or the concentration gradients along the flow channel.

Despite the complexity in a real system, Nernst model affords a simplified mathematical approach which results in expressions that are easy to use and that predict performance adequately for use in the design of electromembrane processes.

C.3. Some derivations of the Model

Since frequent use is made of the assumption that the concentration gradient in the wall layer of an electrodialysis cell is linear, a justification of this assumption with the other main assumptions involved is in order.

C.3.1. General theory of coupled processes

When an ion moves in an electrolyte solution it does not do so in the complete absence of other effects. Its motion is accompanied by a flow of electric current, and there may also be a flow of heat and a flow of solvent. We are faced with the problem of describing simultaneously a minimum of four fluxes: salt, electricity, solvent and heat.

In analyzing systems in which several forces and fluxes are coupled, it is sometimes convenient to make use of the theory of the thermodynamics of irreversible processes. Although an analysis made in these terms cannot deal with the underlying causes of the phenomena that may be observed, it is of great value in clearly defining certain relationships that must necessarily hold between the various forces and flows when the system is in the steady state.

The general equations for flow may be written (Hills et al., 1961) as:

$$\vec{J}_1 = - L_{11}\nabla_T U_1 - L_{12}\nabla_T U_2 - L_{13}\nabla_T U_3 - L_{14}\nabla \ln T$$

$$\vec{J}_2 = - L_{12}\nabla_T U_1 - L_{22}\nabla_T U_2 - L_{23}\nabla_T U_3 - L_{24}\nabla \ln T$$

$$\vec{J}_3 = - L_{13}\nabla_T U_1 - L_{23}\nabla_T U_2 - L_{33}\nabla_T U_3 - L_{34}\nabla \ln T$$

$$\vec{Q} = - L_{14}\nabla_T U_1 - L_{24}\nabla_T U_2 - L_{34}\nabla_T U_3 - L_{44}\nabla \ln T \qquad (C.1.)$$

where L_{ij} are phenomenological coefficients and the subscripts 1,2,3,and 4 refer to the positive ions, negative ions, water and heat respectively. $\nabla_T U$ is the gradient of total chemical potential, taken at constant temperature, and $\vec{Q}$ is the flow of heat.

If we consider an isothermal process in which both non-electrostatic interaction between the ions together with electro-osmosis are neglected, then all the terms except the first will drop out and the ionic flux, J_k is given by

$$J_k = - L_{kk}\nabla_T U_k = - u_k C_k \nabla_T U_k \qquad (C.2.)$$

where J_k is the flux of an ionic species in g-mole/(cm^2)(sec), u_k is the ionic mobility which is defined as the average velocity imparted to the species under the action of a unit generalized force (per mole), and C_k is the concentration in g-moles/cu.cm.

The total chemical potential, U, is meant to include effects due to electricity, as well as temperature, pressure, concentration and gravitational field, if any. Assume that gravitational fields are unimportant, then

$$\nabla_T U = Z F \nabla E + \frac{\partial U}{\partial \rho}\nabla \rho + \frac{\partial U}{\partial C}\nabla C \qquad (C.3.)$$

where ∇E is the electric field in volts/cm

        F is the Faraday constant in coulombs/g.equiv.

        Z is the valence

In real electrodialysis systems the modest differences in temperature and pressure have no significant effect on the current flowing as long as even very small potential differences exist. Therefore $\frac{\partial U}{\partial \rho} \nabla \rho$ term is negligible. For ideal solution,

$$U = U_o + RT \ln a \qquad (C.4.)$$

where U_o is the standard chemical potential and a is the activity. For dilute solutions concentration can be used instead of activity ($a = \gamma C \simeq C$). From Eq.(C.4.) we get

$$\frac{\partial U}{\partial C} \simeq \frac{RT}{C} \nabla C \qquad (C.5.)$$

A term including the derivative of the activity coefficient could be included (see for example, Hills, et al., 1961), but this does not affect the general principle; and, in practice, omission of the term that would arise from differentiation of the activity coefficient is no worse than some of the other assumptions that are needed to facilitate the integration of these equations when they are used to describe real systems.

Substitute Eq.(C.5.) into Eq.(C.3.) and drop the pressure term

$$J_k = - u_k C_k (Z_k F \nabla E + \frac{RT}{C_k} \nabla C_k) \qquad (C.6.)$$

The ionic mobility, u_k (g-moles)(sq.cm)/(joule)(sec), can be related to the ionic-diffusion coefficient, D_k (sq.cm/sec) through the Nernst-Einstein relation:

$$u_k = D_k/RT \qquad (C.7.)$$

where T is the absolute temperature, $^{\circ}$K., and R is the gas constant, 8.3143 joules/($^{\circ}$K)(mole). Eq.(C.7.) is true only when the activity coefficient

is unity, that is, at infinite dilution (Chapman, 1969).

From Eqs.(C.6.) and (C.7.)

$$J_k = - Z_k u_k \, F \, C_k \, \nabla E - D_k \nabla C_k \qquad \text{(C.8.)}$$

Eq.(C.8.) is the well-known Nernst-Planck equation of ionic flux with negligible convection (i.e. $C_k \vec{v} = 0$, where $\vec{v}$ is the stream velocity). Although the Nernst-Planck equation has a number of shortcomings which limit its rigorous applications to dilute solutions, we will use it because it accomplishes a great simplification of a complex problem. To do this however, we must assume the validity of the Nernst-Einstein relation and neglect any gradients in the solvent concentration as well as interactions between the fluxes of the charged species. For a more thorough analysis of ionic transport e.g. concentrated multicomponent solutions, it is necessary to use a more complete flux expression (Chapman, 1969).

C.3.2. Ionic Fluxes

For a uni-directional flow of a 1-1 electrolyte Eqs.(C.7.) and (C.8.) can be written as

$$J_+ = - D_+ \left[\left(\frac{F}{RT} \right) C \left(\frac{dE}{dx} \right) + \left(\frac{dc}{dx} \right) \right]$$

$$J_- = - D_- \left[\left(\frac{-F}{RT} \right) C \left(\frac{dE}{dx} \right) + \left(\frac{dc}{dx} \right) \right] \qquad \text{(C.9.)}$$

Because of electroneutrality in the solution phase

$$C_+ = C_- = C \qquad \text{(C.10.)}$$

and for mono-monovalent electrolyte

$$Z_+ = - Z_- = 1.0 \qquad \text{(C.11.)}$$

In the membrane, the numerical value of the flux ratio, $\dfrac{\overline{J_+}}{\overline{J_-}}$, is

equal to the transport number ratio $\dfrac{\overline{t_+}}{\overline{t_-}}$. Since by definition of the steady

state the fluxes are independent of position x (perpendicular to membrane

face), the same flux ratio prevails also in the solution:

$$\frac{J_+}{J_-} = \frac{\overline{J_+}}{\overline{J_-}} = - \frac{\overline{t_+}}{\overline{t_-}} = - \frac{\overline{t_+}}{(1 - \overline{t_+})} \qquad \text{(C.12.)}$$

The negative sign is introduced because the J's are vectors. In the

membrane $\overline{J_+}$ and $\overline{J_-}$ have opposite signs, while $\overline{t_+}$ and $\overline{t_-}$ are always taken as

positive. It should be noted that the ion flux ratio is equal to the ratio

of the ion transport numbers in the membrane only when ion transport in

membranes takes place entirely by electromigration. Unless the membrane is

ideally permselective, there exist additional ion fluxes due to diffusion

across the membrane caused by the salt concentration difference in the

solutions at the two membrane faces. This back diffusion of the salt will

be neglected here, however, because almost ideally permselective membranes

are used in most electrodialysis installations, and since in practice the

electrical driving forces are in general much larger than the diffusion

driving forces, even when membranes are used which are not fully perm-

selective.

From Eqs.(C.9.) and (C.12.):

$$J_- = - \frac{\overline{t_-} \, J_+}{\overline{t_+} \, D_-} = \frac{FC}{RT} \frac{dE}{dx} - \frac{dc}{dx}$$

OR

$$\frac{FC}{RT} \frac{dE}{dx} = \frac{dc}{dx} - \frac{\overline{t_-} \, J_+}{\overline{t_+} \, D_-} \qquad \text{(C.13.)}$$

substitute Eq.(C.13.) into (C.9.)

$$J_+ = - D_+ \left[\frac{dc}{dx} - \frac{\bar{t}_- J_+}{\bar{t}_+ D_-} + \frac{dc}{dx} \right]$$

$$= - 2D_+ \frac{dc}{dx} + \frac{\bar{t}_- J_+ D_+}{\bar{t}_+ D_-}$$

$$J_+ = \frac{- 2D_+}{1 - (D_+ \bar{t}_-/D_- \bar{t}_+)} \frac{dc}{dx} \qquad (C.14.)$$

and

$$J_- = \frac{- 2D_-}{1 - (D_- \bar{t}_+/D_+ \bar{t}_-)} \frac{dc}{dx} \qquad (C.15.)$$

Since fluxes, ionic diffusion coefficients and membrane transport numbers are constant, it follows that $\frac{dc}{dx}$ is constant also. In other words, the application of the Nernst-Planck equation with the above assumptions leads to a linear concentration gradient in the boundary layer.

It is often more convenient to express the fluxes in terms of the diffusion coefficient of the electrolyte, D, rather than the ionic diffusion coefficients, D_+ and D_-. Noting that in free solution

$$\frac{D_+}{D_-} = \frac{t_+}{t_-} = \frac{t_+}{(1 - t_+)} \qquad (C.16.)$$

and using the Nernst expression for the diffusion coefficient of 1-1 electrolyte in dilute solution

$$\frac{1}{D} = \frac{1}{2} \left(\frac{1}{D_+} + \frac{1}{D_-} \right)$$

OR

$$D = \frac{2D_+ D_-}{D_+ + D_-} = 2D_+ \left(\frac{D_-}{D_+ + D_-} \right) \qquad (C.17.)$$

From Eq.(C.16.)

$$\frac{D_-}{D_+ + D_-} = \frac{t_-}{t_- + t_+} = t_- = (1 - t_+) \tag{C.18.}$$

Substitute Eq.(C.18.) into Eq.(C.17.)

$$D = 2D_+ (1 - t_+) = 2D_- (1 - t_-) \tag{C.19.}$$

From Eqs.(C.14.) and (C.16.)

$$J_+ = - \frac{2D_+}{1 - (t_+ \bar{t}_-/t_- \bar{t}_+)} \frac{dc}{dx} = \frac{- 2D_+ (1-t_+) \bar{t}_+}{(t_- \bar{t}_+ - t_+ \bar{t}_-)} \frac{dc}{dx} \tag{C.20.}$$

But

$$t_- \bar{t}_+ - t_+ \bar{t}_- = (1 - t_+) \bar{t}_+ - t_+ (1 - \bar{t}_+) = \bar{t}_+ - t_+ \tag{C.21.}$$

Substitute Eqs.(C.19.) and (C.21.) into Eq.(C.20.)

$$J_+ = - \frac{D\bar{t}_+}{(\bar{t}_+ - t_+)} \frac{dc}{dx} \tag{C.22.}$$

Similarly

$$J_- = - \frac{D\bar{t}_-}{(\bar{t}_- - t_-)} \frac{dc}{dx} = \frac{Dt_-}{(\bar{t}_+ - t_+)} \frac{dc}{dx} \tag{C.23.}$$

For ideally selective cation exchange membranes, $\bar{t}_+ = 1.0$. Hence from Eqs. (C.22.) and (C.23.):

$$J_+ = - D \left[\frac{1}{t_-} \frac{dc}{dx} \right]; \quad J_- = 0 \tag{C.24.}$$

and for ideally selective anion exchange membrane $\bar{t}_- = 1.0$

$$J_+ = 0; \quad J_- = - D \left[\frac{1}{t_+} \frac{dc}{dx} \right] \tag{C.25.}$$

Note that both Eqs.(C.24.) and (C.25.) are of the type of Fick's law, but the

ratio $\frac{D}{t\pm}$ replaces the ionic coefficient D± (i.e. the flux is higher because the electric field provides additional driving force).

The current density, i, is given by Faraday's law

$$i = F (J_+ - J_-) \tag{C.26.}$$

Substitute for J_+ and J_- from Eqs.(C.22.) and (C.23.)

$$i = -\frac{FD}{(\bar{t}_+ - t_+)} \frac{dc}{dx} = \frac{FD}{(\bar{t}_- - t_-)} \frac{dc}{dx} \tag{C.27.}$$

If i, D and the transport numbers are constant, Eq.(C.27.) then, within the range of applicability of the Nernst-Planck equations, the concentration gradient in the wall layer is linear.

C.4. Wall layer thickness

The wall layer thickness, δ, depends on distance from solution inlet and it varys along the flow path. In the Nernst model it is assumed that a steady state has been reached. It is also assumed that the hydraulic flow conditions of the solutions are chosen such that variation along the membrane can be neglected. In this case, the solution concentration profile in the wall layer is time-invariant and also does not vary along the membrane.

According to the Nernst model an approximate average value (or a critical value) of δ is used and the problem can be solved without integration over the whole flow path. Studies which stress the hydrodynamic aspects of the problem and the influence of non-uniform diffusion layers have been published (Sonin and Probstein, 1968; Solan and Winograd, 1969). It is of interest that the hydrodynamic analysis leads to justification of Nernst's polarization layer concept [replacement of the actual mass-transfer boundary layer (diffusion layer) by a diffusion layer of uniform thickness] as a fairly good approximation for certain flow situations (Spiegler, 1971).

C.5. Conclusion

It can be concluded that the Nernst idealized model is in effect equivalent to the application of the Nernst-Planck equations and the use of an average thickness of the diffusion layer.

Appendix D

Graphical Solution of Constant-Rate Model

Graphical solution for synchronous (in-phase) operation [case (i) - chapter (3)] will be considered here. Graphical solutions for the other cases can be developed in a similar manner.

The system consists of a separator (ED stack) and two end reservoirs as shown in Figure D-1(a). Initially the separator and the bottom reservoir are full of solution of concentration C_o, top reservoir is empty. The abscissa in Figure D-1(b), which represents the vertical coordinate in Figure D-1(a), is divided into three sections:

Section I   : $-\ell \leqslant z \leqslant o$,   the bottom reservoir

Section II : $o \leqslant z \leqslant \ell$,   the separator

Section III: $\ell \leqslant z \leqslant 2\ell$,   the top reservoir

Operation starts with up-stroke (demineralization half cycle). During this period solute is transferred from the mobile phase into the storage compartments of the separator. By the end of the first half cycle the concentration profiles of solution in the separator and the top reservoir are indicated by the lines abc, cde respectively in Figure D-2. The amount of solute stored in the separator during this half cycle is given by the rectangle afgh (Figure D-2) which has the same area as the two triangles acf and cef (i.e. cf = fg). The stored material is returned to the mobile phase during the second half cycle and it distributes itself between

329
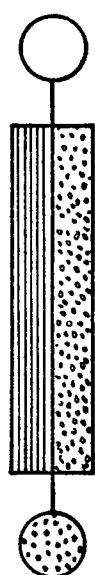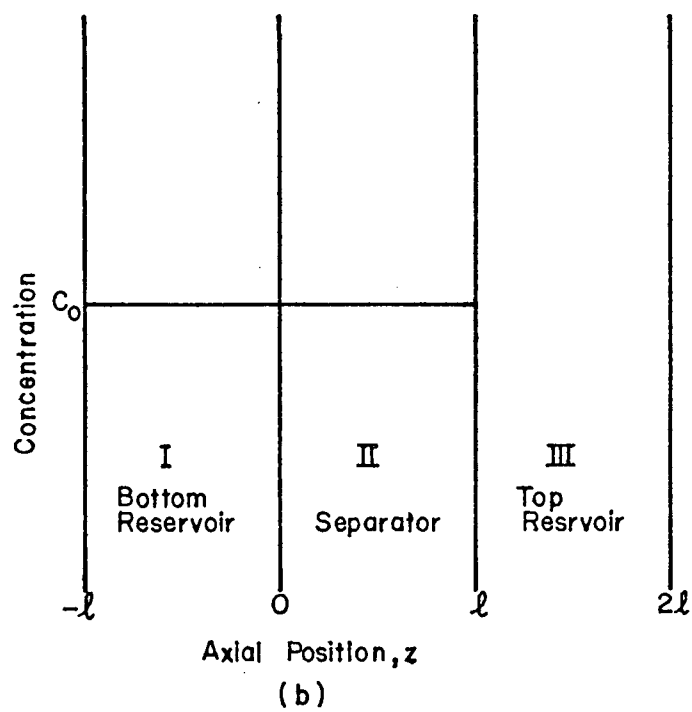
(a) (b)

Figure D_1

(a) Separator (ED Stack) and two end reservoirs.
(b) Initial concentration profile.
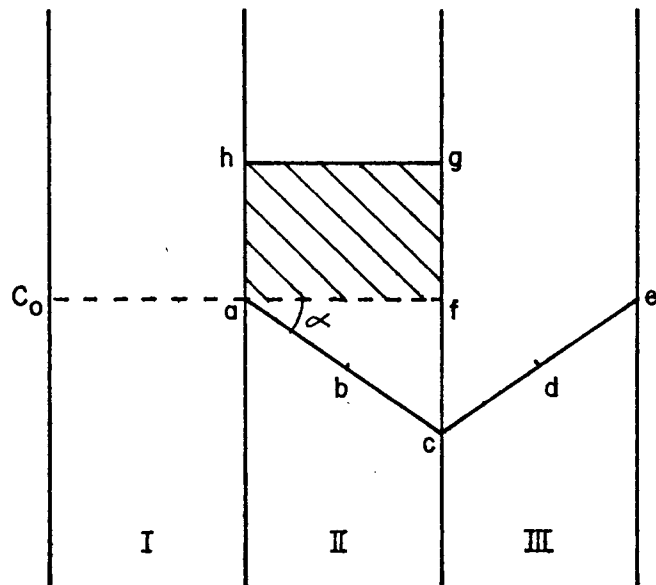
FIGURE D_2

Concentration profile abcde and amount of
material stored afgh at the end of the first half cycle.

regions II and III in different proportions depending on the ratio of the mass transfer rates in the two half-cycles, $\dfrac{K_1}{K_2}$ where

$$\frac{dC_f}{dt} = - K_1 \quad ; \quad \text{for demineralization} \tag{D.1.}$$

$$\frac{dC_f}{dt} = K_2 \quad ; \quad \text{for enrichment} \tag{D.2.}$$

If $K_2 \neq K_1$ and demineralization is assumed to take place for time $\dfrac{T}{2}$, then to maintain the material balance of the solute, the enrichment period should be Δt, where

$$\Delta t = \frac{TK_1}{2K_2} \tag{D.3.}$$

Graphical solutions of three different cases of the ratio $\dfrac{K_1}{K_2}$ will be considered.

(a) $\dfrac{K_1}{K_2} = 1.0$

In this case $\angle\alpha = \angle\beta$ as shown in Figure D-3(a) where $\alpha = \tan^{-1} K_1$ and $\beta = \tan^{-1} K_2$; and the stored material is distributed equally between regions II and III during the second half cycle. Each point along the lines abc, cde will gain a concentration shift given by the length of the corresponding arrow vertically above it (concentrations at points a and e remain constant while that at point c shows the maximum jump). Figure D-3(b) shows that by the end of the first cycle all points along the concentration profiles return to their initial values and no separation is obtained in this case.
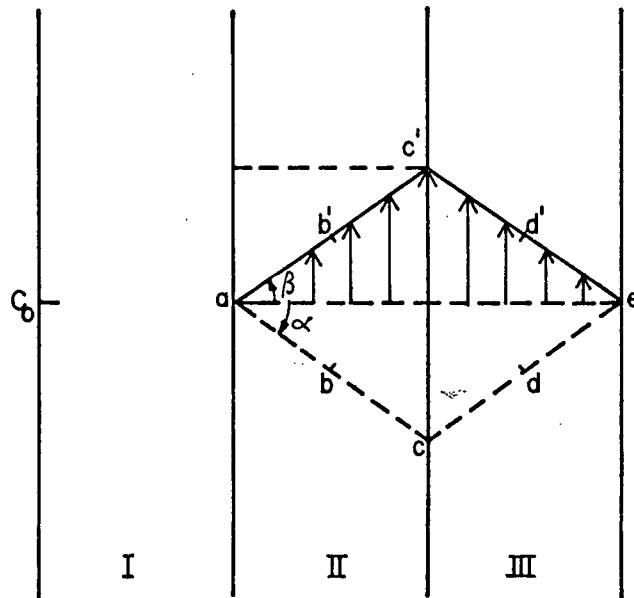
FIGURE D_3(a)

Mass transfer during the second half cycle
(enrichment half cycle)
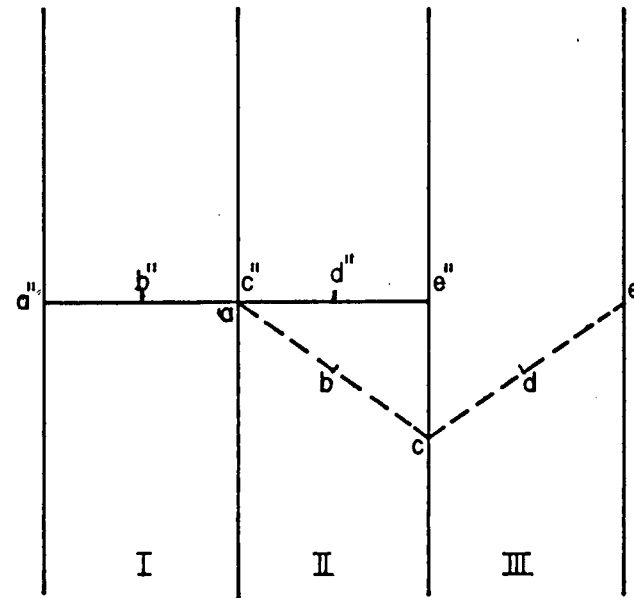
$K_2 = K_1$

FIGURE D_3(b)

Concentration profile at the beginning (dotted line)
and at the end (solid line) of the second half cycle.

$K_2 = K_1$

(b) $K_2 \gg K_1$

In this case $\dfrac{K_1}{K_2} \to 0$. From Equation (D.3.) $\Delta t \to 0$, which means that all the stored material is transferred instantaneously to region II (i.e. $\angle B \to 90°$). Figure D-4(a) shows the mass transfer during this half cycle, where the vertical arrows indicate the concentration shifts at various points along abC_{II}, while Figure D-4(b) shows the concentration profiles at the beginning and at the end of the second (enrichment) half cycle. Due to the instantaneous mass transfer there is a concentration discontinuity at the boundary of the two regions (points C_{II} and C_{III}).

Every cycle the depleted product suffers a loss of material represented by the triangle C_{III} e C'_{III} (Figure D-4(a)) while the enriched product gains a net increase of similar amount. The average top and bottom concentrations after the nth cycle are given by:

$$\frac{C_{T,n}}{C_o} = 1 - \frac{K_1 Tn}{2C_o} \tag{D.4.}$$

and

$$\frac{C_{B,n}}{C_o} = 1 + \frac{K_1 Tn}{2C_o} \tag{D.5.}$$

(c) $K_2 > K_1$

K_2 is assumed to be larger than K_1, but both are of the same order of magnitude e.g. $K_2 = 2K_1$. In this case Equation (D.3.) gives that

$$\Delta t = \frac{T}{4} \tag{D.6.}$$

The mass transfer during the second half cycle is shown in Figure D-5(a) where $\angle B = 2 \angle \alpha$.
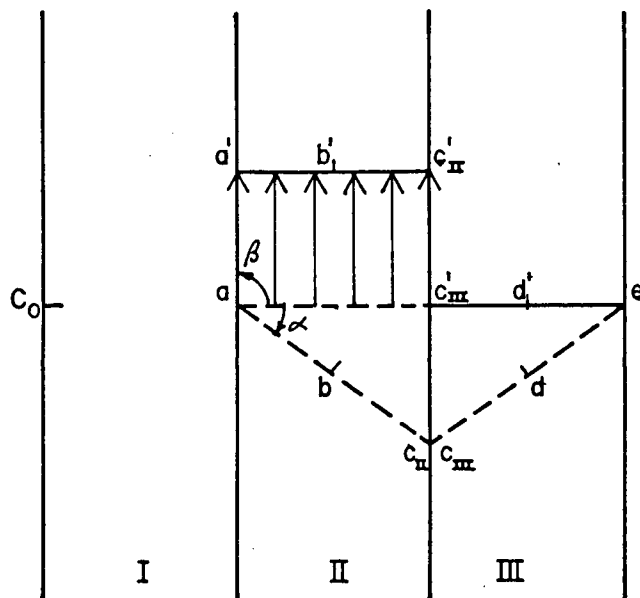
FIGURE D_4(a)

Mass transfer during the second half cycle
(enrichment half cycle).
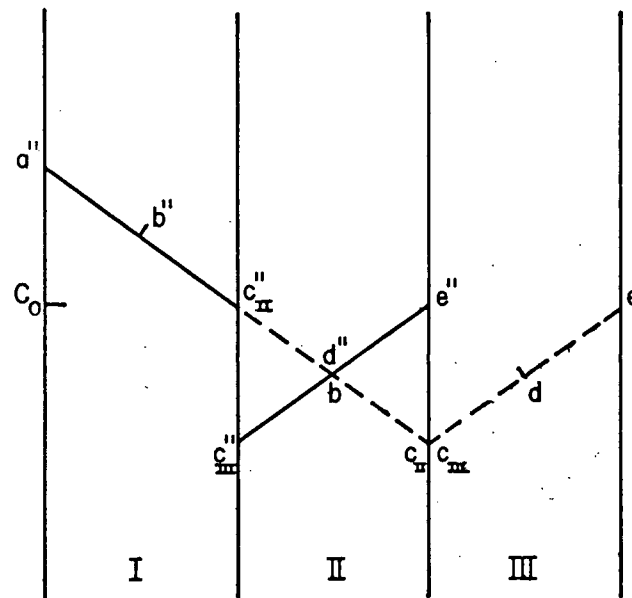
$K_2 \gg K_1$

FIGURE D_4(b)

Concentration profile at the beginning (dotted line)
and at the end (solid line) of the second half cycle.

$K_2 \gg K_1$
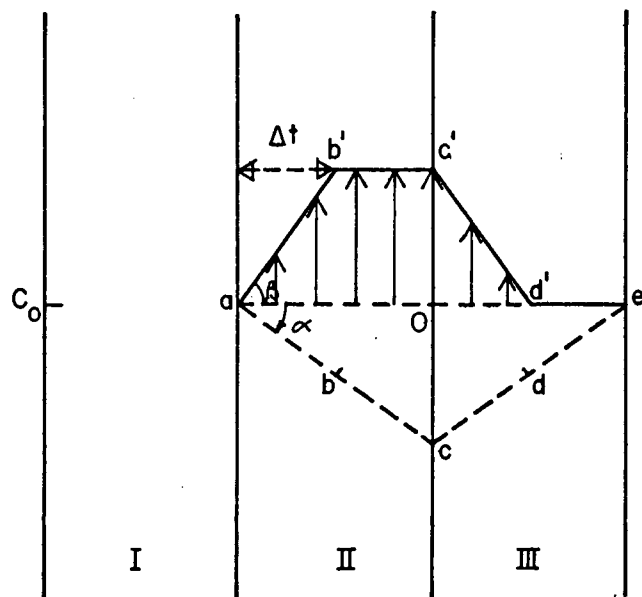
FIGURE D_5(a)

Mass transfe during the second half cycle
(enrichment half cycle).
$K_2 = 2K_1$
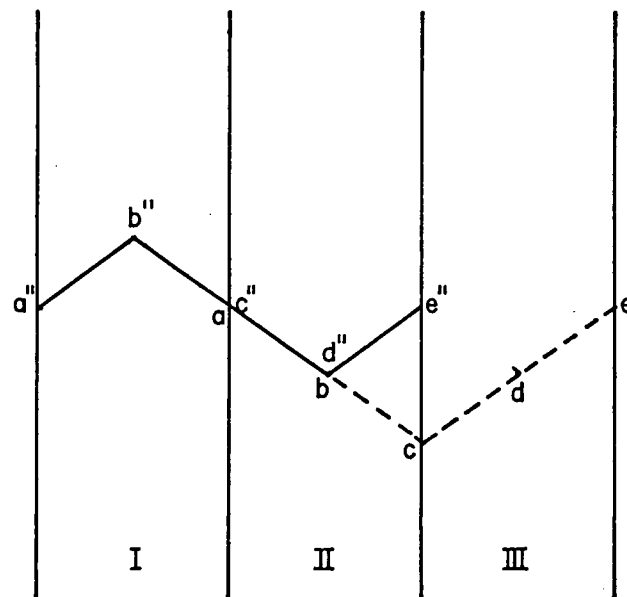
FIGURE D_5(b)

Concentration profile at the beginning (dotted line)
and at the end (solid line) of the second half cycle.
$K_2 = 2K_1$

After the first half cycle the material lost by the top (demineralized) product is given by Δ ceo (Figure D-5(a)) where

$$\Delta \text{ ceo } = \frac{1}{2} \left(\frac{T}{2} \right) \left(\frac{TK_1}{2} \right)$$ (D.7.)

and the average concentration of the top product is given by

$$C_{T,1} = C_o - \frac{TK_1}{4}$$ (D.8.)

Then every cycle the top product will lose a material given by

$$\Delta \text{ ceo } - \Delta c'od' = \frac{1}{2} \left(\frac{K_1 T}{2} \right) \left(\frac{T}{2} \right) - \frac{1}{2} \left(\frac{K_1 T}{2} \right) (\Delta t)$$

$$= \frac{T}{2} \left(\frac{K_1 T}{4} - \frac{\Delta t \, K_1}{2} \right)$$ (D.9.)

and the average concentration change will be given by

$$\frac{\text{material loss}}{(T/2)} = \frac{K_1 T}{4} - \frac{K_1^2 T}{K_2 4}$$ (D.10.)

The average top concentration after the nth cycle is given by

$$\frac{C_{T,n}}{C_o} = 1 - \frac{TK_1}{4C_o} - \frac{TK_1}{4C_o} \left(1 - \frac{K_1}{K_2} \right) (n - 1)$$ (D.11.)

Similarly every cycle the bottom product gains the material given by

trapezium ab'c'o - triangle aoc

$$= \frac{1}{2} \left(\frac{K_1 T}{2} \right) \left(\frac{T}{2} + \frac{T}{2} - \Delta t \right) - \frac{1}{2} \left(\frac{KT_1}{2} \right) \left(\frac{T}{2} \right)$$

$$= \frac{T}{2} \left(\frac{K_1 T}{4} \right) \left(1 - \frac{K_1}{K_2} \right)$$ (D.12.)

The average bottom concentration after the nth cycle is given by

$$\frac{C_{B,n}}{C_o} = 1 + \frac{TK_1}{4C_o} \left(1 - \frac{K_1}{K_2} \right) n$$ (D.13.)

APPENDIX E

COMPUTER PROGRAMS

i

Appendix E

Symbols used in Computer Program

i) DATA

CB = Brine Concentration (ppm)

CD = Dialysate Concentration (ppm)

VB = Volume of Brine product (c.c./cycle)

VD = Volume of dialysate product (c.c./cycle)

CF = Initial (Feed) Concentration (ppm)

Numbers 1, 2, ... 9 stand for Exp. letters A, B, ... I.

ii) RESULTS (A)

This first part of the program computes:

a) Separation factor NS = CB/CD

b) Material balance and % error

$$ERR \% = (\frac{PP - FF}{FF}) 100$$

where PP = BB + DD .... (Salt in product streams)

BB = CB * VB .... (Salt in brine)

DD = CD * VD .... (Salt in dialysate)

FF = CF * (VB + VD) .... (Salt in feed)

iii) RESULTS (B)

This second part of the program computes the amount of salt shifted during separation, AS where

AS = (CB - CF) * VB + (CF - CD) * VD

339

```
        $COMPILE
1            DIMENSION X(12,5) ,BB(12),DD(12),PP(12),VF(12),FF(12),          2
            1ERR(12),CBF(12),CDF(12),BF(12),DF(12),AS(12)                    3
2            REAL MB(12),NS(12)                                              4
3            N=9                                                             5
4            READ(5,15)((X(I,J),J=1,5),I=1,N)                                6
5       15   FORMAT(5F10.2)                                                  7
6            WRITE(6,6)                                                      8
7        6   FORMAT(1X,'DATA'//1X;12X,'CB',9X,'VB',8X,'CD',                  9
            18X,'VD',8X,'CF')                                                10
8            DO 60 I=1,N                                                     11
9       60   WRITE(6,26)I,X(I,1),X(I,2),X(I,3),X(I,4),X(I,5)                 12
10      26   FORMAT(1X,I7,5F10.2)                                            13
11           WRITE(6,36)                                                     14
12      36   FORMAT(//1X,'RESULTS(A)'/1X,'MATERIAL BALANCE & SEPARATION FACTOR' 15
            1//1X,14X,'BB',11X,'DD',11X,                                     16
            1'PP',11X,'FF',10X,'MB',8X,'ERR%',7X,'NS')                       17
13           DO 80 I=1,N                                                     18
14           BB(I)=X(I,1)*X(I,2)                                             19
15           DD(I)=X(I,3)*X(I,4)                                             20
16           PP(I)=BB(I)+DD(I)                                               21
17           VF(I)=X(I,2)+X(I,4)                                             22
18           FF(I)=VF(I)*X(I,5)                                              23
19           MB(I)=PP(I)-FF(I)                                               24
20           ERR(I)=MB(I)*100.0/FF(I)                                        25
21           NS(I)=X(I,1)/X(I,3)                                             26
22           CBF(I)=X(I,1)-X(I,5)                                            27
23           CDF(I)=X(I,5)-X(I,3)                                            28
24           BF(I)=CBF(I)*X(I,2)                                             29
25           DF(I)=CDF(I)*X(I,4)                                             30
26           AS(I)=BF(I)+DF(I)                                               31
27      80   WRITE(6,46)I,BB(I),DD(I),PP(I),FF(I),MB(I),ERR(I),NS(I)         32
28      45   FORMAT(1X,I7,4F13.2,F11.2,2F10.3)                               33
29           WRITE(6,66)                                                     34
30           WRITE(6,86)                                                     35
31           DO 90 I=1,N                                                     36
32      90   WRITE(6,76)I,CBF(I),BF(I),CDF(I),DF(I),AS(I)                    37
33      66   FORMAT(//1X,'RESULTS(B)'/1X,'AMOUNT OF SEPARATION')             38
34      86   FORMAT(//1X,13X,'CB-CF',7X,'BF',10X,'CF-CD',8X,'DF',12X,'AS')   39
35      76   FORMAT(1X,I7,4F12.2,F14.2)                                      40
36           STOP                                                           41
37           END                                                            42
        $DATA
    DATA
```

	CB	VB	CD	VD	CF
1	4000.00	25.37	196.00	24.17	2160.00
2	4075.00	25.52	148.00	24.48	2160.00
3	3875.00	25.87	330.00	24.13	2160.00
4	4125.00	24.67	140.00	24.50	2170.00
5	4250.00	25.00	118.00	25.00	2170.00
6	4350.00	24.57	94.00	25.74	2170.00
7	3825.00	25.79	410.00	24.21	2170.00
8	3675.00	25.88	570.00	24.13	2170.00
9	3375.00	25.45	840.00	24.66	2170.00

RESULTS(A)
MATERIAL BALANCE & SEPARATION FACTOR

	BB	DD	PP	FF	MB	ERR%	NS
1	101479.90	4737.32	106217.20	107006.30	-789.13	-0.737	20.408
2	103994.00	3623.04	107617.00	108000.00	-383.00	-0.355	27.534
3	100246.10	7962.90	108209.00	108000.00	209.06	0.194	11.742
4	101763.60	3430.00	105193.60	106698.80	-1505.19	-1.411	29.464
5	106250.00	2950.00	109200.00	108500.00	700.00	0.645	36.017
6	106879.50	2416.74	109296.10	109107.60	188.56	0.173	46.277
7	98646.69	9926.10	108572.70	108500.00	72.75	0.067	9.329
8	95109.00	13754.10	108863.00	108521.60	341.38	0.315	6.447
9	85893.69	20714.40	106608.00	108738.60	-2130.63	-1.959	4.018

RESULTS(B)
AMOUNT OF SEPARATION

	CB-CF	BF	CF-CD	DF	AS
1	1840.00	46680.79	1964.00	47469.88	94150.63
2	1915.00	48870.80	2012.00	49253.75	98124.50
3	1715.00	44367.04	1830.00	44157.91	88524.94
4	1955.00	48229.84	2030.00	49735.00	97964.81
5	2080.00	52000.00	2052.00	51300.00	103300.00
6	2180.00	53562.61	2076.00	53373.97	106936.50
7	1655.00	42682.44	1760.00	42609.61	85292.00
8	1505.00	38949.41	1600.00	38608.01	77557.38
9	1205.00	30667.25	1330.00	32797.80	63465.05

CORE USAGE   OBJECT CODE=   2608 BYTES,ARRAY AREA=   864 BYTES,TOTAL AREA AVAILABLE= 102400 BYTES

DIAGNOSTICS   NUMBER OF ERRORS=   0, NUMBER OF WARNINGS=   0, NUMBER OF EXTENSIONS=   0

COMPILE TIME=   0.15 SEC,EXECUTION TIME=   0.15 SEC, WATFIV - JUL 1973 V1L4   16:45:00   FRIDAY   21 NOV 75

        $STOP
#EXECUTION TERMINATED
#

```
$r *watfiv scards=exp 5=m4 par=nolist
#EXECUTION BEGINS


          $COMPILE

          $DATA
DATA

             CB         VB         CD         VD         CF
       1    3900.00    101.11     267.00      99.83     2100.00
       2    4000.00     98.85     192.00      96.75     2100.00
       3    3675.00     99.09     575.00      98.86     2100.00
       4    4025.00    101.17     180.00      98.25     2160.00
       5    4125.00     98.88     145.00      96.25     2160.00
       6    4200.00     99.35     125.00      98.15     2160.00
       7    3625.00    100.00     640.00     101.18     2140.00
       8    3300.00     98.17    1100.00     100.00     2140.00
       9    2880.00     98.44    1440.00      99.88     2140.00


RESULTS(A)
MATERIAL BALANCE & SEPARATION FACTOR

             BB          DD          PP          FF          MB       ERR%       NS
       1  394329.00    26654.61   420983.50   421974.00    -990.44   -0.235    14.607
       2  395400.00    18576.00   413976.00   410760.00    3216.00    0.783    20.833
       3  364155.60    56344.50   421000.10   415694.90    5305.25    1.276     6.391
       4  407209.10    17685.00   424894.10   430747.10   -5853.00   -1.359    22.361
       5  407880.00    13956.25   421836.20   421480.70     355.50    0.084    28.448
       6  417270.00    12268.75   429538.60   426600.00    2938.69    0.689    33.600
       7  362500.00    64755.20   427255.10   430525.10   -3269.94   -0.760     5.664
       8  323960.90   110000.00   433960.90   424083.70    9877.19    2.329     3.000
       9  283507.10   143827.10   427334.30   424404.80    2929.56    0.690     2.000


RESULTS(B)
AMOUNT OF SEPARATION

             CB-CF       BF          CF-CD       DF          AS
       1    1800.00   181998.00    1833.00   182938.30   364986.30
       2    1900.00   187815.00    1908.00   184599.00   372414.00
       3    1575.00   156066.60    1525.00   150761.50   306828.10
       4    1865.00   188682.00    1980.00   194535.00   383217.00
       5    1965.00   194299.10    2015.00   193943.70   383242.90
       6    2040.00   202674.00    2035.00   199735.10   402409.10
       7    1485.00   148500.00    1500.00   151769.90   300269.90
       8    1160.00   113877.10    1040.00   104000.00   217877.10
       9     740.00    72845.56     700.00    69916.00   142761.50

CORE USAGE       OBJECT CODE=    2608 BYTES,ARRAY AREA=      864 BYTES,TOTAL AREA AVAILABLE=  102400  BYTES

DIAGNOSTICS      NUMBER OF ERRORS=      0, NUMBER OF WARNINGS=      0, NUMBER OF EXTENSIONS=      0
```

```
$r *watfiv scards=exp 5=m5 par=nolist
*EXECUTION BEGINS
```

          $COMPILE

          $DATA
DATA

             CB   VB   CD   VD   CF
     1   1080.00   24.20   21.10   25.39   540.00
     2   1120.00   24.14   17.10   25.84   540.00
     3   1050.00   24.38   26.30   25.30   549.00
     4   1090.00   24.25   19.70   25.25   560.00
     5   1140.00   23.84   15.70   25.66   560.00
     6   1160.00   24.13   14.90   25.95   560.00
     7   1010.00   25.34   40.00   25.11   530.00
     8   1000.00   25.07   53.00   24.78   530.00
     9   960.00   25.62   90.00   24.84   530.00

RESULTS(A)
MATERIAL BALANCE & SEPARATION FACTOR

             BB   DD   PP   FF   MB   ERR%   NS
     1   26136.00   535.73   26671.72   26778.60   -106.88   -0.399   51.185
     2   27035.80   441.86   27478.66   26989.20   489.46   1.814   65.497
     3   25599.00   665.39   26264.79   26827.20   -562.81   -2.098   39.924
     4   26432.50   497.42   26929.92   27720.00   -790.08   -2.850   55.330
     5   27177.59   402.86   27580.45   27720.00   -139.55   -0.503   72.611
     6   27990.80   386.65   28377.46   28044.80   332.66   1.136   77.352
     7   25593.39   1004.40   26597.79   26738.50   -140.70   -0.526   25.250
     8   25070.00   1313.34   26383.34   26420.50   -37.16   -0.141   18.868
     9   24595.20   2235.60   26830.79   26743.79   87.00   0.325   10.667

RESULTS(B)
AMOUNT OF SEPARATION

             CB-CF   BF   CF-CD   DF   AS
     1   540.00   13068.00   518.90   13174.87   26242.86
     2   580.00   14001.20   522.90   13511.93   27512.93
     3   510.00   12433.80   513.70   12996.61   25430.41
     4   530.00   12852.50   540.30   13642.57   26495.07
     5   580.00   13827.20   544.30   13966.73   27793.93
     6   600.00   14478.00   545.10   14145.34   28623.34
     7   480.00   12163.20   490.00   12303.90   24467.09
     8   470.00   11782.90   477.00   11820.06   23602.96
     9   430.00   11016.60   440.00   10929.60   21946.20

CORE USAGE   OBJECT CODE=   2608 BYTES,ARRAY AREA=   864 BYTES,TOTAL AREA AVAILABLE= 102400 BYTES

DIAGNOSTICS   NUMBER OF ERRORS=   0, NUMBER OF WARNINGS=   0, NUMBER OF EXTENSIONS=   0

COMPILE TIME=   0.03 SEC,EXECUTION TIME=   0.15 SEC, WATFIV - JUL 1973 V1L4   16:11:45   FRIDAY   21 NOV 75

$r *watfiv scards=exp 5=m7 par=nolist
#EXECUTION BEGINS

$COMPILE

$DATA
DATA

	CB	VB	CD	VD	CF
1	1050.00	51.82	26.30	49.24	550.00
2	1090.00	50.17	20.20	51.50	550.00
3	1030.00	51.91	33.00	49.03	550.00
4	1070.00	50.09	24.20	51.00	550.00
5	1100.00	50.77	18.10	51.49	550.00
6	1110.00	50.50	17.60	51.57	550.00
7	1010.00	50.25	44.00	51.25	530.00
8	990.00	50.94	61.00	49.50	530.00
9	950.00	50.77	104.00	49.67	530.00

RESULTS(A)
MATERIAL BALANCE & SEPARATION FACTOR

	BB	DD	PP	FF	MB	ERR%	NS
1	54411.00	1295.01	55706.02	55583.00	123.01	0.221	39.924
2	54635.30	1040.30	55725.59	55918.50	-192.90	-0.345	53.960
3	53467.30	1617.99	55085.29	55517.00	-431.71	-0.778	31.212
4	53596.29	1234.20	54830.49	55599.50	-769.00	-1.383	44.215
5	55847.00	931.97	56778.97	56243.00	535.97	0.953	60.77
6	56055.00	907.63	56962.63	56138.50	824.13	1.468	63.068
7	50752.50	2255.00	53007.50	53795.00	-787.50	-1.464	22.955
8	50430.60	3019.50	53450.10	53233.20	216.90	0.407	16.230
9	48231.50	5165.68	53397.18	53233.20	163.98	0.308	9.135

RESULTS(B)
AMOUNT OF SEPARATION

	CB-CF	BF	CF-CD	DF	AS
1	500.00	25910.00	523.70	25786.99	51696.99
2	540.00	27091.80	529.80	27284.69	54376.48
3	480.00	24916.80	517.00	25348.51	50265.31
4	520.00	26046.80	525.80	26315.79	52362.59
5	550.00	27923.50	531.90	27387.53	55311.03
6	560.00	28280.00	532.40	27455.86	55735.86
7	480.00	24120.00	486.00	24907.50	49027.50
8	460.00	23432.40	463.00	23215.50	46647.90
9	420.00	21323.40	426.00	21159.42	42482.82

CORE USAGE   OBJECT CODE=   2608 BYTES,ARRAY AREA=   864 BYTES,TOTAL AREA AVAILABLE= 102400 BYTES

DIAGNOSTICS   NUMBER OF ERRORS=   0, NUMBER OF WARNINGS=   0, NUMBER OF EXTENSIONS=   0

COMPILE TIME=   0.03 SEC,EXECUTION TIME=   0.15 SEC, WATFIV - JUL 1973 V1L4   16:16:11   FRIDAY   21 NOV 75

```
          $COMPILE

          $DATA
DATA
            CB        VB        CD        VD        CF
       1   1020.00    99.72     36.00     98.12     540.00
       2   1050.00    99.09     26.00     98.18     540.00
       3   1010.00    99.45     48.00     98.79     540.00
       4   1030.00    98.50     32.00     99.65     540.00
       5   1070.00    97.32     23.00     99.92     540.00
       6   1080.00    97.69     23.30     99.82     540.00
       7   1000.00    98.73     55.00     98.55     520.00
       8    970.00    98.15     80.00     98.50     520.00
       9    890.00    97.65    139.00     99.15     520.00
```

RESULTS(A)
MATERIAL BALANCE & SEPARATION FACTOR

```
           BB          DD         PP          FF         MB       ERR%       NS
     1  101714.30    3532.32   105246.60   106833.50   -1586.88   -1.485    28.333
     2  104044.40    2552.68   106597.00   106525.70      71.31    0.067    40.385
     3  100444.40    4741.92   105186.30   107049.50   -1863.25   -1.741    21.042
     4  101455.00    3188.80   104643.70   107000.90   -2357.19   -2.203    32.188
     5  104132.30    2298.16   106430.50   106509.50     -79.06   -0.074    46.522
     6  105505.10    2325.81   107830.90   106655.30    1175.56    1.102    48.430
     7   98729.94    5420.25   104150.10   102585.50    1564.63    1.525    18.182
     8   95205.44    7880.00   103085.40   102257.90     827.50    0.809    12.125
     9   86908.44   13781.85   100690.20   102335.90   -1645.69   -1.608     6.403
```

RESULTS(B)
AMOUNT OF SEPARATION

```
           CB-CF        BF        CF-CD        DF          AS
     1     480.00    47865.60     504.00    49452.48     97318.06
     2     510.00    50535.89     514.00    50464.52    101000.30
     3     470.00    46741.50     492.00    48604.68     95346.13
     4     490.00    48265.00     508.00    50622.20     98887.19
     5     530.00    51579.60     517.00    51658.64    103238.10
     6     540.00    52752.60     516.70    51576.99    104329.50
     7     480.00    47390.39     465.00    45825.75     93215.13
     8     450.00    44167.50     440.00    43340.00     87507.44
     9     370.00    36130.50     381.00    37776.14     73906.63
```

```
CORE USAGE       OBJECT CODE=   2608 BYTES,ARRAY AREA=      864 BYTES,TOTAL AREA AVAILABLE=  102400  BYTES

DIAGNOSTICS      NUMBER OF ERRORS=      0, NUMBER OF WARNINGS=        0, NUMBER OF EXTENSIONS=      0

COMPILE TIME=    0.03 SEC,EXECUTION TIME=      0.15 SEC,  WATFIV - JUL 1973 V1L4    16:20:45    FRIDAY      21 NOV 75
```

$COMPILE

$DATA

DATA

	CB	VB	CD	VD	CF
1	7150.00	26.28	810.00	25.47	4050.00
2	7450.00	26.00	565.00	25.00	4050.00
3	6800.00	26.34	1310.00	25.29	4050.00
4	7600.00	26.50	450.00	25.82	4100.00
5	8100.00	25.17	288.00	26.48	4100.00
6	8150.00	26.78	218.00	26.85	4100.00
7	6625.00	25.87	1700.00	26.65	4175.00
8	6375.00	25.09	2240.00	26.86	4175.00
9	5825.00	25.39	2650.00	25.84	4175.00

RESULTS(A)
MATERIAL BALANCE & SEPARATION FACTOR

	BB	DD	PP	FF	MB	ERR%	NS
1	187901.90	20630.70	208532.60	209587.50	-1054.88	-0.503	8.827
2	193700.00	14125.00	207825.00	206550.00	1275.90	0.617	13.186
3	179111.90	33129.39	212241.80	209101.40	3140.38	1.502	5.191
4	201400.00	11619.00	213019.00	214512.00	-1493.00	-0.696	16.889
5	203876.90	7626.24	211503.10	211764.90	-261.81	-0.124	28.125
6	218256.90	5853.30	224110.10	219883.00	4227.19	1.922	37.385
7	171388.60	45304.99	216693.60	219270.90	-2577.31	-1.175	3.897
8	159948.60	60166.40	220115.00	216891.10	3223.88	1.486	2.846
9	147896.60	68475.94	216372.60	213885.10	2487.44	1.163	2.198

RESULTS(B)
AMOUNT OF SEPARATION

	CB-CF	BF	CF-CD	DF	AS
1	3100.00	81467.94	3240.00	82522.35	163990.60
2	3400.00	88400.00	3485.00	87125.00	175525.00
3	2750.00	72434.94	2740.00	69294.56	141729.50
4	3500.00	92750.00	3650.00	94243.00	186993.00
5	4000.00	100679.90	3812.00	100941.60	201621.60
6	4050.00	108458.90	3882.00	104231.60	212690.60
7	2450.00	63381.48	2475.00	65958.69	129340.10
8	2200.00	55197.99	1935.00	51974.10	107172.00
9	1650.00	41893.50	1525.00	39405.99	81299.44

CORE USAGE   OBJECT CODE=   2608 BYTES,ARRAY AREA=   864 BYTES,TOTAL AREA AVAILABLE= 102400 BYTES

DIAGNOSTICS   NUMBER OF ERRORS=   0, NUMBER OF WARNINGS=   0, NUMBER OF EXTENSIONS=   0

COMPILE TIME=   0.03 SEC,EXECUTION TIME=   0.15 SEC, WATFIV - JUL 1973 V1L4   16:25:07   FRIDAY   21 NOV 75

```
$r *watfiv scards=exp S=mll par=nolist
#EXECUTION BEGINS
```

```
          $COMPILE

          $DATA
DATA

          CB          VB          CD          VD          CF
   1    7050.00      51.23      940.00      48.84     4100.00
   2    7375.00      51.39      625.00      49.61     4100.00
   3    6775.00      51.20     1470.00      49.93     4100.00
   4    7500.00      51.86      490.00      49.14     4175.00
   5    8075.00      50.15      310.00      50.15     4175.00
   6    8125.00      49.21      239.00      50.86     4175.00
   7    6450.00      50.14     2010.00      50.64     4200.00
   8    5975.00      49.70     2490.00      50.97     4200.00
   9    5300.00      49.52     3125.00      50.85     4200.00
```

```
RESULTS(A)
MATERIAL BALANCE & SEPARATION FACTOR

          BB          DD          PP          FF          MB        ERR%       NS
   1   361171.40    45909.59   407081.00   410286.90   -3205.94   -0.781    7.500
   2   379001.10    31005.25   410007.40   414100.00   -4092.56   -0.988   11.800
   3   346879.90    73397.06   420277.00   414632.90    5644.06    1.361    4.609
   4   388950.00    24078.60   413028.50   421575.00   -8546.44   -2.050   15.306
   5   404961.10    15546.50   420507.60   413752.40    1755.19    0.419   26.048
   6   399831.20    12155.54   411986.70   417792.20   -5805.50   -1.390   33.996
   7   323402.90   101786.30   425189.30   423275.90    1913.38    0.452    3.209
   8   295957.40   126915.20   423872.60   422813.90.   1058.5     0.250    2.400
   9   262456.00   158906.20   421362.20   421554.00    -191.75   -0.045    1.696
```

```
RESULTS(B)
AMOUNT OF SEPARATION

          CB-CF        BF         CF-CD         DF          AS
   1     2950.00   151128.40    3160.00    154334.30    305462.80
   2     3275.00   168302.10    3475.00    172394.70    340696.90
   3     2675.00   136959.90    2630.00    131315.80    268275.80
   4     3325.00   172434.50    3685.00    181080.80    353515.30
   5     3900.00   195584.90    3865.00    193829.60    389414.60
   6     3950.00   194379.50    3936.00    200184.90    394564.40
   7     2250.00   112814.90    2190.00    110901.50    223716.50
   8     1775.00    88217.44    1710.00     87158.69    175376.10
   9     1100.00    54472.00    1075.00     54663.5     109135.5
```

```
CORE USAGE      OBJECT CODE=   2608 BYTES,ARRAY AREA=      864 BYTES,TOTAL AREA AVAILABLE=  102400  BYTES

DIAGNOSTICS      NUMBER OF ERRORS=      0, NUMBER OF WARNINGS=        0, NUMBER OF EXTENSIONS=        0

COMPILE TIME=    0.03 SEC,EXECUTION TIME=       0.15 SEC,  WATFIV - JUL 1973 V1L4       16:29:27    FRIDAY      21 NOV 75
```

$COMPILE

$DATA

DATA

	CB	VB	CD	VD	CF
1	6900.00	101.33	1190.00	101.50	4050.00
2	7250.00	99.75	725.00	99.50	4050.00
3	6650.00	99.15	1670.00	101.75	4050.00
4	7400.00	101.75	590.00	99.15	4125.00
5	7925.00	99.11	350.00	99.11	4125.00
6	8100.00	99.25	283.00	100.81	4125.00
7	6400.00	99.11	2210.00	101.58	4200.00
8	5600.00	99.41	2800.00	101.91	4200.00
9	5000.00	99.18	3575.00	101.73	4200.00

RESULTS(A)
MATERIAL BALANCE & SEPARATION FACTOR

	BB	DD	PP	FF	MB	ERR%	NS
1	699177.00	120785.00	819962.00	821461.50	-1499.50	-0.183	5.798
2	723187.50	72137.50	795325.00	806962.50	-11637.50	-1.442	10.000
3	659347.40	169922.50	829269.30	813644.90	15625.00	1.920	3.982
4	752950.00	58498.50	811448.40	828712.40	-17264.80	-2.083	12.542
5	785446.70	34688.50	820135.20	817657.50	2477.75	0.303	22.643
6	803925.00	28529.23	832454.10	825247.40	7206.75	0.873	28.622
7	634304.00	224491.70	858795.70	842898.00	15897.75	1.885	2.896
8	556696.00	285348.00	842044.00	845544.00	-3500.00	-0.414	2.000
9	495899.90	363684.60	859584.60	843821.90	15762.69	1.868	1.399

RESULTS(B)
AMOUNT OF SEPARATION

	CB-CF	BF	CF-CD	DF	AS
1	2850.00	288790.50	2860.00	290290.00	579080.50
2	3200.00	319200.00	3325.00	330837.50	650037.50
3	2600.00	257789.90	2380.00	242165.00	499954.90
4	3275.00	333231.20	3535.00	350495.10	683726.40
5	3800.00	376618.00	3775.00	374140.20	750758.20
6	3975.00	394518.70	3842.00	387312.00	781830.70
7	2200.00	218042.00	1990.00	202144.10	420186.10
8	1400.00	139174.00	1400.00	142674.00	281848.00
9	800.00	79343.94	625.00	63581.25	142925.10

CORE USAGE   OBJECT CODE=   2608 BYTES,ARRAY AREA=   864 BYTES,TOTAL AREA AVAILABLE= 102400 BYTES

DIAGNOSTICS   NUMBER OF ERRORS=   0, NUMBER OF WARNINGS=   0, NUMBER OF EXTENSIONS=   0

COMPILE TIME=   0.03 SEC,EXECUTION TIME=   0.15 SEC, WATFIV - JUL 1973 V1L4   16:33:51   FRIDAY   21 NOV 75

```
        $COMPILE
    1         DIMENSION X(12,4),BB(12),DD(12),PP(12),VF(12),FF(12),           2
              1ERR(12),CBF(12),CDF(12),BF(12),DF(12),AS(12)                   3
    2         REAL MB(12),NS(12)                                             4
    3         N=9                                                            5
    4         READ(5,5)CF                                                    6
    5     5   FORMAT(F10.2)                                                  7
    6         READ(5,15)((X(I,J),J=1,4),I=1,N)                               8
    7    15   FORMAT(4F10.2)                                                 9
    8         WRITE(6,6)                                                    10
    9     6   FORMAT(1X,'DATA'//1X,12X,'CB',9X,'VB',8X,'CD',                11
              18X,'VD')                                                     12
   10         DO 60 I=1,N                                                   13
   11    60   WRITE(6,26)I,X(I,1),X(I,2),X(I,3),X(I,4)                      14
   12    26   FORMAT(1X,I7,4F10.2)                                          15
   13         WRITE(6,36)                                                   16
   14    36   FORMAT(//1X,'RESULTS(A)'/1X,'MATERIAL BALANCE & SEPARATION FACTOR' 17
              1//1X,14X,'BB',11X,'DD',11X,                                  18
              1'PP',11X,'FF',10X,'MB',8X,'ERR%',7X,'NS')                    19
   15         DO 80 I=1,N                                                   20
   16         BB(I)=X(I,1)*X(I,2)                                           21
   17         DD(I)=X(I,3)*X(I,4)                                           22
   18         PP(I)=BB(I)+DD(I)                                             23
   19         VF(I)=X(I,2)+X(I,4)                                           24
   20         FF(I)=VF(I)*CF                                                25
   21         MB(I)=PP(I)-FF(I)                                             26
   22         ERR(I)=MB(I)*100.0/FF(I)                                      27
   23         NS(I)=X(I,1)/X(I,3)                                           28
   24         CBF(I)=X(I,1)-CF                                              29
   25         CDF(I)=CF-X(I,3)                                              30
   26         BF(I)=CBF(I)*X(I,2)                                           31
   27         DF(I)=CDF(I)*X(I,4)                                           32
   28         AS(I)=BF(I)+DF(I)                                             33
   29    80   WRITE(6,46)I,BB(I),DD(I),PP(I),FF(I),MB(I),ERR(I),NS(I)       34
   30    46   FORMAT(1X,I7,4F13.2,F11.2,2F10.3)                             35
   31         WRITE(6,66)                                                   36
   32         WRITE(6,86)                                                   37
   33         DO 90 I=1,N                                                   38
   34    90   WRITE(6,76)I,CBF(I),BF(I),CDF(I),DF(I),AS(I)                  39
   35    66   FORMAT(//1X,'RESULTS(B)'/1X,'AMOUNT OF SEPARATION')           40
   36    86   FORMAT(//1X,13X,'CB-CF',7X,'BF',10X,'CF-CD',8X,'DF',12X,'AS')  41
   37    76   FORMAT(1X,I7,4F12.2,F14.2)                                    42
   38         STOP                                                          43
   39         END                                                          44

        $DATA
```

DATA

	CB	VB	CD	VD
1	3560.00	18.80	400.00	19.83
2	3770.00	18.19	290.00	19.80
3	3310.00	17.90	580.00	18.30
4	3410.00	17.94	455.00	18.11
5	3900.00	17.20	280.00	19.80
6	4025.00	17.73	195.00	19.86
7	3300.00	17.55	735.00	18.16
8	3010.00	18.10	820.00	18.20
9	2795.00	18.00	1020.00	18.13

RESULTS(A)
MATERIAL BALANCE & SEPARATION FACTOR

	BB	DD	PP	FF	MB	ERR%	NS
1	66928.00	7932.00	74860.00	75328.50	-468.50	-0.622	8.900
2	68576.25	5742.00	74318.25	74080.50	237.75	0.321	13.000
3	59248.98	10614.00	69862.94	70589.94	-727.00	-1.030	5.707
4	61175.41	8240.05	69415.44	70297.50	-882.06	-1.255	7.495
5	67079.94	5544.00	72623.94	72150.00	473.94	0.657	13.929
6	71363.19	3872.70	75235.88	73300.44	1935.44	2.640	20.041
7	57915.01	13347.60	71262.56	69634.50	1628.06	2.338	4.490
8	54481.02	14924.00	69405.00	70785.00	-1380.00	-1.950	3.671
9	50310.00	18492.60	68802.56	70453.50	-1650.94	-2.343	2.740

RESULTS(B)
AMOUNT OF SEPARATION

	CB-CF	BF	CF-CD	DF	AS
1	1610.00	30268.00	1550.00	30736.50	61004.50
2	1820.00	33105.80	1660.00	32868.00	65973.75
3	1360.00	24343.99	1370.00	25071.00	49414.99
4	1460.00	26192.40	1495.00	27074.45	53266.85
5	1950.00	33539.99	1670.00	33066.00	66605.94
6	2075.00	36789.74	1755.00	34854.30	71644.00
7	1350.00	23692.50	1215.00	22064.40	45756.91
8	1060.00	19186.00	1130.00	20566.00	39752.00
9	845.00	15210.00	930.00	16860.90	32070.90

CORE USAGE   OBJECT CODE=   2600 BYTES,ARRAY AREA=   816 BYTES,TOTAL AREA AVAILABLE=   102400   BYTES

DIAGNOSTICS   NUMBER OF ERRORS=   0, NUMBER OF WARNINGS=   0, NUMBER OF EXTENSIONS=   0

COMPILE TIME=   0.18 SEC,EXECUTION TIME=   0.13 SEC, WATFIV VERSION 1 LEVEL 3 MARCH 1971   DATE= 07-30-74

$STOP
#EXECUTION TERMINATED
#

```
        $COMPILE

        $DATA
DATA

            CB          VB          CD          VD
    1     3200.00       47.38      640.00       48.30
    2     3460.00       47.41      480.00       48.62
    3     2850.00       47.88      990.00       48.25
    4     3180.00       47.15      830.00       49.85
    5     3500.00       47.34      450.00       49.69
    6     3720.00       46.46      310.00       49.83
    7     2780.00       47.14     1130.00       48.33
    8     2615.00       47.64     1290.00       48.14
    9     2370.00       46.54     1550.00       48.08
```

RESULTS(A)
MATERIAL BALANCE & SEPARATION FACTOR

	BB	DD	PP	FF	MB	ERR%	NS
1	151616.00	30912.00	182528.00	186576.00	-4048.00	-2.170	5.000
2	164038.50	23337.60	187376.10	187258.40	117.69	0.063	7.208
3	136458.00	47767.50	184225.50	187453.50	-3228.00	-1.722	2.879
4	149936.90	41375.50	191312.40	189150.00	2162.44	1.143	3.831
5	165689.90	22360.50	188050.40	189208.40	-1158.00	-0.612	7.778
6	172831.10	15447.30	188278.40	187765.50	512.94	0.273	12.000
7	131049.10	54612.90	185662.00	186166.50	-504.44	-0.271	2.460
8	124578.50	62100.60	186679.10	186770.90	-91.81	-0.049	2.027
9	110299.70	74524.00	184823.70	184508.90	314.81	0.171	1.529

RESULTS(B)
AMOUNT OF SEPARATION

	CB-CF	BF	CF-CD	DF	AS
1	1250.00	59225.00	1310.00	63273.00	122498.00
2	1510.00	71589.07	1470.00	71471.38	143060.40
3	900.00	43092.00	960.00	46320.00	89412.00
4	1230.00	57994.49	1120.00	55832.00	113826.40
5	1550.00	73376.94	1500.00	74535.00	147911.90
6	1770.00	82234.19	1640.00	81721.19	163955.30
7	830.00	39126.20	820.00	39630.60	78755.75
8	665.00	31680.60	660.00	31772.40	63453.00
9	420.00	19546.80	400.00	19232.00	38778.80

```
CORE-USAGE        OBJECT-CODE=   2600 BYTES,ARRAY AREA=      816 BYTES,TOTAL AREA AVAILABLE=  102400 BYTES

DIAGNOSTICS       NUMBER OF ERRORS=      0, NUMBER OF WARNINGS=      0, NUMBER OF EXTENSIONS=      0

COMPILE TIME=    0.03 SEC,EXECUTION TIME=      0.12 SEC,  WATFIV - VERSION 1 LEVEL 3 MARCH  1971      DATE=  07-30-74


        $STOP
#EXECUTION TERMINATED
```

```
$COMPILE
$DATA
```
DATA

	CB	VB	CD	VD
1	3050.00	96.20	1115.00	98.90
2	3270.00	96.54	870.00	98.75
3	2580.00	96.23	1545.00	97.87
4	2910.00	96.94	1190.00	97.11
5	3300.00	97.83	790.00	98.10
6	3615.00	97.89	515.00	98.21
7	2620.00	97.22	1465.00	98.50
8	2500.00	97.15	1590.00	98.43
9	2400.00	96.88	1725.00	98.13

RESULTS(A)

MATERIAL BALANCE & SEPARATION FACTOR

	BB	DD	PP	FF	MB	ERR%	NS
1	293409.90	110273.40	403683.30	400930.40	2752.94	0.687	2.735
2	315685.70	85912.50	401598.20	401320.80	277.38	0.069	3.759
3	248273.30	151209.10	399482.50	398875.40	607.06	0.152	1.670
4	282095.30	115560.80	397656.20	398772.70	-1116.50	-0.280	2.445
5	322839.00	77499.00	400333.00	402636.10	-2298.13	-0.571	4.177
6	353872.30	50578.15	404450.40	402985.50	1464.94	0.364	7.019
7	254716.30	144302.50	399018.80	402204.50	-3185.69	-0.792	1.788
8	242874.90	156503.60	399378.60	401916.80	-2538.19	-0.632	1.572
9	232512.00	169274.20	401786.20	400745.50	-1040.69	-0.260	1.391

RESULTS(B)

AMOUNT OF SEPARATION

	CB-CF	BF	CF-CD	DF	AS
1	995.00	95718.94	940.00	92965.94	188684.80
2	1215.00	117296.00	1185.00	117018.70	234314.80
3	525.00	50520.75	510.00	49913.70	100434.40
4	855.00	82383.69	865.00	84000.13	166883.80
5	1245.00	121798.30	1265.00	124096.50	245894.80
6	1560.00	152708.30	1540.00	151243.30	303951.70
7	565.00	54929.30	590.00	58115.00	113044.20
8	445.00	43231.75	465.00	45769.95	89001.69
9	345.00	33423.60	330.00	32382.90	65806.50

CORE USAGE   OBJECT CODE=   2600 BYTES,ARRAY AREA=   816 BYTES,TOTAL AREA AVAILABLE= 102400 BYTES

DIAGNOSTICS   NUMBER OF ERRORS=   0, NUMBER OF WARNINGS=   0, NUMBER OF EXTENSIONS=   0

COMPILE TIME=   0.03 SEC,EXECUTION TIME=   0.13 SEC, WATFIV - VERSION 1 LEVEL 3 MARCH 1971   DATE= 07-30-74

```
        $STOP
#EXECUTION TERMINATED
```

```
$COMPILE

    $DATA
DATA

          CB          VB          CD          VD
  1     1070.00      17.91       31.50       19.14
  2     1110.00      17.19       24.00       19.38
  3     1040.00      17.94       41.00       19.11
  4     1070.00      17.75       25.00       19.80
  5     1125.00      17.15       20.40       19.79
  6     1150.00      17.14       16.80       19.82
  7      970.00      17.97       95.00       19.16
  8      940.00      17.95      123.00       19.03
  9      850.00      17.94      214.00       19.00


RESULTS(A)
MATERIAL BALANCE & SEPARATION FACTOR

          BB          DD          PP          FF          MB        ERR%        NS
  1     19163.70     602.91    19766.61    19636.50     130.11      0.663     33.968
  2     19080.90     465.12    19546.02    19382.10     163.92      0.846     46.250
  3     18657.60     783.51    19441.11    19636.50    -195.39     -0.995     25.366
  4     18992.50     495.00    19487.50    19901.50    -414.00     -2.080     42.800
  5     19293.74     403.72    19697.46    19578.19     119.27      0.609     55.147
  6     19711.00     332.98    20043.97    19588.80     455.17      2.324     68.452
  7     17430.90    1820.20    19251.10    19678.90    -427.80     -2.174     10.211
  8     16873.00    2340.69    19213.68    19599.39    -385.71     -1.968      7.642
  9     15249.00    4066.00    19315.00    19578.20    -263.20     -1.344      3.972


RESULTS(B)
AMOUNT OF SEPARATION

          CB-CF        BF        CF-CD        DF          AS
  1      540.00     9671.40     498.50     9541.29     19212.69
  2      580.00     9970.20     506.00     9806.28     19776.48
  3      510.00     9147.40     489.00     9344.79     18494.19
  4      540.00     9585.00     505.00     9999.00     19584.00
  5      595.00    10204.25     509.60    10084.98     20289.22
  6      620.00    10626.80     513.20    10171.63     20798.42
  7      440.00     7906.80     435.00     8334.60     16241.40
  8      410.00     7359.50     407.00     7745.21     15104.70
  9      320.00     5740.80     316.00     6004.00     11744.80

  CORE USAGE      OBJECT CODE=    2600 BYTES,ARRAY AREA=      816 BYTES,TOTAL AREA AVAILABLE=   102400   BYTES

  DIAGNOSTICS      NUMBER OF ERRORS=      0, NUMBER OF WARNINGS=      0, NUMBER OF EXTENSIONS=      0

COMPILE TIME=     0.03 SEC;EXECUTION TIME=     0.12 SEC;  WATFIV - VERSION 1 LEVEL 3 MARCH 1971     DATE=  07-30-74


       $STOP
#EXECUTION TERMINATED
```

```
$COMPILE
```

```
                  $DATA
```
DATA

	CB	VB	CD	VD
1	980.00	47.43	38.00	49.14
2	1020.00	46.15	30.00	48.30
3	960.00	47.87	48.00	48.10
4	1016.00	46.17	40.00	49.63
5	1044.00	46.14	32.00	49.89
6	1055.00	46.13	27.00	49.87
7	928.00	46.96	103.00	48.04
8	900.00	47.85	130.00	49.13
9	796.00	47.89	221.00	48.11

RESULTS(A)
MATERIAL BALANCE & SEPARATION FACTOR

	BB	DD	PP	FF	MB	ERR%	NS
1	46481.39	1867.32	48348.71	49250.70	-901.99	-1.831	25.789
2	47072.99	1449.00	48521.99	48169.50	352.50	0.732	34.000
3	45955.20	2308.80	48263.99	48944.70	-680.71	-1.391	20.000
4	46908.71	1985.20	48893.91	48858.00	35.91	0.074	25.400
5	48170.16	1596.48	49766.63	48975.30	791.34	1.616	32.625
6	48667.15	1346.49	50013.64	48960.00	1053.64	2.152	39.074
7	43578.88	4948.12	48527.00	48450.00	77.00	0.159	9.010
8	43065.00	6386.90	49451.90	49459.80	-7.90	-0.016	6.923
9	38120.44	10632.31	48752.75	48960.00	-207.25	-0.423	3.602

RESULTS(B)
AMOUNT OF SEPARATION

	CB-CF	BF	CF-CD	DF	AS
1	470.00	22292.09	472.00	23194.08	45486.17
2	510.00	23536.50	480.00	23184.00	46720.50
3	450.00	21541.50	462.00	22222.20	43763.70
4	506.00	23362.02	470.00	23326.10	46688.12
5	534.00	24638.76	478.00	23847.42	48486.18
6	545.00	25140.85	483.00	24087.21	49228.06
7	418.00	19629.28	407.00	19552.27	39181.55
8	390.00	18661.50	380.00	18669.40	37330.90
9	286.00	13696.54	289.00	13903.79	27600.33

CORE USAGE   OBJECT CODE=   2600 BYTES,ARRAY AREA=   816 BYTES,TOTAL AREA AVAILABLE= 102400 BYTES

DIAGNOSTICS   NUMBER OF ERRORS=   0, NUMBER OF WARNINGS=   0, NUMBER OF EXTENSIONS=   0

COMPILE TIME=   0.03 SEC,EXECUTION TIME=   0.12 SEC, WATFIV - VERSION 1 LEVEL 3 MARCH 1971   DATE= 07-30-74

```
        $STOP
#EXECUTION TERMINATED
#
```

```
$COMPILE
$DATA
```

DATA

	CB	VB	CD	VD
1	935.00	96.94	66.00	97.14
2	950.00	96.72	57.00	97.80
3	915.00	96.16	103.00	97.84
4	920.00	97.80	76.00	98.28
5	948.00	96.30	57.00	96.87
6	960.00	96.15	52.00	98.31
7	852.00	96.26	153.00	97.59
8	800.00	97.40	200.00	97.72
9	706.00	96.03	298.00	98.17

RESULTS(A)
MATERIAL BALANCE & SEPARATION FACTOR

	BB	DD	PP	FF	MB	ERR%	NS
1	90638.88	6411.24	97050.06	97040.00	10.06	0.010	14.167
2	91884.00	5574.60	97458.56	97260.00	198.56	0.204	16.667
3	87986.38	10077.52	98063.88	97000.00	1063.88	1.097	8.883
4	89976.00	7469.28	97445.25	98040.00	-594.75	-0.607	12.105
5	91292.38	5521.59	96813.94	96584.94	229.00	0.237	16.632
6	92303.94	5112.12	97416.00	97229.94	186.06	0.191	18.462
7	82013.50	14931.27	96944.75	96924.94	19.81	0.020	5.569
8	77919.94	19544.00	97463.94	97559.94	-96.00	-0.098	4.000
9	67797.13	29254.66	97051.75	97099.94	-48.19	-0.050	2.369

RESULTS(B)
AMOUNT OF SEPARATION

	CB-CF	BF	CF-CD	DF	AS
1	435.00	42168.90	434.00	42158.76	84327.63
2	450.00	43524.00	443.00	43325.40	86849.38
3	415.00	39906.40	397.00	38842.48	78748.88
4	420.00	41076.00	424.00	41670.72	82746.69
5	448.00	43142.40	443.00	42913.41	86055.75
6	460.00	44229.00	448.00	44042.88	88271.88
7	352.00	33883.52	347.00	33863.73	67747.19
8	300.00	29220.00	300.00	29316.00	58536.00
9	206.00	19782.18	202.00	19830.34	39612.52

CORE USAGE   OBJECT CODE=   2600 BYTES,ARRAY AREA=   816 BYTES,TOTAL AREA AVAILABLE= 102400 BYTES

DIAGNOSTICS   NUMBER OF ERRORS=   0, NUMBER OF WARNINGS=   0, NUMBER OF EXTENSIONS=   0

COMPILE TIME=   0.03 SEC,EXECUTION TIME=   0.12 SEC,   WATFIV - VERSION 1 LEVEL 3 MARCH   1971   DATE= 07-30-74

```
$STOP
#EXECUTION TERMINATED
#
```

$r *watfiv scards=con 5=r9 par=nolist
#EXECUTION BEGINS

$COMPILE

$DATA
DATA

	CB	VB	CD	VD
1	4900.00	17.73	2475.00	19.18
2	5400.00	17.80	2020.00	19.20
3	5420.00	18.61	1750.00	18.72
4	6150.00	18.13	1350.00	18.96

RESULTS(A)
MATERIAL BALANCE & SEPARATION FACTOR

	BB	DD	PP	FF	MB	ERR%	NS
1	86876.94	47470.48	134347.30	135459.60	-1112.25	-0.821	1.980
2	96120.00	38783.99	134903.90	135790.00	-886.06	-0.653	2.673
3	100866.10	32760.00	133626.10	137001.00	-3374.88	-2.463	3.097
4	111499.50	25596.01	137095.50	136120.30	975.19	0.716	4.556

RESULTS(B)
AMOUNT OF SEPARATION

	CB-CF	BF	CF-CD	DF	AS
1	1230.00	21807.39	1195.00	22920.09	44727.98
2	1730.00	30794.00	1650.00	31679.99	62474.00
3	1750.00	32567.50	1920.00	35942.40	68509.88
4	2480.00	44962.41	2320.00	43987.21	88949.63

CORE USAGE   OBJECT CODE=   2592 BYTES,ARRAY AREA=   816 BYTES,TOTAL AREA AVAILABLE= 102400 BYTES

DIAGNOSTICS   NUMBER OF ERRORS=   0, NUMBER OF WARNINGS=   0, NUMBER OF EXTENSIONS=   0

COMPILE TIME=   0.03 SEC,EXECUTION TIME=   0.08 SEC, WATFIV - VERSION 1 LEVEL 3 MARCH 1971   DATE= 07-30-74

$STOP
#EXECUTION TERMINATED
#

$COMPILE

$DATA

DATA

	CB	VB	CD	VD
1	4700.00	47.50	2645.00	48.75
2	5020.00	47.24	2280.00	48.34
3	5300.00	47.45	2120.00	48.25
4	5700.00	46.85	1655.00	47.95

RESULTS(A)
MATERIAL BALANCE & SEPARATION FACTOR

	BB	DD	PP	FF	MB	ERR%	NS
1	223250.00	128943.70	352193.70	353237.50	-1043.75	-0.295	1.777
2	237144.80	110215.10	347360.00	350778.50	-3418.56	-0.975	2.202
3	251484.90	102290.00	353774.90	351218.90	2556.00	0.728	2.500
4	267045.00	79357.19	346402.10	347916.00	-1513.81	-0.435	3.444

RESULTS(B)
AMOUNT OF SEPARATION

	CB-CF	BF	CF-CD	DF	AS
1	1030.00	48925.00	1025.00	49968.75	98893.75
2	1350.00	63774.00	1390.00	67192.56	130966.50
3	1630.00	77343.44	1550.00	74787.50	152130.90
4	2030.00	95105.50	2015.00	96619.19	191724.60

CORE USAGE   OBJECT CODE=   2592 BYTES,ARRAY AREA=   816 BYTES,TOTAL AREA AVAILABLE=   102400 BYTES

DIAGNOSTICS   NUMBER OF ERRORS=   0, NUMBER OF WARNINGS=   0, NUMBER OF EXTENSIONS=   0

COMPILE TIME=   0.03 SEC,EXECUTION TIME=   0.08 SEC, WATFIV - VERSION 1 LEVEL 3 MARCH 1971   DATE= 07-30-74

$STOP
#EXECUTION TERMINATED
#

```
$COMPILE

$DATA
```
DATA

	CB	VB	CD	VD
1	4520.00	96.25	2970.00	98.35
2	4700.00	96.10	2660.00	98.35
3	4850.00	96.74	2540.00	98.00
4	5330.00	96.62	2150.00	98.85

RESULTS(A)
MATERIAL BALANCE & SEPARATION FACTOR

	BB	DD	PP	FF	MB	ERR%	NS
1	435050.00	292099.50	727149.50	723912.00	3237.50	0.447	1.522
2	451670.00	261611.00	713281.00	723354.00	-10073.00	-1.393	1.767
3	469189.00	248920.00	718109.00	724432.80	-6323.81	-0.873	1.909
4	514984.50	212527.50	727512.00	727148.30	363.69	0.050	2.479

RESULTS(B)
AMOUNT OF SEPARATION

	CB-CF	BF	CF-CD	DF	AS
1	800.00	77000.00	750.00	73762.50	150762.50
2	980.00	94178.00	1060.00	104251.00	198429.00
3	1130.00	109316.10	1180.00	115640.00	224956.10
4	1610.00	155558.10	1570.00	155194.50	310752.60

CORE USAGE   OBJECT CODE=   2592 BYTES,ARRAY AREA=   816 BYTES,TOTAL AREA AVAILABLE=   102400 BYTES

DIAGNOSTICS   NUMBER OF ERRORS=   0, NUMBER OF WARNINGS=   0, NUMBER OF EXTENSIONS=   0

COMPILE TIME=   0.03 SEC,EXECUTION TIME=   0.09 SEC, WATFIV = VERSION 1 LEVEL 3 MARCH 1971   DATE= 07-30-74

```
$STOP
```
#EXECUTION TERMINATED
#

APPENDIX F

Theoretical and Practical Energy Requirements
for a Desalting Process

F.1. Minimum Work of Separation

The mixing of two substances always results in an increase in

entropy, due to the increase in "randomness" of the system. This increase

is accompanied by a corresponding decrease in free energy, so that the

separation of the resulting mixture under thermodynamically reversible

conditions requires the supply of an equal amount of energy to counteract

nature's tendency to mix rather than unmix spontaneously.

In general, heat and work both depend on the particular path, and one

cannot calculate the minimum requirement of either without considering

the process in detail. There is however, one particular process - the

isothermal reversible process - for which the work is measured by the change

in the Helmholtz free energy (the work function), A. The term "minimum work

of separation" is usually used to mean the thermodynamic reversible work of

separation for an isothermal process and hence it is independent of the

process mechanism and dependent only on the initial and final states.

The minimum work to separate one mole of a feed solution of composition

x_1 into two product solutions of compositions x_2 and x_3 respectively is

given by (Dodge, 1944)*

---

* Dodge, B.F., Ed., "Chemical Engineering Thermodynamics", McGraw Hill Co.,
  New York, 1944.

$$W_{ideal} = -\Delta A = -RT \left[\frac{x_2 (x_1 - x_3)}{x_2 - x_3} \ln \frac{\rho_{A2}}{\rho_{A1}} + \right.$$

$$\frac{(1 - x_2)(x_1 - x_3)}{x_2 - x_3} \ln \frac{\rho_{B2}}{\rho_{B1}} + \frac{x_3 (x_2 - x_1)}{x_2 - x_3} \ln \frac{\rho_{A3}}{\rho_{A1}}$$

$$\left. + \frac{(1 - x_3)(x_2 - x_1)}{x_2 - x_3} \ln \frac{\rho_{B3}}{\rho_{B1}} \right] \quad \ldots\ldots\ldots\ldots\ldots \quad (F.1.)$$

where ρ is the partial pressure and subscripts 1, 2 and 3 refer to feed, first product, and second product, respectively, and subscripts A and B to the components.

Spiegler (1966 a) developed a general equation for the minimum theoretical energy requirement to separate salt from a saline. For any desalting process in which a 1-1 electrolyte solution of conc. C_f is converted into two product solutions of concs. C_d and C_c at 25°C, the minimum energy is given by

$$U = 1.377 \times \Delta N \left(\frac{\ln \beta}{\beta - 1} - \frac{\ln \alpha}{\alpha - 1} \right) \qquad (F.2.)$$

where U is the energy in kwh/m^3

ΔN = the normality difference between feed and product solution

N = the normality (g-equiv/lit)

$$\beta = \frac{N_f}{N_c} \quad ; \quad \alpha = \frac{N_f}{N_d}$$

subscripts f, d, c identify feed, product (diluate) and concentrate respectively.

F.2. Practical Energy Requirements

The theoretical energy requirements for a desalting process usually represents merely a small portion of the actual energy requirement. When the minimum work requirement for demineralization is compared with the actual requirement of operating process, it is found that this latter have an energy efficiency of the order of only 2 to 5% (Dodge and Eshaya, 1960)*.

These low efficiencies are, of course, attributable to the driving forces which are necessary in any practical process, as contrasted with the reversible process that assumes zero driving forces. These driving forces are the finite temperature differences, pressure differences, concentration differences, e.m.f. differences, etc., which are necessary for equipment of practical size. Any reduction in the driving force always entails an increase in size and hence cost of equipment and because the total costs of a desalting process are about equally divided between costs of energy and fixed costs on equipment, one reaches a cost minimum at an efficiency which is generally less than 20%.

The main irreversible effects that make the actual process differs from the ideal reversible one are:

   i) Pressure drop in lines and equipment due to fluid friction.

   ii) Throttling processes.

   iii) Finite temperature difference between fluids exchanging heat.

   iv) Heat conduction along solids.

   v) Heat leak into the system from the surroundings.

---

* Dodge, B.F. and A.M. Eshaya, in: "Saline Water Conversion" Number 27 in Advances in Chemistry Series, American Chemical Society, Washington, D.C., 1960.

vi) Fluid mixing when there is a difference in temperature or concentration.

vii) Mass transfer with finite concentration gradient.

viii) Joule heating in electric current flow.

ix) Polarization effects at electrodes.

x) Mechanical friction, as in pumps and compressors.

These effects can never be completely eliminated and frequently must remain of considerable magnitude, if the size of the equipment is to be kept within reasonable bounds [Dodge B.F. and A.M. Eshaya, 1960].